EG&G Idaho, Inc.

FORM EG&G-398
(Rev. 12-78)

INTERIM REPORT

Accession No. _____

Report No. RE-A-78-261 Rev. 2

Contract Program or Project Title: Thermal Analysis Branch

Subject of this Document: An Analysis Tool for Predicting Transient Hydrodynamics in Nuclear Piping Systems Containing Swing Check Valves

Type of Document: Internal Final Report

Author(s): R. A. Berry

Date of Document: September 1979

Responsible NRC Individual and NRC Office or Division: C. W. Burger, NRC-RES

This document was prepared primarily for preliminary or internal use. It has not received full review and approval. Since there may be substantive changes, this document should not be considered final.

EG&G Idaho, Inc.
Idaho Falls, Idaho 83401

Kay Rose
for H. P. Pearson, Supervisor
Information Processing

Prepared for the
U.S. Nuclear Regulatory Commission
and the U.S. Department of Energy
Idaho Operations Office
Under contract No. EY-76-C-07-1570
NRC FIN No.
A6164

1215 219

INTERIM REPORT

RE-A-78-261, Rev. 2
For U. S. Nuclear Regulatory Commission

CODE ASSESSMENT AND APPLICATIONS PROGRAM

AN ANALYSIS TOOL FOR PREDICTING TRANSIENT HYDRODYNAMICS IN NUCLEAR PIPING SYSTEMS CONTAINING SWING CHECK VALVES

By

R. A. Berry

Thermal Analysis Branch

September 1979

EG&G Idaho, Inc.

IDAHO NATIONAL ENGINEERING LABORATORY

DEPARTMENT OF ENERGY

IDAHO OPERATIONS OFFICE UNDER CONTRACT DE-AC07-76IDO1570

Report No. RE-A-78-261, Rev. 2

Date September 1979

Contract Program or Project Title: Thermal Analysis Branch

Subject of this Document: An Analysis Tool for Predicting Transient Hydrodynamics in Nuclear Piping Systems Containing Swing Check Valves

Type of Document: Internal Final Report
EG&G Idaho Inc.

Author(s): R. A. Berry
Broadway Facility, Idaho Falls, Idaho
208-526-1254

Date of Document:
September 1979

Responsible NRC Individual and NRC Office or Division:

C. W. Burger, NRC-RES

This document was prepared primarily for preliminary or internal use. It has not received full review and approval. Since there may be substantive changes, this document should not be considered final.

Idaho National Engineering Laboratory
Idaho Falls, Idaho 83401
Operated by
EG&G Idaho, Inc.
for the
U.S. Department of Energy

Prepared for
U.S. Nuclear Regulatory Commission
Washington, D.C. 20555

FIN A6164

ACKNOWLEDGMENTS

The assistance of Dr. V. H. Ransom, Mr. R. J. Wagner, and Mr. K. E. Carlson in the application, operation, and interpretation of results of the RELAP5 Reactor Loss of Coolant Analysis Program is gratefully acknowledged, as is the advice received from many reviewers.

ABSTRACT

An analysis tool is constructed for the purpose of predicting the fluid transient in a piping system as a consequence of (or in spite of) a check valve being present in the system. The development of the check valve model along with its implementation into a fluid flow analysis computer program is documented. The analysis tool requirements are outlined and the valve flow and disk dynamics are established. A sample demonstration problem was run using the analysis tool and the results reported. Several supporting documents for the transient fluid flow analysis computer program are also included in the appendices.

SUMMARY

This report addresses the hydrodynamic consequence of fluid transients in piping systems containing swing-type check valves, particularly the systems and subsystems of nuclear power plants. An analysis tool which can be used to predict these consequences is constructed from the RELAP5 Reactor Loss of Coolant Analysis Program. A dynamic check valve model was developed as a simple, one-dimensional, junction phenomenon which reacts interactively with the local flow field.

A demonstration problem was completed. The problem consisted of a BWR primary feedwater line (with a check valve present) subjected to a postulated pipe rupture. The results from this analysis appear qualitatively and, in many aspects, quantitatively correct. However, due to the complexity of the modeled phenomena, future experimental verification is desirable. The analysis tool shows promise as a predictor of both hydrodynamic effects and valve disk motions.

CONTENTS

FIGURES

FIGURES (Continued)

TABLES

NOMENCLATURE

Variables not defined within the text of the report

A_D	area of valve disk
A_{flow}	minimum flow area through the valve
A_K	flow area at station K
G_{head}	pressure difference across the valve disk due to gravitational effects
I	mass moment of inertia of the valve disk about its rocker axis
L	length of the valve disk moment arm
$\dot{m}$	homogeneous mixture fluid mass flowrate
P_{BP}	valve closing back pressure (minimum pressure difference across the valve disk required to initiate motion)
R	valve disk radius
t	time
T	torque acting on the valve disk
W	valve disk weight

Greek

α	valve disk angular acceleration
ω	valve disk angular velocity
θ	valve disk angular position
ϕ	angle of inclination of valve assembly
ρ	homogeneous mixture fluid density

Subscripts

n	time, $t + n\,\Delta t$
n+1	time, $t + (n+1)\,\Delta t$
max	maximum
min	minimum

I. INTRODUCTION

Swing-check type valves are in wide use in nuclear power plants, e.g., as isolation and non-return valves in the main steam lines connecting the steam generator to the steam turbine and as protective flow limiters on feedwater lines. During the course of the valve closure, high valve disk (see Figure 1) accelerations can develop leading to a substantial disk impact velocity. This is especially true for the severe case of a pipe rupture in which the major driving moment in the disk dynamics, the pressure differential across the disk, is significant due to the severe pressure transient and flow reversal phenomena.

In both the tripped and pipe-break closure situations several questions must be asked, including the following:

* How fast does or can the valve close?
* Can the valve really stop the flow, i.e., if the valve slams shut rapidly, is it possible for the valve disk or seat to fail due to high impact loads?
* For rapid valve closure what fluid transient results in the connecting piping system and what are the consequences of such a fluid transient?

It is the last question to which this report primarily addresses itself, however, the other two questions will be addressed as a consequence of this analysis.

More specifically, the goal of this project is to develop an analysis tool, using existing technology, which can be used to predict fluid transients which may occur in a piping system due to check valve motions. The results of such an analysis can be used directly to calculate the loads or forcing function inputs to a dynamic structural analysis of the system. This analysis tool was constructed for and funded by the U. S. Nuclear Regulatory Commission (USNRC).

In the remainder of this report the basic requirements of the analysis tool will be established and the various system computer codes which were considered for the implementation of the check valve model will be discussed. The check valve model is then developed by consideration of the check valve flow and disk dynamics. A demonstration problem (a BWR reactor primary feedwater line, with a check valve, undergoing a pipe rupture) will be constructed to illustrate the use of the analysis tool. The results of this demonstration problem are reported. The check valve model, BWR demonstration problem hydrodynamic model, and supporting documentation for the analysis tool are included in the appendices.

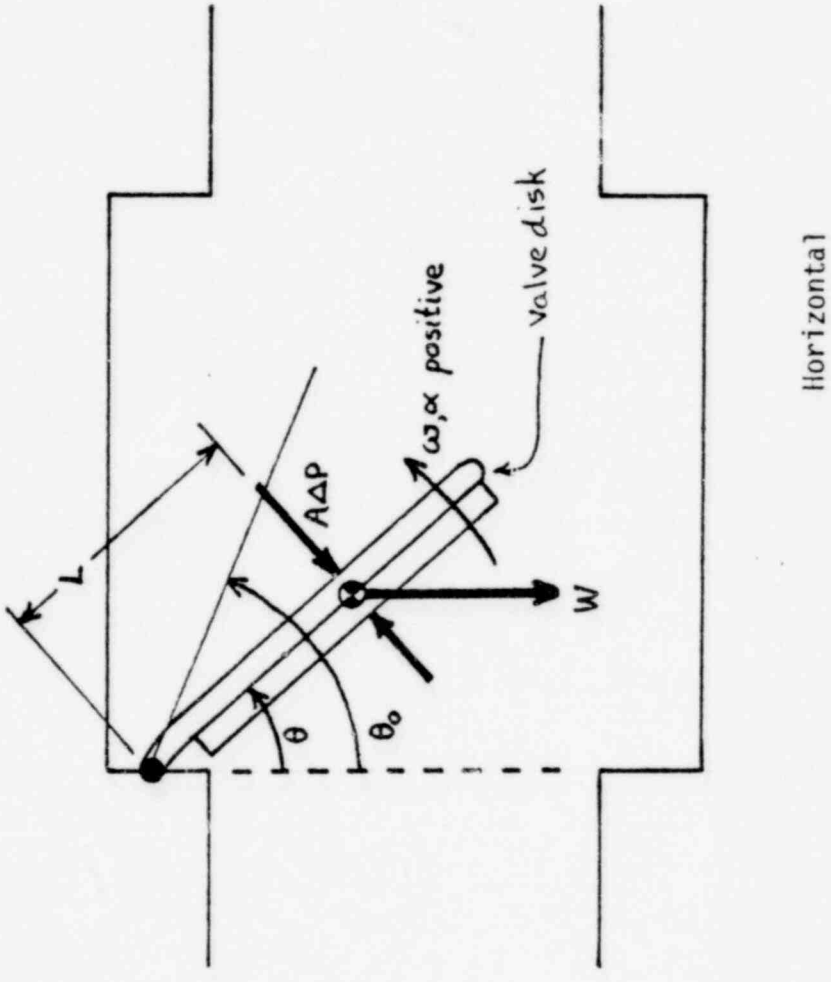

Figure 1

Swing-Type Check Valve Schematic, Nomenclature, and Forces

(The valve is shown horizontally, thus $\phi = 0$)

II. ANALYSIS TOOL DEVELOPMENT

1. REQUIREMENTS

Since the check valve may operate in a system undergoing a pipe rupture (potential blowdown), a primary requisite for the analysis tool is the ability to handle wave phenomena and critical flow in two phase systems as well as single phase (steam or subcooled water) systems. Unfortunately, wave phenomena, and consequently critical flow phenomena, are not understood as well as is desirable when two phases are present. The propagation velocities, as well as several other aspects of wave pheonmena such as damping (diffusion), dispersion of wave trains, and the existence and structure of shocks are strongly affected by the interactions between the phases in two phase media. Consequently, it is essential that single-phase results not, as is too often the case for critical flow and propagation phenomena, be extended to two-phase media without caution[1]. Thermal non-equilibrium and phasic velocity slip considerations are essential.

Another requirement of the analysis tool deals with the availability of check valve flow characteristics. Quite often these flow characteristics are difficult to obtain or just not available. It is therefore desirable that the check valve model utilized in the analysis tool be able to give reasonable results without published valve flow characteristics.

2. ANALYSIS TOOL TEST PROGRAMS

The charter for this project was the development of a dynamic check valve model for implementation into an already existing fluid transient code with perhaps some modification to the fluid transients code to accommodate the valve model and not for the development of a complete fluid transients code. In light of the previous Section II,1, it was evident that if a suitable fluid transients code was available, it would surely be an advanced, state-of-the-art code. Four computer codes were identified as possible candidates into which to incorporate the dynamic check valve model; DAPSY[2,3], SOLA-PLOOP[4,5], TRAC[6], and RELAP[7*].

---

* Included in Appendix C.

DAPSY is a one-dimensional code developed in West Germany for the calculation of pressure wave propagation in light water reactor primary coolant systems. This code uses a method of characteristics solution technique (assuming equal phase velocities and that steam is always on the saturation line) to solve the four equation system representing homogeneous, limited non-equilibrium flows. The equation system solved by DAPSY was considered to marginally meet the requirements placed on the flow physics calculations. An agreement with the West German government to obtain this code was already in progress; however, it became evident that this code would not have been available in a timely manner.

SOLA-PLOOP is a one-dimensional code developed at the Los Alamos Scientific Laboratory (LASL) for calculating transient, non-equilibrium, two-phase flow in networks using a partially implicit algorithm[8]. The code was originally selected as the fluid transient basis for the valve model because of its apparently simple yet capable construction. It was eventually dropped because too much of the coding was simply unchecked, and because its ability to handle abrupt area changes was inadequate; significant, new development of the code itself would have been required.

TRAC is a multi-dimensional code still currently under heavy development at LASL with USNRC funding as a "best estimate" prediction tool for the analysis of postulated light water reactor accidents. The currently released version, TRAC-P1, uses both implicit and semi-implicit solution techniques for a two-phase, five-equation drift-flux model. TRAC has a check valve model; however, it is much too simple for the purpose of this project. TRAC appeared to be a good basis for the valve model; however, TRAC-P1 was not generally released at the initiation of this project and the last alternative code RELAP5, yet to be discussed, was felt to offer superior capabilities for this application because of its equation form.

RELAP5 is a one-dimensional, advanced, "best estimate" code for the transient analysis of light water reactor systems, still under development at the Idaho National Engineering Laboratory for the USNCR. RELAP5 was considered, for the following reasons, to be the superior fluid transient code for implementing the check valve model:

- The hydrodynamic model is a two-fluid non-equilibrium model with one of the phases fixed at saturation.
- The code, with its five equation model (overall continuity, phasic difference continuity, overall momentum, phasic difference momentum, and overall internal energy) also has a unique method for calculating

flow through abrupt area changes[9*].

. The code incorporates some unique and advanced choking models[10**].

. The code is user oriented as far as input and output are concerned.

Although the advanced code is yet to be released, the RELAP5 code was obtained from the authors along with much valuable cooperation and assistance.

3. VALVE FLOW DYNAMICS

From a flow point of view, the check valve is represented by an abrupt area change (see Figure 2). The flow field through the area change is analyzed to calculate the forces acting on the valve disk to cause motion. The disk motion is in turn tracked to get successively new flow area changes. These two steps are repeated continuously in an explicit manner. Appendix D presents a detailed account of the calculation of flow through abrupt area changes.

A normal pressure gradient for a steady-state type flow is shown in Fig. 3 (dashed line). Figure 3 also shows a typical adverse pressure gradient which could result at some time in the area change region (Fig. 2) due to a decompression wave propagation through this region. The decompression wave is of finite length due to a finite break opening time or an instantaneous break in a system experiencing artificial (numerical) viscosity phenomena. The adverse pressure gradient (pressure at K lower than the pressure at L despite a fluid flow from K to L through an area change) could easily occur during a transient; for example, a break may have occurred upstream of point K and a decompression wave may be traveling to the right, decompressing the fluid at point K prior to that at point L. A similar situation could result from a compression wave propagating in the L-to-K direction from somewhere downstream of point L; in this case the fluid at point L would compress prior to that at point K. Since the flow field in the vicinity of the valve (area restriction) is being treated one-dimensionally, the available pressures for application to the valve disk are limited. Sensitivity studies were done to determine the effect that the selection of different applied pressures had on the valve disk motion. Initially the pressure difference applied to the valve disk was $P_L - P_K$, where P_L and P_K are the downstream and upstream static pressures. A second, alternative approach was also taken in which the maximum possible pressure gradient was applied to the disk; $(P_L - P_K) + (P_K - P_C)$ or simply $P_L - P_C$, where P_C is the pressure occurring at the ven contracta point. This latter assumption applies the minimum pressure occurring at the vena (continued on next page)

---

* Included in Appendix).

** Included in Appendix).

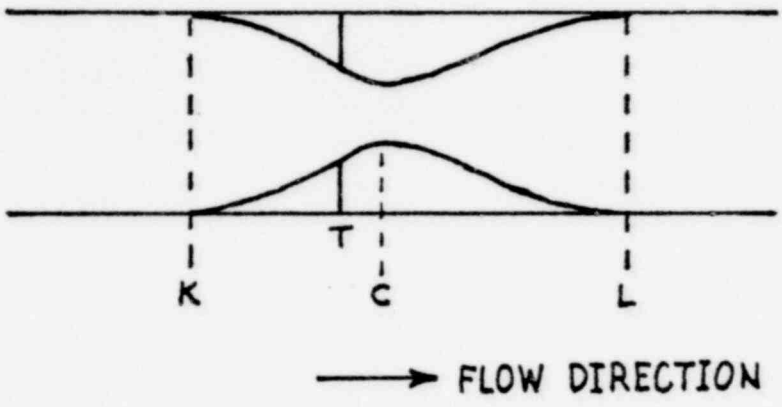

Figure 2
Abrupt Area Change Simulation of Check Valve

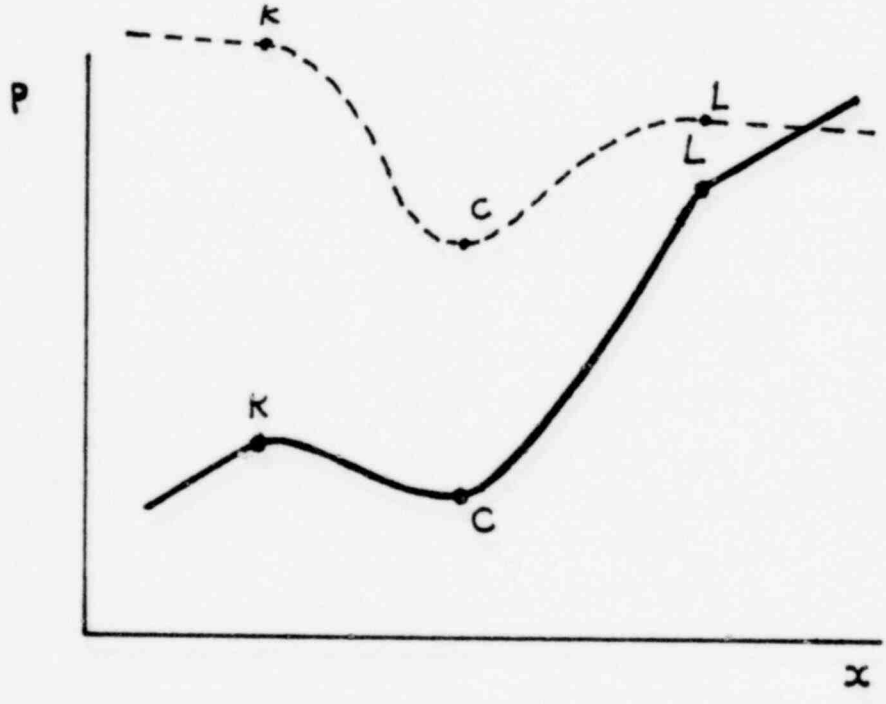

Figure 3
Adverse Pressure Gradient Through an Abrupt Area Change

1216 233

contracta point to one complete side of the disk (conservative assumption). The variation of the valve disk motion history with the two different forms for applying pressure to the disk was found to be very slight. The second approach outlined above for applying pressures to the disk was used in the sample demonstration problem to be reported in Section III.

The pressure at the point of vena contracta, P_C, was calculated using a homogeneous, equilibrium Bernoulli equation. Assuming flow from Point K to Point L in Figure 2, the vena contracta pressure is then calculated as:

$$P_C = P_K + \frac{1}{2}\rho \left[\left(\frac{\dot{m}}{\rho A_K}\right)^2 - \left(\frac{\dot{m}}{\rho A_C}\right)^2\right]$$

where the vena contracta area, A_C, is calculated as shown in Appendix D.

Upon careful inspection of the second approach for applying pressures to the valve disk, outlined above, it becomes evident that for normal gradients a more consistent approach (and probably more accurate) would be $(P_K - P_L) + (P_L - P_C)$ or simply $P_K - P_C$. This variation for normal pressure gradients was not implemented but is recommended for future applications.

The pressure difference across the valve grows rapidly once critical flow conditions are reached, thus a good choked flow model is needed. RELAP5 had an excellent, advanced choked flow model for two-phase flow through the valve (see Appendix E). For the case of subcooled liquid conditions upstream of the valve (minimum area) with two-phase flow possibly existing at the minimum area ($P_C \leq P_{saturation}$) an adequate choking model had to be implemented. The assumption of flow choking upon the vena contracta pressure's reaching the saturation pressure was adopted, realizing that this assumption is only approximate.

4. VALVE DISK DYNAMICS

Refer again to the typical valve disk assembly and the force system acting on it as shown in Figure 1. The motion of the disk assembly about the rocker shaft axis is given by Newton's second law (angular version) as

$$\sum \begin{bmatrix}\text{Torques Acting}\\ \text{On Disk}\end{bmatrix} = \begin{bmatrix}\text{Disk Mass Moment}\\ \text{Of Inertia About}\\ \text{The Axis}\end{bmatrix} * \begin{bmatrix}\text{Disk Angular}\\ \text{Acceleration}\end{bmatrix}$$

or

$$\sum T = I \alpha \tag{2}$$

The external torques acting on the valve disk are given by

$$T = -W L \sin (\theta + \phi) - A_D L (\Delta P + P_{BP} + G_{head}) \tag{3}$$

where the ΔP term may take on the different definitions given previously in Section II,3.

Substituting Equation (3) into (2) gives

$$I \alpha = -W L \sin \theta - \pi R^2 L(\Delta P + P_{BP} + G_{head}) \tag{4}$$

where ϕ has been dropped by assuming the valve is a horizontal pipe. Finite differencing Equation (4) gives

$$\alpha_n = \frac{1}{I} \left[-W L \sin \theta_n - \pi R^2 L(\Delta P_n + P_{BP} + G_{head})\right] \tag{5}$$

where the subscript n indicates the time level $t + n \Delta t$. Integrating Equation (5) with respect to time by forward differencing yields

$$\omega_{n+1} = \omega_n + \alpha_n \Delta t \tag{6}$$

Integrating Equation (6) similarly gives

$$\theta_{n+1} = \theta_n + \omega_{n+1} \Delta t \tag{7}$$

In order to account for valve stops at the minimum and maximum disk positions the following checks on valve disk angle of opening were made

$$\begin{aligned} &\text{If } \theta \geq \theta_{max} \quad \text{then } \theta = \theta_{max} \quad \text{and } \omega = 0 \\ &\text{If } \theta \leq \theta_{min} \quad \text{then } \theta = \theta_{min} \quad \text{and } \omega = 0 \end{aligned} \tag{8}$$

The flow area for the valve (area restriction) is then set. Any arbitrary function may be applied; the one selected here for demonstration is[11,12]

$$A_{\substack{flow \\ n+1}} = 2\pi R^2 \tan \Theta_{n+1} \quad \text{for } \Theta < 26.565° \qquad (9)$$

$$= \pi R^2 \quad \text{for } \Theta > 26.565°$$

Equations (5) through (9) constitute the basic inertial swinging disk check valve model. Figure 4 shows the basic calculational cycle for the check valve. Appendix A contains a FORTRAN listing of the check valve model.

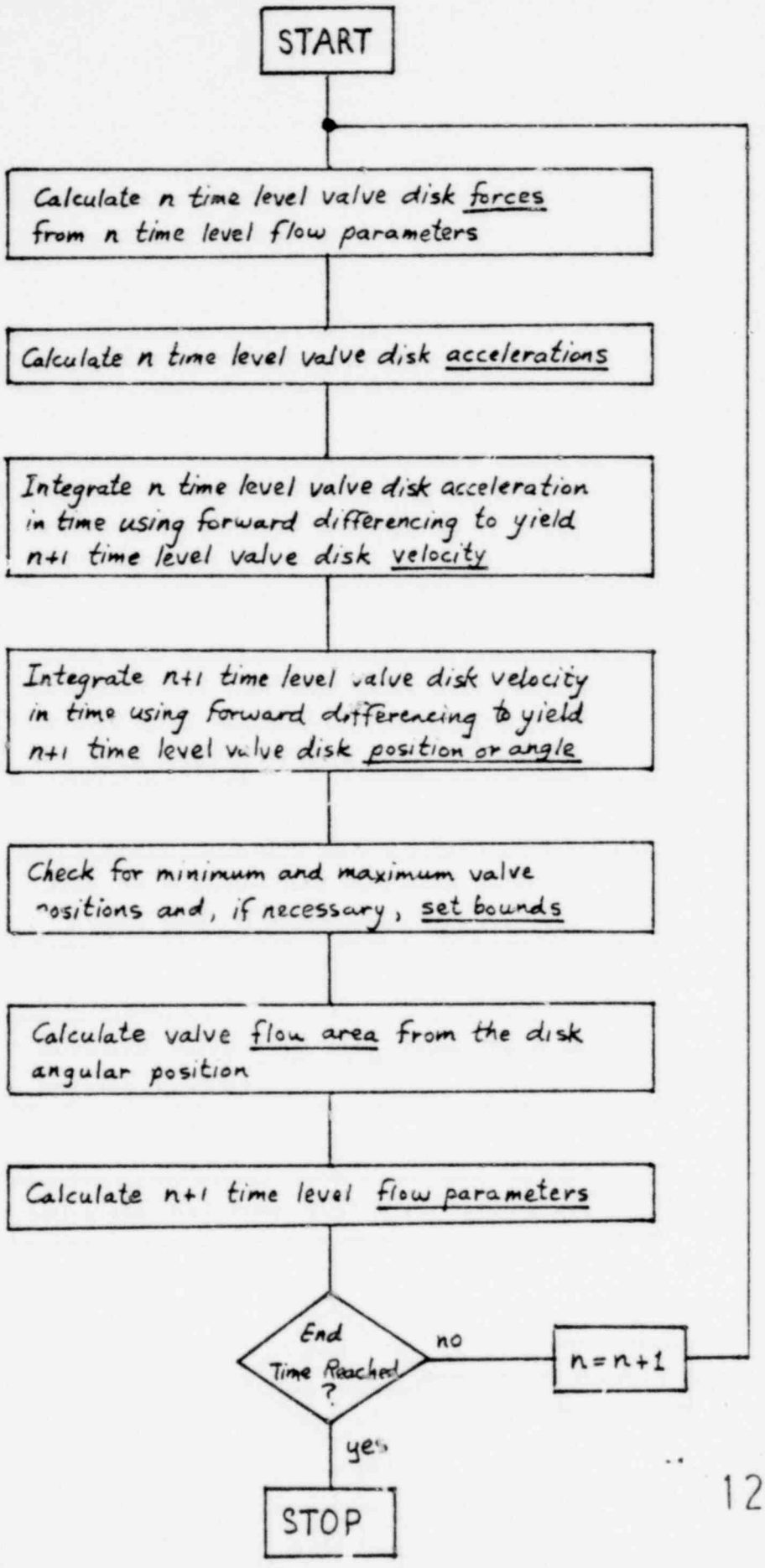

1216 237

Figure 4. Basic Calculational Cycle for the Check Valve Model

III. DEMONSTRATION PROBLEM

1. PROBLEM DEFINITION

The system selected to demonstrate the check valve analysis tool was a BWR reactor primary feedwater line. The piping system was postulated to rupture (instantaneous guillotine break) just outside of the containment. The system analyzed consisted of the piping between the break and the reactor feedring sparger with one control valve and one swing check valve. The analyzed system, containing about 60 meters of piping, is shown isometrically in Figure 5. The cross-hatched pipe runs will be explained later in connection with the presented output.

2. ANALYSIS MODEL

The RELAP5 hydrodynamic model of the analyzed system is shown in Figure 6. The numbered components are identified in Table I. Appendix B gives a complete listing of the RELAP5 model initial conditions and physical dimensions.

The initial system conditions were approximately: pressure, 6.89 MPa; temperature, 496 K; void fraction, 0.0; mass flowrate, 2.268×10^6 Kg/hr. The break boundary volume was set at: pressure, 0.10 MPa; temperature, 373 K; void fraction, 1.0. The two feedring sparger boundary conditions were set at: pressure, 6.89 MPa; temperature, 496 K; and void fraction, 0.0.

The swing check valve disk was assumed to have a moment arm of 0.254 m, a radius of 0.171 m, a weight of 223 N, and a moment of inertia of 1.63 $kg \cdot m^2$.

3. SAMPLE PROBLEM RESULTS

Pressure distributions along the cross-hatched portion of the piping system (see Figure 5) are shown in Figure 7 at several times; 6, 20, 40, 60, 80, 100, 200, 300, 400, 450, and 500 milliseconds. Wave propagations are clearly evident. The abrupt pressure step shown at the check valve at 80 milliseconds results from flow choking (72 milliseconds) and complete check valve closure (75 milliseconds). Comparing the pressure distributions at 400, 450, and 500 milliseconds reveals the cyclic phenomena of the waves reflecting back and

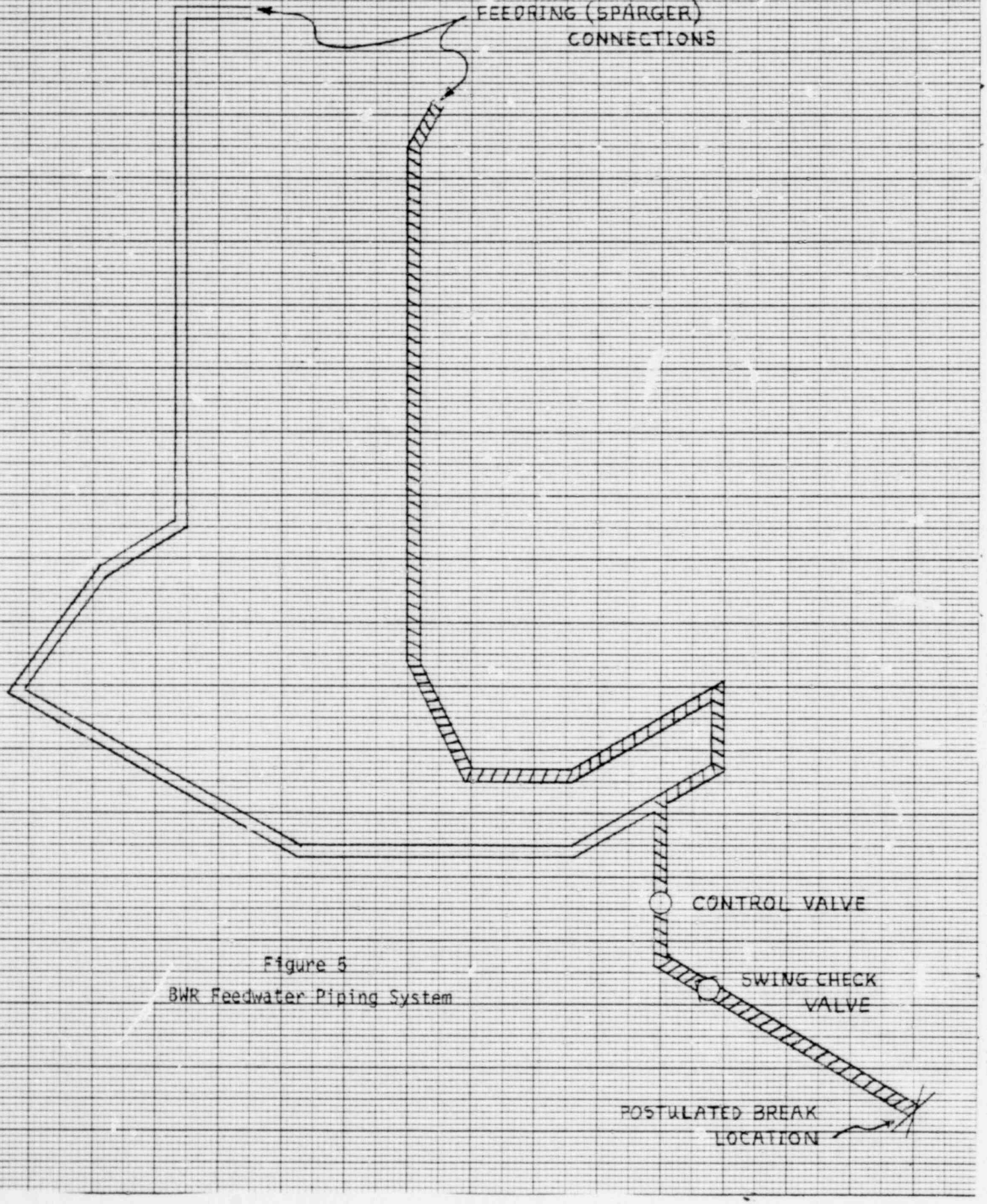

Figure 5
BWR Feedwater Piping System

TABLE I

RELAP5 HYDRODYNAMIC MODEL COMPONENTS

Item #[†]	RELAP5 Type Component	∿ Physical Description
2	Time Dependent Volume	Break Boundary Condition
3	Single Junction	0.112 m^2
4	Pipe	0.118 m^2, 4.42 m
5	Inertial Check Valve	Swing Check Valve
6	Pipe	0.118 m^2, 2.28 m
7	Single Junction	Control Valve, 0.105 m^2
8	Pipe	0.125 m^2, 1.52 m
9	Plenum, 4 ports	Tee, 0.131 m^2, 1.10 m
10	Pipe	0.0656 m^2, 4.57 m
11	Single Junction	0.0656 m^2
12	Pipe	0.0656 m^2, 5.18 m
13	Single Junction	0.0656 m^2
14	Pipe	0.0656 m^2, 6.10 m
15	Single Junction	0.0656 m^2
16	Pipe	0.0656 m^2, 4.57 m
17	Single Junction	0.0622 m^2
18	Time Dependent Volume	Feedring Sparger Boundary Condition
19	Pipe	0.0656 m^2, 7.16 m
20	Single Junction	0.0656 m^2
21	Pipe	0.0656 m^2, 6.71 m
22	Single Junction	0.0656 m^2
23	Pipe	0.0656 m^2, 4.88 m
24	Single Junction	0.0656 m^2
25	Pipe	0.0656 m^2, 6.10 m
26	Single Junction	0.0656 m^2
27	Pipe	0.0656 m^2, 4.58 m
28	Single Junction	0.0622 m^2
29	Time Dependent Volume	Feedring Sparger Boundary Condition

[†]Refer to Figure 6.

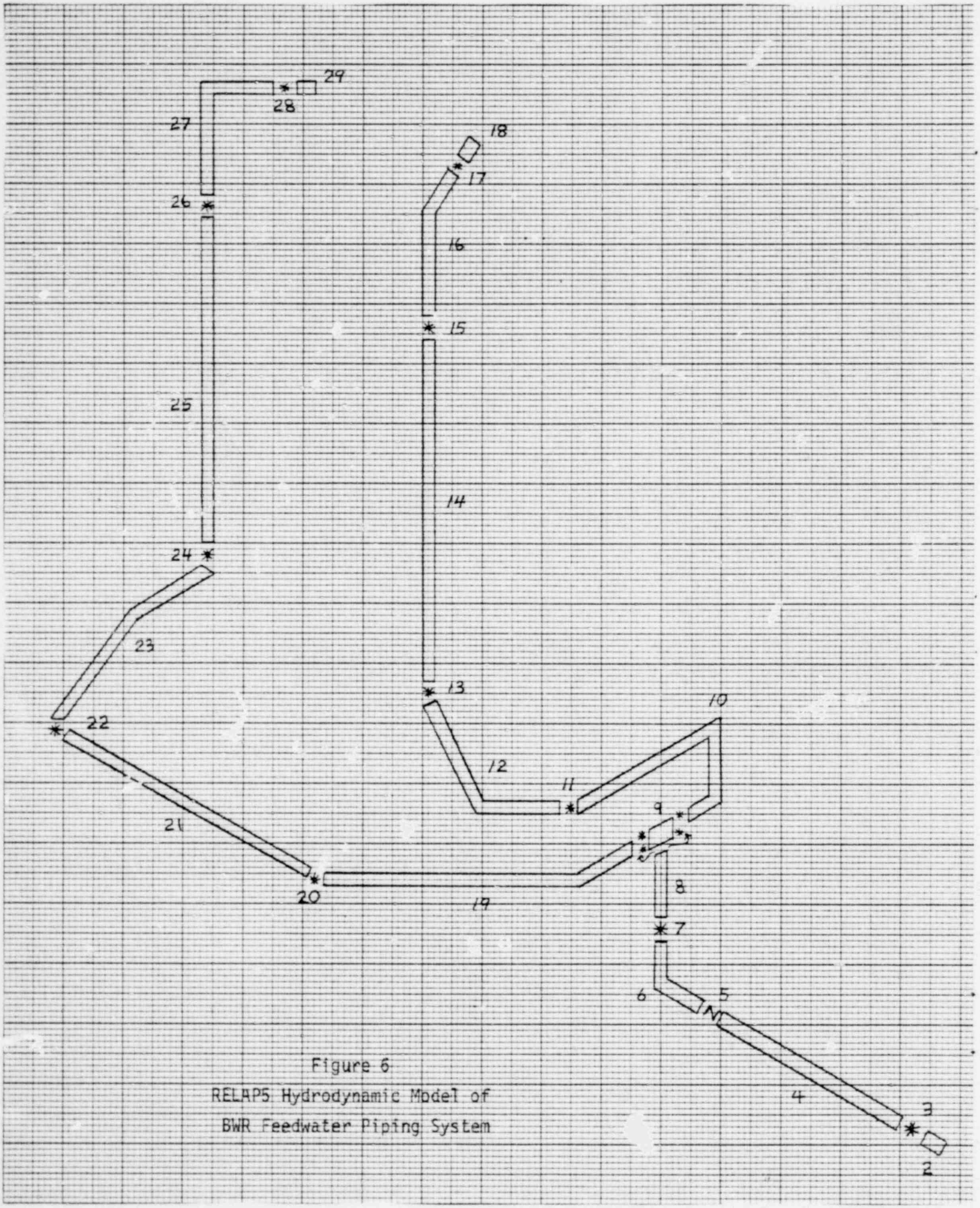

Figure 6
RELAP5 Hydrodynamic Model of
BWR Feedwater Piping System

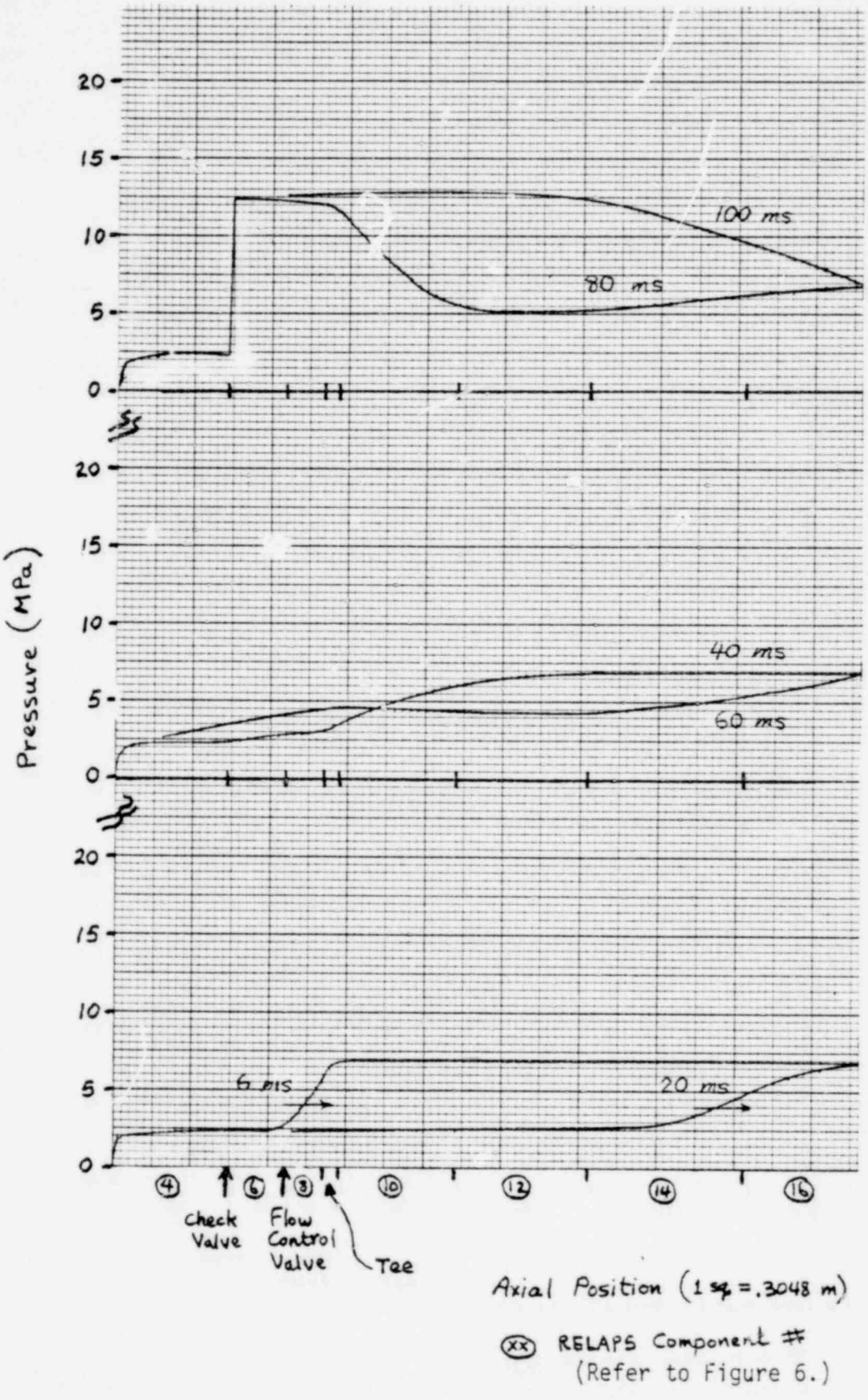

Figure 7

Pressure Distribution Along Cross-Hatched Portion of the Piping System (see Fig. 5) at Various Times

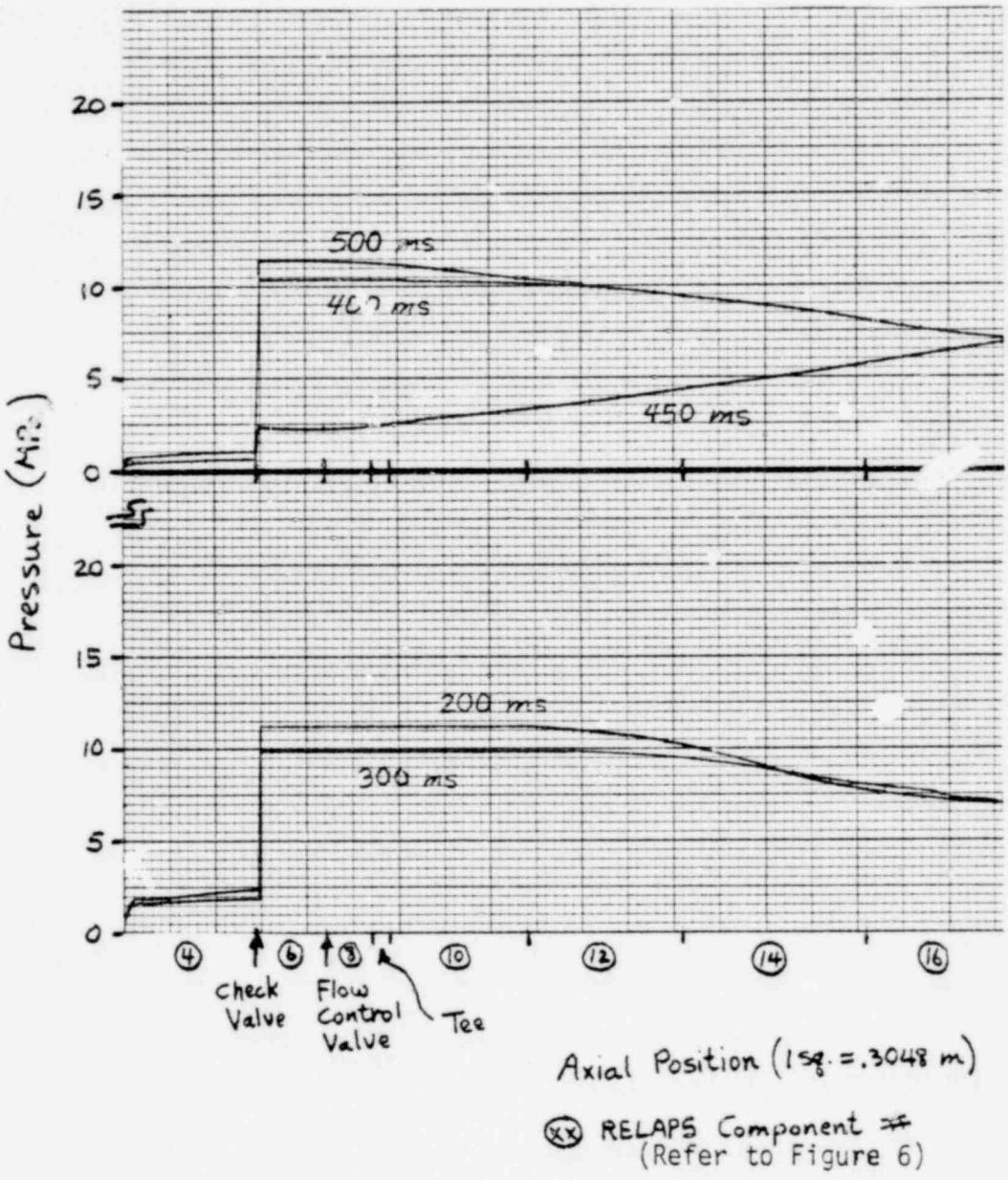

Figure 7 (continued)
Pressure Distribution Along Cross-Hatched Portion of the Piping System (see Fig. 5) at Various Times

1216 243

forth through the piping system. This phenomenon is even more clearly brought out by examining the time history of the pressure difference across the check valve as shown in Figure 8. Clearly the waves are attenuating with time as would be expected.

Figure 9 gives a time history of the valve disk position. The disk was initially open 70 degrees and closed in approximately 75 milliseconds. At 139 milliseconds the valve opened partially for approximately 46 milliseconds. The valve position history shows that the disk impacted the valve seat twice, at 75 and 185 milliseconds, with impact velocities of 5480 and 2050 degrees/second. The initial valve closure history is shown again in Figure 10 with an enlarged time scale. Four distinct regions on the curve can be identified. The initial flat region (0 - 4 milliseconds) shows a very slight valve motion due predominately to gravity acting on the disk. At approximately 4 milliseconds the initial depressurization wave passes the check valve causing a reduced flowrate and an increased pressure gradient tending to shut the valve faster (4 - 48 milliseconds). At 48 milliseconds the flow through the valve reverses, due to pressure wave reflections, causing the valve disk to further accelerate (48 - 72 milliseconds). At 72 milliseconds the flow area through the valve is reduced to the point that flow choking occurs, causing a severe pressure gradient across the disk which further increases the disk acceleration (72 - 75 milliseconds). The valve motions are entirely explainable and, as previously mentioned, appear to be relatively insensitive (based on sensitivity studies) to the variation in technique of applying the disk pressure difference (at least for this particular system). The importance of a good choking model is evident.

The hydrodynamic variable histories necessary to calculate forcing functions for dynamic-structural analysis were written on computer tape for future use.

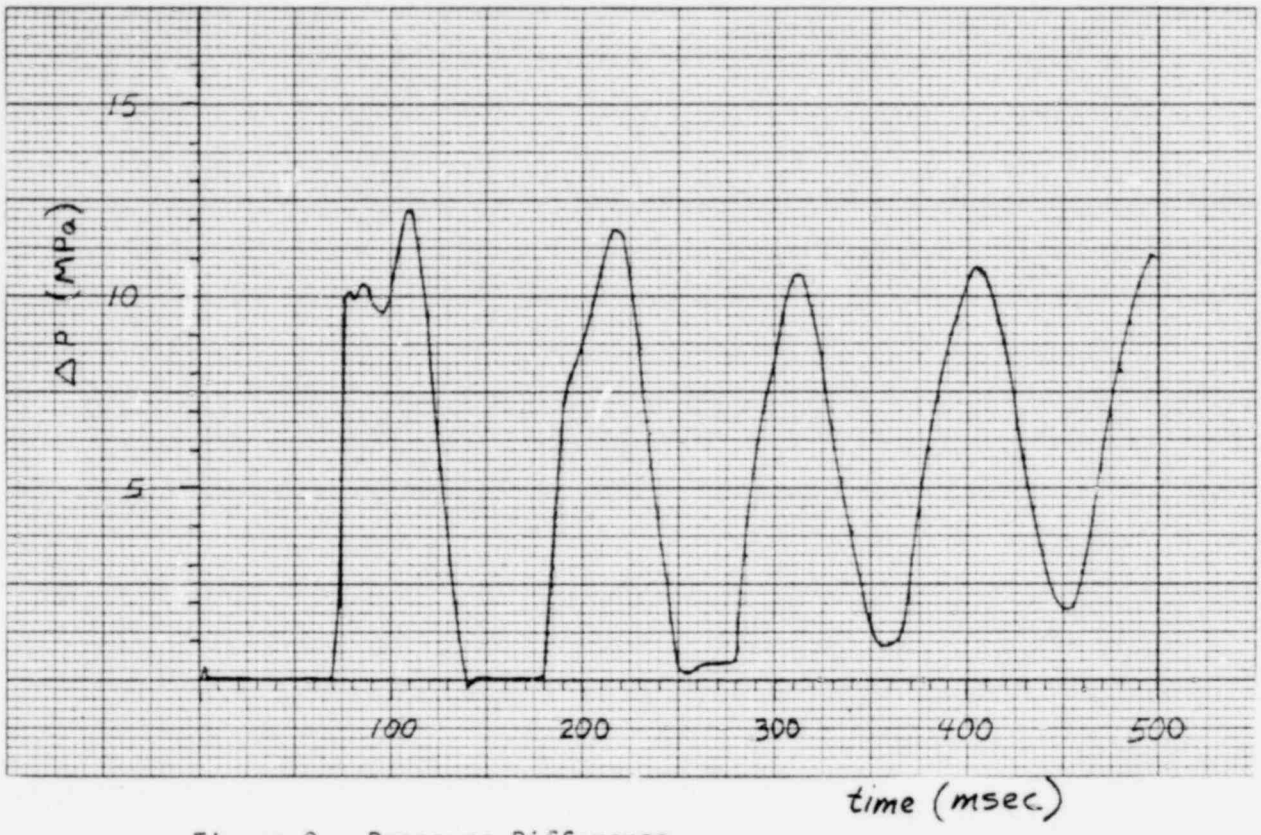

Figure 8. Pressure Difference History Across the Check Valve (P_L - P_K).

Figure 9. Valve Disk Motion History

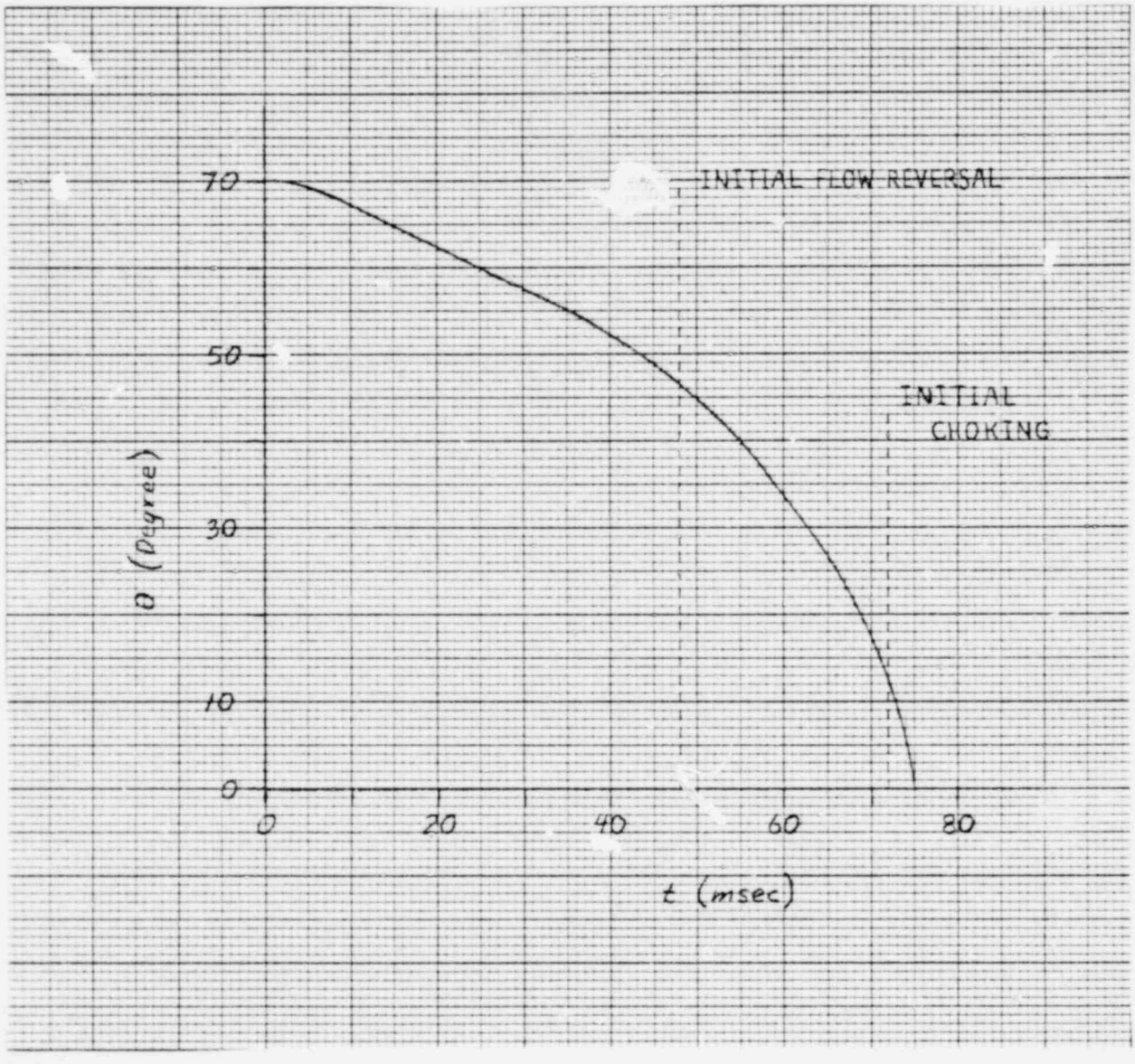

Figure
Initial Valve Disk Motion History

IV. CONCLUSIONS

The transient flow parameters calculated throughout the system may be used to calculate forces acting on components (piping in particular) or to generate forcing functions as input for structural dynamic models.

The analysis tool reported here consisted of the developed check valve model structured into the RELAP5 Reactor Loss of Coolant Analysis Program. Concurrent with the check valve model development, the RELAP5 code was also under heavy development and underwent significant evolutionary change.

There are indications that RELAP5 (and most computational fluid dynamics codes) dissipates and smears sharp waves, particularly those of short duration (due to attenuation of higher frequency Fourier components). It is recommended that further determination of the extent of this phenomenon in RELAP5 be made with simple problems having known analytic solutions.

It should also be pointed out that this analysis tool has not undergone experimental verification. The RELAP5 code, however, has successfully been verified for a limited range of experimental conditions and is currently undergoing an extensive verificational effort. The results presented in the sample demonstration problem appear qualitatively correct and quantitatively close to what would be expected. However, even though this analysis tool has utilized the latest state-of-the-art, the phenomena it represents are of a degree of complexity that clearly recommend future experimental verification. An analyst, in trying to use this tool for problems different than the sample demonstration problem, should give due consideration to the detailed check valve model as well as the hydrodynamic noding structure in the vicinity of the valve.

V. REFERENCES

1. J. A. Boure', "T'. Critical Flow Phenomenon with Reference to Two-Phase Flow and Nuclear Reactor Systems," ASME Winter Annual Meeting, November 1977.

2. T. Grillenberger, The Computer Code DAPSY for the Calculation of Pressure Wave Propagation in the Primary Coolant System of Light Water Reactors, Technische Universität München Report, MRR-I-66 (April 1976).

3. T. Grillenberger, DAPSY - Ein Rechenprogramm Für Die Druckwellenausbreitung Im Reaktorkühlkreislauf, Technische Universität München Report, MRR-P-24 (October 1976).

4. C. W. Hirt and T. A. Oliphant, SOLA-PLOOP: A Non-Equilibrium, Drift-Flux Code for Two-Phase Flow in Networks, LASL Report, LA-UR-76-1200 (August 1976).

5. R. A. Berry, A SOLA-PLOOP User's Guide, EG&G Report RE-A-77-139 (November 1977).

6. TRAC-P1: An Advanced Best Estimate Computer Program for PWR LOCA Analysis; 1. Methods, Models, User Information, and Programming Details, NUREG/CR-0063, LA-7279-MS Vol. 1 (June 1978).

7. V. H..Ransom and J. A. Trapp, RELAP5 Progress Summary: Pilot Code Hydrodynamic Model and Numerical Scheme, EG&G Report CD-AP-TR-005 (January 1978).

8. F. H. Harlow and A. A. Amsden, "A Numerical Fluid Dynamics Calculation Method for All Flow Speeds," Journal of Computational Physics, Vol. 8, No. 2, (October 1971) pp 197-213.

9. J. A. Trapp and V. H. Ransom, RELAP5 Hydrodynamic Model Progress Summary - Abrupt Area Changes and Parallel Branching, EG&G Report PG-R-77-42, (November 1977).

10. V. H. Ransom and J. A. Trapp, RELAP5 Progress Summary: Analytic Choking Criterion for Two-Phase Flow, CDAP-TR-013 (April 1978).

11. R. S. Samra, "Impact Energy Calculations for a Steam Check Valve Following a Postulated Pipe Rupture," ASME Winter Annual Meeting, 76-WA/FE-8, December 1976.

12. V. K. Chexal and J. S. Horowitz, Analysis Report: Maximum Energy of Disc Impact, Main Steam Check and Isolation Valves for Kewaunee Unit 1, Nuclear Services Corporation Report, PIO-02-03 (September 1973).

APPENDIX A

FORTRAN CHECK VALVE MODEL

```
                                IDENT    RX8001
*****    *IDENT RX8001
         *DELETE RPLENM.69
            11 NJ = INIT(1)
               IF( NJ.GE.0 .AND. NJ.LT.10 )   GO TO 13
         *DELETE RJWA.105
         *DELETE RELAP5.3
            * TAPE6=OUTPUT,DEBUG=OUTPUT,PLFILE,PLOTFL,TAPE12)
         *DELETE RELAP5.63
           50C CONTINUE
         *BEFORE PLTREC.43
               WRITE(12)  TIMEHY
               DO 40  I = IV, IVE, IVSKP
                  WRITE(12)  P(I)
            40 CONTINUE
               DO 50  I = IJ, IJE, IJSKP
                  WRITE(12)  VELFJ(I), VELGJ(I)
            5C CONTINUE
               DO 6C  I = IJ, IJE, IJSKP
                  WRITE(  )  RHOFJ(I), RHOGJ(I), VOIDGJ(I)
            6C CONTINUE
         *INSERT REC56.10
         C
               DIMENSION ARG(11), FCT(11)
         C
         *INSERT VALVE.21
         C
         C  DATA STATEMENT
               DATA ARG/ 0.0,0.1,0.2,0.3,0.4,0.5,0.6,0.7,0.8,0.9,1.0 /
               DATA FCT/ 0.617, 0.624, 0.632, 0.643, 0.659, 0.681, 0.712,
              *          0.755, 0.813, 0.892, 1.000 /
         C
         *DELETE        VALVE.102,VALVE.104
         C  *  *  *  *  *  *  *  *  *  *  *  *  *  *  *  *  *  *  *  *  *
         C     INERTIAL SWING CHECK VALVE CODED 08/17/78 BY R. A. BEKRY
         C  *  *  *  *  *  *  *  *  *  *  *  *  *  *  *  *  *  *  *  *  *
           400 K   =   .NOT.MASK(43).AND.SHIFT(IJ1(J),18)
               L   =   .NOT.MASK(43).AND.SHIFT(IJ2(J),18)
               RHOC   =  VOIDFJ(J) * RHOFJ(J) + VOIDGJ(J) * RHOGJ(J)
               GC   =  VOIDFJ(J) * RHOFJ(J) * VELFJO(J)
              *                +   VOIDGJ(J) * RHOGJ(J) * VELGJO(J)
               GHEAD   =  RHOC * ( DZ(K) - DZ(L) )
               WEIGHT   =  -222.86 * LNGVLV(I) * SIN( THETAO(I) * 0.017453 )
               IF( THETAO(I).LE.MINTHT(I).OR.IJ2(J).LT.0 )   GO TO 500
               IF( THETAO(I).LE.0.0.OR.IJ2(J).LT.0 )   GO TO 500
               IF( GC.LT.0.C )   GO TO 430
               P1   =  PJ(K)
               A1   =  AVOL(K)
               ETAT   =  ATHROT(J) * AJUN(J) / AVOL(K)
               GO TO 460
           430 P1   =  PO(L)
               A1   =  AVOL(L)
               ETAT   =  ATHROT(J) * AJUN(J) / AVOL(L)
           460 CONTINUE
               FLORATE=GC*A1
               DO 470  IVI = 2, 11
```

1215 250

A1

```
                    IDENT    RX8001

      SSS  =  ETAT - ARG(IVI)
      IF( SSS.LE.0.0 )   GO TO 480
470   CONTINUE
480   ETAC  =  FCT(IVI-1) + ( FCT(IVI) - FCT(IVI-1) )
     *          * ( ETAT - ARG(IVI-1) ) / ( ARG(IVI) - ARG(IVI-1) )
      ATC  =  ETAC * ATHROT(J) * AJUN(J)
      IF(ATC.LT.1.0E-5) GO TO 490
      PVENC  =          0.5 * RHOC * (( FLORATE/(RHOC*A1))**2. - ( FLORATE/
     *          (RHOC*ATC))**2.)
      GO TO 495
490   PVENC  =          0.0
495   IF(GC.GT.0.0) PVENC = -PVENC
      DELP=(PO(K)-PO(L)+PVENC+PCV(I) + GHEAD ) * (3.1416 * RDSVLV(I)
     *          **2.) * LNGVLV(I)
      GO TO 520
500   DELP = ( PO(K) - PO(L) + PCV(I) + GHEAD ) * (3.1416 * RDSVLV(I)
     *        **2.) * LNGVLV(I)
520   CONTINUE
      ANGACC  =  ( WEIGHT + DELP ) / MOMENT(I)
      OMEGA(I)  =  OMEGAO(I) + ANGACC * DT
      THETA(I)  =  THETAO(I) + OMEGA(I) * DT * 57.2958
      IF ( THETA(I) .LT. MAXTHT(I) )   GO TO 560
      THETA(I)  =  MAXTHT(I)
      OMEGA(I)  =  0.0
560   IF ( THETA(I) .GT. MINTHT(I) )   GO TO 590
      THETA(I)  =  MINTHT(I)
      OMEGA(I)  =  0.0
590   IF ( THETA(I) .LT. 26.565 )   GO TO 591
      ATHROT(J)  =  3.1416 * RDSVLV(I)**2 / AJUN(J)
      GO TO 592
591   ATHROT(J)  =  3.1416 * RDSVLV(I)**2 * 2. * TAN(THETA(I)*.017453)
     *        / AJUN(J)
592   CONTINUE
      IF ( ATHROT(J) .LT. ALEAK(I) )   ATHROT(J) = ALEAK(I)
      DELTAP = PO(K)-PO(L)
      WRITE(6,600) TIMEHY, OMEGA(I), THETA(I), ATHROT(J)
600   FORMAT (1HO,* TIMEHY = *,E10.4,2X,* OMEGA = *,F10.4,2X,
     *        * THETA = *,F10.4,2X,* ATHROT = *,F10.4)
      WRITE (6,900) PVENC,DELTAP
900   FORMAT (1HO,*PVENC = *,E10.4,2X,*DELTAP =*,E10.4)
      IF ( ATHROT(J) .EQ. 0.0 )   GO TO 620
      IJ1(J)  =  .NOT. MASK(1) .AND. IJ1(J)
      GO TO 1000
620   IJ1(J)  =  MASK(1) .OR. IJ1(J)
      VELFJ(J)  =  0.0
      VELGJ(J)  =  0.0
```

APPENDIX B

DEMONSTRATION PROBLEM, RELAP5 MODEL

```
LISTING OF INPUT DATA FOR CASE  1

    1   *BWR FEEDWATER LINE RUPTURE
    2   0000100 NEW TRANSNT
    3   0000102 BRITISH
    4   0000104 NONE
    5   *
    6   * TIME STEP CONTROL CARD(S)
    7   0000201 0.10,1.0-7,.001,1,1,2,200
    8   0000202 0.50,1.0-7,0.001,1,1,5,300
    9   0000400 1,RXB
   10   0000401 TEMPF,2010000,0.0,2,"SUBTITLE"
   11   *
   12   * BREAK BOUNDARY CONDITION
   13   0020000 "BREAK" TMDPVOL
   14   0020101 1.269,0.5,0,0,0,0,1.5-4,0,0
   15   0020200 2
   16   0020201 0.0,14.5,1.0  0.1,14.5,1.0
   17   0030000 "BREAK" SNGLJUN
   18   0030101 2000000 4000000 1.206 0 0 000
   19   0030201 0,19.2501,19.2501,0.0
   20   *
   21   * BEGIN PIPING MODEL
   22   0040000 "18 SCH120" PIPE
   23   0040001 29
   24   0040101 1.269,29
   25   0040301 0.5,29
   26   0040601 0,29
   27   0040801 1.5-4,0,29
   28   0041001 00,29
   29   0041101 00,28
   30   0041201 0,1000.,408.44,0.0,29
   31   0041301 20.8552,20.8552,0.0,28
   32   *
   33   * CHECK VALVE MODEL
   34   0050000 "INERIAL" VALVE
   35   0050101 4010000 6000000 0.994 0 0 100
   36   0050201 1,1389.,0.0,0.0
   37   0050301 INRVLV 0 0 0.0 0.0 70.0 0.0 70.0 1.2 0.0 0.833 0.5625
   38   *
   39   0060000 "18 SCH120" PIPE
   40   0060001 15
   41   0060101 1.269,15
   42   0060301 0.5,15
   43   0060601 0.0,8.90,0.0,15
   44   0060801 1.5-4,0,15
   45   0061001 00,15
   46   0061101 00,14
   47   0061201 0,1000.,408.44,0.0,15
   48   0061300 1
   49   0061301 1389.,0.0,0.0,14
   50   *
   51   * FLOW CONTROL VALVE (GATE)
   52   0070000 "CNT VLV" SNGLJUN
   53   0070101 6010000 8000000 1.127 0 0 000
   54   0070201 1,1389.,0.0,0.0
   55   *
   56   0080000 "18 SCH100" PIPE
   57   0080001 10
   58   0080101 1.342,10
   59   0080301 0.5,10
```

```
0060601 90,0,10
0080801 1.5-4,0,10
0081001 00,10
0081101 00,9
0081201 0,1000,,408.44,0.0,10
0081300 1
0081301 1389.,0.0,0.0,9
*
* BRANCHING TEE MODEL
0090000 "TEE" PLENUM
0090001 4 1
0090101 1.415,3.61,0,0,0,0,1.5-4,0,0
0090200 0,1000,,408.44,0.0
0091101 8010000 9000000 0.671 0 0 000
0091201 694.5,0.0,0.0
0092101 8010000 9000000 0.671 0 0 000
0092201 694.5,0.0,0.0
0093101 9010000 10000000 0.706 0 0 000
0093201 694.5,0.0,0.0
0094101 9010000 19000000 0.706 0 0 000
0094201 694.5,0.0,0.0
*
* FIRST FEED BRANCH
0100000 "12 SCH80" PIPE
0100001 30
0100101 0.706,30
0100301 0.5,30
0100601 0.0,3,90.0,10,0.0,30
0100801 1.5-4,0,30
0101001 00,30
0101101 00,29
0101201 0,1000,,408.44,0.0,30
0101300 1
0101301 694.5,0.0,0.0,29
*
0110000 "JUNCTION" SNGLJUN
0110101 10010000 12000000 0 0 0 000
0110201 1,694.5,0.0,0.0
*
0120000 "12 SCH80" PIPE
0120001 17
0120101 0.706,17
0120301 1.0,17
0120601 0.0,17
0120801 1.5-4,0,17
0121001 00,17
0121101 00,16
0121201 0,1000,,408.44,0.0,17
0121300 1
0121301 694.5,0.0,0.0,16
*
0130000 "JUNCTION" SNGLJUN
0130101 12010000 14000000 0 0 0 000
0130201 1,694.5,0.0,0.0
*
0140000 "12 SCH80" PIPE
0140001 20
0140101 0.706,20
0140301 1.0,20
0140601 90.0,20
0140801 1.5-4,0,20
```

```
0141001 00,20
0141101 00,19
0141201 0,1000.,408.44,0.0,20
0141300 1
0141301 694.5,0.0,0.0,19
*
0150000 "JUNCTION" SNGLJUN
0150101 14010000 16000000 0 0 0 000
0150201 1,694.5,0.0,0.0
*
0160000 "12 SCH80" PIPE
0160001 15
0160101 0.706,15
0160301 1.0,15
0160601 90.0,11.0,0.0,15
0160801 1.5-4,0,15
0161001 00,15
0161101 00,14
0161201 0,1000.,408.44,0.0,15
0161301 18.7431,18.7431,0.0,14
*
* FEEDRING BOUNDARY CONDITION
0170000 "BDY JUN" SNGLJUN
0170101 16010000 18000000 0.670 0 0 000
0170201 0,19.7501,19.7501,0.0
0180000 "BDY VOL" TMDPVOL
0180101 20.0,1.0,0,0,0,0,1.5-4,0,0
0180200 0
0180201 0.0,1000.,408.44,0.0,0.10,1000.,408.44,0.0
*
* SECOND FEED BRANCH
0190000 "12 SCH80" PIPE
0190001 47
0190101 0.706,47
0190301 0.5,47
0190601 0.0,47
0190801 1.5-4,0,47
0191001 00,47
0191101  0,46
0191201 0.1000.,408.44,0.0,47
0191300 1
0191301 694.5,0.0, 0.0,46
*
0200000 "JUNCTION" SNGLJUN
0200101 19010000 21000000 0 0 0 000
0200201 1,694.5,0.0,0.0
*
0210000 "12 SCH80" PIPE
0210001 22
0210101 0.706,22
0210301 1.0,22
0210601 0.0,22
0210801 1.5-4,0,22
0211001 00,22
0211101 00,21
0211201 0,1000.,408.44,0.0,22
0211300 1
0211301 694.5,0.0,0.0,21
*
0220000 "JUNCTION" SNGLJUN
0220101 21010000 23000000 0 0 0 000
```

```
0220201 1,694.5,0.0,0.0
*
0230000 "12 SCH80" PIPE
0230001 16
0230101 0.706,16
0230301 1.0,16
0230601 26.0,10,0.0,16
0230801 1.5-4,0,16
0231001 00,1
0231101 00,1
0231201 0,1000.,408.44,0.0,16
0231300 1
0231301 694.5,0.0,0.0,15
*
0240000 "JUNCTION" SNGLJUN
0240101 23010000 25000000 0 0 0 000
0240201 1,694.5,0.0,0.0
*
0250000 "12 SCH80" PIPE
0250001 20
0250101 0.706,20
0250301 1.0,20
0250601 90.0,20
0250801 1.5-4,0,20
0251001 00,20
0251101 00,19
0251201 0,1000.,408.44,0.0,20
0251300 1
0251301 694.5,0.0,0.0,19
*
0260000 "JUNCTION" SNGLJUN
0260101 25010000 27000000 0 0 0 000
0260201 1,694.5,0.0,0.0
*
0270000 "12 SCH80" PIPE
0270001 15
0270101 0.706,15
0270301 1.0,15
0270601 90.0,11,0.0,15
0270801 1.5-4,0,15
0271001 00,15
0271101 00,14
0271201 0,1000.,408.44,0.0,15
0271301 18.7431,18.7431,0.0,14
*
*FEEDRING BOUNDARY CONDITION
0280000 "BDY JUN" SNGLJUN
0280101 27010000 29000000 0.670 0 0 000
0280201 0,19.7501,19.7501,0.0
0290000 "BDY VOL" TMDPVOL
0290101 20.0,1.0,0,0,0,0,1.5-4,0,0
0290200 0
0290201 0,0,1000.,408.44,0.0,0.1,1000.,408.44,0.0
* END OF CASE
```

1215 256

84

INP-CHK, RUN OPTION IS RUN.

INPUT UNITS ARE ASSUMED BRITISH OUTPUT UNITS ARE SI

NO RESTART-PLOT FILE IS TO BE WRITTEN.

TIME STEP CONTROL DATA

END TIME (SEC)	MIN. TIME STEP (SEC)	MAX. TIME STEP (SEC)	OPTION	MINOR EDIT FREQUENCY	MAJOR EDIT FREQUENCY	RESTART FREQUENCY
1.000000E-01	1.000000E-07	1.000000E-03	1	1	2	200
5.000000E-01	1.000000E-07	1.000000E-03	1	1	5	300

EDIT OF COMPONENT INPUT DATA
(QUANTITIES PRINTED ARE INPUT VALUES, SET BY DEFAULT, OR SET BY ERROR RECOVERY)

INPUT DATA FOR COMPONENT 2, BREAK TMDPVOL , HAVING 1 VOLUMES AND 0 JUNCTIONS

VOL NO.	FLOW AREA (M2)	FLOW LENGTH (M)	VOLUME (M3)	HORIZ. ANGLE (DEG)	VERT. ANGLE (DEG)	ELEV. CHNG. (M)
2010000	1.178940E-01	1.524000E-01	1.796704E-02	0.	0.	0.

VOL.NO.	ROUGHNESS (M)	HYDRAULIC DIAM. (M)	EQUIL. FLAG
2010000	4.572000E-05	3.874368E-01	0

TIME DEPENDENT DATA

TIME (SEC)	PRESSURE (PA)	QUALITY
0.	9.997398E+04	1.000000E+00
1.000000E-01	9.997398E+04	1.000000E+00

INPUT DATA FOR COMPONENT 3, BREAK SNGLJUN , HAVING 0 VOLUMES AND 1 JUNCTIONS

JUN.NO.	FROM VOL.	TO VOL.	JUNCTION AREA (M2)	FORWARD LOSS COEFFICIENT	REVERSE LOSS COEFFICIENT	JUNCTION FLAGS
3000000	2000000	4000000	1.120411E-01	0.	0.	0

JUN.NO.	INIT. LIQ. VEL. (M/SEC)	INIT. VAP. VEL. (M/SEC)	INTERFACE VEL. (M/SEC)
3000000	5.867430E+00	5.867430E+00	0.

INPUT DATA FOR COMPONENT 4, 18 SCH120 PIPE , HAVING 29 VOLUMES AND 28 JUNCTIONS

VOL NO.	FLOW AREA (M2)	FLOW LENGTH (M)	VOLUME (M3)	HORIZ. ANGLE (DEG)	VERT. ANGLE (DEG)	ELEV. CHNG. (M)
4010000	1.178940E-01	1.524000E-01	1.796704E-02	0.	0.	0.
4020000	1.178940E-01	1.524000E-01	1.796704E-02	0.	0.	0.
4030000	1.178940E-01	1.524000E-01	1.796704E-02	0.	0.	0.
4040000	1.178940E-01	1.524000E-01	1.796704E-02	0.	0.	0.
4050000	1.178940E-01	1.524000E-01	1.796704E-02	0.	0.	0.
4060000	1.178940E-01	1.524000E-01	1.796704E-02	0.	0.	0.
4070000	1.178940E-01	1.524000E-01	1.796704E-02	0.	0.	0.
4080000	1.178940E-01	1.524000E-01	1.796704E-02	0.	0.	0.
4090000	1.178940E-01	1.524000E-01	1.796704E-02	0.	0.	0.
4100000	1.178940E-01	1.524000E-01	1.796704E-02	0.	0.	0.
4110000	1.178940E-01	1.524000E-01	1.796704E-02	0.	0.	0.
4120000	1.178940E-01	1.524000E-01	1.796704E-02	0.	0.	0.
4130000	1.178940E-01	1.524000E-01	1.796704E-02	0.	0.	0.
4140000	1.178940E-01	1.524000E-01	1.796704E-02	0.	0.	0.

4150000	1.178940E-01	1.524000E-01	1.796704E-02	0.	0.	0.	
4160000	1.178940E-01	1.524000E-01	1.796704E-02	0.	0.	0.	
4170000	1.178940E-01	1.524000E-01	1.796704E-02	0.	0.	0.	
4180000	1.178940E-01	1.524000E-01	1.796704E-02	0.	0.	0.	
4190000	1.178940E-01	1.524000E-01	1.796704E-02	0.	0.	0.	
4200000	1.178940E-01	1.524000E-01	1.796704E-02	0.	0.	0.	
4210000	1.178940E-01	1.524000E-01	1.796704E-02	0.	0.	0.	
4220000	1.178940E-01	1.524000E-01	1.796704E-02	0.	0.	0.	
4230000	1.178940E-01	1.524000E-01	1.796704E-02	0.	0.	0.	
4240000	1.178940E-01	1.524000E-01	1.796704E-02	0.	0.	0.	
4250000	1.178940E-01	1.524000E-01	1.796704E-02	0.	0.	0.	
4260000	1.178940E-01	1.524000E-01	1.796704E-02	0.	0.	0.	
4270000	1.178940E-01	1.524000E-01	1.796704E-02	0.	0.	0.	
4280000	1.178940E-01	1.524000E-01	1.796704E-02	0.	0.	0.	
4290000	1.178940E-01	1.524000E-01	1.796704E-02	0.	0.	0.	

VOL NO.	ROUGHNESS (M)	HYDRAULIC DIAM. (M)	VOLUME FLAGS	INIT. COND. FLAG	I.C. VALUE 1	I.C. VALUE 2	I.C. VALUE 3
4010000	4.572000E-05	3.874368E-01	0	0	1.000000E+03	4.084400E+02	0.
4020000	4.572000E-05	3.874368E-01	0	0	1.000000E+03	4.084400E+02	0.
4030000	4.572000E-05	3.874368E-01	0	0	1.000000E+03	4.084400E+02	0.
4040000	4.572000E-05	3.874368E-01	0	0	1.000000E+03	4.084400E+02	0.
4050000	4.572000E-05	3.874368E-01	0	0	1.000000E+03	4.084400E+02	0.
4060000	4.572000E-05	3.874368E-01	0	0	1.000000E+03	4.084400E+02	0.
4070000	4.572000E-05	3.874368E-01	0	0	1.000000E+03	4.084400E+02	0.
4080000	4.572000E-05	3.874368E-01	0	0	1.000000E+03	4.084400E+02	0.
4090000	4.572000E-05	3.874368E-01	0	0	1.000000E+03	4.084400E+02	0.
4100000	4.572000E-05	3.874368E-01	0	0	1.000000E+03	4.084400E+02	0.
4110000	4.572000E-05	3.874368E-01	0	0	1.000000E+03	4.084400E+02	0.
4120000	4.572000E-05	3.874368E-01	0	0	1.000000E+03	4.084400E+02	0.
4130000	4.572000E-05	3.874368E-01	0	0	1.000000E+03	4.084400E+02	0.
4140000	4.572000E-05	3.874368E-01	0	0	1.000000E+03	4.084400E+02	0.
4150000	4.572000E-05	3.874368E-01	0	0	1.000000E+03	4.084400E+02	0.
4160000	4.572000E-05	3.874368E-01	0	0	1.000000E+03	4.084400E+02	0.
4170000	4.572000E-05	3.874368E-01	0	0	1.000000E+03	4.084400E+02	0.
4180000	4.572000E-05	3.874368E-01	0	0	1.000000E+03	4.084400E+02	0.
4190000	4.572000E-05	3.874368E-01	0	0	1.000000E+03	4.084400E+02	0.
4200000	4.572000E-05	3.874368E-01	0	0	1.000000E+03	4.084400E+02	0.
4210000	4.572000E-05	3.874368E-01	0	0	1.000000E+03	4.084400E+02	0.
4220000	4.572000E-05	3.874368E-01	0	0	1.000000E+03	4.084400E+02	0.
4230000	4.572000E-05	3.874368E-01	0	0	1.000000E+03	4.084400E+02	0.
4240000	4.572000E-05	3.874368E-01	0	0	1.000000E+03	4.084400E+02	0.
4250000	4.572000E-05	3.874368E-01	0	0	1.000000E+03	4.084400E+02	0.
4260000	4.572000E-05	3.874368E-01	0	0	1.000000E+03	4.084400E+02	0.
4270000	4.572000E-05	3.874368E-01	0	0	1.000000E+03	4.084400E+02	0.
4280000	4.572000E-05	3.874368E-01	0	0	1.000000E+03	4.084400E+02	0.
4290000	4.572000E-05	3.874368E-01	0	0	1.000000E+03	4.084400E+02	0.

JUN.NO.	JUNCTION AREA (M2)	FORWARD LOSS COEFFICIENT	REVERSE LOSS COEFFICIENT	JUNCTION FLAGS	INIT. LIQ. VEL. (M/SEC)	INIT. VAP. VEL. (M/SEC)	INTERFACE VEL. (M/SEC)
4010000	1.178940E-01	0.	0.	0	6.356665E+00	6.356665E+00	0.
4020000	1.178940E-01	0.	0.	0	6.356665E+00	6.356665E+00	0.
4030000	1.178940E-01	0.	0.	0	6.356665E+00	6.356665E+00	0.
4040000	1.178940E-01	0.	0.	0	6.356665E+00	6.356665E+00	0.
4050000	1.178940E-01	0.	0.	0	6.356665E+00	6.356665E+00	0.
4060000	1.178940E-01	0.	0.	0	6.356665E+00	6.356665E+00	0.
4070000	1.178940E-01	0.	0.	0	6.356665E+00	6.356665E+00	0.
4080000	1.178940E-01	0.	0.	0	6.356665E+00	6.356665E+00	0.
4090000	1.178940E-01	0.	0.	0	6.356665E+00	6.356665E+00	0.
4100000	1.178940E-01	0.	0.	0	6.356665E+00	6.356665E+00	0.
4110000	1.178940E-01	0.	0.	0	6.356665E+00	6.356665E+00	0.

4120000	1.178940E-01	0.	0.	0	6.356665E+00	6.356665E+00	0.
4130000	1.178940E-01	0.	0.	0	6.356665E+00	6.356665E+00	0.
4140000	1.178940E-01	0.	0.	0	6.356665E+00	6.356665E+00	0.
4150000	1.178940E-01	0.	0.	0	6.356665E+00	6.356665E+00	0.
4160000	1.178940E-01	0.	0.	0	6.356665E+00	6.356665E+00	0.
4170000	1.178940E-01	0.	0.	0	6.356665E+00	6.356665E+00	0.
4180000	1.178940E-01	0.	0.	0	6.356665E+00	6.356665E+00	0.
4190000	1.178940E-01	0.	0.	0	6.356665E+00	6.356665E+00	0.
4200000	1.178940E-01	0.	0.	0	6.356665E+00	6.356665E+00	0.
4210000	1.178940E-01	0.	0.	0	6.356665E+00	6.356665E+00	0.
4220000	1.178940E-01	0.	0.	0	6.356665E+00	6.356665E+00	0.
4230000	1.178940E-01	0.	0.	0	6.356665E+00	6.356665E+00	0.
4240000	1.178940E-01	0.	0.	0	6.356665E+00	6.356665E+00	0.
4250000	1.178940E-01	0.	0.	0	6.356665E+00	6.356665E+00	0.
4260000	1.178940E-01	0.	0.	0	6.356665E+00	6.356665E+00	0.
4270000	1.178940E-01	0.	0.	0	6.356665E+00	6.356665E+00	0.
4280000	1.178940E-01	0.	0.	0	6.356665E+00	6.356665E+00	0.

INPUT DATA FOR COMPONENT 5, INERIAL VALVE , HAVING 0 VOLUMES AND 1 JUNCTIONS

JUN.NO.	FROM VOL.	TO VOL.	JUNCTION AREA (M2)	FORWARD LOSS COEFFICIENT	REVERSE LOSS COEFFICIENT	JUNCTION FLAGS
5000000	4010000	6000000	9.234562E-02	0.	0.	100

JUN.NO.	INIT. LIQ. FLOW (KG/SEC)	INIT. VAP. FLOW (KG/SEC)	INTERFACE VEL. (M/SEC)
5000000	6.300398E+02	0.	0.

JUN.NO.	BACK PRESSURE (LBF/IN2)	LEAKAGE (% AREA OPEN)	INERTIAL VALVE FLAGS
5000000	0.	0.	0

JUN.NO.	VALVE ANGLE THETA (DEG)	MINIMUM (DEG)	MAXIMUM (DEG)
5000000	7.000000E+01	0.	7.000000E+01

JUN.NO.	INERTIA (FT-LB-S2)	ANG. VEL. (RAD/SEC)	MOMENT LENGTH (FT)	FLAPPER RADIUS (FT)
5000000	1.200000E+00	0.	8.330000E-01	5.625000E-01

INPUT DATA FOR COMPONENT 6, 18 SCH120 PIPE , HAVING 15 VOLUMES AND 14 JUNCTIONS

VOL NO.	FLOW AREA (M2)	FLOW LENGTH (M)	VOLUME (M3)	HORIZ. ANGLE (DEG)	VERT. ANGLE (DEG)	ELEV. CHNG. (M)
6010000	1.178940E-01	1.524000E-01	1.796704E-02	0.	0.	0.
6020000	1.178940E-01	1.524000E-01	1.796704E-02	0.	0.	0.
6030000	1.178940E-01	1.524000E-01	1.796704E-02	0.	0.	0.
6040000	1.178940E-01	1.524000E-01	1.796704E-02	0.	0.	0.
6050000	1.178940E-01	1.524000E-01	1.796704E-02	0.	0.	0.
6060000	1.178940E-01	1.524000E-01	1.796704E-02	0.	0.	0.
6070000	1.178940E-01	1.524000E-01	1.796704E-02	0.	0.	0.
6080000	1.178940E-01	1.524000E-01	1.796704E-02	0.	0.	0.
6090000	1.178940E-01	1.524000E-01	1.796704E-02	0.	9.000000E+01	1.524000E-01
6100000	1.178940E-01	1.524000E-01	1.796704E-02	0.	9.000000E+01	1.524000E-01
6110000	1.178940E-01	1.524000E-01	1.796704E-02	0.	9.000000E+01	1.524000E-01
6120000	1.178940E-01	1.524000E-01	1.796704E-02	0.	9.000000E+01	1.524000E-01
6130000	1.178940E-01	1.524000E-01	1.796704E-02	0.	9.000000E+01	1.524000E-01
6140000	1.178940E-01	1.524000E-01	1.796704E-02	0.	9.000000E+01	1.524000E-01
6150000	1.178940E-01	1.524000E-01	1.796704E-02	0.	9.000000E+01	1.524000E-01

VOL NO.	ROUGHNESS	HYDRAULIC DIAM.	VOLUME	INIT. COND.	I.C. VALUE 1	I.C. VALUE 2	I.C. VALUE 3

	(M)	(M)	FLAGS	FLAG			
6010000	4.572000E-05	3.874368E-01	0	0	1.000000E+03	4.084400E+02	0.
6020000	4.572000E-05	3.874368E-01	0	0	1.000000E+03	4.084400E+02	0.
6030000	4.572000E-05	3.874368E-01	0	0	1.000000E+03	4.084400E+02	0.
6040000	4.572000E-05	3.874368E-01	0	0	1.000000E+03	4.084400E+02	0.
6050000	4.572000E-05	3.874368E-01	0	0	1.000000E+03	4.084400E+02	0.
6060000	4.572000E-05	3.874368E-01	0	0	1.000000E+03	4.084400E+02	0.
6070000	4.572000E-05	3.874368E-01	0	0	1.000000E+03	4.084400E+02	0.
6080000	4.572000E-05	3.874368E-01	0	0	1.000000E+03	4.084400E+02	0.
6090000	4.572000E-05	3.874368E-01	0	0	1.000000E+03	4.084400E+02	0.
6100000	4.572000E-05	3.874368E-01	0	0	1.000000E+03	4.084400E+02	0.
6110000	4.572000E-05	3.874368E-01	0	0	1.000000E+03	4.084400E+02	0.
6120000	4.572000E-05	3.874368E-01	0	0	1.000000E+03	4.084400E+02	0.
6130000	4.572000E-05	3.874368E-01	0	0	1.000000E+03	4.084400E+02	0.
6140000	4.572000E-05	3.874368E-01	0	0	1.000000E+03	4.084400E+02	0.
6150000	4.572000E-05	3.874368E-01	0	0	1.000000E+03	4.084400E+02	0.

JUN.NO.	JUNCTION AREA (M2)	FORWARD LOSS COEFFICIENT	REVERSE LOSS COEFFICIENT	JUNCTION FLAGS	INIT. LIQ. FLOW (KG/SEC)	INIT. VAP. FLOW (KG/SEC)	INTERFACE VEL. (M/SEC)
6010000	1.178940E-01	0.	0.	0	6.300398E+02	0.	0.
6020000	1.178940E-01	0.	0.	0	6.300398E+02	0.	0.
6030000	1.178940E-01	0.	0.	0	6.300398E+02	0.	0.
6040000	1.178940E-01	0.	0.	0	6.300398E+02	0.	0.
6050000	1.178940E-01	0.	0.	0	6.300398E+02	0.	0.
6060000	1.178940E-01	0.	0.	0	6.300398E+02	0.	0.
6070000	1.178940E-01	0.	0.	0	6.300398E+02	0.	0.
6080000	1.178940E-01	0.	0.	0	6.300398E+02	0.	0.
6090000	1.178940E-01	0.	0.	0	6.300398E+02	0.	0.
6100000	1.178940E-01	0.	0.	0	6.300398E+02	0.	0.
6110000	1.178940E-01	0.	0.	0	6.300398E+02	0.	0.
6120000	1.178940E-01	0.	0.	0	6.300398E+02	0.	0.
6130000	1.178940E-01	0.	0.	0	6.300398E+02	0.	0.
6140000	1.178940E-01	0.	0.	0	6.300398E+02	0.	0.

INPUT DATA FOR COMPONENT 7, CHT VLV SNGLJUN , HAVING [illegible]OLUMES AND 1 JUNCTIONS

JUN.NO.	FROM VOL.	TO VOL.	JUNCTION AREA (M2)	FORWARD LOSS COEFFICIENT	REVERSE LOSS COEFFICIENT	JUNCTION FLAGS
7000000	6010000	8000000	1.047017E-01	0.	0.	0

JUN.NO.	INIT. LIQ. FLOW (KG/SEC)	INIT. VAP. FLOW (KG/SEC)	INTERFACE VEL. (M/SEC)
7000000	6.300398E+02	0.	0.

INPUT DATA FOR COMPONENT 8, 18 SCH100 PIPE , HAVING 10 VOLUMES AND 9 JUNCTIONS

VOL NO.	FLOW AREA (M2)	FLOW LENGTH (M)	VOLUME (M3)	HORIZ. ANGLE (DEG)	VERT. ANGLE (DEG)	ELEV. CHNG. (M)
8010000	1.246759E-01	1.524000E-01	1.900060E-02	0.	9.000000E+01	1.524000E-01
8020000	1.246759E-01	1.524000E-01	1.900060E-02	0.	9.000000E+01	1.524000E-01
8030000	1.246759E-01	1.524000E-01	1.900060E-02	0.	9.000000E+01	1.524000E-01
8040000	1.246759E-01	1.524000E-01	1.900060E-02	0.	9.000000E+01	1.524000E-01
8050000	1.246759E-01	1.524000E-01	1.900060E-02	0.	9.000000E+01	1.524000E-01
8060000	1.246759E-01	1.524000E-01	1.900060E-02	0.	9.000000E+01	1.524000E-01
8070000	1.246759E-01	1.524000E-01	1.900060E-02	0.	9.000000E+01	1.524000E-01
8080000	1.246759E-01	1.524000E-01	1.900060E-02	0.	9.000000E+01	1.524000E-01
8090000	1.246759E-01	1.524000E-01	1.900060E-02	0.	9.000000E+01	1.524000E-01
8100000	1.246759E-01	1.524000E-01	1.900060E-02	0.	9.000000E+01	1.524000E-01

VOL NO.	ROUGHNESS (M)	HYDRAULIC DIAM. (M)	VOLUME FLAGS	INIT. COND. FLAG	I.C. VALUE 1	I.C. VALUE 2	I.C. VALUE 3

8010000	4.572000E-05	3.984247E-01	0	0	1.000000E+03	4.084400E+02	0.
8020000	4.572000E-05	3.984247E-01	0	0	1.000000E+03	4.084400E+02	0.
8030000	4.572000E-05	3.984247E-01	0	0	1.000000E+03	4.084400E+02	0.
8040000	4.572000E-05	3.984247E-01	0	0	1.000000E+03	4.084400E+02	0.
8050000	4.572000E-05	3.984247E-01	0	0	1.000000E+03	4.084400E+02	0.
8060000	4.572000E-05	3.984247E-01	0	0	1.000000E+03	4.084400E+02	0.
8070000	4.572000E-05	3.984247E-01	0	0	1.000000E+03	4.084400E+02	0.
8080000	4.572000E-05	3.984247E-01	0	0	1.000000E+03	4.084400E+02	0.
8090000	4.572000E-05	3.984247E-01	0	0	1.000000E+03	4.084400E+02	0.
8100000	4.572000E-05	3.984247E-01	0	0	1.000000E+03	4.084400E+02	0.

JUN.NO.	JUNCTION AREA (M2)	FORWARD LOSS COEFFICIENT	REVERSE LOSS COEFFICIENT	JUNCTION FLAGS	INIT. LIQ. FLOW (KG/SEC)	INIT. VAP. FLOW (KG/SEC)	INTERFACE VEL. (M/SEC)
8010000	1.246759E-01	0.	0.	0	6.300398E+02	0.	0.
8020000	1.246759E-01	0.	0.	0	6.300398E+02	0.	0.
8030000	1.246759E-01	0.	0.	0	6.300398E+02	0.	0.
8040000	1.246759E-01	0.	0.	0	6.300398E+02	0.	0.
8050000	1.246759E-01	0.	0.	0	6.300398E+02	0.	0.
8060000	1.246759E-01	0.	0.	0	6.300398E+02	0.	0.
8070000	1.246759E-01	0.	0.	0	6.300398E+02	0.	0.
8080000	1.246759E-01	0.	0.	0	6.300398E+02	0.	0.
8090000	1.246759E-01	0.	0.	0	6.300398E+02	0.	0.

INPUT DATA FOR COMPONENT 9, TEE PLENUM , HAVING 1 VOLUMES AND 4 JUNCTIONS

VOL NO.	FLOW AREA (M2)	FLOW LENGTH (M)	VOLUME (M3)	HORIZ. ANGLE (DEG)	VERT. ANGLE (DEG)	ELEV. CHNG. (M)
9010000	1.314578E-01	1.100328E+00	1.446467E-01	0.	0.	0.

VOL NO.	ROUGHNESS (M)	HYDRAULIC DIAM. (M)	VOLUME FLAGS	INIT. COND. FLAG	T.C. VALUE 1	I.C. VALUE 2	I.C. VALUE 3
9010000	4.572000E-05	4.091177E-01	0	0	6.894757E+06	9.500314E+05	0.

JUN.NO.	FROM VOL.	TO VOL.	JUNCTION AREA (M2)	FORWARD LOSS COEFFICIENT	REVERSE LOSS COEFFICIENT	JUNCTION FLAGS
9010000	8010000	9000000	6.233794E-02	0.	0.	0
9020000	8010000	9000000	6.233794E-02	0.	0.	0
9030000	9010000	10000000	6.558955E-02	0.	0.	0
9040000	9010000	19000000	6.558955E-02	0.	0.	0

JUN.NO.	INIT. LIQ. FLOW (KG/SEC)	INIT. VAP. FLOW (KG/SEC)	INTERFACE VEL. (M/SEC)
9010000	3.150199E+02	0.	0.
9020000	3.150199E+02	0.	0.
9030000	3.150199E+02	0.	0.
9040000	3.150199E+02	0.	0.

INPUT DATA FOR COMPONENT 10, 12 SCH80 PIPE , HAVING 30 VOLUMES AND 29 JUNCTIONS

VOL NO.	FLOW AREA (M2)	FLOW LENGTH (M)	VOLUME (M3)	HORIZ. ANGLE (DEG)	VERT. ANGLE (DEG)	ELEV. CHNG. (M)
10010000	6.558955E-02	1.524000E-01	9.995847E-03	0.	0.	0.
10020000	6.558955E-02	1.524000E-01	9.995847E-03	0.	0.	0.
10030000	6.558955E-02	1.524000E-01	9.995847E-03	0.	0.	0.
10040000	6.558955E-02	1.524000E-01	9.995847E-03	0.	9.000000E+01	1.524000E-01
10050000	6.558955E-02	1.524000E-01	9.995847E-03	0.	9.000000E+01	1.524000E-01
10060000	6.558955E-02	1.524000E-01	9.995847E-03	0.	9.000000E+01	1.524000E-01
10070000	6.558955E-02	1.524000E-01	9.995847E-03	0.	9.000000E+01	1.524000E-01
10080000	6.558955E-02	1.524000E-01	9.995847E-03	0.	9.000000E+01	1.524000E-01
10090000	6.558955E-02	1.524000E-01	9.995847E-03	0.	9.000000E+01	1.524000E-01
10100000	6.558955E-02	1.524000E-01	9.995847E-03	0.	9.000000E+01	1.524000E-01

10110000	6.558955E-02	1.524000E-01	9.995847E-03	0.	0.	0.	
10120000	6.558955E-02	1.524000E-01	9.995847E-03	0.	0.	0.	
10130000	6.558955E-02	1.524000E-01	9.995847E-03	0.	0.	0.	
10140000	6.558955E-02	1.524000E-01	9.995847E-03	0.	0.	0.	
10150000	6.558955E-02	1.524000E-01	9.995847E-03	0.	0.	0.	
10160000	6.558955E-02	1.524000E-01	9.995847E-03	0.	0.	0.	
10170000	6.558955E-02	1.524000E-01	9.995847E-03	0.	0.	0.	
10180000	6.558955E-02	1.524000E-01	9.995847E-03	0.	0.	0.	
10190000	6.558955E-02	1.524000E-01	9.995847E-03	0.	0.	0.	
10200000	6.558955E-02	1.524000E-01	9.995847E-03	0.	0.	0.	
10210000	6.558955E-02	1.524000E-01	9.995847E-03	0.	0.	0.	
10220000	6.558955E-02	1.524000E-01	9.995847E-03	0.	0.	0.	
10230000	6.558955E-02	1.524000E-01	9.995847E-03	0.	0.	0.	
10240000	6.558955E-02	1.524000E-01	9.995847E-03	0.	0.	0.	
10250000	6.558955E-02	1.524000E-01	9.995847E-03	0.	0.	0.	
10260000	6.558955E-02	1.524000E-01	9.995847E-03	0.	0.	0.	
10270000	6.558955E-02	1.524000E-01	9.995847E-03	0.	0.	0.	
10280000	6.558955E-02	1.524000E-01	9.995847E-03	0.	0.	0.	
10290000	6.558955E-02	1.524000E-01	9.995847E-03	0.	0.	0.	
10300000	6.558955E-02	1.524000E-01	9.995847E-03	0.	0.	0.	

VOL NO.	ROUGHNESS (M)	HYDRAULIC DIAM. (M)	VOLUME FLAGS	INIT. COND. FLAG	I.C. VALUE 1	I.C. VALUE 2	I.C. VALUE 3
10010000	4.572000E-05	2.889831E-01	0	0	1.000000E+03	4.084400E+02	0.
10020000	4.572000E-05	2.889831E-01	0	0	1.000000E+03	4.084400E+02	0.
10030000	4.572000E-05	2.889831E-01	0	0	1.000000E+03	4.084400E+02	0.
10040000	4.572000E-05	2.889831E-01	0	0	1.000000E+03	4.084400E+02	0.
10050000	4.572000E-05	2.889831E-01	0	0	1.000000E+03	4.084400E+02	0.
10060000	4.572000E-05	2.889831E-01	0	0	1.000000E+03	4.084400E+02	0.
10070000	4.572000E-05	2.889831E-01	0	0	1.000000E+03	4.084400E+02	0.
10080000	4.572000E-05	2.889831E-01	0	0	1.000000E+03	4.084400E+02	0.
10090000	4.572000E-05	2.889831E-01	0	0	1.000000E+03	4.084400E+02	0.
10100000	4.572000E-05	2.889831E-01	0	0	1.000000E+03	4.084400E+02	0.
10110000	4.572000E-05	2.889831E-01	0	0	1.000000E+03	4.084400E+02	0.
10120000	4.572000E-05	2.889831E-01	0	0	1.000000E+03	4.084400E+02	0.
10130000	4.572000E-05	2.889831E-01	0	0	1.000000E+03	4.084400E+02	0.
10140000	4.572000E-05	2.889831E-01	0	0	1.000000E+03	4.084400E+02	0.
10150000	4.572000E-05	2.889831E-01	0	0	1.000000E+03	4.084400E+02	0.
10160000	4.572000E-05	2.889831E-01	0	0	1.000000E+03	4.084400E+02	0.
10170000	4.572000E-05	2.889831E-01	0	0	1.000000E+03	4.084400E+02	0.
10180000	4.572000E-05	2.889831E-01	0	0	1.000000E+03	4.084400E+02	0.
10190000	4.572000E-05	2.889831E-01	0	0	1.000000E+03	4.084400E+02	0.
10200000	4.572000E-05	2.889831E-01	0	0	1.000000E+03	4.084400E+02	0.
10210000	4.572000E-05	2.889831E-01	0	0	1.000000E+03	4.084400E+02	0.
10220000	4.572000E-05	2.889831E-01	0	0	1.000000E+03	4.084400E+02	0.
10230000	4.572000E-05	2.889831E-01	0	0	1.000000E+03	4.084400E+02	0.
10240000	4.572000E-05	2.889831E-01	0	0	1.000000E+03	4.084400E+02	0.
10250000	4.572000E-05	2.889831E-01	0	0	1.000000E+03	4.084400E+02	0.
10260000	4.572000E-05	2.889831E-01	0	0	1.000000E+03	4.084400E+02	0.
10270000	4.572000E-05	2.889831E-01	0	0	1.000000E+03	4.084400E+02	0.
10280000	4.572000E-05	2.889831E-01	0	0	1.000000E+03	4.084400E+02	0.
10290000	4.572000E-05	2.889831E-01	0	0	1.000000E+03	4.084400E+02	0.
10300000	4.572000E-05	2.889831E-01	0	0	1.000000E+03	4.084400E+02	0.

JUN.NO.	JUNCTION AREA (M2)	FORWARD LOSS COEFFICIENT	REVERSE LOSS COEFFICIENT	JUNCTION FLAGS	INIT. LIQ. FLOW (KG/SEC)	INIT. VAP. FLOW (KG/SEC)	INTERFACE VEL. (M/SEC)
10010000	6.558955E-02	0.	0.	0	3.150199E+02	0.	0.
10020000	6.558955E-02	0.	0.	0	3.150199E+02	0.	0.
10030000	6.558955E-02	0.	0.	0	3.150199E+02	0.	0.
10040000	6.558955E-02	0.	0.	0	3.150199E+02	0.	0.
10050000	6.558955E-02	0.	0.	0	3.150199E+02	0.	0.

10060000	6.558955E-02	0.	0.	0	3.150199E+02	0.	0.
10070000	6.558955E-02	0.	0.	0	3.150199E+02	0.	0.
10080000	6.558955E-02	0.	0.	0	3.150199E+02	0.	0.
10090000	6.558955E-02	0.	0.	0	3.150199E+02	0.	0.
10100000	6.558955E-02	0.	0.	0	3.150199E+02	0.	0.
10110000	6.558955E-02	0.	0.	0	3.150199E+02	0.	0.
10120000	6.558955E-02	0.	0.	0	3.150199E+02	0.	0.
10130000	6.558955E-02	0.	0.	0	3.150199E+02	0.	0.
10140000	6.558955E-02	0.	0.	0	3.150199E+02	0.	0.
10150000	6.558955E-02	0.	0.	0	3.150199E+02	0.	0.
10160000	6.558955E-02	0.	0.	0	3.150199E+02	0.	0.
10170000	6.558955E-02	0.	0.	0	3.150199E+02	0.	0.
10180000	6.558955E-02	0.	0.	0	3.150199E+02	0.	0.
10190000	6.558955E-02	0.	0.	0	3.150199E+02	0.	0.
10200000	6.558955E-02	0.	0.	0	3.150199E+02	0.	0.
10210000	6.558955E-02	0.	0.	0	3.150199E+02	0.	0.
10220000	6.558955E-02	0.	0.	0	3.150199E+02	0.	0.
10230000	6.558955E-02	0.	0.	0	3.150199E+02	0.	0.
10240000	6.558955E-02	0.	0.	0	3.150199E+02	0.	0.
10250000	6.558955E-02	0.	0.	0	3.150199E+02	0.	0.
10260000	6.558955E-02	0.	0.	0	3.150199E+02	0.	0.
10270000	6.558955E-02	0.	0.	0	3.150199E+02	0.	0.
10280000	6.558955E-02	0.	0.	0	3.150199E+02	0.	0.
10290000	6.558955E-02	0.	0.	0	3.150199E+02	0.	0.

INPUT DATA FOR COMPONENT 11, JUNCTION SNGLJUN , HAVING 0 VOLUMES AND 1 JUNCTIONS

JUN.NO.	FROM VOL.	TO VOL.	JUNCTION AREA (M2)	FORWARD LOSS COEFFICIENT	REVERSE LOSS COEFFICIENT	JUNCTION FLAGS
11000000	10010000	12000000	0.	0.	0.	0

JUN.NO.	INIT. LIQ. FLOW (KG/SEC)	INIT. VAP. FLOW (KG/SEC)	INTERFACE VEL. (M/SEC)
11000000	3.150199E+02	0.	0.

INPUT DATA FOR COMPONENT 12, 12 SCH80 ,IPE , HAVING 17 VOLUMES AND 16 JUNCTIONS

VOL NO.	FLOW AREA (M2)	FLOW LENGTH (F)	VOLUME (M3)	HORIZ. ANGLE (DEG)	VERT. ANGLE (DEG)	ELEV. CHNG. (M)
12010000	6.558955E-02	3.048000E-01	1.999169E-02	0.	0.	0.
12020000	6.558955E-02	3.048000E-01	1.999169E-02	0.	0.	0.
12030000	6.558955E-02	3.048000E-01	1.999169E-02	0.	0.	0.
12040000	6.558955E-02	3.048000E-01	1.999169E-02	0.	0.	0.
12050000	6.558955E-02	3.048000E-01	1.999169E-02	0.	0.	0.
12060000	6.558955E-02	3.048000E-01	1.999169E-02	0.	0.	0.
12070000	6.558955E-02	3.048000E-01	1.999169E-02	0.	0.	0.
12080000	6.558955E-02	3.048000E-01	1.999169E-02	0.	0.	0.
12090000	6.558955E-02	3.048000E-01	1.999169E-02	0.	0.	0.
12100000	6.558955E-02	3.048000E-01	1.999169E-02	0.	0.	0.
12110000	6.558955E-02	3.048000E-01	1.999169E-02	0.	0.	0.
12120000	6.558955E-02	3.048000E-01	1.999169E-02	0.	0.	0.
12130000	6.558955E-02	3.048000E-01	1.999169E-02	0.	0.	0.
12140000	6.558955E-02	3.048000E-01	1.999169E-02	0.	0.	0.
12150000	6.558955E-02	3.048000E-01	1.999169E-02	0.	0.	0.
12160000	6.558955E-02	3.048000E-01	1.999169E-02	0.	0.	0.
12170000	6.558955E-02	3.048000E-01	1.999169E-02	0.	0.	0.

VOL NO.	ROUGHNESS (M)	HYDRAULIC DIAM. (M)	VOLUME FLAGS	INIT. COND. FLAG	I.C. VALUE 1	I.C. VALUE 2	I.C. VALUE 3
12010000	4.572000E-05	2.889831E-01	0	0	1.000000E+03	4.084400E+02	0.
12020000	4.572000E-05	2.889831E-01	0	0	1.000000E+03	4.084400E+02	0.

12030000	4.572000E-05	2.889831E-01	0	0	1.000000E+03	4.084400E+02	0.
12040000	4.572000E-05	2.889831E-01	0	0	1.000000E+03	4.084400E+02	0.
12050000	4.572000E-05	2.889831E-01	0	0	1.000000E+03	4.084400E+02	0.
12060000	4.572000E-05	2.889831E-01	0	0	1.000000E+03	4.084400E+02	0.
12070000	4.572000E-05	2.889831E-01	0	0	1.000000E+03	4.084400E+02	0.
12080000	4.572000E-05	2.889831E-01	0	0	1.000000E+03	4.084400E+02	0.
12090000	4.572000E-05	2.889831E-01	0	0	1.000000E+03	4.084400E+02	0.
12100000	4.572000E-05	2.889831E-01	0	0	1.000000E+03	4.084400E+02	0.
12110000	4.572000E-05	2.889831E-01	0	0	1.000000E+03	4.084400E+02	0.
12120000	4.572000E-05	2.889831E-01	0	0	1.000000E+03	4.084400E+02	0.
12130000	4.572000E-05	2.889831E-01	0	0	1.000000E+03	4.084400E+02	0.
12140000	4.572000E-05	2.889831E-01	0	0	1.000000E+03	4.084400E+02	0.
12150000	4.572000E-05	2.889831E-01	0	0	1.000000E+03	4.084400E+02	0.
12160000	4.572000E-05	2.889831E-01	0	0	1.000000E+03	4.084400E+02	0.
12170000	4.572000E-05	2.889831E-01	0	0	1.000000E+03	4.084400E+02	0.

JUN.NO.	JUNCTION AREA (M2)	FORWARD LOSS COEFFICIENT	REVERSE LOSS COEFFICIENT	JUNCTION FLAGS	INIT. LIQ. FLOW (KG/SEC)	INIT. VAP. FLOW (KG/SEC)	INTERFACE VEL. (M/SEC)
12010000	6.558955E-02	0.	0.	0	3.150199E+02	0.	0.
12020000	6.558955E-02	0.	0.	0	3.150199E+02	0.	0.
12030000	6.558955E-02	0.	0.	0	3.150199E+02	0.	0.
12040000	6.558955E-02	0.	0.	0	3.150199E+02	0.	0.
12050000	6.558955E-02	0.	0.	0	3.150199E+02	0.	0.
12060000	6.558955E-02	0.	0.	0	3.150199E+02	0.	0.
12070000	6.558955E-02	0.	0.	0	3.150199E+02	0.	0.
12080000	6.558955E-02	0.	0.	0	3.150199E+02	0.	0.
12090000	6.558955E-02	0.	0.	0	3.150199E+02	0.	0.
12100000	6.558955E-02	0.	0.	0	3.150199E+02	0.	0.
12110000	6.558955E-02	0.	0.	0	3.150199E+02	0.	0.
12120000	6.558955E-02	0.	0.	0	3.150199E+02	0.	0.
12130000	6.558955E-02	0.	0.	0	3.150199E+02	0.	0.
12140000	6.558955E-02	0.	0.	0	3.150199E+02	0.	0.
12150000	6.558955E-02	0.	0.	0	3.150199E+02	0.	0.
12160000	6.558955E-02	0.	0.	0	3.150199E+02	0.	0.

INPUT DATA FOR COMPONENT 13, JUNCTION SNGLJUN • HAVING 0 VOLUMES AND 1 JUNCTIONS

JUN.NO.	FROM VOL.	TO VOL.	JUNCTION AREA (M2)	FORWARD LOSS COEFFICIENT	REVERSE LOSS COEFFICIENT	JUNCTION FLAGS
13000000	12010000	14000000	0.	0.	0.	0

JUN.NO.	INIT. LIQ. FLOW (KG/SEC)	INIT. VAP. FLOW (KG/SEC)	INTERFACE VEL. (M/SEC)
13000000	3.150199E+02	0.	0.

INPUT DATA FOR COMPONENT 14, 12 SCH80 PIPE • HAVING 20 VOLUMES AND 19 JUNCTIONS

VOL NO.	FLOW AREA (M2)	FLOW LENGTH (M)	VOLUME (M3)	HORIZ. ANGLE (DEG)	VERT. ANGLE (DEG)	ELEV. CHNG. (M)
14010000	6.558955E-02	3.048000E-01	1.999169E-02	0.	9.000000E+01	3.048000E-01
14020000	6.558955E-02	3.048000E-01	1.999169E-02	0.	9.000000E+01	3.048000E-01
14030000	6.558955E-02	3.048000E-01	1.999169E-02	0.	9.000000E+01	3.048000E-01
14040000	6.558955E-02	3.048000E-01	1.999169E-02	0.	9.000000E+01	3.048000E-01
14050000	6.558955E-02	3.048000E-01	1.999169E-02	0.	9.000000E+01	3.048000E-01
14060000	6.558955E-02	3.048000E-01	1.999169E-02	0.	9.000000E+01	3.048000E-01
14070000	6.558955E-02	3.048000E-01	1.999169E-02	0.	9.000000E+01	3.048000E-01
14080000	6.558955E-02	3.048000E-01	1.999169E-02	0.	9.000000E+01	3.048000E-01
14090000	6.558955E-02	3.048000E-01	1.999169E-02	0.	9.000000E+01	3.048000E-01
14100000	6.558955E-02	3.048000E-01	1.999169E-02	0.	9.000000E+01	3.048000E-01
14110000	6.558955E-02	3.048000E-01	1.999169E-02	0.	9.000000E+01	3.048000E-01
14120000	6.558955E-02	3.048000E-01	1.999169E-02	0.	9.000000E+01	3.048000E-01

14130000	6.558955E-02	3.048000E-01	1.999169E-02	0.	9.000000E+01	3.048000E-01	
14140000	6.558955E-02	3.048000E-01	1.999169E-02	0.	9.000000E+01	3.048000E-01	
14150000	6.558955E-02	3.048000E-01	1.999169E-02	0.	9.000000E+01	3.048000E-01	
14160000	6.558955E-02	3.048000E-01	1.999169E-02	0.	9.000000E+01	3.048000E-01	
14170000	6.558955E-02	3.048000E-01	1.999169E-02	0.	9.000000E+01	3.048000E-01	
14180000	6.558955E-02	3.048000E-01	1.999169E-02	0.	9.000000E+01	3.048000E-01	
14190000	6.558955E-02	3.048000E-01	1.999169E-02	0.	9.000000E+01	3.048000E-01	
14200000	6.558955E-02	3.048000E-01	1.999169E-02	0.	9.000000E+01	3.048000E-01	

VOL NO.	ROUGHNESS (M)	HYDRAULIC DIAM. (M)	VOLUME FLAGS	INIT. COND. FLAG	I.C. VALUE 1	I.C. VALUE 2	I.C. VALUE 3
14010000	4.572000E-05	2.889831E-01	0	0	1.000000E+03	4.084400E+02	0.
14020000	4.572000E-05	2.889831E-01	0	0	1.000000E+03	4.084400E+02	0.
14030000	4.572000E-05	2.889831E-01	0	0	1.000000E+03	4.084400E+02	0.
14040000	4.572000E-05	2.889831E-01	0	0	1.000000E+03	4.084400E+02	0.
14050000	4.572000E-05	2.889831E-01	0	0	1.000000E+03	4.084400E+02	0.
14060000	4.572000E-05	2.889831E-01	0	0	1.000000E+03	4.084400E+02	0.
14070000	4.572000E-05	2.889831E-01	0	0	1.000000E+03	4.084400E+02	0.
14080000	4.572000E-05	2.889831E-01	0	0	1.000000E+03	4.084400E+02	0.
14090000	4.572000E-05	2.889831E-01	0	0	1.000000E+03	4.084400E+02	0.
14100000	4.572000E-05	2.889831E-01	0	0	1.000000E+03	4.084400E+02	0.
14110000	4.572000E-05	2.889831E-01	0	0	1.000000E+03	4.084400E+02	0.
14120000	4.572000E-05	2.889831E-01	0	0	1.000000E+03	4.084400E+02	0.
14130000	4.572000E-05	2.889831E-01	0	0	1.000000E+03	4.084400E+02	0.
14140000	4.572000E-05	2.889831E-01	0	0	1.000000E+03	4.084400E+02	0.
14150000	4.572000E-05	2.889831E-01	0	0	1.000000E+03	4.084400E+02	0.
14160000	4.572000E-05	2.889831E-01	0	0	1.000000E+03	4.084400E+02	0.
14170000	4.572000E-05	2.889831E-01	0	0	1.000000E+03	4.084400E+02	0.
14180000	4.572000E-05	2.889831E-01	0	0	1.000000E+03	4.084400E+02	0.
14190000	4.572000E-05	2.889831E-01	0	0	1.000000E+03	4.084400E+02	0.
14200000	4.572000E-05	2.889831E-01	0	0	1.000000E+03	4.084400E+02	0.

JUN.NO.	JUNCTION AREA (M2)	FORWARD LOSS COEFFICIENT	REVERSE LOSS COEFFICIENT	JUNCTION FLAGS	INIT. LIQ. FLOW (KG/SEC)	INIT. VAP. FLOW (KG/SEC)	INTERFACE VEL. (M/SEC)
14010000	6.558955E-02	0.	0.	0	3.150199E+02	0.	0.
14020000	6.558955E-02	0.	0.	0	3.150199E+02	0.	0.
14030000	6.558955E-02	0.	0.	0	3.150199E+02	0.	0.
14040000	6.558955E-02	0.	0.	0	3.150199E+02	0.	0.
14050000	6.558955E-02	0.	0.	0	3.150199E+02	0.	0.
14060000	6.558955E-02	0.	0.	0	3.150199E+02	0.	0.
14070000	6.558955E-02	0.	0.	0	3.150199E+02	0.	0.
14080000	6.558955E-02	0.	0.	0	3.150199E+02	0.	0.
14090000	6.558955E-02	0.	0.	0	3.150199E+02	0.	0.
14100000	6.558955E-02	0.	0.	0	3.150199E+02	0.	0.
14110000	6.558955E-02	0.	0.	0	3.150199E+02	0.	0.
14120000	6.558955E-02	0.	0.	0	3.150199E+02	0.	0.
14130000	6.558955E-02	0.	0.	0	3.150199E+02	0.	0.
14140000	6.558955E-02	0.	0.	0	3.150199E+02	0.	0.
14150000	6.558955E-02	0.	0.	0	3.150199E+02	0.	0.
14160000	6.558955E-02	0.	0.	0	3.150199E+02	0.	0.
14170000	6.558955E-02	0.	0.	0	3.150199E+02	0.	0.
14180000	6.558955E-02	0.	0.	0	3.150199E+02	0.	0.
14190000	6.558955E-02	0.	0.	0	3.150199E+02	0.	0.

INPUT DATA FOR COMPONENT 15, JUNCTION SNGLJUN , HAVING 0 VOLUMES AND 1 JUNCTIONS

JUN.NO.	FROM VOL.	TO VOL.	JUNCTION AREA (M2)	FORWARD LOSS COEFFICIENT	REVERSE LOSS COEFFICIENT	JUNCTION FLAGS
15000000	14010000	16000000	0.	0.	0.	0

JUN.NO.	INIT. LIQ. FLOW	INIT. VAP. FLOW	INTERFACE VEL.

	(KG/SEC)	(KG/SEC)	(M/SEC)
15000000	3.150199E+02	0.	0.

INPUT DATA FOR COMPONENT 16, 12 SCH80 PIPE , HAVING 15 VOLUMES AND 14 JUNCTIONS

VOL NO.	FLOW AREA (M2)	FLOW LENGTH (M)	VOLUME (M3)	HORIZ. ANGLE (DEG)	VERT. ANGLE (DEG)	ELEV. CHNG. (M)
16010000	6.558955E-02	3.048000E-01	1.999169E-02	0.	9.000000E+01	3.048000E-01
16020000	6.558955E-02	3.048000E-01	1.999169E-02	0.	9.000000E+01	3.048000E-01
16030000	6.558955E-02	3.048000E-01	1.999169E-02	0.	9.000000E+01	3.048000E-01
16040000	6.558955E-02	3.048000E-01	1.999169E-02	0.	9.000000E+01	3.048000E-01
16050000	6.558955E-02	3.048000E-01	1.999169E-02	0.	9.000000E+01	3.048000E-01
16060000	6.558955E-02	3.048000E-01	1.999169E-02	0.	9.000000E+01	3.048000E-01
16070000	6.558955E-02	3.048000E-01	1.999169E-02	0.	9.000000E+01	3.048000E-01
16080000	6.558955E-02	3.048000E-01	1.999169E-02	0.	9.000000E+01	3.048000E-01
16090000	6.558955E-02	3.048000E-01	1.999169E-02	0.	9.000000E+01	3.048000E-01
16100000	6.558955E-02	3.048000E-01	1.999169E-02	0.	9.000000E+01	3.048000E-01
16110000	6.558955E-02	3.048000E-01	1.999169E-02	0.	9.000000E+01	3.048000E-01
16120000	6.558955E-02	3.048000E-01	1.999169E-02	0.	0.	0.
16130000	6.558955E-02	3.048000E-01	1.999169E-02	0.	0.	0.
16140000	6.558955E-02	3.048000E-01	1.999169E-02	0.	0.	0.
16150000	6.558955E-02	3.048000E-01	1.999169E-02	0.	0.	0.

VOL NO.	ROUGHNESS (M)	HYDRAULIC DIAM. (M)	VOLUME FLAGS	INIT. COND. FLAG	I.C. VALUE 1	I.C. VALUE 2	I.C. VALUE 3
16010000	4.572000E-05	2.889831E-01	0	0	1.000000E+03	4.084400E+02	0.
16020000	4.572000E-05	2.889831E-01	0	0	1.000000E+03	4.084400E+02	0.
16030000	4.572000E-05	2.889831E-01	0	0	1.000000E+03	4.084400E+02	0.
16040000	4.572000E-05	2.889831E-01	0	0	1.000000E+03	4.084400E+02	0.
16050000	4.572000E-05	2.889831E-01	0	0	1.000000E+03	4.084400E+02	0.
16060000	4.572000E-05	2.889831E-01	0	0	1.000000E+03	4.084400E+02	0.
16070000	4.572000E-05	2.889831E-01	0	0	1.000000E+03	4.084400E+02	0.
16080000	4.572000E-05	2.889831E-01	0	0	1.000000E+03	4.084400E+02	0.
16090000	4.572000E-05	2.889831E-01	0	0	1.000000E+03	4.084400E+02	0.
16100000	4.572000E-05	2.889831E-01	0	0	1.000000E+03	4.084400E+02	0.
16110000	4.572000E-05	2.889831E-01	0	0	1.000000E+03	4.084400E+02	0.
16120000	4.572000E-05	2.889831E-01	0	0	1.000000E+03	4.084400E+02	0.
16130000	4.572000E-05	2.889831E-01	0	0	1.000000E+03	4.084400E+02	0.
16140000	4.572000E-05	2.889831E-01	0	0	1.000000E+03	4.084400E+02	0.
16150000	4.572000E-05	2.889831E-01	0	0	1.000000E+03	4.084400E+02	0.

JUN.NO.	JUNCTION AREA (M2)	FORWARD LOSS COEFFICIENT	REVERSE LOSS COEFFICIENT	JUNCTION FLAGS	INIT. LIQ. VEL. (M/SEC)	INIT. VAP. VEL. (M/SEC)	INTERFACE VEL. (M/SEC)
16010000	6.558955E-02	0.	0.	0	5.712897E+00	5.712897E+00	0.
16020000	6.558955E-02	0.	0.	0	5.712897E+00	5.712897E+00	0.
16030000	6.558955E-02	0.	0.	0	5.712897E+00	5.712897E+00	0.
16040000	6.558955E-02	0.	0.	0	5.712897E+00	5.712897E+00	0.
16050000	6.558955E-02	0.	0.	0	5.712897E+00	5.712897E+00	0.
16060000	6.558955E-02	0.	0.	0	5.712897E+00	5.712897E+00	0.
16070000	6.558955E-02	0.	0.	0	5.712897E+00	5.712897E+00	0.
16080000	6.558955E-02	0.	0.	0	5.712897E+00	5.712897E+00	0.
16090000	6.558955E-02	0.	0.	0	5.712897E+00	5.712897E+00	0.
16100000	6.558955E-02	0.	0.	0	5.712897E+00	5.712897E+00	0.
16110000	6.558955E-02	0.	0.	0	5.712897E+00	5.712897E+00	0.
16120000	6.558955E-02	0.	0.	0	5.712897E+00	5.712897E+00	0.
16130000	6.558955E-02	0.	0.	0	5.712897E+00	5.712897E+00	0.
16140000	6.558955E-02	0.	0.	0	5.712897E+00	5.712897E+00	0.

INPUT DATA FOR COMPONENT 17, BDY JUN SNGLJUN , HAVING 0 VOLUMES AND 1 JUNCTIONS

JUN.NO.	FROM VOL.	TO VOL.	JUNCTION AREA	FORWARD LOSS	REVERSE LOSS	JUNCTION

			(M2)	COEFFICIENT	COEFFICIENT	FLAGS
17000000	16010000	18000000	6.224504E-02	0.	0.	0

JUN.NO.	INIT. LIQ. VEL. (M/SEC)	INIT. VAP. VEL. (M/SEC)	INTERFACE VEL. (M/SEC)
17000000	6.019830E+00	6.019830E+00	0.

INPUT DATA FOR COMPONENT 18, BDY VOL TMDPVOL , HAVING 1 VOLUMES AND 0 JUNCTIONS

VOL NO.	FLOW AREA (M2)	FLOW LENGTH (M)	VOLUME (M3)	HORIZ. ANGLE (DEG)	VERT. ANGLE (DEG)	ELEV. CHNG. (M)
18010000	1.858061E+00	3.048000E-01	5.663369E-01	0.	0.	0.

VOL.NO.	ROUGHNESS (M)	HYDRAULIC DIAM. (M)	EQUIL. FLAG
18010000	4.572000E-05	1.538102E+00	0

TIME DEPENDENT DATA

TIME (SEC)	PRESSURE (PA)	INTERNAL ENERGY (J/KG)	STATIC QUALITY
0.	6.894757E+06	9.500314E+05	0.
1.000000E-01	6.894757E+06	9.500314E+05	0.

INPUT DATA FOR COMPONENT 19, 12 SCH80 PIPE , HAVING 47 VOLUMES AND 46 JUNCTIONS

VOL NO.	FLOW AREA (M2)	FLOW LENGTH (M)	VOLUME (M3)	HORIZ. ANGLE (DEG)	VERT. ANGLE (DEG)	ELEV. CHNG. (M)
19010000	6.558955E-02	1.524000E-01	9.995847E-03	0.	0.	0.
19020000	6.558955E-02	1.524000E-01	9.995847E-03	0.	0.	0.
19030000	6.558955E-02	1.524000E-01	9.995847E-03	0.	0.	0.
19040000	6.558955E-02	1.524000E-01	9.995847E-03	0.	0.	0.
19050000	6.558955E-02	1.524000E-01	9.995847E-03	0.	0.	0.
19060000	6.558955E-02	1.524000E-01	9.995847E-03	0.	0.	0.
19070000	6.558955E-02	1.524000E-01	9.995847E-03	0.	0.	0.
19080000	6.558955E-02	1.524000E-01	9.995847E-03	0.	0.	0.
19090000	6.558955E-02	1.524000E-01	9.995847E-03	0.	0.	0.
19100000	6.558955E-02	1.524000E-01	9.995847E-03	0.	0.	0.
19110000	6.558955E-02	1.524000E-01	9.995847E-03	0.	0.	0.
19120000	6.558955E-02	1.524000E-01	9.995847E-03	0.	0.	0.
19130000	6.558955E-02	1.524000E-01	9.995847E-03	0.	0.	0.
19140000	6.558955E-02	1.524000E-01	9.995847E-03	0.	0.	0.
19150000	6.558955E-02	1.524000E-01	9.995847E-03	0.	0.	0.
19160000	6.558955E-02	1.524000E-01	9.995847E-03	0.	0.	0.
19170000	6.558955E-02	1.524000E-01	9.995847E-03	0.	0.	0.
19180000	6.558955E-02	1.524000E-01	9.995847E-03	0.	0.	0.
19190000	6.558955E-02	1.524000E-01	9.995847E-03	0.	0.	0.
19200000	6.558955E-02	1.524000E-01	9.995847E-03	0.	0.	0.
19210000	6.558955E-02	1.524000E-01	9.995847E-03	0.	0.	0.
19220000	6.558955E-02	1.524000E-01	9.995847E-03	0.	0.	0.
19230000	6.558955E-02	1.524000E-01	9.995847E-03	0.	0.	0.
19240000	6.558955E-02	1.524000E-01	9.995847E-03	0.	0.	0.
19250000	6.558955E-02	1.524000E-01	9.995847E-03	0.	0.	0.
19260000	6.558955E-02	1.524000E-01	9.995847E-03	0.	0.	0.
19270000	6.558955E-02	1.524000E-01	9.995847E-03	0.	0.	0.
19280000	6.558955E-02	1.524000E-01	9.995847E-03	0.	0.	0.
19290000	6.558955E-02	1.524000E-01	9.995847E-03	0.	0.	0.
19300000	6.558955E-02	1.524000E-01	9.995847E-03	0.	0.	0.
19310000	6.558955E-02	1.524000E-01	9.995847E-03	0.	0.	0.
19320000	6.558955E-02	1.524000E-01	9.995847E-03	0.	0.	0.
19330000	6.558955E-02	1.524000E-01	9.995847E-03	0.	0.	0.
19340000	6.558955E-02	1.524000E-01	9.995847E-03	0.	0.	0.

19350000	6.558955E-02	1.524000E-01	9.995847E-03	0.	0.	0.	
19360000	6.558955E-02	1.524000E-01	9.995847E-03	0.	0.	0.	
19370000	6.558955E-02	1.524000E-01	9.995847E-03	0.	0.	0.	
19380000	6.558955E-02	1.524000E-01	9.995847E-03	0.	0.	0.	
19390000	6.558955E-02	1.524000E-01	9.995847E-03	0.	0.	0.	
19400000	6.558955E-02	1.524000E-01	9.995847E-03	0.	0.	0.	
19410000	6.558955E-02	1.524000E-01	9.995847E-03	0.	0.	0.	
19420000	6.558955E-02	1.524000E-01	9.995847E-03	0.	0.	0.	
19430000	6.558955E-02	1.524000E-01	9.995847E-03	0.	0.	0.	
19440000	6.558955E-02	1.524000E-01	9.995847E-03	0.	0.	0.	
19450000	6.558955E-02	1.524000E-01	9.995847E-03	0.	0.	0.	
19460000	6.558955E-02	1.524000E-01	9.995847E-03	0.	0.	0.	
19470000	6.558955E-02	1.524000E-01	9.995847E-03	0.	0.	0.	

VOL NO.	ROUGHNESS (M)	HYDRAULIC DIAM. (M)	VOLUME FLAGS	INIT. COND. FLAG	T.C. VALUE 1	I.C. VALUE 2	I.C. VALUE 3
19010000	4.572000E-05	2.889831E-01	0	0	1.000000E+03	4.084400E+02	0.
19020000	4.572000E-05	2.889831E-01	0	0	1.000000E+03	4.084400E+02	0.
19030000	4.572000E-05	2.889831E-01	0	0	1.000000E+03	4.084400E+02	0.
19040000	4.572000E-05	2.889831E-01	0	0	1.000000E+03	4.084400E+02	0.
19050000	4.572000E-05	2.889831E-01	0	0	1.000000E+03	4.084400E+02	0.
19060000	4.572000E-05	2.889831E-01	0	0	1.000000E+03	4.084400E+02	0.
19070000	4.572000E-05	2.889831E-01	0	0	1.000000E+03	4.084400E+02	0.
19080000	4.572000E-05	2.889831E-01	0	0	1.000000E+03	4.084400E+02	0.
19090000	4.572000E-05	2.889831E-01	0	0	1.000000E+03	4.084400E+02	0.
19100000	4.572000E-05	2.889831E-01	0	0	1.000000E+03	4.084400E+02	0.
19110000	4.572000E-05	2.889831E-01	0	0	1.000000E+03	4.084400E+02	0.
19120000	4.572000E-05	2.889831E-01	0	0	1.000000E+03	4.084400E+02	0.
19130000	4.572000E-05	2.889831E-01	0	0	1.000000E+03	4.084400E+02	0.
19140000	4.572000E-05	2.889831E-01	0	0	1.000000E+03	4.084400E+02	0.
19150000	4.572000E-05	2.889831E-01	0	0	1.000000E+03	4.084400E+02	0.
19160000	4.572000E-05	2.889831E-01	0	0	1.000000E+03	4.084400E+02	0.
19170000	4.572000E-05	2.889831E-01	0	0	1.000000E+03	4.084400E+02	0.
19180000	4.572000E-05	2.889831E-01	0	0	1.000000E+03	4.084400E+02	0.
19190000	4.572000E-05	2.889831E-01	0	0	1.000000E+03	4.084400E+02	0.
19200000	4.572000E-05	2.889831E-01	0	0	1.000000E+03	4.084400E+02	0.
19210000	4.572000E-05	2.889831E-01	0	0	1.000000E+03	4.084400E+02	0.
19220000	4.572000E-05	2.889831E-01	0	0	1.000000E+03	4.084400E+02	0.
19230000	4.572000E-05	2.889831E-01	0	0	1.000000E+03	4.084400E+02	0.
19240000	4.572000E-05	2.889831E-01	0	0	1.000000E+03	4.084400E+02	0.
19250000	4.572000E-05	2.889831E-01	0	0	1.000000E+03	4.084400E+02	0.
19260000	4.572000E-05	2.889831E-01	0	0	1.000000E+03	4.084400E+02	0.
19270000	4.572000E-05	2.889831E-01	0	0	1.000000E+03	4.084400E+02	0.
19280000	4.572000E-05	2.889831E-01	0	0	1.000000E+03	4.084400E+02	0.
19290000	4.572000E-05	2.889831E-01	0	0	1.000000E+03	4.084400E+02	0.
19300000	4.572000E-05	2.889831E-01	0	0	1.000000E+03	4.084400E+02	0.
19310000	4.572000E-05	2.889831E-01	0	0	1.000000E+03	4.084400E+02	0.
19320000	4.572000E-05	2.889831E-01	0	0	1.000000E+03	4.084400E+02	0.
19330000	4.572000E-05	2.889831E-01	0	0	1.000000E+03	4.084400E+02	0.
19340000	4.572000E-05	2.889831E-01	0	0	1.000000E+03	4.084400E+02	0.
19350000	4.572000E-05	2.889831E-01	0	0	1.000000E+03	4.084400E+02	0.
19360000	4.572000E-05	2.889831E-01	0	0	1.000000E+03	4.084400E+02	0.
19370000	4.572000E-05	2.889831E-01	0	0	1.000000E+03	4.084400E+02	0.
19380000	4.572000E-05	2.889831E-01	0	0	1.000000E+03	4.084400E+02	0.
19390000	4.572000E-05	2.889831E-01	0	0	1.000000E+03	4.084400E+02	0.
19400000	4.572000E-05	2.889831E-01	0	0	1.000000E+03	4.084400E+02	0.
19410000	4.572000E-05	2.889831E-01	0	0	1.000000E+03	4.084400E+02	0.
19420000	4.572000E-05	2.889831E-01	0	0	1.000000E+03	4.084400E+02	0.
19430000	4.572000E-05	2.889831E-01	0	0	1.000000E+03	4.084400E+02	0.
19440000	4.572000E-05	2.889831E-01	0	0	1.000000E+03	4.084400E+02	0.
19450000	4.572000E-05	2.889831E-01	0	0	1.000000E+03	4.084400E+02	0.

19460000	4.572000E-05	2.889831E-01	0	0	1.000000E+03	4.084400E+02	0.
19470000	4.572000E-05	2.889831E-01	0	0	1.000000E+03	4.084400E+02	0.

JUN.NO.	JUNCTION AREA (M2)	FORWARD LOSS COEFFICIENT	REVERSE LOSS COEFFICIENT	JUNCTION FLAGS	INIT. LIQ. FLOW (KG/SEC)	INIT. VAP. FLOW (KG/SEC)	INTERFACE VEL. (M/SEC)
19010000	6.558955E-02	0.	0.	0	3.150199E+02	0.	0.
19020000	6.558955E-02	0.	0.	0	3.150199E+02	0.	0.
19030000	6.558955E-02	0.	0.	0	3.150199E+02	0.	0.
19040000	6.558955E-02	0.	0.	0	3.150199E+02	0.	0.
19050000	6.558955E-02	0.	0.	0	3.150199E+02	0.	0.
19060000	6.558955E-02	0.	0.	0	3.150199E+02	0.	0.
19070000	6.558955E-02	0.	0.	0	3.150199E+02	0.	0.
19080000	6.558955E-02	0.	0.	0	3.150199E+02	0.	0.
19090000	6.558955E-02	0.	0.	0	3.150199E+02	0.	0.
19100000	6.558955E-02	0.	0.	0	3.150199E+02	0.	0.
19110000	6.558955E-02	0.	0.	0	3.150199E+02	0.	0.
19120000	6.558955E-02	0.	0.	0	3.150199E+02	0.	0.
19130000	6.558955E-02	0.	0.	0	3.150199E+02	0.	0.
19140000	6.558955E-02	0.	0.	0	3.150199E+02	0.	0.
19150000	6.558955E-02	0.	0.	0	3.150199E+02	0.	0.
19160000	6.558955E-02	0.	0.	0	3.150199E+02	0.	0.
19170000	6.558955E-02	0.	0.	0	3.150199E+02	0.	0.
19180000	6.558955E-02	0.	0.	0	3.150199E+02	0.	0.
19190000	6.558955E-02	0.	0.	0	3.150199E+02	0.	0.
19200000	6.558955E-02	0.	0.	0	3.150199E+02	0.	0.
19210000	6.558955E-02	0.	0.	0	3.150199E+02	0.	0.
19220000	6.558955E-02	0.	0.	0	3.150199E+02	0.	0.
19230000	6.558955E-02	0.	0.	0	3.150199E+02	0.	0.
19240000	6.558955E-02	0.	0.	0	3.150199E+02	0.	0.
19250000	6.558955E-02	0.	0.	0	3.150199E+02	0.	0.
19260000	6.558955E-02	0.	0.	0	3.150199E+02	0.	0.
19270000	6.558955E-02	0.	0.	0	3.150199E+02	0.	0.
19280000	6.558955E-02	0.	0.	0	3.150199E+02	0.	0.
19290000	6.558955E-02	0.	0.	0	3.150199E+02	0.	0.
19300000	6.558955E-02	0.	0.	0	3.150199E+02	0.	0.
19310000	6.558955E-02	0.	0.	0	3.150199E+02	0.	0.
19320000	6.558955E-02	0.	0.	0	3.150199E+02	0.	0.
19330000	6.558955E-02	0.	0.	0	3.150199E+02	0.	0.
19340000	6.558955E-02	0.	0.	0	3.150199E+02	0.	0.
19350000	6.558955E-02	0.	0.	0	3.150199E+02	0.	0.
19360000	6.558955E-02	0.	0.	0	3.150199E+02	0.	0.
19370000	6.558955E-02	0.	0.	0	3.150199E+02	0.	0.
19380000	6.558955E-02	0.	0.	0	3.150199E+02	0.	0.
19390000	6.558955E-02	0.	0.	0	3.150199E+02	0.	0.
19400000	6.558955E-02	0.	0.	0	3.150199E+02	0.	0.
19410000	6.558955E-02	0.	0.	0	3.150199E+02	0.	0.
19420000	6.558955E-02	0.	0.	0	3.150199E+02	0.	0.
19430000	6.558955E-02	0.	0.	0	3.150199E+02	0.	0.
19440000	6.558955E-02	0.	0.	0	3.150199E+02	0.	0.
19450000	6.558955E-02	0.	0.	0	3.150199E+02	0.	0.
19460000	6.558955E-02	0.	0.	0	3.150199E+02	0.	0.

INPUT DATA FOR COMPONENT 20, JUNCTION SNGLJUN , HAVING 0 VOLUMES AND 1 JUNCTIONS

JUN.NO.	FROM VOL.	TO VOL.	JUNCTION AREA (M2)	FORWARD LOSS COEFFICIENT	REVERSE LOSS COEFFICIENT	JUNCTION FLAGS
20000000	19010000	21000000	0.	0.	0.	0

JUN.NO.	INIT. LIQ. FLOW (KG/SEC)	INIT. VAP. FLOW (KG/SEC)	INTERFACE VEL. (M/SEC)
20000000	3.150199E+02	0.	0.

INPUT DATA FOR COMPONENT 21, 12 SCH80 PIPE , HAVING 22 VOLUMES AND 21 JUNCTIONS

VOL NO.	FLOW AREA (M2)	FLOW LENGTH (M)	VOLUME (M3)	HORIZ. ANGLE (DEG)	VERT. ANGLE (DEG)	ELEV. CHNG. (M)
21010000	6.558955E-02	3.048000E-01	1.999169E-02	0.	0.	0.
21020000	6.558955E-02	3.048000E-01	1.999169E-02	0.	0.	0.
21030000	6.558955E-02	3.048000E-01	1.999169E-02	0.	0.	0.
21040000	6.558955E-02	3.048000E-01	1.999169E-02	0.	0.	0.
21050000	6.558955E-02	3.048000E-01	1.999169E-02	0.	0.	0.
21060000	6.558955E-02	3.048000E-01	1.999169E-02	0.	0.	0.
21070000	6.558955E-02	3.048000E-01	1.999169E-02	0.	0.	0.
21080000	6.558955E-02	3.048000E-01	1.999169E-02	0.	0.	0.
21090000	6.558955E-02	3.048000E-01	1.999169E-02	0.	0.	0.
21100000	6.558955E-02	3.048000E-01	1.999169E-02	0.	0.	0.
21110000	6.558955E-02	3.048000E-01	1.999169E-02	0.	0.	0.
21120000	6.558955E-02	3.048000E-01	1.999169E-02	0.	0.	0.
21130000	6.558955E-02	3.048000E-01	1.999169E-02	0.	0.	0.
21140000	6.558955E-02	3.048000E-01	1.999169E-02	0.	0.	0.
21150000	6.558955E-02	3.048000E-01	1.999169E-02	0.	0.	0.
21160000	6.558955E-02	3.048000E-01	1.999169E-02	0.	0.	0.
21170000	6.558955E-02	3.048000E-01	1.999169E-02	0.	0.	0.
21180000	6.558955E-02	3.048000E-01	1.999169E-02	0.	0.	0.
21190000	6.558955E-02	3.048000E-01	1.999169E-02	0.	0.	0.
21200000	6.558955E-02	3.048000E-01	1.999169E-02	0.	0.	0.
21210000	6.558955E-02	3.048000E-01	1.999169E-02	0.	0.	0.
21220000	6.558955E-02	3.048000E-01	1.999169E-02	0.	0.	0.

VOL NO.	ROUGHNESS (M)	HYDRAULIC DIAM. (M)	VOLUME FLAGS	INIT. COND. FLAG	I.C. VALUE 1	I.C. VALUE 2	I.C. VALUE 3
21010000	4.572000E-05	2.889831E-01	0	0	1.000000E+03	4.084400E+02	0.
21020000	4.572000E-05	2.889831E-01	0	0	1.000000E+03	4.084400E+02	0.
21030000	4.572000E-05	2.889831E-01	0	0	1.000000E+03	4.084400E+02	0.
21040000	4.572000E-05	2.889831E-01	0	0	1.000000E+03	4.084400E+02	0.
21050000	4.572000E-05	2.889831E-01	0	0	1.000000E+03	4.084400E+02	0.
21060000	4.572000E-05	2.889831E-01	0	0	1.000000E+03	4.084400E+02	0.
21070000	4.572000E-05	2.889831E-01	0	0	1.000000E+03	4.084400E+02	0.
21080000	4.572000E-05	2.889831E-01	0	0	1.000000E+03	4.084400E+02	0.
21090000	4.572000E-05	2.889831E-01	0	0	1.000000E+03	4.084400E+02	0.
21100000	4.572000E-05	2.889831E-01	0	0	1.000000E+03	4.084400E+02	0.
21110000	4.572000E-05	2.889831E-01	0	0	1.000000E+03	4.084400E+02	0.
21120000	4.572000E-05	2.889831E-01	0	0	1.000000E+03	4.084400E+02	0.
21130000	4.572000E-05	2.889831E-01	0	0	1.000000E+03	4.084400E+02	0.
21140000	4.572000E-05	2.889831E-01	0	0	1.000000E+03	4.084400E+02	0.
21150000	4.572000E-05	2.889831E-01	0	0	1.000000E+03	4.084400E+02	0.
21160000	4.572000E-05	2.889831E-01	0	0	1.000000E+03	4.084400E+02	0.
21170000	4.572000E-05	2.889831E-01	0	0	1.000000E+03	4.084400E+02	0.
21180000	4.572000E-05	2.889831E-01	0	0	1.000000E+03	4.084400E+02	0.
21190000	4.572000E-05	2.889831E-01	0	0	1.000000E+03	4.084400E+02	0.
21200000	4.572000E-05	2.889831E-01	0	0	1.000000E+03	4.084400E+02	0.
21210000	4.572000E-05	2.889831E-01	0	0	1.000000E+03	4.084400E+02	0.
21220000	4.572000E-05	2.889831E-01	0	0	1.000000E+03	4.084400E+02	0.

JUN.NO.	JUNCTION AREA (M2)	FORWARD LOSS COEFFICIENT	REVERSE LOSS COEFFICIENT	JUNCTION FLAGS	INIT. LIQ. FLOW (KG/SEC)	INIT. VAP. FLOW (KG/SEC)	INTERFACE VEL. (M/SEC)
21010000	6.558955E-02	0.	0.	0	3.150199E+02	0.	0.
21020000	6.558955E-02	0.	0.	0	3.150199E+02	0.	0.
21030000	6.558955E-02	0.	0.	0	3.150199E+02	0.	0.
21040000	6.558955E-02	0.	0.	0	3.150199E+02	0.	0.
21050000	6.558955E-02	0.	0.	0	3.150199E+02	0.	0.
21060000	6.558955E-02	0.	0.	0	3.150199E+02	0.	0.

21070000	6.558955E-02	0.	0.	0	3.150199E+02	0.	0.
21080000	6.558955E-02	0.	0.	0	3.150199E+02	0.	0.
21090000	6.558955E-02	0.	0.	0	3.150199E+02	0.	0.
21100000	6.558955E-02	0.	0.	0	3.150199E+02	0.	0.
21110000	6.558955E-02	0.	0.	0	3.150199E+02	0.	0.
21120000	6.558955E-02	0.	0.	0	3.150199E+02	0.	0.
21130000	6.558955E-02	0.	0.	0	3.150199E+02	0.	0.
21140000	6.558955E-02	0.	0.	0	3.150199E+02	0.	0.
21150000	6.558955E-02	0.	0.	0	3.150199E+02	0.	0.
21160000	6.558955E-02	0.	0.	0	3.150199E+02	0.	0.
21170000	6.558955E-02	0.	0.	0	3.150199E+02	0.	0.
21180000	6.558955E-02	0.	0.	0	3.150199E+02	0.	0.
21190000	6.558955E-02	0.	0.	0	3.150199E+02	0.	0.
21200000	6.558955E-02	0.	0.	0	3.150199E+02	0.	0.
21210000	6.558955E-02	0.	0.	0	3.150199E+02	0.	0.

INPUT DATA FOR COMPONENT 22, JUNCTION SNGLJUN , HAVING 0 VOLUMES AND 1 JUNCTIONS

JUN.NO.	FROM VOL.	TO VOL.	JUNCTION AREA (M2)	FORWARD LOSS COEFFICIENT	REVERSE LOSS COEFFICIENT	JUNCTION FLAGS
22000000	21010000	23000000	0.	0.	0.	0

JUN.NO.	INIT. LIQ. FLOW (KG/SEC)	INIT. VAP. FLOW (KG/SEC)	INTERFACE VEL. (M/SEC)
22000000	3.150199E+02	0.	0.

INPUT DATA FOR COMPONENT 23, 12 SCH80 PIPE , HAVING 16 VOLUMES AND 15 JUNCTIONS

VOL NO.	FLOW AREA (M2)	FLOW LENGTH (M)	VOLUME (M3)	HORIZ. ANGLE (DEG)	VERT. ANGLE (DEG)	ELEV. CHNG. (M)
23010000	6.558955E-02	3.048000E-01	1.999169E-02	0.	2.600000E+01	1.336155E-01
23020000	6.558955E-02	3.048000E-01	1.999169E-02	0.	2.600000E+01	1.336155E-01
23030000	6.558955E-02	3.048000E-01	1.999169E-02	0.	2.600000E+01	1.336155E-01
23040000	6.558955E-02	3.048000E-01	1.999169E-02	0.	2.600000E+01	1.336155E-01
23050000	6.558955E-02	3.048000E-01	1.999169E-02	0.	2.600000E+01	1.336155E-01
23060000	6.558955E-02	3.048000E-01	1.999169E-02	0.	2.600000E+01	1.336155E-01
23070000	6.558955E-02	3.048000E-01	1.999169E-02	0.	2.600000E+01	1.336155E-01
23080000	6.558955E-02	3.048000E-01	1.999169E-02	0.	2.600000E+01	1.336155E-01
23090000	6.558955E-02	3.048000E-01	1.999169E-02	0.	2.600000E+01	1.336155E-01
23100000	6.558955E-02	3.048000E-01	1.999169E-02	0.	2.600000E+01	1.336155E-01
23110000	6.558955E-02	3.048000E-01	1.999169E-02	0.	0.	0.
23120000	6.558955E-02	3.048000E-01	1.999169E-02	0.	0.	0.
23130000	6.558955E-02	3.048000E-01	1.999169E-02	0.	0.	0.
23140000	6.558955E-02	3.048000E-01	1.999169E-02	0.	0.	0.
23150000	6.558955E-02	3.048000E-01	1.999169E-02	0.	0.	0.
23160000	6.558955E-02	3.048000E-01	1.999169E-02	0.	0.	0.

VOL NO.	ROUGHNESS (M)	HYDRAULIC DIAM. (M)	VOLUME FLAGS	INIT. COND. FLAG	I.C. VALUE 1	I.C. VALUE 2	I.C. VALUE 3
23010000	4.572000E-05	2.889831E-01	0	0	1.000000E+03	4.084400E+02	0.
23020000	4.572000E-05	2.889831E-01	0	0	1.000000E+03	4.084400E+02	0.
23030000	4.572000E-05	2.889831E-01	0	0	1.000000E+03	4.084400E+02	0.
23040000	4.572000E-05	2.889831E-01	0	0	1.000000E+03	4.084400E+02	0.
23050000	4.572000E-05	2.889831E-01	0	0	1.000000E+03	4.084400E+02	0.
23060000	4.572000E-05	2.889831E-01	0	0	1.000000E+03	4.084400E+02	0.
23070000	4.572000E-05	2.889831E-01	0	0	1.000000E+03	4.084400E+02	0.
23080000	4.572000E-05	2.889831E-01	0	0	1.000000E+03	4.084400E+02	0.
23090000	4.572000E-05	2.889831E-01	0	0	1.000000E+03	4.084400E+02	0.
23100000	4.572000E-05	2.889831E-01	0	0	1.000000E+03	4.084400E+02	0.
23110000	4.572000E-05	2.889831E-01	0	0	1.000000E+03	4.084400E+02	0.
23120000	4.572000E-05	2.889831E-01	0	0	1.000000E+03	4.084400E+02	0.

23130000	4.572000E-05	2.889831E-01	0	0	1.000000E+03	4.084400E+02	0.
23140000	4.572000E-05	2.889831E-01	0	0	1.000000E+03	4.084400E+02	0.
23150000	4.572000E-05	2.889831E-01	0	0	1.000000E+03	4.084400E+02	0.
23160000	4.572000E-05	2.889831E-01	0	0	1.000000E+03	4.084400E+02	0.

JUN.NO.	JUNCTION AREA (M2)	FORWARD LOSS COEFFICIENT	REVERSE LOSS COEFFICIENT	JUNCTION FLAGS	INIT. LIQ. FLOW (KG/SEC)	INIT. VAP. FLOW (KG/SEC)	INTERFACE VEL. (M/SEC)
23010000	6.558955E-02	0.	0.	0	3.150199E+02	0.	0.
23020000	6.558955E-02	0.	0.	0	3.150199E+02	0.	0.
23030000	6.558955E-02	0.	0.	0	3.150199E+02	0.	0.
23040000	6.558955E-02	0.	0.	0	3.150199E+02	0.	0.
23050000	6.558955E-02	0.	0.	0	3.150199E+02	0.	0.
23060000	6.558955E-02	0.	0.	0	3.150199E+02	0.	0.
23070000	6.558955E-02	0.	0.	0	3.150199E+02	0.	0.
23080000	6.558955E-02	0.	0.	0	3.150199E+02	0.	0.
23090000	6.558955E-02	0.	0.	0	3.150199E+02	0.	0.
23100000	6.558955E-02	0.	0.	0	3.150199E+02	0.	0.
23110000	6.558955E-02	0.	0.	0	3.150199E+02	0.	0.
23120000	6.558955E-02	0.	0.	0	3.150199E+02	0.	0.
23130000	6.558955E-02	0.	0.	0	3.150199E+02	0.	0.
23140000	6.558955E-02	0.	0.	0	3.150199E+02	0.	0.
23150000	6.558955E-02	0.	0.	0	3.150199E+02	0.	0.

INPUT DATA FOR COMPONENT 24, JUNCTION SNGLJUN , HAVING 0 VOLUMES AND 1 JUNCTIONS

JUN.NO.	FROM VOL.	TO VOL.	JUNCTION AREA (M2)	FORWARD LOSS COEFFICIENT	REVERSE LOSS COEFFICIENT	JUNCTION FLAGS
24000000	23010000	25000000	0.	0.	0.	0

JUN.NO.	INIT. LIQ. FLOW (KG/SEC)	INIT. VAP. FLOW (KG/SEC)	INTERFACE VEL. (M/SEC)
24000000	3.150199E+02	0.	0.

INPUT DATA FOR COMPONENT 25, 12 SCH80 PIPE , HAVING 20 VOLUMES AND 19 JUNCTIONS

VOL NO.	FLOW AREA (M2)	FLOW LENGTH (M)	VOLUME (M3)	HORIZ. ANGLE (DEG)	VERT. ANGLE (DEG)	ELEV. CHNG. (M)
25010000	6.558955E-02	3.048000E-01	1.999169E-02	0.	9.000000E+01	3.048000E-01
25020000	6.558955E-02	3.048000E-01	1.999169E-02	0.	9.000000E+01	3.048000E-01
25030000	6.558955E-02	3.048000E-01	1.999169E-02	0.	9.000000E+01	3.048000E-01
25040000	6.558955E-02	3.048000E-01	1.999169E-02	0.	9.000000E+01	3.048000E-01
25050000	6.558955E-02	3.048000E-01	1.999169E-02	0.	9.000000E+01	3.048000E-01
25060000	6.558955E-02	3.048000E-01	1.999169E-02	0.	9.000000E+01	3.048000E-01
25070000	6.558955E-02	3.048000E-01	1.999169E-02	0.	9.000000E+01	3.048000E-01
25080000	6.558955E-02	3.048000E-01	1.999169E-02	0.	9.000000E+01	3.048000E-01
25090000	6.558955E-02	3.048000E-01	1.999169E-02	0.	9.000000E+01	3.048000E-01
25100000	6.558955E-02	3.048000E-01	1.999169E-02	0.	9.000000E+01	3.048000E-01
25110000	6.558955E-02	3.048000E-01	1.999169E-02	0.	9.000000E+01	3.048000E-01
25120000	6.558955E-02	3.048000E-01	1.999169E-02	0.	9.000000E+01	3.048000E-01
25130000	6.558955E-02	3.048000E-01	1.999169E-02	0.	9.000000E+01	3.048000E-01
25140000	6.558955E-02	3.048000E-01	1.999169E-02	0.	9.000000E+01	3.048000E-01
25150000	6.558955E-02	3.048000E-01	1.999169E-02	0.	9.000000E+01	3.048000E-01
25160000	6.558955E-02	3.048000E-01	1.999169E-02	0.	9.000000E+01	3.048000E-01
25170000	6.558955E-02	3.048000E-01	1.999169E-02	0.	9.000000E+01	3.048000E-01
25180000	6.558955E-02	3.048000E-01	1.999169E-02	0.	9.000000E+01	3.048000E-01
25190000	6.558955E-02	3.048000E-01	1.999169E-02	0.	9.000000E+01	3.048000E-01
25200000	6.558955E-02	3.048000E-01	1.999169E-02	0.	9.000000E+01	3.048000E-01

VOL NO.	ROUGHNESS (M)	HYDRAULIC DIAM. (M)	VOLUME FLAGS	INIT. COND. FLAG	I.C. VALUE 1	I.C. VALUE 2	I.C. VALUE 3
25010000	4.572000E-05	2.889831E-01	0	0	1.000000E+03	4.084400E+02	0.

25020000	4.572000E-05	2.889831E-01	0	0	1.000000E+03	4.084400E+02	0.
25030000	4.572000E-05	2.889831E-01	0	0	1.000000E+03	4.084400E+02	0.
25040000	4.572000E-05	2.889831E-01	0	0	1.000000E+03	4.084400E+02	0.
25050000	4.572000E-05	2.889831E-01	0	0	1.000000E+03	4.084400E+02	0.
25060000	4.572000E-05	2.889831E-01	0	0	1.000000E+03	4.084400E+02	0.
25070000	4.572000E-05	2.889831E-01	0	0	1.000000E+03	4.084400E+02	0.
25080000	4.572000E-05	2.889831E-01	0	0	1.000000E+03	4.084400E+02	0.
25090000	4.572000E-05	2.889831E-01	0	0	1.000000E+03	4.084400E+02	0.
25100000	4.572000E-05	2.889831E-01	0	0	1.000000E+03	4.084400E+02	0.
25110000	4.572000E-05	2.889831E-01	0	0	1.000000E+03	4.084400E+02	0.
25120000	4.572000E-05	2.889831E-01	0	0	1.000000E+03	4.084400E+02	0.
25130000	4.572000E-05	2.889831E-01	0	0	1.000000E+03	4.084400E+02	0.
25140000	4.572000E-05	2.889831E-01	0	0	1.000000E+03	4.084400E+02	0.
25150000	4.572000E-05	2.889831E-01	0	0	1.000000E+03	4.084400E+02	0.
25160000	4.572000E-05	2.889831E-01	0	0	1.000000E+03	4.084400E+02	0.
25170000	4.572000E-05	2.889831E-01	0	0	1.000000E+03	4.084400E+02	0.
25180000	4.572000E-05	2.889831E-01	0	0	1.000000E+03	4.084400E+02	0.
25190000	4.572000E-05	2.889831E-01	0	0	1.000000E+03	4.084400E+02	0.
25200000	4.572000E-05	2.889831E-01	0	0	1.000000E+03	4.084400E+02	0.

JUN.NO.	JUNCTION AREA (M2)	FORWARD LOSS COEFFICIENT	REVERSE LOSS COEFFICIENT	JUNCTION FLAGS	INIT. LIQ. FLOW (KG/SEC)	INIT. VAP. FLOW (KG/SEC)	INTERFACE VEL. (M/SEC)
25010000	6.558955E-02	0.	0.	0	3.150199E+02	0.	0.
25020000	6.558955E-02	0.	0.	0	3.150199E+02	0.	0.
25030000	6.558955E-02	0.	0.	0	3.150199E+02	0.	0.
25040000	6.558955E-02	0.	0.	0	3.150199E+02	0.	0.
25050000	6.558955E-02	0.	0.	0	3.150199E+02	0.	0.
25060000	6.558955E-02	0.	0.	0	3.150199E+02	0.	0.
25070000	6.558955E-02	0.	0.	0	3.150199E+02	0.	0.
25080000	6.558955E-02	0.	0.	0	3.150199E+02	0.	0.
25090000	6.558955E-02	0.	0.	0	3.150199E+02	0.	0.
25100000	6.558955E-02	0.	0.	0	3.150199E+02	0.	0.
25110000	6.558955E-02	0.	0.	0	3.150199E+02	0.	0.
25120000	6.558955E-02	0.	0.	0	3.150199E+02	0.	0.
25130000	6.558955E-02	0.	0.	0	3.150199E+02	0.	0.
25140000	6.558955E-02	0.	0.	0	3.150199E+02	0.	0.
25150000	6.558955E-02	0.	0.	0	3.150199E+02	0.	0.
25160000	6.558955E-02	0.	0.	0	3.150199E+02	0.	0.
25170000	6.558955E-02	0.	0.	0	3.150199E+02	0.	0.
25180000	6.558955E-02	0.	0.	0	3.150199E+02	0.	0.
25190000	6.558955E-02	0.	0.	0	3.150199E+02	0.	0.

INPUT DATA FOR COMPONENT 26, JUNCTION SNGLJUN , HAVING 0 VOLUMES AND 1 JUNCTIONS

JUN.NO.	FROM VOL.	TO VOL.	JUNCTION AREA (M2)	FORWARD LOSS COEFFICIENT	REVERSE LOSS COEFFICIENT	JUNCTION FLAGS
26000000	25010000	27000000	0.	0.	0.	0

JUN.NO.	INIT. LIQ. FLOW (KG/SEC)	INIT. VAP. FLOW (KG/SEC)	INTERFACE VEL. (M/SEC)
26000000	3.150199E+02	0.	0.

INPUT DATA FOR COMPONENT 27, 12 SCHED PIPE , HAVING 15 VOLUMES AND 14 JUNCTIONS

VOL NO.	FLOW AREA (M2)	FLOW LENGTH (M)	VOLUME (M3)	HORIZ. ANGLE (DEG)	VERT. ANGLE (DEG)	ELEV. CHNG. (M)
27010000	6.558955E-02	3.048000E-01	1.999169E-02	0.	9.000000E+01	3.048000E-01
27020000	6.558955E-02	3.048000E-01	1.999169E-02	0.	9.000000E+01	3.048000E-01
27030000	6.558955E-02	3.048000E-01	1.999169E-02	0.	9.000000E+01	3.048000E-01
27040000	6.558955E-02	3.048000E-01	1.999169E-02	0.	9.000000E+01	3.048000E-01
27050000	6.558955E-02	3.048000E-01	1.999169E-02	0.	9.000000E+01	3.048000E-01

27060000	6.558955E-02	3.048000E-01	1.999169E-02	0.	9.000000E+01	3.048000E-01	
27070000	6.558955E-02	3.048000E-01	1.999169E-02	0.	9.000000E+01	3.048000E-01	
27080000	6.558955E-02	3.048000E-01	1.999169E-02	0.	9.000000E+01	3.048000E-01	
27090000	6.558955E-02	3.048000E-01	1.999169E-02	0.	9.000000E+01	3.048000E-01	
27100000	6.558955E-02	3.048000E-01	1.999169E-02	0.	9.000000E+01	3.048000E-01	
27110000	6.558955E-02	3.048000E-01	1.999169E-02	0.	9.000000E+01	3.048000E-01	
27120000	6.558955E-02	3.048000E-01	1.999169E-02	0.	0.	0.	
27130000	6.558955E-02	3.048000E-01	1.999169E-02	0.	0.	0.	
27140000	6.558955E-02	3.048000E-01	1.999169E-02	0.	0.	0.	
27150000	6.558955E-02	3.048000E-01	1.999169E-02	0.	0.	0.	

VOL NO.	ROUGHNESS (M)	HYDRAULIC DIAM. (M)	VOLUME FLAGS	INIT. COND. FLAG	I.C. VALUE 1	I.C. VALUE 2	I.C. VALUE 3
27010000	4.572000E-05	2.889831E-01	0	0	1.000000E+03	4.084400E+02	0.
27020000	4.572000E-05	2.889831E-01	0	0	1.000000E+03	4.084400E+02	0.
27030000	4.572000E-05	2.889831E-01	0	0	1.000000E+03	4.084400E+02	0.
27040000	4.572000E-05	2.889831E-01	0	0	1.000000E+03	4.084400E+02	0.
27050000	4.572000E-05	2.889831E-01	0	0	1.000000E+03	4.084400E+02	0.
27060000	4.572000E-05	2.889831E-01	0	0	1.000000E+03	4.084400E+02	0.
27070000	4.572000E-05	2.889831E-01	0	0	1.000000E+03	4.084400E+02	0.
27080000	4.572000E-05	2.889831E-01	0	0	1.000000E+03	4.084400E+02	0.
27090000	4.572000E-05	2.889831E-01	0	0	1.000000E+03	4.084400E+02	0.
27100000	4.572000E-05	2.889831E-01	0	0	1.000000E+03	4.084400E+02	0.
27110000	4.572000E-05	2.889831E-01	0	0	1.000000E+03	4.084400E+02	0.
27120000	4.572000E-05	2.889831E-01	0	0	1.000000E+03	4.084400E+02	0.
27130000	4.572000E-05	2.889831E-01	0	0	1.000000E+03	4.084400E+02	0.
27140000	4.572000E-05	2.889831E-01	0	0	1.000000E+03	4.084400E+02	0.
27150000	4.572000E-05	2.889831E-01	0	0	1.000000E+03	4.084400E+02	0.

JUN.NO.	JUNCTION AREA (M2)	FORWARD LOSS COEFFICIENT	REVERSE LOSS COEFFICIENT	JUNCTION FLAGS	INIT. LIQ. VEL. (M/SEC)	INIT. VAP. VEL. (M/SEC)	INTERFACE VEL. (M/SEC)
27010000	6.558955E-02	0.	0.	0	5.712897E+00	5.712897E+00	0.
27020000	6.558955E-02	0.	0.	0	5.712897E+00	5.712897E+00	0.
27030000	6.558955E-02	0.	0.	0	5.712897E+00	5.712897E+00	0.
27040000	6.558955E-02	0.	0.	0	5.712897E+00	5.712897E+00	0.
27050000	6.558955E-02	0.	0.	0	5.712897E+00	5.712897E+00	0.
27060000	6.558955E-02	0.	0.	0	5.712897E+00	5.712897E+00	0.
27070000	6.558955E-02	0.	0.	0	5.712897E+00	5.712897E+00	0.
27080000	6.558955E-02	0.	0.	0	5.712897E+00	5.712897E+00	0.
27090000	6.558955E-02	0.	0.	0	5.712897E+00	5.712897E+00	0.
27100000	6.558955E-02	0.	0.	0	5.712897E+00	5.712897E+00	0.
27110000	6.558955E-02	0.	0.	0	5.712897E+00	5.712897E+00	0.
27120000	6.558955E-02	0.	0.	0	5.712897E+00	5.712897E+00	0.
27130000	6.558955E-02	0.	0.	0	5.712897E+00	5.712897E+00	0.
27140000	6.558955E-02	0.	0.	0	5.712897E+00	5.712897E+00	0.

1215 274

INPUT DATA FOR COMPONENT 28, BDY JUN SNGLJUN , HAVING 0 VOLUMES AND 1 JUNCTIONS

JUN.NO.	FROM VOL.	TO VOL.	JUNCTION AREA (M2)	FORWARD LOSS COEFFICIENT	REVERSE LOSS COEFFICIENT	JUNCTION FLAGS
28000000	27010000	29000000	6.224504E-02	0.	0.	0

JUN.NO.	INIT. LIQ. VEL. (M/SEC)	INIT. VAP. VEL. (M/SEC)	INTERFACE VEL. (M/SEC)
28000000	6.019830E+00	6.019830E+00	0.

INPUT DATA FOR COMPONENT 29, BDY VOL TMDPVOL , HAVING 1 VOLUMES AND 0 JUNCTIONS

VOL NO.	FLOW AREA (M2)	FLOW LENGTH (M)	VOLUME (M3)	HORIZ. ANGLE (DEG)	VERT. ANGLE (DEG)	ELEV. CHNG. (M)
29010000	1.858061E+00	3.048000E-01	5.663369E-01	0.	0.	0.

B22

VOL.NO.	ROUGHNESS (F)	HYDRAULIC DIAM. (M)	EQUIL. FLAG
29010000	4.572000E-05	1.538102E+00	0

TIME DEPENDENT DATA

TIME (SEC)	PRESSURE (PA)	INTERNAL ENERGY (J/KG)	STATIC QUALITY
0.	6.894757E+06	9.500314E+05	0.
1.000000E-01	6.894757E+06	9.500314E+05	0.

ATTEMPTED ADV: TOT.=	0	EDIT=	0	MIN.DT=	0.	SEC	LAST DT=	1.000000E-03	SEC	MS.ERR=	0.	KG			
REPEATED ADV: TOT.=	0	EDIT=	0	MAX.DT=	1.000000E-03	SEC	CRNT.DT=	0.	SEC	TOT.MS=	3.693984E+03	KG			
SUCCESSFUL ADV: TOT.=	0	EDIT=	0	AVG.DT=	0.	SEC	ERR.EST=	0.		M.RATE=	0.				
REQUESTED ADV: TOT.=	0	EDIT=	0	REQ.DT=	1.000000E-03	SEC	CPU=	1.760000E+00	SEC	TIME=	0.	SEC			

VOL.NO.	PRESSURE (PA)	INT. ENERGY (J/KG)	STATIC QUAL.	EQU.QUAL.	TEMPF (K)	TEMPG (K)	TEMPE (K)	VOLUME (M3)	VOLUME FLAGS
BREAK TMDPVOL	COMPONENT								
2010000	9.99740E+04	2.50605E+06	1.00000E+00	1.00000E+00	3.72774E+02	3.72774E+02	3.72774E+02	0.	0
18 SCH120	PIPE	COMPONENT							
4010000	6.89476E+06	9.50031E+05	0.	0.	4.96021E+02	5.57917E+02	4.96021E+02	1.79670E-02	0
4020000	6.89476E+06	9.50031E+05	0.	0.	4.96021E+02	5.57917E+02	4.96021E+02	1.79670E-02	0
4030000	6.89476E+06	9.50031E+05	0.	0.	4.96021E+02	5.57917E+02	4.96021E+02	1.79670E-02	0
4040000	6.89476E+06	9.50031E+05	0.	0.	4.96021E+02	5.57917E+02	4.96021E+02	1.79670E-02	0
4050000	6.89476E+06	9.50031E+05	0.	0.	4.96021E+02	5.57917E+02	4.96021E+02	1.79670E-02	0
4060000	6.89476E+06	9.50031E+05	0.	0.	4.96021E+02	5.57917E+02	4.96021E+02	1.79670E-02	0
4070000	6.89476E+06	9.50031E+05	0.	0.	4.96021E+02	5.57917E+02	4.96021E+02	1.79670E-02	0
4080000	6.89476E+06	9.50031E+05	0.	0.	4.96021E+02	5.57917E+02	4.96021E+02	1.79670E-02	0
4090000	6.89476E+06	9.50031E+05	0.	0.	4.96021E+02	5.57917E+02	4.96021E+02	1.79670E-02	0
4100000	6.89476E+06	9.50031E+05	0.	0.	4.96021E+02	5.57917E+02	4.96021E+02	1.79670E-02	0
4110000	6.89476E+06	9.50031E+05	0.	0.	4.96021E+02	5.57917E+02	4.96021E+02	1.79670E-02	0
4120000	6.89476E+06	9.50031E+05	0.	0.	4.96021E+02	5.57917E+02	4.96021E+02	1.79670E-02	0
4130000	6.89476E+06	9.50031E+05	0.	0.	4.96021E+02	5.57917E+02	4.96021E+02	1.79670E-02	0
4140000	6.89476E+06	9.50031E+05	0.	0.	4.96021E+02	5.57917E+02	4.96021E+02	1.79670E-02	0
4150000	6.89476E+06	9.50031E+05	0.	0.	4.96021E+02	5.57917E+02	4.96021E+02	1.79670E-02	0
4160000	6.89476E+06	9.50031E+05	0.	0.	4.96021E+02	5.57917E+02	4.96021E+02	1.79670E-02	0
4170000	6.89476E+06	9.50031E+05	0.	0.	4.96021E+02	5.57917E+02	4.96021E+02	1.79670E-02	0
4180000	6.89476E+06	9.50031E+05	0.	0.	4.96021E+02	5.57917E+02	4.96021E+02	1.79670E-02	0
4190000	6.89476E+06	9.50031E+05	0.	0.	4.96021E+02	5.57917E+02	4.96021E+02	1.79670E-02	0
4200000	6.89476E+06	9.50031E+05	0.	0.	4.96021E+02	5.57917E+02	4.96021E+02	1.79670E-02	0
4210000	6.89476E+06	9.50031E+05	0.	0.	4.96021E+02	5.57917E+02	4.96021E+02	1.79670E-02	0
4220000	6.89476E+06	9.50031E+05	0.	0.	4.96021E+02	5.57917E+02	4.96021E+02	1.79670E-02	0
4230000	6.89476E+06	9.50031E+05	0.	0.	4.96021E+02	5.57917E+02	4.96021E+02	1.79670E-02	0
4240000	6.89476E+06	9.50031E+05	0.	0.	4.96021E+02	5.57917E+02	4.96021E+02	1.79670E-02	0
4250000	6.89476E+06	9.50031E+05	0.	0.	4.96021E+02	5.57917E+02	4.96021E+02	1.79670E-02	0
4260000	6.89476E+06	9.50031E+05	0.	0.	4.96021E+02	5.57917E+02	4.96021E+02	1.79670E-02	0
4270000	6.89476E+06	9.50031E+05	0.	0.	4.96021E+02	5.57917E+02	4.96021E+02	1.79670E-02	0
4280000	6.89476E+06	9.50031E+05	0.	0.	4.96021E+02	5.57917E+02	4.96021E+02	1.79670E-02	0
4290000	6.89476E+06	9.50031E+05	0.	0.	4.96021E+02	5.57917E+02	4.96021E+02	1.79670E-02	0
18 SCH120	PIPE	COMPONENT							
6010000	6.89476E+06	9.50031E+05	0.	0.	4.96021E+02	5.57917E+02	4.96021E+02	1.79670E-02	0
6020000	6.89476E+06	9.50031E+05	0.	0.	4.96021E+02	5.57917E+02	4.96021E+02	1.79670E-02	0
6030000	6.89476E+06	9.50031E+05	0.	0.	4.96021E+02	5.57917E+02	4.96021E+02	1.79670E-02	0
6040000	6.89476E+06	9.50031E+05	0.	0.	4.96021E+02	5.57917E+02	4.96021E+02	1.79670E-02	0
6050000	6.89476E+06	9.50031E+05	0.	0.	4.96021E+02	5.57917E+02	4.96021E+02	1.79670E-02	0
6060000	6.89476E+06	9.50031E+05	0.	0.	4.96021E+02	5.57917E+02	4.96021E+02	1.79670E-02	0
6070000	6.89476E+06	9.50031E+05	0.	0.	4.96021E+02	5.57917E+02	4.96021E+02	1.79670E-02	0
6080000	6.89476E+06	9.50031E+05	0.	0.	4.96021E+02	5.57917E+02	4.96021E+02	1.79670E-02	0
6090000	6.89476E+06	9.50031E+05	0.	0.	4.96021E+02	5.57917E+02	4.96021E+02	1.79670E-02	0
6100000	6.89476E+06	9.50031E+05	0.	0.	4.96021E+02	5.57917E+02	4.96021E+02	1.79670E-02	0
6110000	6.89476E+06	9.50031E+05	0.	0.	4.96021E+02	5.57917E+02	4.96021E+02	1.79670E-02	0
6120000	6.89476E+06	9.50031E+05	0.	0.	4.96021E+02	5.57917E+02	4.96021E+02	1.79670E-02	0
6130000	6.89476E+06	9.50031E+05	0.	0.	4.96021E+02	5.57917E+02	4.96021E+02	1.79670E-02	0
6140000	6.89476E+06	9.50031E+05	0.	0.	4.96021E+02	5.57917E+02	4.96021E+02	1.79670E-02	0
6150000	6.89476E+06	9.50031E+05	0.	0.	4.96021E+02	5.57917E+02	4.96021E+02	1.79670E-02	0
18 SCH100	PIPE	COMPONENT							
8010000	6.89476E+06	9.50031E+05	0.	0.	4.96021E+02	5.57917E+02	4.96021E+02	1.90006E-02	0
8020000	6.89476E+06	9.50031E+05	0.	0.	4.96021E+02	5.57917E+02	4.96021E+02	1.90006E-02	0
8030000	6.89476E+06	9.50031E+05	0.	0.	4.96021E+02	5.57917E+02	4.96021E+02	1.90006E-02	0
8040000	6.89476E+06	9.50031E+05	0.	0.	4.96021E+02	5.57917E+02	4.96021E+02	1.90006E-02	0
8050000	6.89476E+06	9.50031E+05	0.	0.	4.96021E+02	5.57917E+02	4.96021E+02	1.90006E-02	0

80600000	6.89476E+06	9.50031E+05	0.	0.	4.96021E+02	5.57917E+02	4.96021E+02	1.90006E-02	0
80700000	6.89476E+06	9.50031E+05	0.	0.	4.96021E+02	5.57917E+02	4.96021E+02	1.90006E-02	0
80800000	6.89476E+06	9.50031E+05	0.	0.	4.96021E+02	5.57917E+02	4.96021E+02	1.90006E-02	0
80900000	6.89476E+06	9.50031E+05	0.	0.	4.96021E+02	5.57917E+02	4.96021E+02	1.90006E-02	0
81000000	6.89476E+06	9.50031E+05	0.	0.	4.96021E+02	5.57917E+02	4.96021E+02	1.90006E-02	0
TEE	PLENUM	COMPONENT							
90100000	6.89476E+06	9.50031E+05	0.	0.	4.96021E+02	5.57917E+02	4.96021E+02	1.44647E-01	0
12 SCH80	PIPE	COMPONENT							
100100000	6.89476E+06	9.50031E+05	0.	0.	4.96021E+02	5.57917E+02	4.96021E+02	9.99585E-03	0
100200000	6.89476E+06	9.50031E+05	0.	0.	4.96021E+02	5.57917E+02	4.96021E+02	9.99585E-03	0
100300000	6.89476E+06	9.50031E+05	0.	0.	4.96021E+02	5.57917E+02	4.96021E+02	9.99585E-03	0
100400000	6.89476E+06	9.50031E+05	0.	0.	4.96021E+02	5.57917E+02	4.96021E+02	9.99585E-03	0
100500000	6.89476E+06	9.50031E+05	0.	0.	4.96021E+02	5.57917E+02	4.96021E+02	9.99585E-03	0
100600000	6.89476E+06	9.50031E+05	0.	0.	4.96021E+02	5.57917E+02	4.96021E+02	9.99585E-03	0
100700000	6.89476E+06	9.50031E+05	0.	0.	4.96021E+02	5.57917E+02	4.96021E+02	9.99585E-03	0
100800000	6.89476E+06	9.50031E+05	0.	0.	4.96021E+02	5.57917E+02	4.96021E+02	9.99585E-03	0
100900000	6.89476E+06	9.50031E+05	0.	0.	4.96021E+02	5.57917E+02	4.96021E+02	9.99585E-03	0
101000000	6.89476E+06	9.50031E+05	0.	0.	4.96021E+02	5.57917E+02	4.96021E+02	9.99585E-03	0
101100000	6.89476E+06	9.50031E+05	0.	0.	4.96021E+02	5.57917E+02	4.96021E+02	9.99585E-03	0
101200000	6.89476E+06	9.50031E+05	0.	0.	4.96021E+02	5.57917E+02	4.96021E+02	9.99585E-03	0
101300000	6.89476E+06	9.50031E+05	0.	0.	4.96021E+02	5.57917E+02	4.96021E+02	9.99585E-03	0
101400000	6.89476E+06	9.50031E+05	0.	0.	4.96021E+02	5.57917E+02	4.96021E+02	9.99585E-03	0
101500000	6.89476E+06	9.50031E+05	0.	0.	4.96021E+02	5.57917E+02	4.96021E+02	9.99585E-03	0
101600000	6.89476E+06	9.50031E+05	0.	0.	4.96021E+02	5.57917E+02	4.96021E+02	9.99585E-03	0
101700000	6.89476E+06	9.50031E+05	0.	0.	4.96021E+02	5.57917E+02	4.96021E+02	9.99585E-03	0
101800000	6.89476E+06	9.50031E+05	0.	0.	4.96021E+02	5.57917E+02	4.96021E+02	9.99585E-03	0
101900000	6.89476E+06	9.50031E+05	0.	0.	4.96021E+02	5.57917E+02	4.96021E+02	9.99585E-03	0
102000000	6.89476E+06	9.50031E+05	0.	0.	4.96021E+02	5.57917E+02	4.96021E+02	9.99585E-03	0
102100000	6.89476E+06	9.50031E+05	0.	0.	4.96021E+02	5.57917E+02	4.96021E+02	9.99585E-03	0
102200000	6.89476E+06	9.50031E+05	0.	0.	4.96021E+02	5.57917E+02	4.96021E+02	9.99585E-03	0
102300000	6.89476E+06	9.50031E+05	0.	0.	4.96021E+02	5.57917E+02	4.96021E+02	9.99585E-03	0
102400000	6.89476E+06	9.50031E+05	0.	0.	4.96021E+02	5.57917E+02	4.96021E+02	9.99585E-03	0
102500000	6.89476E+06	9.50031E+05	0.	0.	4.96021E+02	5.57917E+02	4.96021E+02	9.99585E-03	0
102600000	6.89476E+06	9.50031E+05	0.	0.	4.96021E+02	5.57917E+02	4.96021E+02	9.99585E-03	0
102700000	6.89476E+06	9.50031E+05	0.	0.	4.96021E+02	5.57917E+02	4.96021E+02	9.99585E-03	0
102800000	6.89476E+06	9.50031E+05	0.	0.	4.96021E+02	5.57917E+02	4.96021E+02	9.99585E-03	0
102900000	6.89476E+06	9.50031E+05	0.	0.	4.96021E+02	5.57917E+02	4.96021E+02	9.99585E-03	0
103000000	6.89476E+06	9.50031E+05	0.	0.	4.96021E+02	5.57917E+02	4.96021E+02	9.99585E-03	0
12 SCH80	PIPE	COMPONENT							
120100000	6.89476E+06	9.50031E+05	0.	0.	4.96021E+02	5.57917E+02	4.96021E+02	1.99917E-02	0
120200000	6.89476E+06	9.50031E+05	0.	0.	4.96021E+02	5.57917E+02	4.96021E+02	1.99917E-02	0
120300000	6.89476E+06	9.50031E+05	0.	0.	4.96021E+02	5.57917E+02	4.96021E+02	1.99917E-02	0
120400000	6.89476E+06	9.50031E+05	0.	0.	4.96021E+02	5.57917E+02	4.96021E+02	1.99917E-02	0
120500000	6.89476E+06	9.50031E+05	0.	0.	4.96021E+02	5.57917E+02	4.96021E+02	1.99917E-02	0
120600000	6.89476E+06	9.50031E+05	0.	0.	4.96021E+02	5.57917E+02	4.96021E+02	1.99917E-02	0
120700000	6.89476E+06	9.50031E+05	0.	0.	4.96021E+02	5.57917E+02	4.96021E+02	1.99917E-02	0
120800000	6.89476E+06	9.50031E+05	0.	0.	4.96021E+02	5.57917E+02	4.96021E+02	1.99917E-02	0
120900000	6.89476E+06	9.50031E+05	0.	0.	4.96021E+02	5.57917E+02	4.96021E+02	1.99917E-02	0
121000000	6.89476E+06	9.50031E+05	0.	0.	4.96021E+02	5.57917E+02	4.96021E+02	1.99917E-02	0
121100000	6.89476E+06	9.50031E+05	0.	0.	4.96021E+02	5.57917E+02	4.96021E+02	1.99917E-02	0
121200000	6.89476E+06	9.50031E+05	0.	0.	4.96021E+02	5.57917E+02	4.96021E+02	1.99917E-02	0
121300000	6.89476E+06	9.50031E+05	0.	0.	4.96021E+02	5.57917E+02	4.96021E+02	1.99917E-02	0
121400000	6.89476E+06	9.50031E+05	0.	0.	4.96021E+02	5.57917E+02	4.96021E+02	1.99917E-02	0
121500000	6.89476E+06	9.50031E+05	0.	0.	4.96021E+02	5.57917E+02	4.96021E+02	1.99917E-02	0
121600000	6.89476E+06	9.50031E+05	0.	0.	4.96021E+02	5.57917E+02	4.96021E+02	1.99917E-02	0
121700000	6.89476E+06	9.50031E+05	0.	0.	4.96021E+02	5.57917E+02	4.96021E+02	1.99917E-02	0
12 SCH80	PIPE	COMPONENT							
140100000	6.89476E+06	9.50031E+05	0.	0.	4.96021E+02	5.57917E+02	4.96021E+02	1.99917E-02	0
140200000	6.89476E+06	9.50031E+05	0.	0.	4.96021E+02	5.57917E+02	4.96021E+02	1.99917E-02	0
140300000	6.89476E+06	9.50031E+05	0.	0.	4.96021E+02	5.57917E+02	4.96021E+02	1.99917E-02	0
140400000	6.89476E+06	9.50031E+05	0.	0.	4.96021E+02	5.57917E+02	4.96021E+02	1.99917E-02	0

1215 278

14050000	6.89476E+06	9.50031E+05	0.	0.	4.96021E+02	5.57917E+02	4.96021E+02	1.99917E-02	0
14060000	6.89476E+06	9.50031E+05	0.	0.	4.96021E+02	5.57917E+02	4.96021E+02	1.99917E-02	0
14070000	6.89476E+06	9.50031E+05	0.	0.	4.96021E+02	5.57917E+02	4.96021E+02	1.99917E-02	0
14080000	6.89476E+06	9.50031E+05	0.	0.	4.96021E+02	5.57917E+02	4.96021E+02	1.99917E-02	0
14090000	6.89476E+06	9.50031E+05	0.	0.	4.96021E+02	5.57917E+02	4.96021E+02	1.99917E-02	0
14100000	6.89476E+06	9.50031E+05	0.	0.	4.96021E+02	5.57917E+02	4.96021E+02	1.99917E-02	0
14110000	6.89476E+06	9.50031E+05	0.	0.	4.96021E+02	5.57917E+02	4.96021E+02	1.99917E-02	0
14120000	6.89476E+06	9.50031E+05	0.	0.	4.96021E+02	5.57917E+02	4.96021E+02	1.99917E-02	0
14130000	6.89476E+06	9.50031E+05	0.	0.	4.96021E+02	5.57917E+02	4.96021E+02	1.99917E-02	0
14140000	6.89476E+06	9.50031E+05	0.	0.	4.96021E+02	5.57917E+02	4.96021E+02	1.99917E-02	0
14150000	6.89476E+06	9.50031E+05	0.	0.	4.96021E+02	5.57917E+02	4.96021E+02	1.99917E-02	0
14160000	6.89476E+06	9.50031E+05	0.	0.	4.96021E+02	5.57917E+02	4.96021E+02	1.99917E-02	0
14170000	6.89476E+06	9.50031E+05	0.	0.	4.96021E+02	5.57917E+02	4.96021E+02	1.99917E-02	0
14180000	6.89476E+06	9.50031E+05	0.	0.	4.96021E+02	5.57917E+02	4.96021E+02	1.99917E-02	0
14190000	6.89476E+06	9.50031E+05	0.	0.	4.96021E+02	5.57917E+02	4.96021E+02	1.99917E-02	0
14200000	6.89476E+06	9.50031E+05	0.	0.	4.96021E+02	5.57917E+02	4.96021E+02	1.99917E-02	0
12 SCH80	PIPE	COMPONENT							
16010000	6.89476E+06	9.50031E+05	0.	0.	4.96021E+02	5.57917E+02	4.96021E+02	1.99917E-02	0
16020000	6.89476E+06	9.50031E+05	0.	0.	4.96021E+02	5.57917E+02	4.96021E+02	1.99917E-02	0
16030000	6.89476E+06	9.50031E+05	0.	0.	4.96021E+02	5.57917E+02	4.96021E+02	1.99917E-02	0
16040000	6.89476E+06	9.50031E+05	0.	0.	4.96021E+02	5.57917E+02	4.96021E+02	1.99917E-02	0
16050000	6.89476E+06	9.50031E+05	0.	0.	4.96021E+02	5.57917E+02	4.96021E+02	1.99917E-02	0
16060000	6.89476E+06	9.50031E+05	0.	0.	4.96021E+02	5.57917E+02	4.96021E+02	1.99917E-02	0
16070000	6.89476E+06	9.50031E+05	0.	0.	4.96021E+02	5.57917E+02	4.96021E+02	1.99917E-02	0
16080000	6.89476E+06	9.50031E+05	0.	0.	4.96021E+02	5.57917E+02	4.96021E+02	1.99917E-02	0
16090000	6.89476E+06	9.50031E+05	0.	0.	4.96021E+02	5.57917E+02	4.96021E+02	1.99917E-02	0
16100000	6.89476E+06	9.50031E+05	0.	0.	4.96021E+02	5.57917E+02	4.96021E+02	1.99917E-02	0
16110000	6.89476E+06	9.50031E+05	0.	0.	4.96021E+02	5.57917E+02	4.96021E+02	1.99917E-02	0
16120000	6.89476E+06	9.50031E+05	0.	0.	4.96021E+02	5.57917E+02	4.96021E+02	1.99917E-02	0
16130000	6.89476E+06	9.50031E+05	0.	0.	4.96021E+02	5.57917E+02	4.96021E+02	1.99917E-02	0
16140000	6.89476E+06	9.50031E+05	0.	0.	4.96021E+02	5.57917E+02	4.96021E+02	1.99917E-02	0
16150000	6.89476E+06	9.50031E+05	0.	0.	4.96021E+02	5.57917E+02	4.96021E+02	1.99917E-02	0
BDY VOL	TMDPVOL	COMPONENT							
18010000	6.89476E+06	9.50031E+05	0.	0.	4.96021E+02	5.57917E+02	4.96021E+02	0.	0
12 SCH80	PIPE	COMPONENT							
19010000	6.89476E+06	9.50031E+05	0.	0.	4.96021E+02	5.57917E+02	4.96021E+02	9.99585E-03	0
19020000	6.89476E+06	9.50031E+05	0.	0.	4.96021E+02	5.57917E+02	4.96021E+02	9.99585E-03	0
19030000	6.89476E+06	9.50031E+05	0.	0.	4.96021E+02	5.57917E+02	4.96021E+02	9.99585E-03	0
19040000	6.89476E+06	9.50031E+05	0.	0.	4.96021E+02	5.57917E+02	4.96021E+02	9.99585E-03	0
19050000	6.89476E+06	9.50031E+05	0.	0.	4.96021E+02	5.57917E+02	4.96021E+02	9.99585E-03	0
19060000	6.89476E+06	9.50031E+05	0.	0.	4.96021E+02	5.57917E+02	4.96021E+02	9.99585E-03	0
19070000	6.89476E+06	9.50031E+05	0.	0.	4.96021E+02	5.57917E+02	4.96021E+02	9.99585E-03	0
19080000	6.89476E+06	9.50031E+05	0.	0.	4.96021E+02	5.57917E+02	4.96021E+02	9.99585E-03	0
19090000	6.89476E+06	9.50031E+05	0.	0.	4.96021E+02	5.57917E+02	4.96021E+02	9.99585E-03	0
19100000	6.89476E+06	9.50031E+05	0.	0.	4.96021E+02	5.57917E+02	4.96021E+02	9.99585E-03	0
19110000	6.89476E+06	9.50031E+05	0.	0.	4.96021E+02	5.57917E+02	4.96021E+02	9.99585E-03	0
19120000	6.89476E+06	9.50031E+05	0.	0.	4.96021E+02	5.57917E+02	4.96021E+02	9.99585E-03	0
19130000	6.89476E+06	9.50031E+05	0.	0.	4.96021E+02	5.57917E+02	4.96021E+02	9.99585E-03	0
19140000	6.89476E+06	9.50031E+05	0.	0.	4.96021E+02	5.57917E+02	4.96021E+02	9.99585E-03	0
19150000	6.89476E+06	9.50031E+05	0.	0.	4.96021E+02	5.57917E+02	4.96021E+02	9.99585E-03	0
19160000	6.89476E+06	9.50031E+05	0.	0.	4.96021E+02	5.57917E+02	4.96021E+02	9.99585E-03	0
19170000	6.89476E+06	9.50031E+05	0.	0.	4.96021E+02	5.57917E+02	4.96021E+02	9.99585E-03	0
19180000	6.89476E+06	9.50031E+05	0.	0.	4.96021E+02	5.57917E+02	4.96021E+02	9.99585E-03	0
19190000	6.89476E+06	9.50031E+05	0.	0.	4.96021E+02	5.57917E+02	4.96021E+02	9.99585E-03	0
19200000	6.89476E+06	9.50031E+05	0.	0.	4.96021E+02	5.57917E+02	4.96021E+02	9.99585E-03	0
19210000	6.89476E+06	9.50031E+05	0.	0.	4.96021E+02	5.57917E+02	4.96021E+02	9.99585E-03	0
19220000	6.89476E+06	9.50031E+05	0.	0.	4.96021E+02	5.57917E+02	4.96021E+02	9.99585E-03	0
19230000	6.89476E+06	9.50031E+05	0.	0.	4.96021E+02	5.57917E+02	4.96021E+02	9.99585E-03	0
19240000	6.89476E+06	9.50031E+05	0.	0.	4.96021E+02	5.57917E+02	4.96021E+02	9.99585E-03	0
19250000	6.89476E+06	9.50031E+05	0.	0.	4.96021E+02	5.57917E+02	4.96021E+02	9.99585E-03	0
19260000	6.89476E+06	9.50031E+05	0.	0.	4.96021E+02	5.57917E+02	4.96021E+02	9.99585E-03	0

TMI-2 UFSAR

826

19270000	6.89476E+06	9.50031E+05	0.	0.	4.96021E+02	5.57917E+02	4.96021E+02	9.99585E-03	0
19280000	6.89476E+06	9.50031E+05	0.	0.	4.96021E+02	5.57917E+02	4.96021E+02	9.99585E-03	0
19290000	6.89476E+06	9.50031E+05	0.	0.	4.96021E+02	5.57917E+02	4.96021E+02	9.99585E-03	0
19300000	6.89476E+06	9.50031E+05	0.	0.	4.96021E+02	5.57917E+02	4.96021E+02	9.99585E-03	0
19310000	6.89476E+06	9.50031E+05	0.	0.	4.96021E+02	5.57917E+02	4.96021E+02	9.99585E-03	0
19320000	6.89476E+06	9.50031E+05	0.	0.	4.96021E+02	5.57917E+02	4.96021E+02	9.99585E-03	0
19330000	6.89476E+06	9.50031E+05	0.	0.	4.96021E+02	5.57917E+02	4.96021E+02	9.99585E-03	0
19340000	6.89476E+06	9.50031E+05	0.	0.	4.96021E+02	5.57917E+02	4.96021E+02	9.99585E-03	0
19350000	6.89476E+06	9.50031E+05	0.	0.	4.96021E+02	5.57917E+02	4.96021E+02	9.99585E-03	0
19360000	6.89476E+06	9.50031E+05	0.	0.	4.96021E+02	5.57917E+02	4.96021E+02	9.99585E-03	0
19370000	6.89476E+06	9.50031E+05	0.	0.	4.96021E+02	5.57917E+02	4.96021E+02	9.99585E-03	0
19380000	6.89476E+06	9.50031E+05	0.	0.	4.96021E+02	5.57917E+02	4.96021E+02	9.99585E-03	0
19390000	6.89476E+06	9.50031E+05	0.	0.	4.96021E+02	5.57917E+02	4.96021E+02	9.99585E-03	0
19400000	6.89476E+06	9.50031E+05	0.	0.	4.96021E+02	5.57917E+02	4.96021E+02	9.99585E-03	0
19410000	6.89476E+06	9.50031E+05	0.	0.	4.96021E+02	5.57917E+02	4.96021E+02	9.99585E-03	0
19420000	6.89476E+06	9.50031E+05	0.	0.	4.96021E+02	5.57917E+02	4.96021E+02	9.99585E-03	0
19430000	6.89476E+06	9.50031E+05	0.	0.	4.96021E+02	5.57917E+02	4.96021E+02	9.99585E-03	0
19440000	6.89476E+06	9.50031E+05	0.	0.	4.96021E+02	5.57917E+02	4.96021E+02	9.99585E-03	0
19450000	6.89476E+06	9.50031E+05	0.	0.	4.96021E+02	5.57917E+02	4.96021E+02	9.99585E-03	0
19460000	6.89476E+06	9.50031E+05	0.	0.	4.96021E+02	5.57917E+02	4.96021E+02	9.99585E-03	0
19470000	6.89476E+06	9.50031E+05	0.	0.	4.96021E+02	5.57917E+02	4.96021E+02	9.99585E-03	0
12 SCH80	PIPE	COMPONENT							
21010000	6.89476E+06	9.50031E+05	0.	0.	4.96021E+02	5.57917E+02	4.96021E+02	1.99917E-02	0
21020000	6.89476E+06	9.50031E+05	0.	0.	4.96021E+02	5.57917E+02	4.96021E+02	1.99917E-02	0
21030000	6.89476E+06	9.50031E+05	0.	0.	4.96021E+02	5.57917E+02	4.96021E+02	1.99917E-02	0
21040000	6.89476E+06	9.50031E+05	0.	0.	4.96021E+02	5.57917E+02	4.96021E+02	1.99917E-02	0
21050000	6.89476E+06	9.50031E+05	0.	0.	4.96021E+02	5.57917E+02	4.96021E+02	1.99917E-02	0
21060000	6.89476E+06	9.50031E+05	0.	0.	4.96021E+02	5.57917E+02	4.96021E+02	1.99917E-02	0
21070000	6.89476E+06	9.50031E+05	0.	0.	4.96021E+02	5.57917E+02	4.96021E+02	1.99917E-02	0
21080000	6.89476E+06	9.50031E+05	0.	0.	4.96021E+02	5.57917E+02	4.96021E+02	1.99917E-02	0
21090000	6.89476E+06	9.50031E+05	0.	0.	4.96021E+02	5.57917E+02	4.96021E+02	1.99917E-02	0
21100000	6.89476E+06	9.50031E+05	0.	0.	4.96021E+02	5.57917E+02	4.96021E+02	1.99917E-02	0
21110000	6.89476E+06	9.50031E+05	0.	0.	4.96021E+02	5.57917E+02	4.96021E+02	1.99917E-02	0
21120000	6.89476E+06	9.50031E+05	0.	0.	4.96021E+02	5.57917E+02	4.96021E+02	1.99917E-02	0
21130000	6.89476E+06	9.50031E+05	0.	0.	4.96021E+02	5.57917E+02	4.96021E+02	1.99917E-02	0
21140000	6.89476E+06	9.50031E+05	0.	0.	4.96021E+02	5.57917E+02	4.96021E+02	1.99917E-02	0
21150000	6.89476E+06	9.50031E+05	0.	0.	4.96021E+02	5.57917E+02	4.96021E+02	1.99917E-02	0
21160000	6.89476E+06	9.50031E+05	0.	0.	4.96021E+02	5.57917E+02	4.96021E+02	1.99917E-02	0
21170000	6.89476E+06	9.50031E+05	0.	0.	4.96021E+02	5.57917E+02	4.96021E+02	1.99917E-02	0
21180000	6.89476E+06	9.50031E+05	0.	0.	4.96021E+02	5.57917E+02	4.96021E+02	1.99917E-02	0
21190000	6.89476E+06	9.50031E+05	0.	0.	4.96021E+02	5.57917E+02	4.96021E+02	1.99917E-02	0
21200000	6.89476E+06	9.50031E+05	0.	0.	4.96021E+02	5.57917E+02	4.96021E+02	1.99917E-02	0
21210000	6.89476E+06	9.50031E+05	0.	0.	4.96021E+02	5.57917E+02	4.96021E+02	1.99917E-02	0
21220000	6.89476E+06	9.50031E+05	0.	0.	4.96021E+02	5.57917E+02	4.96021E+02	1.99917E-02	0
12 SCH80	PIPE	COMPONENT							
23010000	6.89476E+06	9.50031E+05	0.	0.	4.96021E+02	5.57917E+02	4.96021E+02	1.99917E-02	0
23020000	6.89476E+06	9.50031E+05	0.	0.	4.96021E+02	5.57917E+02	4.96021E+02	1.99917E-02	0
23030000	6.89476E+06	9.50031E+05	0.	0.	4.96021E+02	5.57917E+02	4.96021E+02	1.99917E-02	0
23040000	6.89476E+06	9.50031E+05	0.	0.	4.96021E+02	5.57917E+02	4.96021E+02	1.99917E-02	0
23050000	6.89476E+06	9.50031E+05	0.	0.	4.96021E+02	5.57917E+02	4.96021E+02	1.99917E-02	0
23060000	6.89476E+06	9.50031E+05	0.	0.	4.96021E+02	5.57917E+02	4.96021E+02	1.99917E-02	0
23070000	6.89476E+06	9.50031E+05	0.	0.	4.96021E+02	5.57917E+02	4.96021E+02	1.99917E-02	0
23080000	6.89476E+06	9.50031E+05	0.	0.	4.96021E+02	5.57917E+02	4.96021E+02	1.99917E-02	0
23090000	6.89476E+06	9.50031E+05	0.	0.	4.96021E+02	5.57917E+02	4.96021E+02	1.99917E-02	0
23100000	6.89476E+06	9.50031E+05	0.	0.	4.96021E+02	5.57917E+02	4.96021E+02	1.99917E-02	0
23110000	6.89476E+06	9.50031E+05	0.	0.	4.96021E+02	5.57917E+02	4.96021E+02	1.99917E-02	0
23120000	6.89476E+06	9.50031E+05	0.	0.	4.96021E+02	5.57917E+02	4.96021E+02	1.99917E-02	0
23130000	6.89476E+06	9.50031E+05	0.	0.	4.96021E+02	5.57917E+02	4.96021E+02	1.99917E-02	0
23140000	6.89476E+06	9.50031E+05	0.	0.	4.96021E+02	5.57917E+02	4.96021E+02	1.99917E-02	0
23150000	6.89476E+06	9.50031E+05	0.	0.	4.96021E+02	5.57917E+02	4.96021E+02	1.99917E-02	0
23160000	6.89476E+06	9.50031E+05	0.	0.	4.96021E+02	5.57917E+02	4.96021E+02	1.99917E-02	0

12 SCH80	PIPE	COMPONENT							
25010000	6.89476E+06	9.50031E+05	0.	0.	4.96021E+02	5.57917E+02	4.96021E+02	1.99917E-02	0
25020000	6.89476E+06	9.50031E+05	0.	0.	4.96021E+02	5.57917E+02	4.96021E+02	1.99917E-02	0
25030000	6.89476E+06	9.50031E+05	0.	0.	4.96021E+02	5.57917E+02	4.96021E+02	1.99917E-02	0
25040000	6.89476E+06	9.50031E+05	0.	0.	4.96021E+02	5.57917E+02	4.96021E+02	1.99917E-02	0
25050000	6.89476E+06	9.50031E+05	0.	0.	4.96021E+02	5.57917E+02	4.96021E+02	1.99917E-02	0
25060000	6.89476E+06	9.50031E+05	0.	0.	4.96021E+02	5.57917E+02	4.96021E+02	1.99917E-02	0
25070000	6.89476E+06	9.50031E+05	0.	0.	4.96021E+02	5.57917E+02	4.96021E+02	1.99917E-02	0
25080000	6.89476E+06	9.50031E+05	0.	0.	4.96021E+02	5.57917E+02	4.96021E+02	1.99917E-02	0
25090000	6.89476E+06	9.50031E+05	0.	0.	4.96021E+02	5.57917E+02	4.96021E+02	1.99917E-02	0
25100000	6.89476E+06	9.50031E+05	0.	0.	4.96021E+02	5.57917E+02	4.96021E+02	1.99917E-02	0
25110000	6.89476E+06	9.50031E+05	0.	0.	4.96021E+02	5.57917E+02	4.96021E+02	1.99917E-02	0
25120000	6.89476E+06	9.50031E+05	0.	0.	4.96021E+02	5.57917E+02	4.96021E+02	1.99917E-02	0
25130000	6.89476E+06	9.50031E+05	0.	0.	4.96021E+02	5.57917E+02	4.96021E+02	1.99917E-02	0
25140000	6.89476E+06	9.50031E+05	0.	0.	4.96021E+02	5.57917E+02	4.96021E+02	1.99917E-02	0
25150000	6.89476E+06	9.50031E+05	0.	0.	4.96021E+02	5.57917E+02	4.96021E+02	1.99917E-02	0
25160000	6.89476E+06	9.50031E+05	0.	0.	4.96021E+02	5.57917E+02	4.96021E+02	1.99917E-02	0
25170000	6.89476E+06	9.50031E+05	0.	0.	4.96021E+02	5.57917E+02	4.96021E+02	1.99917E-02	0
25180000	6.89476E+06	9.50031E+05	0.	0.	4.96021E+02	5.57917E+02	4.96021E+02	1.99917E-02	0
25190000	6.89476E+06	9.50031E+05	0.	0.	4.96021E+02	5.57917E+02	4.96021E+02	1.99917E-02	0
25200000	6.89476E+06	9.50031E+05	0.	0.	4.96021E+02	5.57917E+02	4.96021E+02	1.99917E-02	0
12 SCH80	PIPE	COMPONENT							
27010000	6.89476E+06	9.50031E+05	0.	0.	4.96021E+02	5.57917E+02	4.96021E+02	1.99917E-02	0
27020000	6.89476E+06	9.50031E+05	0.	0.	4.96021E+02	5.57917E+02	4.96021E+02	1.99917E-02	0
27030000	6.89476E+06	9.50031E+05	0.	0.	4.96021E+02	5.57917E+02	4.96021E+02	1.99917E-02	0
27040000	6.89476E+06	9.50031E+05	0.	0.	4.96021E+02	5.57917E+02	4.96021E+02	1.99917E-02	0
27050000	6.89476E+06	9.50031E+05	0.	0.	4.96021E+02	5.57917E+02	4.96021E+02	1.99917E-02	0
27060000	6.89476E+06	9.50031E+05	0.	0.	4.96021E+02	5.57917E+02	4.96021E+02	1.99917E-02	0
27070000	6.89476E+06	9.50031E+05	0.	0.	4.96021E+02	5.57917E+02	4.96021E+02	1.99917E-02	0
27080000	6.89476E+06	9.50031E+05	0.	0.	4.96021E+02	5.57917E+02	4.96021E+02	1.99917E-02	0
27090000	6.89476E+06	9.50031E+05	0.	0.	4.96021E+02	5.57917E+02	4.96021E+02	1.99917E-02	0
27100000	6.89476E+06	9.50031E+05	0.	0.	4.96021E+02	5.57917E+02	4.96021E+02	1.99917E-02	0
27110000	6.89476E+06	9.50031E+05	0.	0.	4.96021E+02	5.57917E+02	4.96021E+02	1.99917E-02	0
27120000	6.89476E+06	9.50031E+05	0.	0.	4.96021E+02	5.57917E+02	4.96021E+02	1.99917E-02	0
27130000	6.89476E+06	9.50031E+05	0.	0.	4.96021E+02	5.57917E+02	4.96021E+02	1.99917E-02	0
27140000	6.89476E+06	9.50031E+05	0.	0.	4.96021E+02	5.57917E+02	4.96021E+02	1.99917E-02	0
27150000	6.89476E+06	9.50031E+05	0.	0.	4.96021E+02	5.57917E+02	4.96021E+02	1.99917E-02	0
BDY VOL	TMDPVOL	COMPONENT							
29010000	6.89476E+06	9.50031E+05	0.	0.	4.96021E+02	5.57917E+02	4.96021E+02	0.	0

VOL.NO.	RHO (KG/M3)	RHOF (KG/M3)	RHOG (KG/M3)	VOIDG	UF (J/KG)	UG (J/KG)	SOUNDE (M/SEC)	HEAT INPUT (WATTS)
2010000	5.90269E-01	9.58393E+02	5.90269E-01	1.00000E+00	4.17376E+05	2.50605E+06	4.38734E+02	0.
4010000	8.40714E+02	8.40714E+02	3.59188E+01	0.	9.50031E+05	2.58260E+06	1.25691E+03	0.
4020000	8.40714E+02	8.40714E+02	3.59188E+01	0.	9.50031E+05	2.58260E+06	1.25691E+03	0.
4030000	8.40714E+02	8.40714E+02	3.59188E+01	0.	9.50031E+05	2.58260E+06	1.25691E+03	0.
4040000	8.40714E+02	8.40714E+02	3.59188E+01	0.	9.50031E+05	2.58260E+06	1.25691E+03	0.
4050000	8.40714E+02	8.40714E+02	3.59188E+01	0.	9.50031E+05	2.58260E+06	1.25691E+03	0.
4060000	8.40714E+02	8.40714E+02	3.59188E+01	0.	9.50031E+05	2.58260E+06	1.25691E+03	0.
4070000	8.40714E+02	8.40714E+02	3.59188E+01	0.	9.50031E+05	2.58260E+06	1.25691E+03	0.
4080000	8.40714E+02	8.40714E+02	3.59188E+01	0.	9.50031E+05	2.58260E+06	1.25691E+03	0.
4090000	8.40714E+02	8.40714E+02	3.59188E+01	0.	9.50031E+05	2.58260E+06	1.25691E+03	0.
4100000	8.40714E+02	8.40714E+02	3.59188E+01	0.	9.50031E+05	2.58260E+06	1.25691E+03	0.
4110000	8.40714E+02	8.40714E+02	3.59188E+01	0.	9.50031E+05	2.58260E+06	1.25691E+03	0.
4120000	8.40714E+02	8.40714E+02	3.59188E+01	0.	9.50031E+05	2.58260E+06	1.25691E+03	0.
4130000	8.40714E+02	8.40714E+02	3.59188E+01	0.	9.50031E+05	2.58260E+06	1.25691E+03	0.
4140000	8.40714E+02	8.40714E+02	3.59188E+01	0.	9.50031E+05	2.58260E+06	1.25691E+03	0.
4150000	8.40714E+02	8.40714E+02	3.59188E+01	0.	9.50031E+05	2.58260E+06	1.25691E+03	0.
4160000	8.40714E+02	8.40714E+02	3.59188E+01	0.	9.50031E+05	2.58260E+06	1.25691E+03	0.
4170000	8.40714E+02	8.40714E+02	3.59188E+01	0.	9.50031E+05	2.58260E+06	1.25691E+03	0.
4180000	8.40714E+02	8.40714E+02	3.59188E+01	0.	9.50031E+05	2.58260E+06	1.25691E+03	0.

4190000	8.40714E+02	8.40714E+02	3.59188E+01	0.	9.50031E+05	2.58260E+06	1.25691E+03	0.
4200000	8.40714E+02	8.40714E+02	3.59188E+01	0.	9.50031E+05	2.58260E+06	1.25691E+03	0.
4210000	8.40714E+02	8.40714E+02	3.59188E+01	0.	9.50031E+05	2.58260E+06	1.25691E+03	0.
4220000	8.40714E+02	8.40714E+02	3.59188E+01	0.	9.50031E+05	2.58260E+06	1.25691E+03	0.
4230000	8.40714E+02	8.40714E+02	3.59188E+01	0.	9.50031E+05	2.58260E+06	1.25691E+03	0.
4240000	8.40714E+02	8.40714E+02	3.59188E+01	0.	9.50031E+05	2.58260E+06	1.25691E+03	0.
4250000	8.40714E+02	8.40714E+02	3.59188E+01	0.	9.50031E+05	2.58260E+06	1.25691E+03	0.
4260000	8.40714E+02	8.40714E+02	3.59188E+01	0.	9.50031E+05	2.58260E+06	1.25691E+03	0.
4270000	8.40714E+02	8.40714E+02	3.59188E+01	0.	9.50031E+05	2.58260E+06	1.25691E+03	0.
4280000	8.40714E+02	8.40714E+02	3.59188E+01	0.	9.50031E+05	2.58260E+06	1.25691E+03	0.
4290000	8.40714E+02	8.40714E+02	3.59188E+01	0.	9.50031E+05	2.58260E+06	1.25691E+03	0.
6010000	8.40714E+02	8.40714E+02	3.59188E+01	0.	9.50031E+05	2.58260E+06	1.25691E+03	0.
6020000	8.40714E+02	8.40714E+02	3.59188E+01	0.	9.50031E+05	2.58260E+06	1.25691E+03	0.
6030000	8.40714E+02	8.40714E+02	3.59188E+01	0.	9.50031E+05	2.58260E+06	1.25691E+03	0.
6040000	8.40714E+02	8.40714E+02	3.59188E+01	0.	9.50031E+05	2.58260E+06	1.25691E+03	0.
6050000	8.40714E+02	8.40714E+02	3.59188E+01	0.	9.50031E+05	2.58260E+06	1.25691E+03	0.
6060000	8.40714E+02	8.40714E+02	3.59188E+01	0.	9.50031E+05	2.58260E+06	1.25691E+03	0.
6070000	8.40714E+02	8.40714E+02	3.59188E+01	0.	9.50031E+05	2.58260E+06	1.25691E+03	0.
6080000	8.40714E+02	8.40714E+02	3.59188E+01	0.	9.50031E+05	2.58260E+06	1.25691E+03	0.
6090000	8.40714E+02	8.40714E+02	3.59188E+01	0.	9.50031E+05	2.58260E+06	1.25691E+03	0.
6100000	8.40714E+02	8.40714E+02	3.59188E+01	0.	9.50031E+05	2.58260E+06	1.25691E+03	0.
6110000	8.40714E+02	8.40714E+02	3.59188E+01	0.	9.50031E+05	2.58260E+06	1.25691E+03	0.
6120000	8.40714E+02	8.40714E+02	3.59188E+01	0.	9.50031E+05	2.58260E+06	1.25691E+03	0.
6130000	8.40714E+02	8.40714E+02	3.59188E+01	0.	9.50031E+05	2.58260E+06	1.25691E+03	0.
6140000	8.40714E+02	8.40714E+02	3.59188E+01	0.	9.50031E+05	2.58260E+06	1.25691E+03	0.
6150000	8.40714E+02	8.40714E+02	3.59188E+01	0.	9.50031E+05	2.58260E+06	1.25691E+03	0.
8010000	8.40714E+02	8.40714E+02	3.59188E+01	0.	9.50031E+05	2.58260E+06	1.25691E+03	0.
8020000	8.40714E+02	8.40714E+02	3.59188E+01	0.	9.50031E+05	2.58260E+06	1.25691E+03	0.
8030000	8.40714E+02	8.40714E+02	3.59188E+01	0.	9.50031E+05	2.58260E+06	1.25691E+03	0.
8040000	8.40714E+02	8.40714E+02	3.59188E+01	0.	9.50031E+05	2.58260E+06	1.25691E+03	0.
8050000	8.40714E+02	8.40714E+02	3.59188E+01	0.	9.50031E+05	2.58260E+06	1.25691E+03	0.
8060000	8.40714E+02	8.40714E+02	3.59188E+01	0.	9.50031E+05	2.58260E+06	1.25691E+03	0.
8070000	8.40714E+02	8.40714E+02	3.59188E+01	0.	9.50031E+05	2.58260E+06	1.25691E+03	0.
8080000	8.40714E+02	8.40714E+02	3.59188E+01	0.	9.50031E+05	2.58260E+06	1.25691E+03	0.
8090000	8.40714E+02	8.40714E+02	3.59188E+01	0.	9.50031E+05	2.58260E+06	1.25691E+03	0.
8100000	8.40714E+02	8.40714E+02	3.59188E+01	0.	9.50031E+05	2.58260E+06	1.25691E+03	0.
9010000	8.40714E+02	8.40714E+02	3.59188E+01	0.	9.50031E+05	2.58260E+06	1.25691E+03	0.
10010000	8.40714E+02	8.40714E+02	3.59188E+01	0.	9.50031E+05	2.58260E+06	1.25691E+03	0.
10020000	8.40714E+02	8.40714E+02	3.59188E+01	0.	9.50031E+05	2.58260E+06	1.25691E+03	0.
10030000	8.40714E+02	8.40714E+02	3.59188E+01	0.	9.50031E+05	2.58260E+06	1.25691E+03	0.
10040000	8.40714E+02	8.40714E+02	3.59188E+01	0.	9.50031E+05	2.58260E+06	1.25691E+03	0.
10050000	8.40714E+02	8.40714E+02	3.59188E+01	0.	9.50031E+05	2.58260E+06	1.25691E+03	0.
10060000	8.40714E+02	8.40714E+02	3.59188E+01	0.	9.50031E+05	2.58260E+06	1.25691E+03	0.
10070000	8.40714E+02	8.40714E+02	3.59188E+01	0.	9.50031E+05	2.58260E+06	1.25691E+03	0.
10080000	8.40714E+02	8.40714E+02	3.59188E+01	0.	9.50031E+05	2.58260E+06	1.25691E+03	0.
10090000	8.40714E+02	8.40714E+02	3.59188E+01	0.	9.50031E+05	2.58260E+06	1.25691E+03	0.
10100000	8.40714E+02	8.40714E+02	3.59188E+01	0.	9.50031E+05	2.58260E+06	1.25691E+03	0.
10110000	8.40714E+02	8.40714E+02	3.59188E+01	0.	9.50031E+05	2.58260E+06	1.25691E+03	0.
10120000	8.40714E+02	8.40714E+02	3.59188E+01	0.	9.50031E+05	2.58260E+06	1.25691E+03	0.
10130000	8.40714E+02	8.40714E+02	3.59188E+01	0.	9.50031E+05	2.58260E+06	1.25691E+03	0.
10140000	8.40714E+02	8.40714E+02	3.59188E+01	0.	9.50031E+05	2.58260E+06	1.25691E+03	0.
10150000	8.40714E+02	8.40714E+02	3.59188E+01	0.	9.50031E+05	2.58260E+06	1.25691E+03	0.
10160000	8.40714E+02	8.40714E+02	3.59188E+01	0.	9.50031E+05	2.58260E+06	1.25691E+03	0.
10170000	8.40714E+02	8.40714E+02	3.59188E+01	0.	9.50031E+05	2.58260E+06	1.25691E+03	0.
10180000	8.40714E+02	8.40714E+02	3.59188E+01	0.	9.50031E+05	2.58260E+06	1.25691E+03	0.
10190000	8.40714E+02	8.40714E+02	3.59188E+01	0.	9.50031E+05	2.58260E+06	1.25691E+03	0.
10200000	8.40714E+02	8.40714E+02	3.59188E+01	0.	9.50031E+05	2.58260E+06	1.25691E+03	0.
10210000	8.40714E+02	8.40714E+02	3.59188E+01	0.	9.50031E+05	2.58260E+06	1.25691E+03	0.
10220000	8.40714E+02	8.40714E+02	3.59188E+01	0.	9.50031E+05	2.58260E+06	1.25691E+03	0.
10230000	8.40714E+02	8.40714E+02	3.59188E+01	0.	9.50031E+05	2.58260E+06	1.25691E+03	0.
10240000	8.40714E+02	8.40714E+02	3.59188E+01	0.	9.50031E+05	2.58260E+06	1.25691E+03	0.

1215 281

10250000	8.40714E+02	8.40714E+02	3.59188E+01	0.	9.50031E+05	2.58260E+06	1.25691E+03	0.
10260000	8.40714E+02	8.40714E+02	3.59188E+01	0.	9.50031E+05	2.58260E+06	1.25691E+03	0.
10270000	8.40714E+02	8.40714E+02	3.59188E+01	0.	9.50031E+05	2.58260E+06	1.25691E+03	0.
10280000	8.40714E+02	8.40714E+02	3.59188E+01	0.	9.50031E+05	2.58260E+06	1.25691E+03	0.
10290000	8.40714E+02	8.40714E+02	3.59188E+01	0.	9.50031E+05	2.58260E+06	1.25691E+03	0.
10300000	8.40714E+02	8.40714E+02	3.59188E+01	0.	9.50031E+05	2.58260E+06	1.25691E+03	0.
12010000	8.40714E+02	8.40714E+02	3.59188E+01	0.	9.50031E+05	2.58260E+06	1.25691E+03	0.
12020000	8.40714E+02	8.40714E+02	3.59188E+01	0.	9.50031E+05	2.58260E+06	1.25691E+03	0.
12030000	8.40714E+02	8.40714E+02	3.59188E+01	0.	9.50031E+05	2.58260E+06	1.25691E+03	0.
12040000	8.40714E+02	8.40714E+02	3.59188E+01	0.	9.50031E+05	2.58260E+06	1.25691E+03	0.
12050000	8.40714E+02	8.40714E+02	3.59188E+01	0.	9.50031E+05	2.58260E+06	1.25691E+03	0.
12060000	8.40714E+02	8.40714E+02	3.59188E+01	0.	9.50031E+05	2.58260E+06	1.25691E+03	0.
12070000	8.40714E+02	8.40714E+02	3.59188E+01	0.	9.50031E+05	2.58260E+06	1.25691E+03	0.
12080000	8.40714E+02	8.40714E+02	3.59188E+01	0.	9.50031E+05	2.58260E+06	1.25691E+03	0.
12090000	8.40714E+02	8.40714E+02	3.59188E+01	0.	9.50031E+05	2.58260E+06	1.25691E+03	0.
12100000	8.40714E+02	8.40714E+02	3.59188E+01	0.	9.50031E+05	2.58260E+06	1.25691E+03	0.
12110000	8.40714E+02	8.40714E+02	3.59188E+01	0.	9.50031E+05	2.58260E+06	1.25691E+03	0.
12120000	8.40714E+02	8.40714E+02	3.59188E+01	0.	9.50031E+05	2.58260E+06	1.25691E+03	0.
12130000	8.40714E+02	8.40714E+02	3.59188E+01	0.	9.50031E+05	2.58260E+06	1.25691E+03	0.
12140000	8.40714E+02	8.40714E+02	3.59188E+01	0.	9.50031E+05	2.58260E+06	1.25691E+03	0.
12150000	8.40714E+02	8.40714E+02	3.59188E+01	0.	9.50031E+05	2.58260E+06	1.25691E+03	0.
12160000	8.40714E+02	8.40714E+02	3.59188E+01	0.	9.50031E+05	2.58260E+06	1.25691E+03	0.
12170000	8.40714E+02	8.40714E+02	3.59188E+01	0.	9.50031E+05	2.58260E+06	1.25691E+03	0.
14010000	8.40714E+02	8.40714E+02	3.59188E+01	0.	9.50031E+05	2.58260E+06	1.25691E+03	0.
14020000	8.40714E+02	8.40714E+02	3.59188E+01	0.	9.50031E+05	2.58260E+06	1.25691E+03	0.
14030000	8.40714E+02	8.40714E+02	3.59188E+01	0.	9.50031E+05	2.58260E+06	1.25691E+03	0.
14040000	8.40714E+02	8.40714E+02	3.59188E+01	0.	9.50031E+05	2.58260E+06	1.25691E+03	0.
14050000	8.40714E+02	8.40714E+02	3.59188E+01	0.	9.50031E+05	2.58260E+06	1.25691E+03	0.
14060000	8.40714E+02	8.40714E+02	3.59188E+01	0.	9.50031E+05	2.58260E+06	1.25691E+03	0.
14070000	8.40714E+02	8.40714E+02	3.59188E+01	0.	9.50031E+05	2.58260E+06	1.25691E+03	0.
14080000	8.40714E+02	8.40714E+02	3.59188E+01	0.	9.50031E+05	2.58260E+06	1.25691E+03	0.
14090000	8.40714E+02	8.40714E+02	3.59188E+01	0.	9.50031E+05	2.58260E+06	1.25691E+03	0.
14100000	8.40714E+02	8.40714E+02	3.59188E+01	0.	9.50031E+05	2.58260E+06	1.25691E+03	0.
14110000	8.40714E+02	8.40714E+02	3.59188E+01	0.	9.50031E+05	2.58260E+06	1.25691E+03	0.
14120000	8.40714E+02	8.40714E+02	3.59188E+01	0.	9.50031E+05	2.58260E+06	1.25691E+03	0.
14130000	8.40714E+02	8.40714E+02	3.59188E+01	0.	9.50031E+05	2.58260E+06	1.25691E+03	0.
14140000	8.40714E+02	8.40714E+02	3.59188E+01	0.	9.50031E+05	2.58260E+06	1.25691E+03	0.
14150000	8.40714E+02	8.40714E+02	3.59188E+01	0.	9.50031E+05	2.58260E+06	1.25691E+03	0.
14160000	8.40714E+02	8.40714E+02	3.59188E+01	0.	9.50031E+05	2.58260E+06	1.25691E+03	0.
14170000	8.40714E+02	8.40714E+02	3.59188E+01	0.	9.50031E+05	2.58260E+06	1.25691E+03	0.
14180000	8.40714E+02	8.40714E+02	3.59188E+01	0.	9.50031E+05	2.58260E+06	1.25691E+03	0.
14190000	8.40714E+02	8.40714E+02	3.59188E+01	0.	9.50031E+05	2.58260E+06	1.25691E+03	0.
14200000	8.40714E+02	8.40714E+02	3.59188E+01	0.	9.50031E+05	2.58260E+06	1.25691E+03	0.
16010000	8.40714E+02	8.40714E+02	3.59188E+01	0.	9.50031E+05	2.58260E+06	1.25691E+03	0.
16020000	8.40714E+02	8.40714E+02	3.59188E+01	0.	9.50031E+05	2.58260E+06	1.25691E+03	0.
16030000	8.40714E+02	8.40714E+02	3.59188E+01	0.	9.50031E+05	2.58260E+06	1.25691E+03	0.
16040000	8.40714E+02	8.40714E+02	3.59188E+01	0.	9.50031E+05	2.58260E+06	1.25691E+03	0.
16050000	8.40714E+02	8.40714E+02	3.59188E+01	0.	9.50031E+05	2.58260E+06	1.25691E+03	0.
16060000	8.40714E+02	8.40714E+02	3.59188E+01	0.	9.50031E+05	2.58260E+06	1.25691E+03	0.
16070000	8.40714E+02	8.40714E+02	3.59188E+01	0.	9.50031E+05	2.58260E+06	1.25691E+03	0.
16080000	8.40714E+02	8.40714E+02	3.59188E+01	0.	9.50031E+05	2.58260E+06	1.25691E+03	0.
16090000	8.40714E+02	8.40714E+02	3.59188E+01	0.	9.50031E+05	2.58260E+06	1.25691E+03	0.
16100000	8.40714E+02	8.40714E+02	3.59188E+01	0.	9.50031E+05	2.58260E+06	1.25691E+03	0.
16110000	8.40714E+02	8.40714E+02	3.59188E+01	0.	9.50031E+05	2.58260E+06	1.25691E+03	0.
16120000	8.40714E+02	8.40714E+02	3.59188E+01	0.	9.50031E+05	2.58260E+06	1.25691E+03	0.
16130000	8.40714E+02	8.40714E+02	3.59188E+01	0.	9.50031E+05	2.58260E+06	1.25691E+03	0.
16140000	8.40714E+02	8.40714E+02	3.59188E+01	0.	9.50031E+05	2.58260E+06	1.25691E+03	0.
16150000	8.40714E+02	8.40714E+02	3.59188E+01	0.	9.50031E+05	2.58260E+06	1.25691E+03	0.
18010000	8.40714E+02	8.40714E+02	3.59188E+01	0.	9.50031E+05	2.58260E+06	1.25691E+03	0.
19010000	8.40714E+02	8.40714E+02	3.59188E+01	0.	9.50031E+05	2.58260E+06	1.25691E+03	0.
19020000	8.40714E+02	8.40714E+02	3.59188E+01	0.	9.50031E+05	2.58260E+06	1.25691E+03	0.

19030000	8.40714E+02	8.40714E+02	3.59188E+01	0.	9.50031E+05	2.58260E+06	1.25691E+03	0.
19040000	8.40714E+02	8.40714E+02	3.59188E+01	0.	9.50031E+05	2.58260E+06	1.25691E+03	0.
19050000	8.40714E+02	8.40714E+02	3.59188E+01	0.	9.50031E+05	2.58260E+06	1.25691E+03	0.
19060000	8.40714E+02	8.40714E+02	3.59188E+01	0.	9.50031E+05	2.58260E+06	1.25691E+03	0.
19070000	8.40714E+02	8.40714E+02	3.59188E+01	0.	9.50031E+05	2.58260E+06	1.25691E+03	0.
19080000	8.40714E+02	8.40714E+02	3.59188E+01	0.	9.50031E+05	2.58260E+06	1.25691E+03	0.
19090000	8.40714E+02	8.40714E+02	3.59188E+01	0.	9.50031E+05	2.58260E+06	1.25691E+03	0.
19100000	8.40714E+02	8.40714E+02	3.59188E+01	0.	9.50031E+05	2.58260E+06	1.25691E+03	0.
19110000	8.40714E+02	8.40714E+02	3.59188E+01	0.	9.50031E+05	2.58260E+06	1.25691E+03	0.
19120000	8.40714E+02	8.40714E+02	3.59188E+01	0.	9.50031E+05	2.58260E+06	1.25691E+03	0.
19130000	8.40714E+02	8.40714E+02	3.59188E+01	0.	9.50031E+05	2.58260E+06	1.25691E+03	0.
19140000	8.40714E+02	8.40714E+02	3.59188E+01	0.	9.50031E+05	2.58260E+06	1.25691E+03	0.
19150000	8.40714E+02	8.40714E+02	3.59188E+01	0.	9.50031E+05	2.58260E+06	1.25691E+03	0.
19160000	8.40714E+02	8.40714E+02	3.59188E+01	0.	9.50031E+05	2.58260E+06	1.25691E+03	0.
19170000	8.40714E+02	8.40714E+02	3.59188E+01	0.	9.50031E+05	2.58260E+06	1.25691E+03	0.
19180000	8.40714E+02	8.40714E+02	3.59188E+01	0.	9.50031E+05	2.58260E+06	1.25691E+03	0.
19190000	8.40714E+02	8.40714E+02	3.59188E+01	0.	9.50031E+05	2.58260E+06	1.25691E+03	0.
19200000	8.40714E+02	8.40714E+02	3.59188E+01	0.	9.50031E+05	2.58260E+06	1.25691E+03	0.
19210000	8.40714E+02	8.40714E+02	3.59188E+01	0.	9.50031E+05	2.58260E+06	1.25691E+03	0.
19220000	8.40714E+02	8.40714E+02	3.59188E+01	0.	9.50031E+05	2.58260E+06	1.25691E+03	0.
19230000	8.40714E+02	8.40714E+02	3.59188E+01	0.	9.50031E+05	2.58260E+06	1.25691E+03	0.
19240000	8.40714E+02	8.40714E+02	3.59188E+01	0.	9.50031E+05	2.58260E+06	1.25691E+03	0.
19250000	8.40714E+02	8.40714E+02	3.59188E+01	0.	9.50031E+05	2.58260E+06	1.25691E+03	0.
19260000	8.40714E+02	8.40714E+02	3.59188E+01	0.	9.50031E+05	2.58260E+06	1.25691E+03	0.
19270000	8.40714E+02	8.40714E+02	3.59188E+01	0.	9.50031E+05	2.58260E+06	1.25691E+03	0.
19280000	8.40714E+02	8.40714E+02	3.59188E+01	0.	9.50031E+05	2.58260E+06	1.25691E+03	0.
19290000	8.40714E+02	8.40714E+02	3.59188E+01	0.	9.50031E+05	2.58260E+06	1.25691E+03	0.
19300000	8.40714E+02	8.40714E+02	3.59188E+01	0.	9.50031E+05	2.58260E+06	1.25691E+03	0.
19310000	8.40714E+02	8.40714E+02	3.59188E+01	0.	9.50031E+05	2.58260E+06	1.25691E+03	0.
19320000	8.40714E+02	8.40714E+02	3.59188E+01	0.	9.50031E+05	2.58260E+06	1.25691E+03	0.
19330000	8.40714E+02	8.40714E+02	3.59188E+01	0.	9.50031E+05	2.58260E+06	1.25691E+03	0.
19340000	8.40714E+02	8.40714E+02	3.59188E+01	0.	9.50031E+05	2.58260E+06	1.25691E+03	0.
19350000	8.40714E+02	8.40714E+02	3.59188E+01	0.	9.50031E+05	2.58260E+06	1.25691E+03	0.
19360000	8.40714E+02	8.40714E+02	3.59188E+01	0.	9.50031E+05	2.58260E+06	1.25691E+03	0.
19370000	8.40714E+02	8.40714E+02	3.59188E+01	0.	9.50031E+05	2.58260E+06	1.25691E+03	0.
19380000	8.40714E+02	8.40714E+02	3.59188E+01	0.	9.50031E+05	2.58260E+06	1.25691E+03	0.
19390000	8.40714E+02	8.40714E+02	3.59188E+01	0.	9.50031E+05	2.58260E+06	1.25691E+03	0.
19400000	8.40714E+02	8.40714E+02	3.59188E+01	0.	9.50031E+05	2.58260E+06	1.25691E+03	0.
19410000	8.40714E+02	8.40714E+02	3.59188E+01	0.	9.50031E+05	2.58260E+06	1.25691E+03	0.
19420000	8.40714E+02	8.40714E+02	3.59188E+01	0.	9.50031E+05	2.58260E+06	1.25691E+03	0.
19430000	8.40714E+02	8.40714E+02	3.59188E+01	0.	9.50031E+05	2.58260E+06	1.25691E+03	0.
19440000	8.40714E+02	8.40714E+02	3.59188E+01	0.	9.50031E+05	2.58260E+06	1.25691E+03	0.
19450000	8.40714E+02	8.40714E+02	3.59188E+01	0.	9.50031E+05	2.58260E+06	1.25691E+03	0.
19460000	8.40714E+02	8.40714E+02	3.59188E+01	0.	9.50031E+05	2.58260E+06	1.25691E+03	0.
19470000	8.40714E+02	8.40714E+02	3.59188E+01	0.	9.50031E+05	2.58260E+06	1.25691E+03	0.
21010000	8.40714E+02	8.40714E+02	3.59188E+01	0.	9.50031E+05	2.58260E+06	1.25691E+03	0.
21020000	8.40714E+02	8.40714E+02	3.59188E+01	0.	9.50031E+05	2.58260E+06	1.25691E+03	0.
21030000	8.40714E+02	8.40714E+02	3.59188E+01	0.	9.50031E+05	2.58260E+06	1.25691E+03	0.
21040000	8.40714E+02	8.40714E+02	3.59188E+01	0.	9.50031E+05	2.58260E+06	1.25691E+03	0.
21050000	8.40714E+02	8.40714E+02	3.59188E+01	0.	9.50031E+05	2.58260E+06	1.25691E+03	0.
21060000	8.40714E+02	8.40714E+02	3.59188E+01	0.	9.50031E+05	2.58260E+06	1.25691E+03	0.
21070000	8.40714E+02	8.40714E+02	3.59188E+01	0.	9.50031E+05	2.58260E+06	1.25691E+03	0.
21080000	8.40714E+02	8.40714E+02	3.59188E+01	0.	9.50031E+05	2.58260E+06	1.25691E+03	0.
21090000	8.40714E+02	8.40714E+02	3.59188E+01	0.	9.50031E+05	2.58260E+06	1.25691E+03	0.
21100000	8.40714E+02	8.40714E+02	3.59188E+01	0.	9.50031E+05	2.58260E+06	1.25691E+03	0.
21110000	8.40714E+02	8.40714E+02	3.59188E+01	0.	9.50031E+05	2.58260E+06	1.25691E+03	0.
21120000	8.40714E+02	8.40714E+02	3.59188E+01	0.	9.50031E+05	2.58260E+06	1.25691E+03	0.
21130000	8.40714E+02	8.40714E+02	3.59188E+01	0.	9.50031E+05	2.58260E+06	1.25691E+03	0.
21140000	8.40714E+02	8.40714E+02	3.59188E+01	0.	9.50031E+05	2.58260E+06	1.25691E+03	0.
21150000	8.40714E+02	8.40714E+02	3.59188E+01	0.	9.50031E+05	2.58260E+06	1.25691E+03	0.
21160000	8.40714E+02	8.40714E+02	3.59188E+01	0.	9.50031E+05	2.58260E+06	1.25691E+03	0.

VOL.NO.	LRGST.MASS ERR. EDIT	LRGST.MASS ERR. TOTAL	REDUCE-QUALITY EDIT	REDUCE-QUALITY TOTAL	REDUCE-EXTRAP. EDIT	REDUCE-EXTRAP. TOTAL	REDUCE-MASS EDIT	REDUCE-MASS TOTAL	REDUCE-PROPTY. EDIT	REDUCE-PROPTY. TOTAL	MIN.COURANT EDIT	MIN.COURANT TOTAL	REDUCE-COURANT EDIT	REDUCE-COURANT TOTAL
21170000	8.40714E+02	8.40714E+02	3.59188E+01	0.	9.50031E+05	2.58260E+06	1.25691E+03	0.						
21180000	8.40714E+02	8.40714E+02	3.59188E+01	0.	9.50031E+05	2.58260E+06	1.25691E+03	0.						
21190000	8.40714E+02	8.40714E+02	3.59188E+01	0.	9.50031E+05	2.58260E+06	1.25691E+03	0.						
21200000	8.40714E+02	8.40714E+02	3.59188E+01	0.	9.50031E+05	2.58260E+06	1.25691E+03	0.						
21210000	8.40714E+02	8.40714E+02	3.59188E+01	0.	9.50031E+05	2.58260E+06	1.25691E+03	0.						
21220000	8.40714E+02	8.40714E+02	3.59188E+01	0.	9.50031E+05	2.58260E+06	1.25691E+03	0.						
23010000	8.40714E+02	8.40714E+02	3.59188E+01	0.	9.50031E+05	2.58260E+06	1.25691E+03	0.						
23020000	8.40714E+02	8.40714E+02	3.59188E+01	0.	9.50031E+05	2.58260E+06	1.25691E+03	0.						
23030000	8.40714E+02	8.40714E+02	3.59188E+01	0.	9.50031E+05	2.58260E+06	1.25691E+03	0.						
23040000	8.40714E+02	8.40714E+02	3.59188E+01	0.	9.50031E+05	2.58260E+06	1.25691E+03	0.						
23050000	8.40714E+02	8.40714E+02	3.59188E+01	0.	9.50031E+05	2.58260E+06	1.25691E+03	0.						
23060000	8.40714E+02	8.40714E+02	3.59188E+01	0.	9.50031E+05	2.58260E+06	1.25691E+03	0.						
23070000	8.40714E+02	8.40714E+02	3.59188E+01	0.	9.50031E+05	2.58260E+06	1.25691E+03	0.						
23080000	8.40714E+02	8.40714E+02	3.59188E+01	0.	9.50031E+05	2.58260E+06	1.25691E+03	0.						
23090000	8.40714E+02	8.40714E+02	3.59188E+01	0.	9.50031E+05	2.58260E+06	1.25691E+03	0.						
23100000	8.40714E+02	8.40714E+02	3.59188E+01	0.	9.50031E+05	2.58260E+06	1.25691E+03	0.						
23110000	8.40714E+02	8.40714E+02	3.59188E+01	0.	9.50031E+05	2.58260E+06	1.25691E+03	0.						
23120000	8.40714E+02	8.40714E+02	3.59188E+01	0.	9.50031E+05	2.58260E+06	1.25691E+03	0.						
23130000	8.40714E+02	8.40714E+02	3.59188E+01	0.	9.50031E+05	2.58260E+06	1.25691E+03	0.						
23140000	8.40714E+02	8.40714E+02	3.59188E+01	0.	9.50031E+05	2.58260E+06	1.25691E+03	0.						
23150000	8.40714E+02	8.40714E+02	3.59188E+01	0.	9.50031E+05	2.58260E+06	1.25691E+03	0.						
23160000	8.40714E+02	8.40714E+02	3.59188E+01	0.	9.50031E+05	2.58260E+06	1.25691E+03	0.						
25010000	8.40714E+02	8.40714E+02	3.59188E+01	0.	9.50031E+05	2.58260E+06	1.25691E+03	0.						
25020000	8.40714E+02	8.40714E+02	3.59188E+01	0.	9.50031E+05	2.58260E+06	1.25691E+03	0.						
25030000	8.40714E+02	8.40714E+02	3.59188E+01	0.	9.50031E+05	2.58260E+06	1.25691E+03	0.						
25040000	8.40714E+02	8.40714E+02	3.59188E+01	0.	9.50031E+05	2.58260E+06	1.25691E+03	0.						
25050000	8.40714E+02	8.40714E+02	3.59188E+01	0.	9.50031E+05	2.58260E+06	1.25691E+03	0.						
25060000	8.40714E+02	8.40714E+02	3.59188E+01	0.	9.50031E+05	2.58260E+06	1.25691E+03	0.						
25070000	8.40714E+02	8.40714E+02	3.59188E+01	0.	9.50031E+05	2.58260E+06	1.25691E+03	0.						
25080000	8.40714E+02	8.40714E+02	3.59188E+01	0.	9.50031E+05	2.58260E+06	1.25691E+03	0.						
25090000	8.40714E+02	8.40714E+02	3.59188E+01	0.	9.50031E+05	2.58260E+06	1.25691E+03	0.						
25100000	8.40714E+02	8.40714E+02	3.59188E+01	0.	9.50031E+05	2.58260E+06	1.25691E+03	0.						
25110000	8.40714E+02	8.40714E+02	3.59188E+01	0.	9.50031E+05	2.58260E+06	1.25691E+03	0.						
25120000	8.40714E+02	8.40714E+02	3.59188E+01	0.	9.50031E+05	2.58260E+06	1.25691E+03	0.						
25130000	8.40714E+02	8.40714E+02	3.59188E+01	0.	9.50031E+05	2.58260E+06	1.25691E+03	0.						
25140000	8.40714E+02	8.40714E+02	3.59188E+01	0.	9.50031E+05	2.58260E+06	1.25691E+03	0.						
25150000	8.40714E+02	8.40714E+02	3.59188E+01	0.	9.50031E+05	2.58260E+06	1.25691E+03	0.						
25160000	8.40714E+02	8.40714E+02	3.59188E+01	0.	9.50031E+05	2.58260E+06	1.25691E+03	0.						
25170000	8.40714E+02	8.40714E+02	3.59188E+01	0.	9.50031E+05	2.58260E+06	1.25691E+03	0.						
25180000	8.40714E+02	8.40714E+02	3.59188E+01	0.	9.50031E+05	2.58260E+06	1.25691E+03	0.						
25190000	8.40714E+02	8.40714E+02	3.59188E+01	0.	9.50031E+05	2.58260E+06	1.25691E+03	0.						
25200000	8.40714E+02	8.40714E+02	3.59188E+01	0.	9.50031E+05	2.58260E+06	1.25691E+03	0.						
27010000	8.40714E+02	8.40714E+02	3.59188E+01	0.	9.50031E+05	2.58260E+06	1.25691E+03	0.						
27020000	8.40714E+02	8.40714E+02	3.59188E+01	0.	9.50031E+05	2.58260E+06	1.25691E+03	0.						
27030000	8.40714E+02	8.40714E+02	3.59188E+01	0.	9.50031E+05	2.58260E+06	1.25691E+03	0.						
27040000	8.40714E+02	8.40714E+02	3.59188E+01	0.	9.50031E+05	2.58260E+06	1.25691E+03	0.						
27050000	8.40714E+02	8.40714E+02	3.59188E+01	0.	9.50031E+05	2.58260E+06	1.25691E+03	0.						
27060000	8.40714E+02	8.40714E+02	3.59188E+01	0.	9.50031E+05	2.58260E+06	1.25691E+03	0.						
27070000	8.40714E+02	8.40714E+02	3.59188E+01	0.	9.50031E+05	2.58260E+06	1.25691E+03	0.						
27080000	8.40714E+02	8.40714E+02	3.59188E+01	0.	9.50031E+05	2.58260E+06	1.25691E+03	0.						
27090000	8.40714E+02	8.40714E+02	3.59188E+01	0.	9.50031E+05	2.58260E+06	1.25691E+03	0.						
27100000	8.40714E+02	8.40714E+02	3.59188E+01	0.	9.50031E+05	2.58260E+06	1.25691E+03	0.						
27110000	8.40714E+02	8.40714E+02	3.59188E+01	0.	9.50031E+05	2.58260E+06	1.25691E+03	0.						
27120000	8.40714E+02	8.40714E+02	3.59188E+01	0.	9.50031E+05	2.58260E+06	1.25691E+03	0.						
27130000	8.40714E+02	8.40714E+02	3.59188E+01	0.	9.50031E+05	2.58260E+06	1.25691E+03	0.						
27140000	8.40714E+02	8.40714E+02	3.59188E+01	0.	9.50031E+05	2.58260E+06	1.25691E+03	0.						
27150000	8.40714E+02	8.40714E+02	3.59188E+01	0.	9.50031E+05	2.58260E+06	1.25691E+03	0.						
29010000	8.40714E+02	8.40714E+02	3.59188E+01	0.	9.50031E+05	2.58260E+06	1.25691E+03	0.						

12215 284

B32

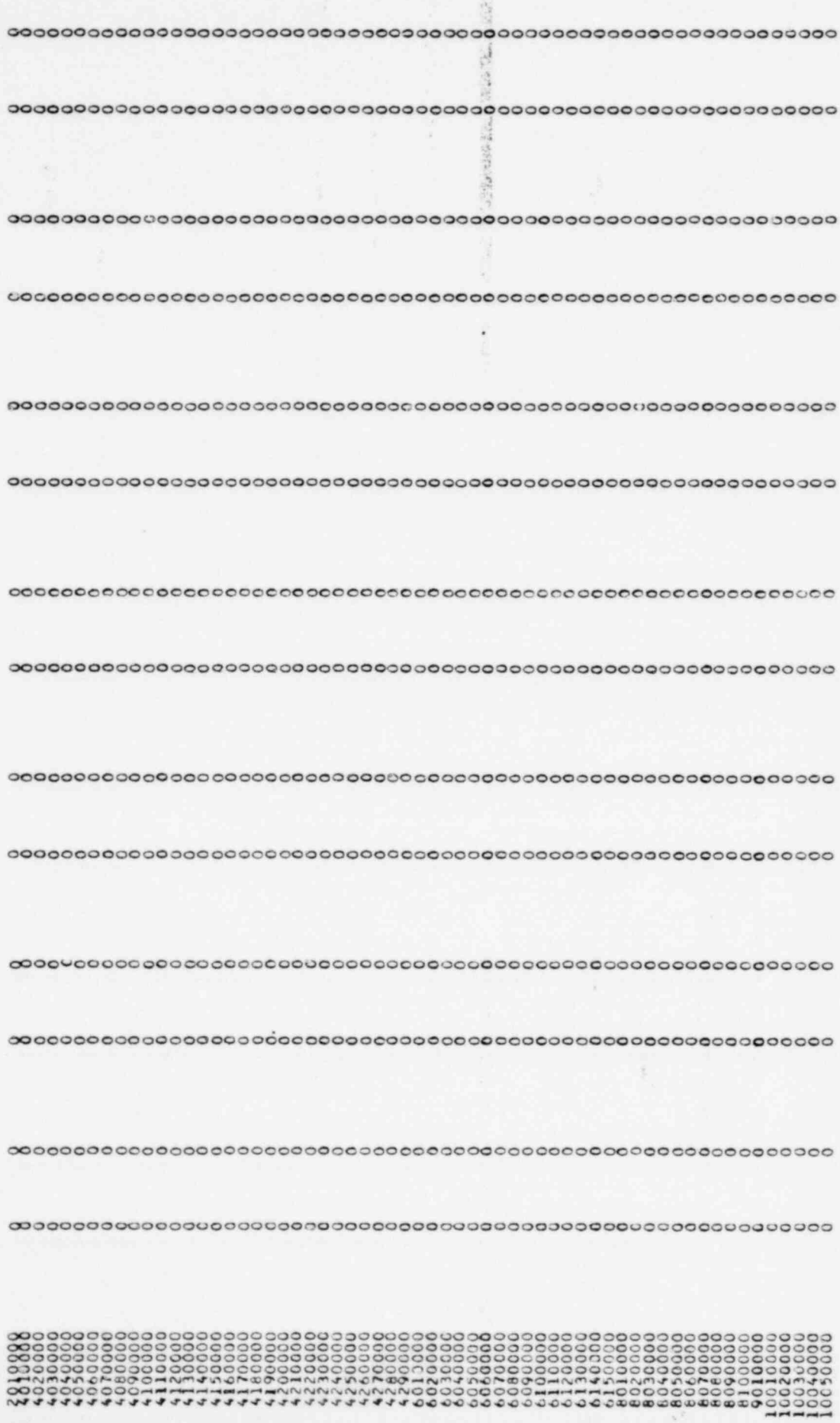

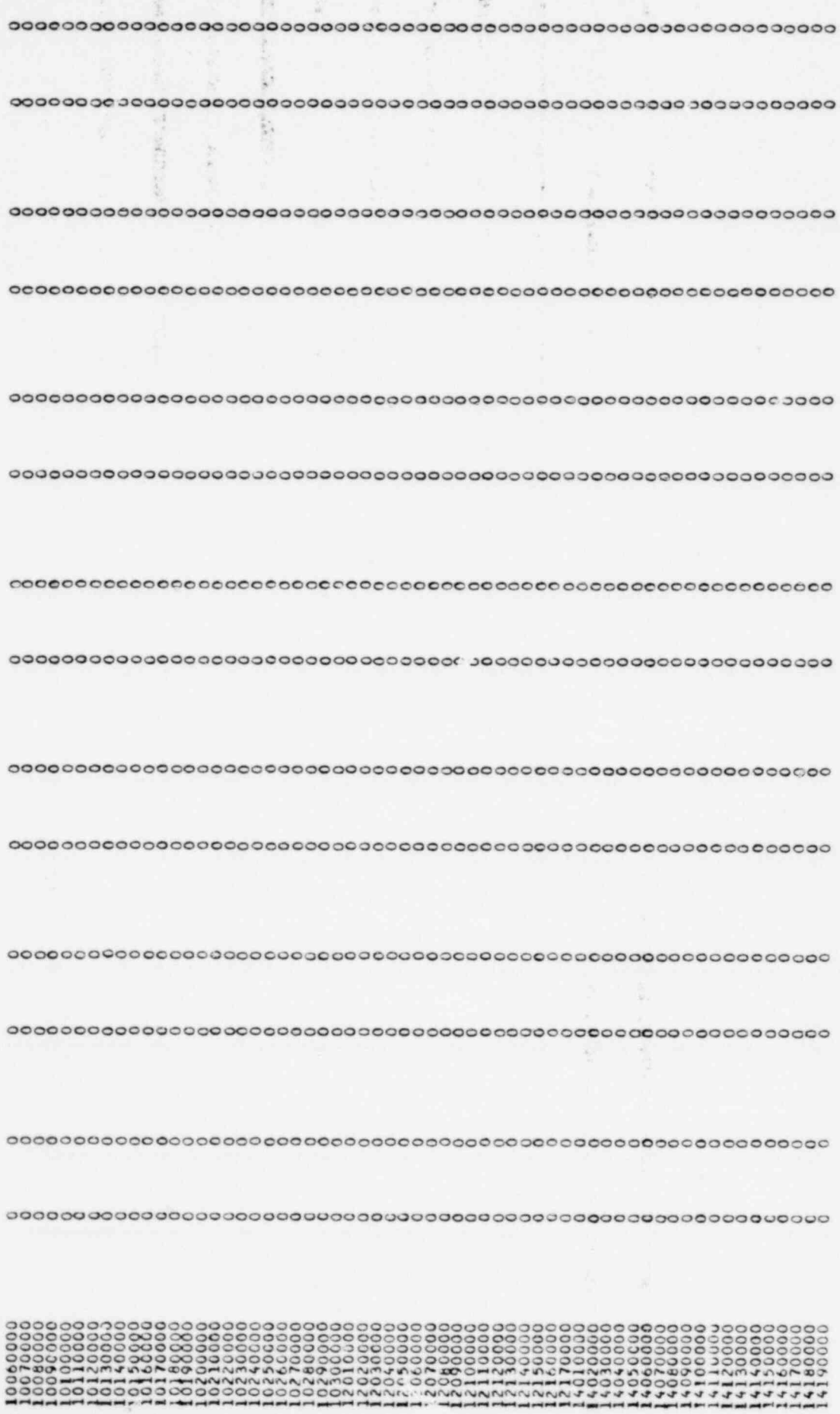

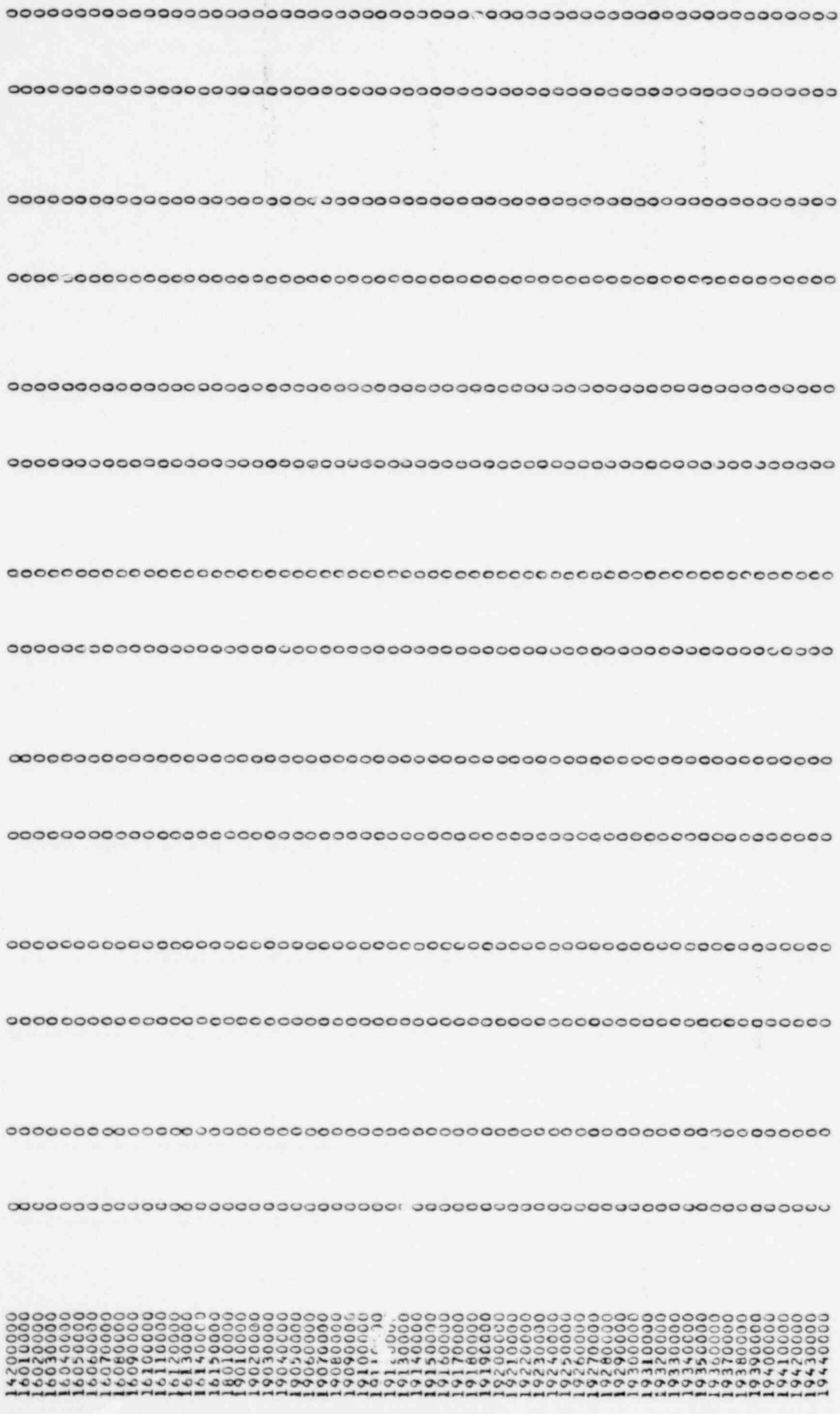

B35

1216-287

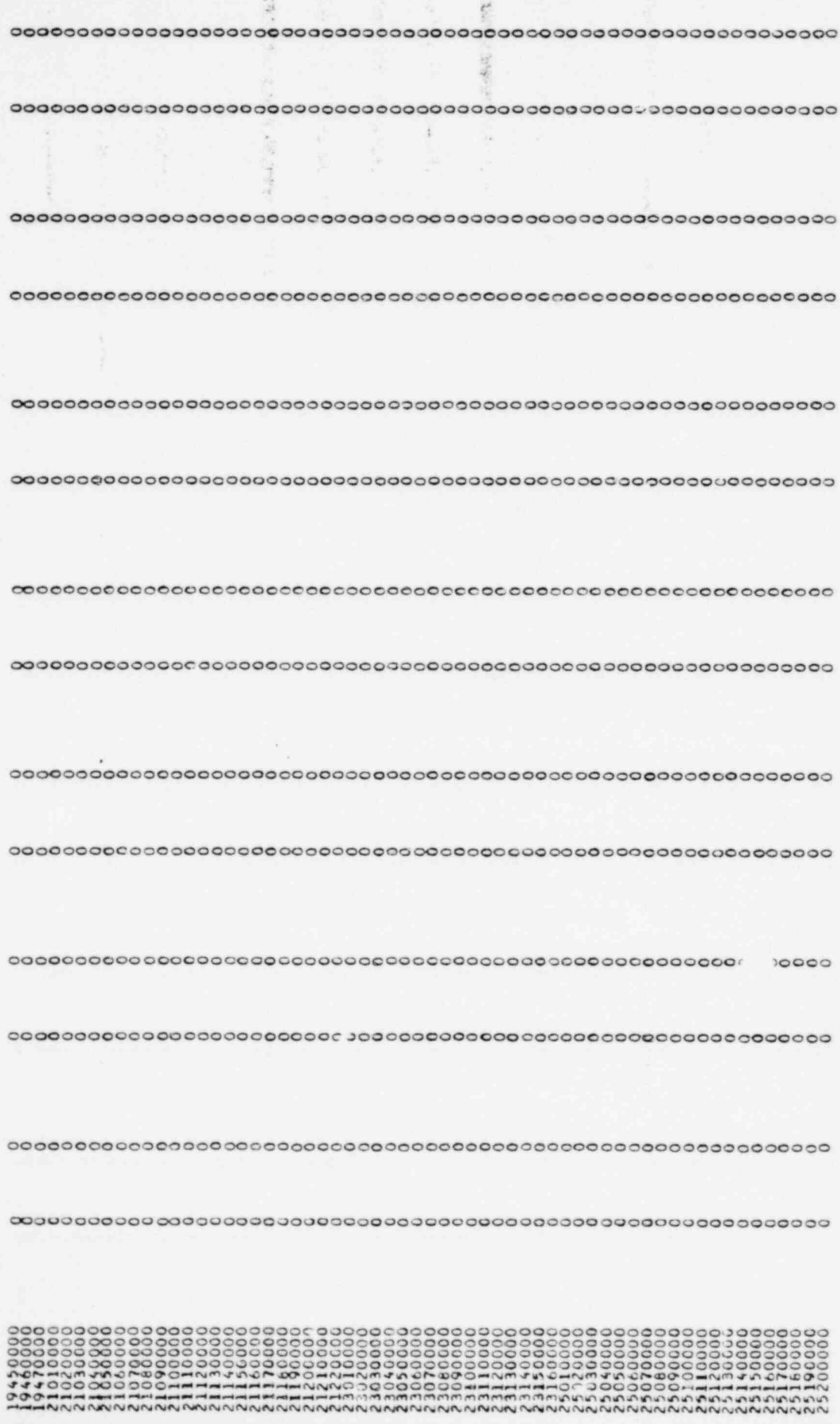

B36

27010000	0	0	0	0	0	0	0	0	0	0	0	0	0
27020000	0	0	0	0	0	0	0	0	0	0	0	0	0
27030000	0	0	0	0	0	0	0	0	0	0	0	0	0
27040000	0	0	0	0	0	0	0	0	0	0	0	0	0
27050000	0	0	0	0	0	0	0	0	0	0	0	0	0
27060000	0	0	0	0	0	0	0	0	0	0	0	0	0
27070000	0	0	0	0	0	0	0	0	0	0	0	0	0
27080000	0	0	0	0	0	0	0	0	0	0	0	0	0
27090000	0	0	0	0	0	0	0	0	0	0	0	0	0
27100000	0	0	0	0	0	0	0	0	0	0	0	0	0
27110000	0	0	0	0	0	0	0	0	0	0	0	0	0
27120000	0	0	0	0	0	0	0	0	0	0	0	0	0
27130000	0	0	0	0	0	0	0	0	0	0	0	0	0
27140000	0	0	0	0	0	0	0	0	0	0	0	0	0
27150000	0	0	0	0	0	0	0	0	0	0	0	0	0
29010000	0	0	0	0	0	0	0	0	0	0	0	0	0

JUN.NO.	FROM VOL.	TO VOL.	LIQ. VEL. (M/SEC)	VAP. VEL. (M/SEC)	INTRFC.VEL. (M/SEC)	JUN.AREA (M2)	THROAT RATIO	JUNCTION FLAGS	CHOKE FLAG	NO.ADVS.CHOKED EDIT	TOTAL
BREAK	SNGLJUN	COMPONENT									
3000000	2010000	4010000	5.86743E+00	5.86743E+00	3.46336E+00	1.12041E-01	1.00000E+00	0	0	0	0
18 SCH120	PIPE	COMPONENT									
4010000	4010000	4020000	6.35666E+00	6.35666E+00	5.34413E+03	1.17894E-01	1.00000E+00	0	0	0	0
4020000	4020000	4030000	6.35666E+00	6.35666E+00	5.34413E+03	1.17894E-01	1.00000E+00	0	0	0	0
4030000	4030000	4040000	6.35666E+00	6.35666E+00	5.34413E+03	1.17894E-01	1.00000E+00	0	0	0	0
4040000	4040000	4050000	6.35666E+00	6.35666E+00	5.34413E+03	1.17894E-01	1.00000E+00	0	0	0	0
4050000	4050000	4060000	6.35666E+00	6.35666E+00	5.34413E+03	1.17894E-01	1.00000E+00	0	0	0	0
4060000	4060000	4070000	6.35666E+00	6.35666E+00	5.34413E+03	1.17894E-01	1.00000E+00	0	0	0	0
4070000	4070000	4080000	6.35666E+00	6.35666E+00	5.34413E+03	1.17894E-01	1.00000E+00	0	0	0	0
4080000	4080000	4090000	6.35666E+00	6.35666E+00	5.34413E+03	1.17894E-01	1.00000E+00	0	0	0	0
4090000	4090000	4100000	6.35666E+00	6.35666E+00	5.34413E+03	1.17894E-01	1.00000E+00	0	0	0	0
4100000	4100000	4110000	6.35666E+00	6.35666E+00	5.34413E+03	1.17894E-01	1.00000E+00	0	0	0	0
4110000	4110000	4120000	6.35666E+00	6.35666E+00	5.34413E+03	1.17894E-01	1.00000E+00	0	0	0	0
4120000	4120000	4130000	6.35666E+00	6.35666E+00	5.34413E+03	1.17894E-01	1.00000E+00	0	0	0	0
4130000	4130000	4140000	6.35666E+00	6.35666E+00	5.34413E+03	1.17894E-01	1.00000E+00	0	0	0	0
4140000	4140000	4150000	6.35666E+00	6.35666E+00	5.34413E+03	1.17894E-01	1.00000E+00	0	0	0	0
4150000	4150000	4160000	6.35666E+00	6.35666E+00	5.34413E+03	1.17894E-01	1.00000E+00	0	0	0	0
4160000	4160000	4170000	6.35666E+00	6.35666E+00	5.34413E+03	1.17894E-01	1.00000E+00	0	0	0	0
4170000	4170000	4180000	6.35666E+00	6.35666E+00	5.34413E+03	1.17894E-01	1.00000E+00	0	0	0	0
4180000	4180000	4190000	6.35666E+00	6.35666E+00	5.34413E+03	1.17894E-01	1.00000E+00	0	0	0	0
4190000	4190000	4200000	6.35666E+00	6.35666E+00	5.34413E+03	1.17894E-01	1.00000E+00	0	0	0	0
4200000	4200000	4210000	6.35666E+00	6.35666E+00	5.34413E+03	1.17894E-01	1.00000E+00	0	0	0	0
4210000	4210000	4220000	6.35666E+00	6.35666E+00	5.34413E+03	1.17894E-01	1.00000E+00	0	0	0	0
4220000	4220000	4230000	6.35666E+00	6.35666E+00	5.34413E+03	1.17894E-01	1.00000E+00	0	0	0	0
4230000	4230000	4240000	6.35666E+00	6.35666E+00	5.34413E+03	1.17894E-01	1.00000E+00	0	0	0	0
4240000	4240000	4250000	6.35666E+00	6.35666E+00	5.34413E+03	1.17894E-01	1.00000E+00	0	0	0	0
4250000	4250000	4260000	6.35666E+00	6.35666E+00	5.34413E+03	1.17894E-01	1.00000E+00	0	0	0	0
4260000	4260000	4270000	6.35666E+00	6.35666E+00	5.34413E+03	1.17894E-01	1.00000E+00	0	0	0	0
4270000	4270000	4280000	6.35666E+00	6.35666E+00	5.34413E+03	1.17894E-01	1.00000E+00	0	0	0	0
4280000	4280000	4290000	6.35666E+00	6.35666E+00	5.34413E+03	1.17894E-01	1.00000E+00	0	0	0	0
INERIAL	VALVE	COMPONENT									
5000000	4290000	6010000	6.35665E+00	0.	5.34412E+03	1.17894E-01	7.83294E-01	100	0	0	0
18 SCH120	PIPE	COMPONENT									
6010000	6010000	6020000	6.35665E+00	0.	5.34412E+03	1.17894E-01	1.00000E+00	0	0	0	0
6020000	6020000	6030000	6.35665E+00	0.	5.34412E+03	1.17894E-01	1.00000E+00	0	0	0	0
6030000	6030000	6040000	6.35665E+00	0.	5.34412E+03	1.17894E-01	1.00000E+00	0	0	0	0
6040000	6040000	6050000	6.35665E+00	0.	5.34412E+03	1.17894E-01	1.00000E+00	0	0	0	0
6050000	6050000	6060000	6.35665E+00	0.	5.34412E+03	1.17894E-01	1.00000E+00	0	0	0	0
6060000	6060000	6070000	6.35665E+00	0.	5.34412E+03	1.17894E-01	1.00000E+00	0	0	0	0
6070000	6070000	6080000	6.35665E+00	0.	5.34412E+03	1.17894E-01	1.00000E+00	0	0	0	0
6080000	6080000	6090000	6.35665E+00	0.	5.34412E+03	1.17894E-01	1.00000E+00	0	0	0	0

6090000	6090000	6100000	6.35665E+00	0.	5.34412E+03	1.17894E-01	1.00000E+00	0	0	0	0
6100000	6100000	6110000	6.35665E+00	0.	5.34412E+03	1.17894E-01	1.00000E+00	0	0	0	0
6110000	6110000	6120000	6.35665E+00	0.	5.34412E+03	1.17894E-01	1.00000E+00	0	0	0	0
6120000	6120000	6130000	6.35665E+00	0.	5.34412E+03	1.17894E-01	1.00000E+00	0	0	0	0
6130000	6130000	6140000	6.35665E+00	0.	5.34412E+03	1.17894E-01	1.00000E+00	0	0	0	0
6140000	6140000	6150000	6.35665E+00	0.	5.34412E+03	1.17894E-01	1.00000E+00	0	0	0	0
CNT VLV	SNGLJUN	COMPONENT									
7000000	6150000	8010000	7.15758E+00	0.	6.01747E+03	1.04702E-01	1.00000E+00	0	0	0	0
18 SCH100	PIPE	COMPONENT									
8010000	8010000	8020000	6.01087E+00	0.	5.05342E+03	1.24676E-01	1.00000E+00	0	0	0	0
8020000	8020000	8030000	6.01087E+00	0.	5.05342E+03	1.24676E-01	1.00000E+00	0	0	0	0
8030000	8030000	8040000	6.01087E+00	0.	5.05342E+03	1.24676E-01	1.00000E+00	0	0	0	0
8040000	8040000	8050000	6.01087E+00	0.	5.05342E+03	1.24676E-01	1.00000E+00	0	0	0	0
8050000	8050000	8060000	6.01087E+00	0.	5.05342E+03	1.24676E-01	1.00000E+00	0	0	0	0
8060000	8060000	8070000	6.01087E+00	0.	5.05342E+03	1.24676E-01	1.00000E+00	0	0	0	0
8070000	8070000	8080000	6.01087E+00	0.	5.05342E+03	1.24676E-01	1.00000E+00	0	0	0	0
8080000	8080000	8090000	6.01087E+00	0.	5.05342E+03	1.24676E-01	1.00000E+00	0	0	0	0
8090000	8090000	8100000	6.01087E+00	0.	5.05342E+03	1.24676E-01	1.00000E+00	0	0	0	0
TEE	PLENUM	COMPONENT									
9010000	8100000	9010000	6.01087E+00	0.	5.05342E+03	6.23379E-02	1.00000E+00	0	0	0	0
9020000	8100000	9010000	6.01087E+00	0.	5.05342E+03	6.23379E-02	1.00000E+00	0	0	0	0
9030000	9010000	10010000	5.71288E+00	0.	4.80290E+03	6.55895E-02	1.00000E+00	0	0	0	0
9040000	9010000	10010000	5.71288E+00	0.	4.80290E+03	6.55895E-02	1.00000E+00	0	0	0	0
12 SCH80	PIPE	COMPONENT									
10010000	10010000	10020000	5.71288E+00	0.	4.80290E+03	6.55895E-02	1.00000E+00	0	0	0	0
10020000	10020000	10030000	5.71288E+00	0.	4.80290E+03	6.55895E-02	1.00000E+00	0	0	0	0
10030000	10030000	10040000	5.71288E+00	0.	4.80290E+03	6.55895E-02	1.00000E+00	0	0	0	0
10040000	10040000	10050000	5.71288E+00	0.	4.80290E+03	6.55895E-02	1.00000E+00	0	0	0	0
10050000	10050000	10060000	5.71288E+00	0.	4.80290E+03	6.55895E-02	1.00000E+00	0	0	0	0
10060000	10060000	10070000	5.71288E+00	0.	4.80290E+03	6.55895E-02	1.00000E+00	0	0	0	0
10070000	10070000	10080000	5.71288E+00	0.	4.80290E+03	6.55895E-02	1.00000E+00	0	0	0	0
10080000	10080000	10090000	5.71288E+00	0.	4.80290E+03	6.55895E-02	1.00000E+00	0	0	0	0
10090000	10090000	10100000	5.71288E+00	0.	4.80290E+03	6.55895E-02	1.00000E+00	0	0	0	0
10100000	10100000	10110000	5.71288E+00	0.	4.80290E+03	6.55895E-02	1.00000E+00	0	0	0	0
10110000	10110000	10120000	5.71288E+00	0.	4.80290E+03	6.55895E-02	1.00000E+00	0	0	0	0
10120000	10120000	10130000	5.71288E+00	0.	4.80290E+03	6.55895E-02	1.00000E+00	0	0	0	0
10130000	10130000	10140000	5.71288E+00	0.	4.80290E+03	6.55895E-02	1.00000E+00	0	0	0	0
10140000	10140000	10150000	5.71288E+00	0.	4.80290E+03	6.55895E-02	1.00000E+00	0	0	0	0
10150000	10150000	10160000	5.71288E+00	0.	4.80290E+03	6.55895E-02	1.00000E+00	0	0	0	0
10160000	10160000	10170000	5.71288E+00	0.	4.80290E+03	6.55895E-02	1.00000E+00	0	0	0	0
10170000	10170000	10180000	5.71288E+00	0.	4.80290E+03	6.55895E-02	1.00000E+00	0	0	0	0
10180000	10180000	10190000	5.71288E+00	0.	4.80290E+03	6.55895E-02	1.00000E+00	0	0	0	0
10190000	10190000	10200000	5.71288E+00	0.	4.80290E+03	6.55895E-02	1.00000E+00	0	0	0	0
10200000	10200000	10210000	5.71288E+00	0.	4.80290E+03	6.55895E-02	1.00000E+00	0	0	0	0
10210000	10210000	10220000	5.71288E+00	0.	4.80290E+03	6.55895E-02	1.00000E+00	0	0	0	0
10220000	10220000	10230000	5.71288E+00	0.	4.80290E+03	6.55895E-02	1.00000E+00	0	0	0	0
10230000	10230000	10240000	5.71288E+00	0.	4.80290E+03	6.55895E-02	1.00000E+00	0	0	0	0
10240000	10240000	10250000	5.71288E+00	0.	4.80290E+03	6.55895E-02	1.00000E+00	0	0	0	0
10250000	10250000	10260000	5.71288E+00	0.	4.80290E+03	6.55895E-02	1.00000E+00	0	0	0	0
10260000	10260000	10270000	5.71288E+00	0.	4.80290E+03	6.55895E-02	1.00000E+00	0	0	0	0
10270000	10270000	10280000	5.71288E+00	0.	4.80290E+03	6.55895E-02	1.00000E+00	0	0	0	0
10280000	10280000	10290000	5.71288E+00	0.	4.80290E+03	6.55895E-02	1.00000E+00	0	0	0	0
10290000	10290000	10300000	5.71288E+00	0.	4.80290E+03	6.55895E-02	1.00000E+00	0	0	0	0
JUNCTION	SNGLJUN	COMPONENT									
11000000	10300000	12010000	5.71288E+00	0.	4.80290E+03	6.55895E-02	1.00000E+00	0	0	0	0
12 SCH80	PIPE	COMPONENT									
12010000	12010000	12020000	5.71288E+00	0.	4.80290E+03	6.55895E-02	1.00000E+00	0	0	0	0
12020000	12020000	12030000	5.71288E+00	0.	4.80290E+03	6.55895E-02	1.00000E+00	0	0	0	0
12030000	12030000	12040000	5.71288E+00	0.	4.80290E+03	6.55895E-02	1.00000E+00	0	0	0	0
12040000	12040000	12050000	5.71288E+00	0.	4.80290E+03	6.55895E-02	1.00000E+00	0	0	0	0
12050000	12050000	12060000	5.71288E+00	0.	4.80290E+03	6.55895E-02	1.00000E+00	0	0	0	0

12060000	12060000	12070000	5.71288E+00	0.		4.80290E+03	6.55895E-02	1.00000E+00	0	0	0	0
12070000	12070000	12080000	5.71288E+00	0.		4.80290E+03	6.55895E-02	1.00000E+00	0	0	0	0
12080000	12080000	12090000	5.71288E+00	0.		4.80290E+03	6.55895E-02	1.00000E+00	0	0	0	0
12090000	12090000	12100000	5.71288E+00	0.		4.80290E+03	6.55895E-02	1.00000E+00	0	0	0	0
12100000	12100000	12110000	5.71288E+00	0.		4.80290E+03	6.55895E-02	1.00000E+00	0	0	0	0
12110000	12110000	12120000	5.71288E+00	0.		4.80290E+03	6.55895E-02	1.00000E+00	0	0	0	0
12120000	12120000	12130000	5.71288E+00	0.		4.80290E+03	6.55895E-02	1.00000E+00	0	0	0	0
12130000	12130000	12140000	5.71288E+00	0.		4.80290E+03	6.55895E-02	1.00000E+00	0	0	0	0
12140000	12140000	12150000	5.71288E+00	0.		4.80290E+03	6.55895E-02	1.00000E+00	0	0	0	0
12150000	12150000	12160000	5.71288E+00	0.		4.80290E+03	6.55895E-02	1.00000E+00	0	0	0	0
12160000	12160000	12170000	5.71288E+00	0.		4.80290E+03	6.55895E-02	1.00000E+00	0	0	0	0
JUNCTION	SNGLJUN	COMPONENT										
13000000	12170000	14010000	5.71288E+00	0.		4.80290E+03	6.55895E-02	1.00000E+00	0	0	0	0
12 SCH80	PIPE	COMPONENT										
14010000	14010000	14020000	5.71288E+00	0.		4.80290E+03	6.55895E-02	1.00000E+00	0	0	0	0
14020000	14020000	14030000	5.71288E+00	0.		4.80290E+03	6.55895E-02	1.00000E+00	0	0	0	0
14030000	14030000	14040000	5.71288E+00	0.		4.80290E+03	6.55895E-02	1.00000E+00	0	0	0	0
14040000	14040000	14050000	5.71288E+00	0.		4.80290E+03	6.55895E-02	1.00000E+00	0	0	0	0
14050000	14050000	14060000	5.71288E+00	0.		4.80290E+03	6.55895E-02	1.00000E+00	0	0	0	0
14060000	14060000	14070000	5.71288E+00	0.		4.80290E+03	6.55895E-02	1.00000E+00	0	0	0	0
14070000	14070000	14080000	5.71288E+00	0.		4.80290E+03	6.55895E-02	1.00000E+00	0	0	0	0
14080000	14080000	14090000	5.71288E+00	0.		4.80290E+03	6.55895E-02	1.00000E+00	0	0	0	0
14090000	14090000	14100000	5.71288E+00	0.		4.80290E+03	6.55895E-02	1.00000E+00	0	0	0	0
14100000	14100000	14110000	5.71288E+00	0.		4.80290E+03	6.55895E-02	1.00000E+00	0	0	0	0
14110000	14110000	14120000	5.71288E+00	0.		4.80290E+03	6.55895E-02	1.00000E+00	0	0	0	0
14120000	14120000	14130000	5.71288E+00	0.		4.80290E+03	6.55895E-02	1.00000E+00	0	0	0	0
14130000	14130000	14140000	5.71288E+00	0.		4.80290E+03	6.55895E-02	1.00000E+00	0	0	0	0
14140000	14140000	14150000	5.71288E+00	0.		4.80290E+03	6.55895E-02	1.00000E+00	0	0	0	0
14150000	14150000	14160000	5.71288E+00	0.		4.80290E+03	6.55895E-02	1.00000E+00	0	0	0	0
14160000	14160000	14170000	5.71288E+00	0.		4.80290E+03	6.55895E-02	1.00000E+00	0	0	0	0
14170000	14170000	14180000	5.71288E+00	0.		4.80290E+03	6.55895E-02	1.00000E+00	0	0	0	0
14180000	14180000	14190000	5.71288E+00	0.		4.80290E+03	6.55895E-02	1.00000E+00	0	0	0	0
14190000	14190000	14200000	5.71288E+00	0.		4.80290E+03	6.55895E-02	1.00000E+00	0	0	0	0
JUNCTION	SNGLJUN	COMPONENT										
15000000	14200000	16010000	5.71288E+00	0.		4.80290E+03	6.55895E-02	1.00000E+00	0	0	0	0
12 SCH80	PIPE	COMPONENT										
16010000	16010000	16020000	5.71290E+00	5.71290E+00		4.80291E+03	6.55895E-02	1.00000E+00	0	0	0	0
16020000	16020000	16030000	5.71290E+00	5.71290E+00		4.80291E+03	6.55895E-02	1.00000E+00	0	0	0	0
16030000	16030000	16040000	5.71290E+00	5.71290E+00		4.80291E+03	6.55895E-02	1.00000E+00	0	0	0	0
16040000	16040000	16050000	5.71290E+00	5.71290E+00		4.80291E+03	6.55895E-02	1.00000E+00	0	0	0	0
16050000	16050000	16060000	5.71290E+00	5.71290E+00		4.80291E+03	6.55895E-02	1.00000E+00	0	0	0	0
16060000	16060000	16070000	5.71290E+00	5.71290E+00		4.80291E+03	6.55895E-02	1.00000E+00	0	0	0	0
16070000	16070000	16080000	5.71290E+00	5.71290E+00		4.80291E+03	6.55895E-02	1.00000E+00	0	0	0	0
16080000	16080000	16090000	5.71290E+00	5.71290E+00		4.80291E+03	6.55895E-02	1.00000E+00	0	0	0	0
16090000	16090000	16100000	5.71290E+00	5.71290E+00		4.80291E+03	6.55895E-02	1.00000E+00	0	0	0	0
16100000	16100000	16110000	5.71290E+00	5.71290E+00		4.80291E+03	6.55895E-02	1.00000E+00	0	0	0	0
16110000	16110000	16120000	5.71290E+00	5.71290E+00		4.80291E+03	6.55895E-02	1.00000E+00	0	0	0	0
16120000	16120000	16130000	5.71290E+00	5.71290E+00		4.80291E+03	6.55895E-02	1.00000E+00	0	0	0	0
16130000	16130000	16140000	5.71290E+00	5.71290E+00		4.80291E+03	6.55895E-02	1.00000E+00	0	0	0	0
16140000	16140000	16150000	5.71290E+00	5.71290E+00		4.80291E+03	6.55895E-02	1.00000E+00	0	0	0	0
BDY JUN	SNGLJUN	COMPONENT										
17000000	16150000	18010000	6.01983E+00	6.01983E+00		5.06095E+03	6.22450E-02	1.00000E+00	0	0	0	0
12 SCH80	PIPE	COMPONENT										
19010000	19010000	19020000	5.71288E+00	0.		4.80290E+03	6.55895E-02	1.00000E+00	0	0	0	0
19020000	19020000	19030000	5.71288E+00	0.		4.80290E+03	6.55895E-02	1.00000E+00	0	0	0	0
19030000	19030000	19040000	5.71288E+00	0.		4.80290E+03	6.55895E-02	1.00000E+00	0	0	0	0
19040000	19040000	19050000	5.71288E+00	0.		4.80290E+03	6.55895E-02	1.00000E+00	0	0	0	0
19050000	19050000	19060000	5.71288E+00	0.		4.80290E+03	6.55895E-02	1.00000E+00	0	0	0	0
19060000	19060000	19070000	5.71288E+00	0.		4.80290E+03	6.55895E-02	1.00000E+00	0	0	0	0
19070000	19070000	19080000	5.71288E+00	0.		4.80290E+03	6.55895E-02	1.00000E+00	0	0	0	0
19080000	19080000	19090000	5.71288E+00	0.		4.80290E+03	6.55895E-02	1.00000E+00	0	0	0	0

12215 291

839

19090000	19090000	19100000	5.71288E+00	0.	4.80290E+03	6.55895E-02	1.00000E+00	0	0	0	0
19100000	19100000	19110000	5.71288E+00	0.	4.80290E+03	6.55895E-02	1.00000E+00	0	0	0	0
19110000	19110000	19120000	5.71288E+00	0.	4.80290E+03	6.55895E-02	1.00000E+00	0	0	0	0
19120000	19120000	19130000	5.71288E+00	0.	4.80290E+03	6.55895E-02	1.00000E+00	0	0	0	0
19130000	19130000	19140000	5.71288E+00	0.	4.80290E+03	6.55895E-02	1.00000E+00	0	0	0	0
19140000	19140000	19150000	5.71288E+00	0.	4.80290E+03	6.55895E-02	1.00000E+00	0	0	0	0
19150000	19150000	19160000	5.71288E+00	0.	4.80290E+03	6.55895E-02	1.00000E+00	0	0	0	0
19160000	19160000	19170000	5.71288E+00	0.	4.80290E+03	6.55895E-02	1.00000E+00	0	0	0	0
19170000	19170000	19180000	5.71288E+00	0.	4.80290E+03	6.55895E-02	1.00000E+00	0	0	0	0
19180000	19180000	19190000	5.71288E+00	0.	4.80290E+03	6.55895E-02	1.00000E+00	0	0	0	0
19190000	19190000	19200000	5.71288E+00	0.	4.80290E+03	6.55895E-02	1.00000E+00	0	0	0	0
19200000	19200000	19210000	5.71288E+00	0.	4.80290E+03	6.55895E-02	1.00000E+00	0	0	0	0
19210000	19210000	19220000	5.71288E+00	0.	4.80290E+03	6.55895E-02	1.00000E+00	0	0	0	0
19220000	19220000	19230000	5.71288E+00	0.	4.80290E+03	6.55895E-02	1.00000E+00	0	0	0	0
19230000	19230000	19240000	5.71288E+00	0.	4.80290E+03	6.55895E-02	1.00000E+00	0	0	0	0
19240000	19240000	19250000	5.71288E+00	0.	4.80290E+03	6.55895E-02	1.00000E+00	0	0	0	0
19250000	19250000	19260000	5.71288E+00	0.	4.80290E+03	6.55895E-02	1.00000E+00	0	0	0	0
19260000	19260000	19270000	5.71288E+00	0.	4.80290E+03	6.55895E-02	1.00000E+00	0	0	0	0
19270000	19270000	19280000	5.71288E+00	0.	4.80290E+03	6.55895E-02	1.00000E+00	0	0	0	0
19280000	19280000	19290000	5.71288E+00	0.	4.80290E+03	6.55895E-02	1.00000E+00	0	0	0	0
19290000	19290000	19300000	5.71288E+00	0.	4.80290E+03	6.55895E-02	1.00000E+00	0	0	0	0
19300000	19300000	19310000	5.71288E+00	0.	4.80290E+03	6.55895E-02	1.00000E+00	0	0	0	0
19310000	19310000	19320000	5.71288E+00	0.	4.80290E+03	6.55895E-02	1.00000E+00	0	0	0	0
19320000	19320000	19330000	5.71288E+00	0.	4.80290E+03	6.55895E-02	1.00000E+00	0	0	0	0
19330000	19330000	19340000	5.71288E+00	0.	4.80290E+03	6.55895E-02	1.00000E+00	0	0	0	0
19340000	19340000	19350000	5.71288E+00	0.	4.80290E+03	6.55895E-02	1.00000E+00	0	0	0	0
19350000	19350000	19360000	5.71288E+00	0.	4.80290E+03	6.55895E-02	1.00000E+00	0	0	0	0
19360000	19360000	19370000	5.71288E+00	0.	4.80290E+03	6.55895E-02	1.00000E+00	0	0	0	0
19370000	19370000	19380000	5.71288E+00	0.	4.80290E+03	6.55895E-02	1.00000E+00	0	0	0	0
19380000	19380000	19390000	5.71288E+00	0.	4.80290E+03	6.55895E-02	1.00000E+00	0	0	0	0
19390000	19390000	19400000	5.71288E+00	0.	4.80290E+03	6.55895E-02	1.00000E+00	0	0	0	0
19400000	19400000	19410000	5.71288E+00	0.	4.80290E+03	6.55895E-02	1.00000E+00	0	0	0	0
19410000	19410000	19420000	5.71288E+00	0.	4.80290E+03	6.55895E-02	1.00000E+00	0	0	0	0
19420000	19420000	19430000	5.71288E+00	0.	4.80290E+03	6.55895E-02	1.00000E+00	0	0	0	0
19430000	19430000	19440000	5.71288E+00	0.	4.80290E+03	6.55895E-02	1.00000E+00	0	0	0	0
19440000	19440000	19450000	5.71288E+00	0.	4.80290E+03	6.55895E-02	1.00000E+00	0	0	0	0
19450000	19450000	19460000	5.71288E+00	0.	4.80290E+03	6.55895E-02	1.00000E+00	0	0	0	0
19460000	19460000	19470000	5.71288E+00	0.	4.80290E+03	6.55895E-02	1.00000E+00	0	0	0	0
JUNCTION	SNGLJUN	COMPONENT									
20000000	19470000	21010000	5.71288E+00	0.	4.80290E+03	6.55895E-02	1.00000E+00	0	0	0	0
12 SCH80	PIPE	COMPONENT									
21010000	21010000	21020000	5.71288E+00	0.	4.80290E+03	6.55895E-02	1.00000E+00	0	0	0	0
21020000	21020000	21030000	5.71288E+00	0.	4.80290E+03	6.55895E-02	1.00000E+00	0	0	0	0
21030000	21030000	21040000	5.71288E+00	0.	4.80290E+03	6.55895E-02	1.00000E+00	0	0	0	0
21040000	21040000	21050000	5.71288E+00	0.	4.80290E+03	6.55895E-02	1.00000E+00	0	0	0	0
21050000	21050000	21060000	5.71288E+00	0.	4.80290E+03	6.55895E-02	1.00000E+00	0	0	0	0
21060000	21060000	21070000	5.71288E+00	0.	4.80290E+03	6.55895E-02	1.00000E+00	0	0	0	0
21070000	21070000	21080000	5.71288E+00	0.	4.80290E+03	6.55895E-02	1.00000E+00	0	0	0	0
21080000	21080000	21090000	5.71288E+00	0.	4.80290E+03	6.55895E-02	1.00000E+00	0	0	0	0
21090000	21090000	21100000	5.71288E+00	0.	4.80290E+03	6.55895E-02	1.00000E+00	0	0	0	0
21100000	21100000	21110000	5.71288E+00	0.	4.80290E+03	6.55895E-02	1.00000E+00	0	0	0	0
21110000	21110000	21120000	5.71288E+00	0.	4.80290E+03	6.55895E-02	1.00000E+00	0	0	0	0
21120000	21120000	21130000	5.71288E+00	0.	4.80290E+03	6.55895E-02	1.00000E+00	0	0	0	0
21130000	21130000	21140000	5.71288E+00	0.	4.80290E+03	6.55895E-02	1.00000E+00	0	0	0	0
21140000	21140000	21150000	5.71288E+00	0.	4.80290E+03	6.55895E-02	1.00000E+00	0	0	0	0
21150000	21150000	21160000	5.71288E+00	0.	4.80290E+03	6.55895E-02	1.00000E+00	0	0	0	0
21160000	21160000	21170000	5.71288E+00	0.	4.80290E+03	6.55895E-02	1.00000E+00	0	0	0	0
21170000	21170000	21180000	5.71288E+00	0.	4.80290E+03	6.55895E-02	1.00000E+00	0	0	0	0
21180000	21180000	21190000	5.71288E+00	0.	4.80290E+03	6.55895E-02	1.00000E+00	0	0	0	0
21190000	21190000	21200000	5.71288E+00	0.	4.80290E+03	6.55895E-02	1.00000E+00	0	0	0	0
21200000	21200000	21210000	5.71288E+00	0.	4.80290E+03	6.55895E-02	1.00000E+00	0	0	0	0

21210000	21210000	21220000	5.71288E+00	0.	4.80290E+03	6.55895E-02	1.00000E+00	0	0	0	0
JUNCTION	SNGL JUN	COMPONENT									
22000000	21220000	23010000	5.71288E+00	0.	4.80290E+03	6.55895E-02	1.00000E+00	0	0	0	0
12 SCH80	PIPE	COMPONENT									
23010000	23010000	23020000	5.71288E+00	0.	4.80290E+03	6.55895E-02	1.00000E+00	0	0	0	0
23020000	23020000	23030000	5.71288E+00	0.	4.80290E+03	6.55895E-02	1.00000E+00	0	0	0	0
23030000	23030000	23040000	5.71288E+00	0.	4.80290E+03	6.55895E-02	1.00000E+00	0	0	0	0
23040000	23040000	23050000	5.71288E+00	0.	4.80290E+03	6.55895E-02	1.00000E+00	0	0	0	0
23050000	23050000	23060000	5.71288E+00	0.	4.80290E+03	6.55895E-02	1.00000E+00	0	0	0	0
23060000	23060000	23070000	5.71288E+00	0.	4.80290E+03	6.55895E-02	1.00000E+00	0	0	0	0
23070000	23070000	23080000	5.71288E+00	0.	4.80290E+03	6.55895E-02	1.00000E+00	0	0	0	0
23080000	23080000	23090000	5.71288E+00	0.	4.80290E+03	6.55895E-02	1.00000E+00	0	0	0	0
23090000	23090000	23100000	5.71288E+00	0.	4.80290E+03	6.55895E-02	1.00000E+00	0	0	0	0
23100000	23100000	23110000	5.71288E+00	0.	4.80290E+03	6.55895E-02	1.00000E+00	0	0	0	0
23110000	23110000	23120000	5.71288E+00	0.	4.80290E+03	6.55895E-02	1.00000E+00	0	0	0	0
23120000	23120000	23130000	5.71288E+00	0.	4.80290E+03	6.55895E-02	1.00000E+00	0	0	0	0
23130000	23130000	23140000	5.71288E+00	0.	4.80290E+03	6.55895E-02	1.00000E+00	0	0	0	0
23140000	23140000	23150000	5.71288E+00	0.	4.80290E+03	6.55895E-02	1.00000E+00	0	0	0	0
23150000	23150000	23160000	5.71288E+00	0.	4.80290E+03	6.55895E-02	1.00000E+00	0	0	0	0
JUNCTION	SNGL JUN	COMPONENT									
24000000	23160000	25010000	5.71288E+00	0.	4.80290E+03	6.55895E-02	1.00000E+00	0	0	0	0
12 SCH80	PIPE	COMPONENT									
25010000	25010000	25020000	5.71288E+00	0.	4.80290E+03	6.55895E-02	1.00000E+00	0	0	0	0
25020000	25020000	25030000	5.71288E+00	0.	4.80290E+03	6.55895E-02	1.00000E+00	0	0	0	0
25030000	25030000	25040000	5.71288E+00	0.	4.80290E+03	6.55895E-02	1.00000E+00	0	0	0	0
25040000	25040000	25050000	5.71288E+00	0.	4.80290E+03	6.55895E-02	1.00000E+00	0	0	0	0
25050000	25050000	25060000	5.71288E+00	0.	4.80290E+03	6.55895E-02	1.00000E+00	0	0	0	0
25060000	25060000	25070000	5.71288E+00	0.	4.80290E+03	6.55895E-02	1.00000E+00	0	0	0	0
25070000	25070000	25080000	5.71288E+00	0.	4.80290E+03	6.55895E-02	1.00000E+00	0	0	0	0
25080000	25080000	25090000	5.71288E+00	0.	4.80290E+03	6.55895E-02	1.00000E+00	0	0	0	0
25090000	25090000	25100000	5.71288E+00	0.	4.80290E+03	6.55895E-02	1.00000E+00	0	0	0	0
25100000	25100000	25110000	5.71288E+00	0.	4.80290E+03	6.55895E-02	1.00000E+00	0	0	0	0
25110000	25110000	25120000	5.71288E+00	0.	4.80290E+03	6.55895E-02	1.00000E+00	0	0	0	0
25120000	25120000	25130000	5.71288E+00	0.	4.80290E+03	6.55895E-02	1.00000E+00	0	0	0	0
25130000	25130000	25140000	5.71288E+00	0.	4.80290E+03	6.55895E-02	1.00000E+00	0	0	0	0
25140000	25140000	25150000	5.71288E+00	0.	4.80290E+03	6.55895E-02	1.00000E+00	0	0	0	0
25150000	25150000	25160000	5.71288E+00	0.	4.80290E+03	6.55895E-02	1.00000E+00	0	0	0	0
25160000	25160000	25170000	5.71288E+00	0.	4.80290E+03	6.55895E-02	1.00000E+00	0	0	0	0
25170000	25170000	25180000	5.71288E+00	0.	4.80290E+03	6.55895E-02	1.00000E+00	0	0	0	0
25180000	25180000	25190000	5.71288E+00	0.	4.80290E+03	6.55895E-02	1.00000E+00	0	0	0	0
25190000	25190000	25200000	5.71288E+00	0.	4.80290E+03	6.55895E-02	1.00000E+00	0	0	0	0
JUNCTION	SNGL JUN	COMPONENT									
26000000	25200000	27010000	5.71288E+00	0.	4.80290E+03	6.55895E-02	1.00000E+00	0	0	0	0
12 SCH80	PIPE	COMPONENT									
27010000	27010000	27020000	5.71290E+00	5.71290E+00	4.80291E+03	6.55895E-02	1.00000E+00	0	0	0	0
27020000	27020000	27030000	5.71290E+00	5.71290E+00	4.80291E+03	6.55895E-02	1.00000E+00	0	0	0	0
27030000	27030000	27040000	5.71290E+00	5.71290E+00	4.80291E+03	6.55895E-02	1.00000E+00	0	0	0	0
27040000	27040000	27050000	5.71290E+00	5.71290E+00	4.80291E+03	6.55895E-02	1.00000E+00	0	0	0	0
27050000	27050000	27060000	5.71290E+00	5.71290E+00	4.80291E+03	6.55895E-02	1.00000E+00	0	0	0	0
27060000	27060000	27070000	5.71290E+00	5.71290E+00	4.80291E+03	6.55895E-02	1.00000E+00	0	0	0	0
27070000	27070000	27080000	5.71290E+00	5.71290E+00	4.80291E+03	6.55895E-02	1.00000E+00	0	0	0	0
27080000	27080000	27090000	5.71290E+00	5.71290E+00	4.80291E+03	6.55895E-02	1.00000E+00	0	0	0	0
27090000	27090000	27100000	5.71290E+00	5.71290E+00	4.80291E+03	6.55895E-02	1.00000E+00	0	0	0	0
27100000	27100000	27110000	5.71290E+00	5.71290E+00	4.80291E+03	6.55895E-02	1.00000E+00	0	0	0	0
27110000	27110000	27120000	5.71290E+00	5.71290E+00	4.80291E+03	6.55895E-02	1.00000E+00	0	0	0	0
27120000	27120000	27130000	5.71290E+00	5.71290E+00	4.80291E+03	6.55895E-02	1.00000E+00	0	0	0	0
27130000	27130000	27140000	5.71290E+00	5.71290E+00	4.80291E+03	6.55895E-02	1.00000E+00	0	0	0	0
27140000	27140000	27150000	5.71290E+00	5.71290E+00	4.80291E+03	6.55895E-02	1.00000E+00	0	0	0	0
BDY JUN	SNGL JUN	COMPONENT									
28000000	27150000	29010000	6.01983E+00	6.01983E+00	5.06095E+03	6.22450E-02	1.00000E+00	0	0	0	0

JUN.NO.	RHOFJ (KG/M3)	RHOGJ (KG/M3)	UFJ (J/KG)	UGJ (J/KG)	VOIDGJ	VOIDD	VOIDT
3000000	9.58393E+02	5.90269E-01	4.17376E+05	2.50605E+06	1.00000E+00	1.00000E+00	1.00000E+00
4010000	8.40714E+02	3.59188E+01	9.50031E+05	2.58260E+06	0.	0.	0.
4020000	8.40714E+02	3.59188E+01	9.50031E+05	2.58260E+06	0.	0.	0.
4030000	8.40714E+02	3.59188E+01	9.50031E+05	2.58260E+06	0.	0.	0.
4040000	8.40714E+02	3.59188E+01	9.50031E+05	2.58260E+06	0.	0.	0.
4050000	8.40714E+02	3.59188E+01	9.50031E+05	2.58260E+06	0.	0.	0.
4060000	8.40714E+02	3.59188E+01	9.50031E+05	2.58260E+06	0.	0.	0.
4070000	8.40714E+02	3.59188E+01	9.50031E+05	2.58260E+06	0.	0.	0.
4080000	8.40714E+02	3.59188E+01	9.50031E+05	2.58260E+06	0.	0.	0.
4090000	8.40714E+02	3.59188E+01	9.50031E+05	2.58260E+06	0.	0.	0.
4100000	8.40714E+02	3.59188E+01	9.50031E+05	2.58260E+06	0.	0.	0.
4110000	8.40714E+02	3.59188E+01	9.50031E+05	2.58260E+06	0.	0.	0.
4120000	8.40714E+02	3.59188E+01	9.50031E+05	2.58260E+06	0.	0.	0.
4130000	8.40714E+02	3.59188E+01	9.50031E+05	2.58260E+06	0.	0.	0.
4140000	8.40714E+02	3.59188E+01	9.50031E+05	2.58260E+06	0.	0.	0.
4150000	8.40714E+02	3.59188E+01	9.50031E+05	2.58260E+06	0.	0.	0.
4160000	8.40714E+02	3.59188E+01	9.50031E+05	2.58260E+06	0.	0.	0.
4170000	8.40714E+02	3.59188E+01	9.50031E+05	2.58260E+06	0.	0.	0.
4180000	8.40714E+02	3.59188E+01	9.50031E+05	2.58260E+06	0.	0.	0.
4190000	8.40714E+02	3.59188E+01	9.50031E+05	2.58260E+06	0.	0.	0.
4200000	8.40714E+02	3.59188E+01	9.50031E+05	2.58260E+06	0.	0.	0.
4210000	8.40714E+02	3.59188E+01	9.50031E+05	2.58260E+06	0.	0.	0.
4220000	8.40714E+02	3.59188E+01	9.50031E+05	2.58260E+06	0.	0.	0.
4230000	8.40714E+02	3.59188E+01	9.50031E+05	2.58260E+06	0.	0.	0.
4240000	8.40714E+02	3.59188E+01	9.50031E+05	2.58260E+06	0.	0.	0.
4250000	8.40714E+02	3.59188E+01	9.50031E+05	2.58260E+06	0.	0.	0.
4260000	8.40714E+02	3.59188E+01	9.50031E+05	2.58260E+06	0.	0.	0.
4270000	8.40714E+02	3.59188E+01	9.50031E+05	2.58260E+06	0.	0.	0.
4280000	8.40714E+02	3.59188E+01	9.50031E+05	2.58260E+06	0.	0.	0.
5000000	8.40714E+02	3.59188E+01	9.50031E+05	2.58260E+06	0.	1.00000E-05	1.00000E-05
6010000	8.40714E+02	3.59188E+01	9.50031E+05	2.58260E+06	0.	0.	0.
6020000	8.40714E+02	3.59188E+01	9.50031E+05	2.58260E+06	0.	0.	0.
6030000	8.40714E+02	3.59188E+01	9.50031E+05	2.58260E+06	0.	0.	0.
6040000	8.40714E+02	3.59188E+01	9.50031E+05	2.58260E+06	0.	0.	0.
6050000	8.40714E+02	3.59188E+01	9.50031E+05	2.58260E+06	0.	0.	0.
6060000	8.40714E+02	3.59188E+01	9.50031E+05	2.58260E+06	0.	0.	0.
6070000	8.40714E+02	3.59188E+01	9.50031E+05	2.58260E+06	0.	0.	0.
6080000	8.40714E+02	3.59188E+01	9.50031E+05	2.58260E+06	0.	0.	0.
6090000	8.40714E+02	3.59188E+01	9.50031E+05	2.58260E+06	0.	0.	0.
6100000	8.40714E+02	3.59188E+01	9.50031E+05	2.58260E+06	0.	0.	0.
6110000	8.40714E+02	3.59188E+01	9.50031E+05	2.58260E+06	0.	0.	0.
6120000	8.40714E+02	3.59188E+01	9.50031E+05	2.58260E+06	0.	0.	0.
6130000	8.40714E+02	3.59188E+01	9.50031E+05	2.58260E+06	0.	0.	0.
6140000	8.40714E+02	3.59188E+01	9.50031E+05	2.58260E+06	0.	0.	0.
7000000	8.40714E+02	3.59188E+01	9.50031E+05	2.58260E+06	0.	0.	0.
8010000	8.40714E+02	3.59188E+01	9.50031E+05	2.58260E+06	0.	0.	0.
8020000	8.40714E+02	3.59188E+01	9.50031E+05	2.58260E+06	0.	0.	0.
8030000	8.40714E+02	3.59188E+01	9.50031E+05	2.58260E+06	0.	0.	0.
8040000	8.40714E+02	3.59188E+01	9.50031E+05	2.58260E+06	0.	0.	0.
8050000	8.40714E+02	3.59188E+01	9.50031E+05	2.58260E+06	0.	0.	0.
8060000	8.40714E+02	3.59188E+01	9.50031E+05	2.58260E+06	0.	0.	0.
8070000	8.40714E+02	3.59188E+01	9.50031E+05	2.58260E+06	0.	0.	0.
8080000	8.40714E+02	3.59188E+01	9.50031E+05	2.58260E+06	0.	0.	0.
8090000	8.40714E+02	3.59188E+01	9.50031E+05	2.58260E+06	0.	0.	0.
9010000	8.40714E+02	3.59188E+01	9.50031E+05	2.58260E+06	0.	0.	0.
9020000	8.40714E+02	3.59188E+01	9.50031E+05	2.58260E+06	0.	0.	0.
9030000	8.40714E+02	3.59188E+01	9.50031E+05	2.58260E+06	0.	0.	0.
9040000	8.40714E+02	3.59188E+01	9.50031E+05	2.58260E+06	0.	0.	0.
10010000	8.40714E+02	3.59188E+01	9.50031E+05	2.58260E+06	0.	0.	0.

10020000	8.40714E+02	3.59188E+01	9.50031E+05	2.58260E+06	0.	0.	0.
10030000	8.40714E+02	3.59188E+01	9.50031E+05	2.58260E+06	0.	0.	0.
10040000	8.40714E+02	3.59188E+01	9.50031E+05	2.58260E+06	0.	0.	0.
10050000	8.40714E+02	3.59188E+01	9.50031E+05	2.58260E+06	0.	0.	0.
10060000	8.40714E+02	3.59188E+01	9.50031E+05	2.58260E+06	0.	0.	0.
10070000	8.40714E+02	3.59188E+01	9.50031E+05	2.58260E+06	0.	0.	0.
10080000	8.40714E+02	3.59188E+01	9.50031E+05	2.58260E+06	0.	0.	0.
10090000	8.40714E+02	3.59188E+01	9.50031E+05	2.58260E+06	0.	0.	0.
10100000	8.40714E+02	3.59188E+01	9.50031E+05	2.58260E+06	0.	0.	0.
10110000	8.40714E+02	3.59188E+01	9.50031E+05	2.58260E+06	0.	0.	0.
10120000	8.40714E+02	3.59188E+01	9.50031E+05	2.58260E+06	0.	0.	0.
10130000	8.40714E+02	3.59188E+01	9.50031E+05	2.58260E+06	0.	0.	0.
10140000	8.40714E+02	3.59188E+01	9.50031E+05	2.58260E+06	0.	0.	0.
10150000	8.40714E+02	3.59188E+01	9.50031E+05	2.58260E+06	0.	0.	0.
10160000	8.40714E+02	3.59188E+01	9.50031E+05	2.58260E+06	0.	0.	0.
10170000	8.40714E+02	3.59188E+01	9.50031E+05	2.58260E+06	0.	0.	0.
10180000	8.40714E+02	3.59188E+01	9.50031E+05	2.58260E+06	0.	0.	0.
10190000	8.40714E+02	3.59188E+01	9.50031E+05	2.58260E+06	0.	0.	0.
10200000	8.40714E+02	3.59188E+01	9.50031E+05	2.58260E+06	0.	0.	0.
10210000	8.40714E+02	3.59188E+01	9.50031E+05	2.58260E+06	0.	0.	0.
10220000	8.40714E+02	3.59188E+01	9.50031E+05	2.58260E+06	0.	0.	0.
10230000	8.40714E+02	3.59188E+01	9.50031E+05	2.58260E+06	0.	0.	0.
10240000	8.40714E+02	3.59188E+01	9.50031E+05	2.58260E+06	0.	0.	0.
10250000	8.40714E+02	3.59188E+01	9.50031E+05	2.58260E+06	0.	0.	0.
10260000	8.40714E+02	3.59188E+01	9.50031E+05	2.58260E+06	0.	0.	0.
10270000	8.40714E+02	3.59188E+01	9.50031E+05	2.58260E+06	0.	0.	0.
10280000	8.40714E+02	3.59188E+01	9.50031E+05	2.58260E+06	0.	0.	0.
10290000	8.40714E+02	3.59188E+01	9.50031E+05	2.58260E+06	0.	0.	0.
11000000	8.40714E+02	3.59188E+01	9.50031E+05	2.58260E+06	0.	0.	0.
12010000	8.40714E+02	3.59188E+01	9.50031E+05	2.58260E+06	0.	0.	0.
12020000	8.40714E+02	3.59188E+01	9.50031E+05	2.58260E+06	0.	0.	0.
12030000	8.40714E+02	3.59188E+01	9.50031E+05	2.58260E+06	0.	0.	0.
12040000	8.40714E+02	3.59188E+01	9.50031E+05	2.58260E+06	0.	0.	0.
12050000	8.40714E+02	3.59188E+01	9.50031E+05	2.58260E+06	0.	0.	0.
12060000	8.40714E+02	3.59188E+01	9.50031E+05	2.58260E+06	0.	0.	0.
12070000	8.40714E+02	3.59188E+01	9.50031E+05	2.58260E+06	0.	0.	0.
12080000	8.40714E+02	3.59188E+01	9.50031E+05	2.58260E+06	0.	0.	0.
12090000	8.40714E+02	3.59188E+01	9.50031E+05	2.58260E+06	0.	0.	0.
12100000	8.40714E+02	3.59188E+01	9.50031E+05	2.58260E+06	0.	0.	0.
12110000	8.40714E+02	3.59188E+01	9.50031E+05	2.58260E+06	0.	0.	0.
12120000	8.40714E+02	3.59188E+01	9.50031E+05	2.58260E+06	0.	0.	0.
12130000	8.40714E+02	3.59188E+01	9.50031E+05	2.58260E+06	0.	0.	0.
12140000	8.40714E+02	3.59188E+01	9.50031E+05	2.58260E+06	0.	0.	0.
12150000	8.40714E+02	3.59188E+01	9.50031E+05	2.58260E+06	0.	0.	0.
12160000	8.40714E+02	3.59188E+01	9.50031E+05	2.58260E+06	0.	0.	0.
13000000	8.40714E+02	3.59188E+01	9.50031E+05	2.58260E+06	0.	0.	0.
14010000	8.40714E+02	3.59188E+01	9.50031E+05	2.58260E+06	0.	0.	0.
14020000	8.40714E+02	3.59188E+01	9.50031E+05	2.58260E+06	0.	0.	0.
14030000	8.40714E+02	3.59188E+01	9.50031E+05	2.58260E+06	0.	0.	0.
14040000	8.40714E+02	3.59188E+01	9.50031E+05	2.58260E+06	0.	0.	0.
14050000	8.40714E+02	3.59188E+01	9.50031E+05	2.58260E+06	0.	0.	0.
14060000	8.40714E+02	3.59188E+01	9.50031E+05	2.58260E+06	0.	0.	0.
14070000	8.40714E+02	3.59188E+01	9.50031E+05	2.58260E+06	0.	0.	0.
14080000	8.40714E+02	3.59188E+01	9.50031E+05	2.58260E+06	0.	0.	0.
14090000	8.40714E+02	3.59188E+01	9.50031E+05	2.58260E+06	0.	0.	0.
14100000	8.40714E+02	3.59188E+01	9.50031E+05	2.58260E+06	0.	0.	0.
14110000	8.40714E+02	3.59188E+01	9.50031E+05	2.58260E+06	0.	0.	0.
14120000	8.40714E+02	3.59188E+01	9.50031E+05	2.58260E+06	0.	0.	0.
14130000	8.40714E+02	3.59188E+01	9.50031E+05	2.58260E+06	0.	0.	0.
14140000	8.40714E+02	3.59188E+01	9.50031E+05	2.58260E+06	0.	0.	0.
14150000	8.40714E+02	3.59188E+01	9.50031E+05	2.58260E+06	0.	0.	0.

1215 295

B43

14160000	8.40714E+02	3.59188E+01	9.50031E+05	2.58260E+06	0.	0.
14170000	8.40714E+02	3.59188E+01	9.50031E+05	2.58260E+06	0.	0.
14180000	8.40714E+02	3.59188E+01	9.50031E+05	2.58260E+06	0.	0.
14190000	8.40714E+02	3.59188E+01	9.50031E+05	2.58260E+06	0.	0.
15000000	8.40714E+02	3.59188E+01	9.50031E+05	2.58260E+06	0.	0.
16010000	8.40714E+02	3.59188E+01	9.50031E+05	2.58260E+06	0.	0.
16020000	8.40714E+02	3.59188E+01	9.50031E+05	2.58260E+06	0.	0.
16030000	8.40714E+02	3.59188E+01	9.50031E+05	2.58260E+06	0.	0.
16040000	8.40714E+02	3.59188E+01	9.50031E+05	2.58260E+06	0.	0.
16050000	8.40714E+02	3.59188E+01	9.50031E+05	2.58260E+06	0.	0.
16060000	8.40714E+02	3.59188E+01	9.50031E+05	2.58260E+06	0.	0.
16070000	8.40714E+02	3.59188E+01	9.50031E+05	2.58260E+06	0.	0.
16080000	8.40714E+02	3.59188E+01	9.50031E+05	2.58260E+06	0.	0.
16090000	8.40714E+02	3.59188E+01	9.50031E+05	2.58260E+06	0.	0.
16100000	8.40714E+02	3.59188E+01	9.50031E+05	2.58260E+06	0.	0.
16110000	8.40714E+02	3.59188E+01	9.50031E+05	2.58260E+06	0.	0.
16120000	8.40714E+02	3.59188E+01	9.50031E+05	2.58260E+06	0.	0.
16130000	8.40714E+02	3.59188E+01	9.50031E+05	2.58260E+06	0.	0.
16140000	8.40714E+02	3.59188E+01	9.50031E+05	2.58260E+06	0.	0.
17000000	8.40714E+02	3.59188E+01	9.50031E+05	2.58260E+06	0.	0.
19010000	8.40714E+02	3.59188E+01	9.50031E+05	2.58260E+06	0.	0.
19020000	8.40714E+02	3.59188E+01	9.50031E+05	2.58260E+06	0.	0.
19030000	8.40714E+02	3.59188E+01	9.50031E+05	2.58260E+06	0.	0.
19040000	8.40714E+02	3.59188E+01	9.50031E+05	2.58260E+06	0.	0.
19050000	8.40714E+02	3.59188E+01	9.50031E+05	2.58260E+06	0.	0.
19060000	8.40714E+02	3.59188E+01	9.50031E+05	2.58260E+06	0.	0.
19070000	8.40714E+02	3.59188E+01	9.50031E+05	2.58260E+06	0.	0.
19080000	8.40714E+02	3.59188E+01	9.50031E+05	2.58260E+06	0.	0.
19090000	8.40714E+02	3.59188E+01	9.50031E+05	2.58260E+06	0.	0.
19100000	8.40714E+02	3.59188E+01	9.50031E+05	2.58260E+06	0.	0.
19110000	8.40714E+02	3.59188E+01	9.50031E+05	2.58260E+06	0.	0.
19120000	8.40714E+02	3.59188E+01	9.50031E+05	2.58260E+06	0.	0.
19130000	8.40714E+02	3.59188E+01	9.50031E+05	2.58260E+06	0.	0.
19140000	8.40714E+02	3.59188E+01	9.50031E+05	2.58260E+06	0.	0.
19150000	8.40714E+02	3.59188E+01	9.50031E+05	2.58260E+06	0.	0.
19160000	8.40714E+02	3.59188E+01	9.50031E+05	2.58260E+06	0.	0.
19170000	8.40714E+02	3.59188E+01	9.50031E+05	2.58260E+06	0.	0.
19180000	8.40714E+02	3.59188E+01	9.50031E+05	2.58260E+06	0.	0.
19190000	8.40714E+02	3.59188E+01	9.50031E+05	2.58260E+06	0.	0.
19200000	8.40714E+02	3.59188E+01	9.50031E+05	2.58260E+06	0.	0.
19210000	8.40714E+02	3.59188E+01	9.50031E+05	2.58260E+06	0.	0.
19220000	8.40714E+02	3.59188E+01	9.50031E+05	2.58260E+06	0.	0.
19230000	8.40714E+02	3.59188E+01	9.50031E+05	2.58260E+06	0.	0.
19240000	8.40714E+02	3.59188E+01	9.50031E+05	2.58260E+06	0.	0.
19250000	8.40714E+02	3.59188E+01	9.50031E+05	2.58260E+06	0.	0.
19260000	8.40714E+02	3.59188E+01	9.50031E+05	2.58260E+06	0.	0.
19270000	8.40714E+02	3.59188E+01	9.50031E+05	2.58260E+06	0.	0.
19280000	8.40714E+02	3.59188E+01	9.50031E+05	2.58260E+06	0.	0.
19290000	8.40714E+02	3.59188E+01	9.50031E+05	2.58260E+06	0.	0.
19300000	8.40714E+02	3.59188E+01	9.50031E+05	2.58260E+06	0.	0.
19310000	8.40714E+02	3.59188E+01	9.50031E+05	2.58260E+06	0.	0.
19320000	8.40714E+02	3.59188E+01	9.50031E+05	2.58260E+06	0.	0.
19330000	8.40714E+02	3.59188E+01	9.50031E+05	2.58260E+06	0.	0.
19340000	8.40714E+02	3.59188E+01	9.50031E+05	2.58260E+06	0.	0.
19350000	8.40714E+02	3.59188E+01	9.50031E+05	2.58260E+06	0.	0.
19360000	8.40714E+02	3.59188E+01	9.50031E+05	2.58260E+06	0.	0.
19370000	8.40714E+02	3.59188E+01	9.50031E+05	2.58260E+06	0.	0.
19380000	8.40714E+02	3.59188E+01	9.50031E+05	2.58260E+06	0.	0.
19390000	8.40714E+02	3.59188E+01	9.50031E+05	2.58260E+06	0.	0.
19400000	8.40714E+02	3.59188E+01	9.50031E+05	2.58260E+06	0.	0.
19410000	8.40714E+02	3.59188E+01	9.50031E+05	2.58260E+06	0.	0.

1215 2960 ft

844

19420000	8.40714E+02	3.59188E+01	9.50031E+05	2.58260E+06	0.	0.
19430000	8.40714E+02	3.59188E+01	9.50031E+05	2.58260E+06	0.	0.
19440000	8.40714E+02	3.59188E+01	9.50031E+05	2.58260E+06	0.	0.
19450000	8.40714E+02	3.59188E+01	9.50031E+05	2.58260E+06	0.	0.
19460000	8.40714E+02	3.59188E+01	9.50031E+05	2.58260E+06	0.	0.
20000000	8.40714E+02	3.59188E+01	9.50031E+05	2.58260E+06	0.	0.
21010000	8.40714E+02	3.59188E+01	9.50031E+05	2.58260E+06	0.	0.
21020000	8.40714E+02	3.59188E+01	9.50031E+05	2.58260E+06	0.	0.
21030000	8.40714E+02	3.59188E+01	9.50031E+05	2.58260E+06	0.	0.
21040000	8.40714E+02	3.59188E+01	9.50031E+05	2.58260E+06	0.	0.
21050000	8.40714E+02	3.59188E+01	9.50031E+05	2.58260E+06	0.	0.
21060000	8.40714E+02	3.59188E+01	9.50031E+05	2.58260E+06	0.	0.
21070000	8.40714E+02	3.59188E+01	9.50031E+05	2.58260E+06	0.	0.
21080000	8.40714E+02	3.59188E+01	9.50031E+05	2.58260E+06	0.	0.
21090000	8.40714E+02	3.59188E+01	9.50031E+05	2.58260E+06	0.	0.
21100000	8.40714E+02	3.59188E+01	9.50031E+05	2.58260E+06	0.	0.
21110000	8.40714E+02	3.59188E+01	9.50031E+05	2.58260E+06	0.	0.
21120000	8.40714E+02	3.59188E+01	9.50031E+05	2.58260E+06	0.	0.
21130000	8.40714E+02	3.59188E+01	9.50031E+05	2.58260E+06	0.	0.
21140000	8.40714E+02	3.59188E+01	9.50031E+05	2.58260E+06	0.	0.
21150000	8.40714E+02	3.59188E+01	9.50031E+05	2.58260E+06	0.	0.
21160000	8.40714E+02	3.59188E+01	9.50031E+05	2.58260E+06	0.	0.
21170000	8.40714E+02	3.59188E+01	9.50031E+05	2.58260E+06	0.	0.
21180000	8.40714E+02	3.59188E+01	9.50031E+05	2.58260E+06	0.	0.
21190000	8.40714E+02	3.59188E+01	9.50031E+05	2.58260E+06	0.	0.
21200000	8.40714E+02	3.59188E+01	9.50031E+05	2.58260E+06	0.	0.
21210000	8.40714E+02	3.59188E+01	9.50031E+05	2.58260E+06	0.	0.
22000000	8.40714E+02	3.59188E+01	9.50031E+05	2.58260E+06	0.	0.
23010000	8.40714E+02	3.59188E+01	9.50031E+05	2.58260E+06	0.	0.
23020000	8.40714E+02	3.59188E+01	9.50031E+05	2.58260E+06	0.	0.
23030000	8.40714E+02	3.59188E+01	9.50031E+05	2.58260E+06	0.	0.
23040000	8.40714E+02	3.59188E+01	9.50031E+05	2.58260E+06	0.	0.
23050000	8.40714E+02	3.59188E+01	9.50031E+05	2.58260E+06	0.	0.
23060000	8.40714E+02	3.59188E+01	9.50031E+05	2.58260E+06	0.	0.
23070000	8.40714E+02	3.59188E+01	9.50031E+05	2.58260E+06	0.	0.
23080000	8.40714E+02	3.59188E+01	9.50031E+05	2.58260E+06	0.	0.
23090000	8.40714E+02	3.59188E+01	9.50031E+05	2.58260E+06	0.	0.
23100000	8.40714E+02	3.59188E+01	9.50031E+05	2.58260E+06	0.	0.
23110000	8.40714E+02	3.59188E+01	9.50031E+05	2.58260E+06	0.	0.
23120000	8.40714E+02	3.59188E+01	9.50031E+05	2.58260E+06	0.	0.
23130000	8.40714E+02	3.59188E+01	9.50031E+05	2.58260E+06	0.	0.
23140000	8.40714E+02	3.59188E+01	9.50031E+05	2.58260E+06	0.	0.
23150000	8.40714E+02	3.59188E+01	9.50031E+05	2.58260E+06	0.	0.
24000000	8.40714E+02	3.59188E+01	9.50031E+05	2.58260E+06	0.	0.
25010000	8.40714E+02	3.59188E+01	9.50031E+05	2.58260E+06	0.	0.
25020000	8.40714E+02	3.59188E+01	9.50031E+05	2.58260E+06	0.	0.
25030000	8.40714E+02	3.59188E+01	9.50031E+05	2.58260E+06	0.	0.
25040000	8.40714E+02	3.59188E+01	9.50031E+05	2.58260E+06	0.	0.
25050000	8.40714E+02	3.59188E+01	9.50031E+05	2.58260E+06	0.	0.
25060000	8.40714E+02	3.59188E+01	9.50031E+05	2.58260E+06	0.	0.
25070000	8.40714E+02	3.59188E+01	9.50031E+05	2.58260E+06	0.	0.
25080000	8.40714E+02	3.59188E+01	9.50031E+05	2.58260E+06	0.	0.
25090000	8.40714E+02	3.59188E+01	9.50031E+05	2.58260E+06	0.	0.
25100000	8.40714E+02	3.59188E+01	9.50031E+05	2.58260E+06	0.	0.
25110000	8.40714E+02	3.59188E+01	9.50031E+05	2.58260E+06	0.	0.
25120000	8.40714E+02	3.59188E+01	9.50031E+05	2.58260E+06	0.	0.
25130000	8.40714E+02	3.59188E+01	9.50031E+05	2.58260E+06	0.	0.
25140000	8.40714E+02	3.59188E+01	9.50031E+05	2.58260E+06	0.	0.
25150000	8.40714E+02	3.59188E+01	9.50031E+05	2.58260E+06	0.	0.
25160000	8.40714E+02	3.59188E+01	9.50031E+05	2.58260E+06	0.	0.
25170000	8.40714E+02	3.59188E+01	9.50031E+05	2.58260E+06	0.	0.

25180000	8.40714E+02	3.59188E+01	9.50031E+05	2.58260E+06	0.	0.	0.
25190000	8.40714E+02	3.59188E+01	9.50031E+05	2.58260E+06	0.	0.	0.
26000000	8.40714E+02	3.59188E+01	9.50031E+05	2.58260E+06	0.	0.	0.
27010000	8.40714E+02	3.59188E+01	9.50031E+05	2.58260E+06	0.	0.	0.
27020000	8.40714E+02	3.59188E+01	9.50031E+05	2.58260E+06	0.	0.	0.
27030000	8.40714E+02	3.59188E+01	9.50031E+05	2.58260E+06	0.	0.	0.
27040000	8.40714E+02	3.59188E+01	9.50031E+05	2.58260E+06	0.	0.	0.
27050000	8.40714E+02	3.59188E+01	9.50031E+05	2.58260E+06	0.	0.	0.
27060000	8.40714E+02	3.59188E+01	9.50031E+05	2.58260E+06	0.	0.	0.
27070000	8.40714E+02	3.59188E+01	9.50031E+05	2.58260E+06	0.	0.	0.
27080000	8.40714E+02	3.59188E+01	9.50031E+05	2.58260E+06	0.	0.	0.
27090000	8.40714E+02	3.59188E+01	9.50031E+05	2.58260E+06	0.	0.	0.
27100000	8.40714E+02	3.59188E+01	9.50031E+05	2.58260E+06	0.	0.	0.
27110000	8.40714E+02	3.59188E+01	9.50031E+05	2.58260E+06	0.	0.	0.
27120000	8.40714E+02	3.59188E+01	9.50031E+05	2.58260E+06	0.	0.	0.
27130000	8.40714E+02	3.59188E+01	9.50031E+05	2.58260E+06	0.	0.	0.
27140000	8.40714E+02	3.59188E+01	9.50031E+05	2.58260E+06	0.	0.	0.
28000000	8.40714E+02	3.59188E+01	9.50031E+05	2.58260E+06	0.	0.	0.

TIMEHY = .1000E-02 OMEGA = 0.0000 THETA = 70.0000 ATHROT = .7833

PVENC = .2591E+05 DELTAP =0.
$$$$ 770 1.000000E-12

TIMEHY = .5000E-03 OMEGA = 0.0000 THETA = 70.0000 ATHROT = .7833

PVENC = .2591E+05 DELTAP =0.

TIMEHY = .2500E-03 OMEGA = 0.0000 THETA = 70.0000 ATHROT = .7833

PVENC = .2591E+05 DELTAP =0.

TIMEHY = .5000E-03 OMEGA = 0.0000 THETA = 70.0000 ATHROT = .7833

PVENC = .2591E+05 DELTAP = .9796E+03

TIMEHY = .3750E-03 OMEGA = 0.0000 THETA = 70.0000 ATHROT = .7833

PVENC = .2591E+05 DELTAP = .9796E+03

TIMEHY = .3125E-03 OMEGA = 0.0000 THETA = 70.0000 ATHROT = .7833

PVENC = .2591E+05 DELTAP = .9796E+03

TIMEHY = .2813E-03 OMEGA = 0.0000 THETA = 70.0000 ATHROT = .7833

PVENC = .2591E+05 DELTAP = .9796E+03

TIMEHY = .2656E-03 OMEGA = 0.0000 THETA = 70.0000 ATHROT = .7833

PVENC = .2591E+05 DELTAP = .9796E+03

TIMEHY = .2578E-03 OMEGA = 0.0000 THETA = 70.0000 ATHROT = .7833

PVENC = .2591E+05 DELTAP = .9796E+03

TIMEHY = .2656E-03 OMEGA = 0.0000 THETA = 70.0000 ATHROT = .7833

PVENC = .2591E+05 DELTAP = .1010E+04
$$$$ 770 1.000000E-12

12159 298

848

APPENDIX C

RELAP5 HYDRODYNAMICS

Report No. CD-AP-TR-005

Date: January 1978

CODE DEVELOPMENT AND ANALYSIS PROGRAM

RELAP5 PROGRESS SUMMARY

PILOT CODE HYDRODYNAMIC MODEL AND NUMERICAL SCHEME

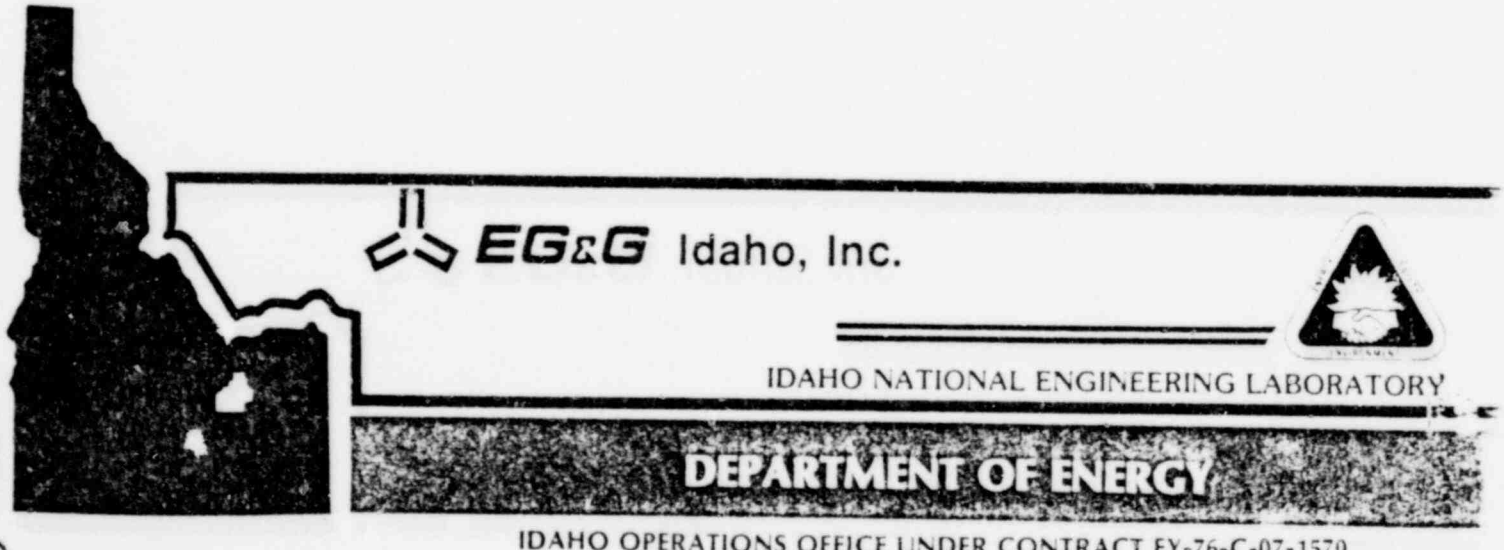

IDAHO OPERATIONS OFFICE UNDER CONTRACT EY-76-C-07-1570

NOTICE

This report was prepared as an account of work sponsored by the United States Government. Neither the United States nor the Department of Energy, nor the Nuclear Regulatory Commission, nor any of their employees, nor any of their contractors, subcontractors, or their employees, makes any warranty, express or implied, or assumes any legal liability or responsibility for the accuracy, completeness or usefulness of any information, apparatus, product or process disclosed, or represents that its use would not infringe privately owned rights.

Report No.: CD-AP-TR-005

Date: January 1978

RELAP5 PROGRESS SUMMARY
PILOT CODE HYDRODYNAMIC MODEL AND NUMERICAL SCHEME

V. H. Ransom

J. A. Trapp

REVIEWED BY:

Paul North

Paul North
Acting Branch Manager

APPROVED BY:

Paul North

Paul North, Manager
Code Development and
Analysis Program

ABSTRACT

The objective of the RELAP5 project is to provide NRC with an efficient, advanced LWR system transient analysis code. A major goal in meeting this objective has been to develop a hydrodynamic model which is both numerically efficient and which includes the important nonhomogeneous and nonequilibrium characteristics of two-phase flow. This goal has been achieved and the resulting hydrodynamic model and the associated numerical scheme is documented herein. The model has been tested in a PILOT code and applied to the analysis of pipe blowdown experiments as well as hypothetical checkout problems. Good agreement with data has been obtained. The PILOT code effort is summarized and continued development will proceed in a computer efficient and user-convenient system code structure.

SUMMARY AND CONCLUSIONS

The objective of the RELAP5 project is to provide NRC with an advanced, fast running, one-dimensional, transient best estimate systems code which is also suitable for a next generation evaluation model and is capable of economically performing repetitive calculations in both the best estimate and evaluation model modes. This objective is being accomplished in a timely manner by development of a relatively simple two-phase nonhomogeneous and nonequilibrium hydrodynamic model in a PILOT code, by utilizing the reactor system modeling technology already developed in the RELAP4 series of codes, and by combining these developments in a computer efficient and user convenient RELAP5 system code structure. The pilot code phase of the RELAP5 hydrodynamic model development[1][2][3][4][5] and associated numerical scheme development is now complete and the purpose of this report is to document the results of this work. The hydrodynamic model has also been installed in the RELAP5 system code structure and all future development will be done using this version of the code.

The RELAP5 hydrodynamic model is a two-fluid nonequilibrium model in which one of the phases is fixed at saturation. Five field equations are employed: (1) the overall continuity equation, (2) the difference of the phasic continuity equations, (3) the overall momentum equation, (4) a difference of the phasic momentum equations, and (5) the overall internal energy equation. The field equations are supplemented with constitutive relations for the equation of state, interphase mass exchange, interphase momentum exchange, and wall friction. An existing water properties subroutine has been improved and incorporated, and preliminary models have been developed for the other constitutive relations. The models were formulated primarly for the purpose of code checkout and are relatively simple. However, simulation of blowdown and steady critical flow experiments

have produced results in good agreement with data. The constitutive relations will be improved as more comprehensive modeling results become available from LWR research programs.

Process models are included in the PILOT code for flow choking, abrupt area change[4], and parallel branching. These models permit the code to be applied to a variety of experimental data for developmental verification. Additional process models for pumps, valves, ECC injection, etc. will be required for reactor systems description. Many of these models will be obtained by conversion of RELAP4 models for inclusion into the RELAP5 system code structure.

The RELAP5 field equations are numerically approximated by difference equations through use of a staggered computational grid. Mass and energy control volumes are connected by flow junctions at which the momentum equations are applied. The spatial derivatives and source terms are evaluated through use of limited implicitness. The general guidelines used in selecting the degree of implicitness are: (1) consistent evaluation of mass and energy flux terms, (2) numerical stability, and (3) tight interphase coupling to provide damping. The differencing scheme is such that all implicit terms are linear in the new time variables. In addition, by judicious choice of implicit terms, the difference equations are easily reduced to a single equation per control volume in terms of the new time pressures. Thus, for a system of N fluid volumes it is only necessary to solve an NxN linear time advancement matrix either directly or by iteration, whichever is faster.

The numerical scheme includes a time step control algorithm based on mass conservation. The time step is continuously adjusted to maintain a preset accuracy. In particular, mass truncation error is controlled at phase boundary crossing, where the system bulk properties are essentially discontinuous. A

small time step is used at the point of phase boundary crossing and then is rapidly increased once the discontinuity is crossed. A restart feature is included which allows rejection of a time step having excessive truncation error and permits restart from the previous solution point with a smaller time step. This feature is used whenever the truncation error exceeds a preset limit or a dependent variable exceeds the legitimate range within a constitutive relationship.

The PILOT code has been tested on many "thought" problems for checkout of the basic numerical scheme, constitutive models, and process models. In particular, two-phase steady flow calculations for abrupt enlargements, contractions, and branched systems have been made to checkout the abrupt area change model[4]. The results appear qualitatively correct when compared with single-phase data. The branching model has been applied to blowdown of a symmetric loop with the result that symmetric and qualitatively correct results were obtained.

The PILOT code has been used to simulate the Edward's 73 mm and 206 mm pipe blowdown[3][5]. The results of the 73 mm pipe simulations are in excellent agreement with the data, both long- and short-term. Nodalization studies using 10, 20 and 40 volumes have demonstrated rapid convergence. The use of proper exit boundary conditions (a velocity model when choked) is primarily responsible for the sharp convergence. The Edward's pipe blowdown simulation using 20 fluid volumes required less than 17 cpu seconds of CDC 7600 computer time to complete blowdown to 0.5 second. The cpu time per node per time step is 0.0005 second (these calculations have also been made using the RELAP5 system code with slightly faster execution times).

The computational efficiency of the RELAP5 hydrodynamic model and associated numerical scheme has been successfully demonstrated in a PILOT code framework. Good agreement between calculated and experimental results have been achieved in application of the code. Develcpment of the efficient and user-convenient system code structure has progressed to the point that it now includes the PILOT code hydrodynamic model and process models for abrupt area change, branching, flow choking and time step control. In addition, the systems code has general heat conductors, generalized system component coupling and a preliminary version of the RELAP4/MOD6 heat transfer surface. All future model development work can now be most effectively accomplished directly in the system code framework.

NOMENCLATURE

Latin Symbols

A	Cross sectional area, coefficient matrix
B	Coefficient matrix
B_x	Body force in x coordinate direction
C	Virtual mass coefficient
C_d	Drag Coefficient
C_p	Specific heat at constant pressure
C_v	Specific heat at constant volume
c	Speed of sound
DISS	Energy dissipation function
E	Total energy $(U + v^2/2)$
FIF,FIG	Interphase drag coefficients, liquid and vapor
FI	Interphase drag coefficient
FWF, FWG	Wall frictional drag coefficients, liquid and vapor
G	Mass velocity
h	Enthalpy, heat transfer coefficient
J	Junction velocity
N	Number of system nodes, number density
n	Unit vector
P	Pressure
Q	Volumetric heat addition
T	Temperature
t	Time
U	Internal energy, vector of dependent variables
V	Volume, specific volume with subscript

v	Fluid velocity
X	Static quality
x	Spatial coordinate

Greek Symbols

α	Volume fraction
β	Coefficient of isobaric thermal expansion
ϕ	Donored property
Γ	Mass volumetric generation rate
λ	Eigenvalue, interface velocity parameter
κ	Coefficient of isothermal compressibility
ρ	Mixture density, component density with subscript
ν	Kinematic viscosity
Δx	Increment in spatial variable
Δt	Increment in time variable

Subscripts

e	Thermodynamic equilibrium
f	Liquid phase
fg	Heat of vaporization
g	Vapor phase
I	Interface
j,j+1,j-1	Spatial noding index, junctions
K,L	Spatial noding index, volumes
m	Mixture property
o	Reference value
p	Particle number density

Superscripts

n,n+1	Time level index
s	Saturation value

Overscore

-	Vector
.	Donored quantity

CONTENTS

CONTENTS (contd.)

TABLE

FIGURES

RELAP5 PROGRESS SUMMARY

PILOT CODE HYDRODYNAMIC MODEL AND NUMERICAL SCHEME

I. INTRODUCTION

The objective of the RELAP5 project is to develop an advanced, one-dimensional, transient, system analysis code for use in light water reactor safety analysis. This objective is being accomplished in a timely manner by development of a relatively simple two-phase nonhomogeneous and non-equilibrium hydrodynamic model and by utilizing the reactor system modeling technology from the RELAP4 series of codes. A new computer efficient and user-convenient system code structure has been designed and both the hydrodynamic model and converted RELAP4 models are being systematically incorporated into this structure.

The hydrodynamic model was initially developed in a simple PILOT code which could be readily modified to test flow modeling techniques and numerical solution schemes. This phase of the effort is now complete and the purpose of this report is to document the hydrodynamic model and associated numerical scheme which has been developed. The goal of this phase of the RELAP5 project has been achieved; i.e., a relatively simple, fast running nonhomogeneous, nonequilibrium hydrodynamic model has been developed, tested and shown to be feasible for use in a light water reactor transient system analysis code.

The logical continuation of the RELAP5 project will emphasize development of the hydrodynamic model and process/component models within the system code structure. This approach will yield maximum benefit for the effort expended since model conversion from the PILOT code to the system code is eliminated. A second benefit is that more experience with application of the

system code version is accumulated as the code is developed, thus enhancing early reliability of the code.

This report records the PILOT code phase of the hydrodynamic model development. The phasic conservation equations are recorded in differential form and subsequently the numerical solution scheme and the associated thermodynamic relations are developed in detail. The process models for abrupt area change, branching and flow choking are briefly described. However, the flow choking model is still under development and complete documentation will follow completion of this work. Finally, the results from the application of the code to pipe blowdown problems are given.

II. NONEQUILIBRIUM HYDRODYNAMIC MODEL ($2VT_kT_{sat}$)

1. GENERAL

The hydrodynamic model selected for development in the RELAP5 code was chosen to include the important physics of the two-phase flow process, while incorporating any simplifying assumptions consistent with the end use of the model; i.e., light water reactor transient analysis including LOCA. The principal simplification used is the specification that one of the phases be at saturation. Generally it is sufficient to specify that the least massive phase be at saturation; i.e., the phase which is either appearing or disappearing. The specification of one phase temperature greatly reduces the amount of constitutive information which must be provided relative to interphase and overall energy transfer. All interphase energy transfer mechanisms are implicitly lumped into the vapor mass generation model. Thus, a single correlation replaces the need for constitutive relations for interphase energy transfer, interphase mass transfer, distribution of external energy transfer between phases, and distribution of energy transfer between sensible and heat of vaporization. In addition, only a single overall energy equation is required.

The two-fluid nonequilibrium hydrodynamic model as implemented in the PILOT code includes several options for simpler hydrodynamic models. These include a drift-flux model, a homogeneous flow model, and a thermal equilibrium model. The two-fluid, drift-flux or homogeneous flow models can be used with either the nonequilibrium or equilibrium thermal models; i.e., six combinations. All six of these models have been checked out, however, most of the developmental effort has been performed using the $2VT_kT_{sat}$ model.

The primary reason for inclusion of the homogeneous equilibrium option is permit the RELAP5 code to be compared to existing homogeneous equilibrium code results for the purpose of checkout and development. However, this option might also be of use in establishing EM versions of the code. The drift-flux option was included to permit comparisons of results with other advanced codes based on the drift-flux model.

2. FIELD EQUATIONS

The basic field equations for the $2VT_kT_{sat}$ model consist of the two phasic continuity equations, the two phasic momentum equations and the mixture total energy equation, a total of five equations. The equations will be recorded here in differential stream-tube form for time and one space dimension as independent variables and in terms of dependent variables which are time and volume average quantities. The development of such equations for the two-phase process has been recorded in several references[6][7][8] and will not be reported herein. The equations will be recorded in the basic form with discussion of those terms which may differ from other developments. Subsequently, the manipulations will be described which are required to obtain the form of the equations from which the numerical scheme was developed.

The phasic mass conservations equations are:

$$\partial(\alpha_g\rho_g)/\partial t + (1/A)\partial(\alpha_g\rho_g v_g A)/\partial x = \Gamma_g, \tag{1}$$

$$\partial(\alpha_f\rho_f)/\partial t + (1/A)\partial(\alpha_f\rho_f v_f A)/\partial x = \Gamma_f. \tag{2}$$

Here A is the cross-sectional area of the flow passage normal to the stream direction (the remaining variables are described in the table of nomenclature).

In general the flow does not include mass sources or sinks and overall continuity consideration yields the requirement that the liquid generation term be the negative of the vapor generation; i.e.,

$$\Gamma_f = -\Gamma_g . \tag{3}$$

The phasic conservation of momentum equations are used, and recorded herein, in the so-called nonconservative form as follows:

Vapor;
$$\alpha_g\rho_g A(\partial v_g/\partial t) + \alpha_g\rho_g v_g A(\partial V_g/\partial x) = -\alpha_g A(\partial P/\partial x)$$
$$+ \alpha_g\rho_g B_x A - (\alpha_g\rho_g A)FWG(v_g) + \Gamma_g A(v_{gI}-v_g) - (\alpha_g\rho_g A)FIG(v_g-v_f)$$
$$- C\alpha_g\alpha_f\rho A[\partial(v_g-v_f)/\partial t + v_f(\partial v_g/\partial x) - v_g(\partial v_f/\partial x)] \tag{4}$$

Liquid;
$$\alpha_f\rho_f A(\partial v_f/\partial t) + \alpha_f\rho_f v_f A(\partial v_f/\partial x) = -\alpha_f A(\partial P/\partial x)$$
$$+ \alpha_f\rho_f B_x A - (\alpha_f\rho_f A)FWF(v_f) + \Gamma_f A(v_{fI}-v_f) - (\alpha_f\rho_f A)FIF(v_f-v_g)$$
$$- C\alpha_f\alpha_g\rho A[\partial(v_f-v_g)/\partial t + v_g(\partial v_f/\partial x) - v_f(\partial v_g/\partial x)] . \tag{5}$$

The force terms appearing on the right-hand sides of Equations (4) and (5) are: the pressure gradient, the body force, wall friction, momenta due to interphase mass transfer, interphase frictional drag and force due to "virtual" mass. The coefficients, FWG and FWF, are the part of the wall frictional drag which is linear in the velocity and is the product of the friction coefficient, the frictional reference area per unit volume, and the magnitude of the fluid bulk velocity. The interfacial velocity appearing in the interphase momentum transfer term is the unit momentum with which phase appearance or disappearance occurs. The coefficients FIG and FIF are the parts of the interphase frictional drag which is linear in the relative velocity and are products of the interphase friction coefficients, the frictional reference area per unit volume and the magnitude of interphase relative velocity

The virtual mass acceleration terms appearing in Equations (4) and (5) are a special case of the objective or frame indifferent formulations proposed by Lahey[9]. The coefficient of virtual mass is the same as that used by Anderson[10] in the RISQUE code, where the value for C depends on the flow regime. A value of $C > \frac{1}{2}$ has been shown to be appropriate for bubbly or dispersed flows[11][12], while $C = 0$ may be appropriate for a separated or stratified flow.

Conservation of interphase momentum requires that the sum of the force terms associated with interphase mass and momentum exchange sum to zero; i.e.,

$$\Gamma_g v_{gI} + (\alpha_g \rho_g) FIG(v_g - v_f) - C\alpha_g \alpha_f \rho [\partial(v_g - v_f)/\partial t + v_f(\partial v_g/\partial x) - v_g(\partial v_f/\partial x)]$$

$$+ \Gamma_f v_{fI} + (\alpha_f \rho_f) FIF(v_f - v_g)$$

$$+ C\alpha_f \alpha_g \rho [\partial(v_f - v_g)/\partial t + v_g(\partial v_f/\partial x) - v_f(\partial v_g/\partial x)] = 0 . \qquad (6)$$

This particular form for the interphase momentum balance results from consideration of the momentum equations in conservative form. In particular, the terms $\Gamma_g v_g$ and $\Gamma_f v_f$ are not interphase momentum transfer terms, but are a result of writing the equations in nonconservative form. The force terms associated with "virtual" mass acceleration in Equation (6) sum to zero identically as a result of the particular form chosen. In addition, it is usually assumed (although not required by any basic conservation principle) that the interphase momentum transfer due to friction and due to mass transfer are independently equal; i.e.,

$$v_{gI} = v_{fI} \equiv v_I \qquad (7)$$

and

$$\alpha_g \rho_g \, FIG = \alpha_f \rho_f \, FIF \equiv \alpha_g \alpha_f \rho_g \rho_f \, FI . \qquad (8)$$

These conditions are sufficient to assure that Equation (6) is satisfied.

The fifth field equation used as a basis for the RELAP5 hydrodynamic model development is the mixture energy equation.

$$\partial(\alpha_g\rho_g E_g + \alpha_f\rho_f E_f)/\partial t + (1/A)\partial(\alpha_g\rho_g v_g E_g A + \alpha_f\rho_f v_f E_f A)/\partial x$$

$$= -(1/A)\partial(\alpha_g v_g PA + \alpha_f v_f PA)/\partial x$$

$$+ (\alpha_g\rho_g v_g + \alpha_f\rho_f v_f)B_x + Q \qquad (9)$$

The viscous work term due to dilation of the fluid in the flow direction is small and is neglected (normal viscous work) and $E = U + v^2/2$.

In all the field equations recorded herein the correlation coefficients are assumed unity so that the average of a product is shown as the product of the averaged variables. While these correlations are neglected in the development of the basic numerical fluid dynamic model, the effect of nonunity correlations will be considered in component modeling where consideration of such effects may be important. The case of a dividing tee is one example of a component where correlations of cross-sectional area average properties must be considered. This model is under development in the systems code and will not be described further.

The mass, momentum and energy field equations have been recorded in a basic form in order to most clearly indicate the standard and general nature of these relationships. However, these forms are not the most convenient for development of the numerical model and the following discussion will describe the manipulation necessary to obtain the particular forms actually used.

The phasic mass conservation equations are summed and differenced to obtain

$$\partial\rho/\partial t + (1/A)\partial(\alpha_g\rho_g v_g A + \alpha_f\rho_f v_f A)/\partial x = 0, \qquad (10)$$

and

$$\rho(\partial X/\partial t) + (1-X)/A[\partial(\alpha_g\rho_g v_g A)/\partial x] - (X/A)[\partial(\alpha_f\rho_f v_f A)/\partial x] = \Gamma_g . \qquad (11)$$

Equation (3) has been used to eliminate the term Γ_f and the relation between quality and void fraction has been employed; i.e.,

$$X = \alpha_g \rho_g / \rho \, . \tag{12}$$

Equations (10) and (11) are the phasic mass conservation field equations used for numerical scheme development.

The momentum equations are also used as a sum and difference. The sum equation is obtained by direct summation of Equations (4) and (5) with the interface conditions, Equations (6), (7) and (8), substituted where appropriate and the cross-sectional area canceled throughout. The resulting sum equation is

$$\alpha_g \rho_g (\partial v_g/\partial t) + \alpha_f \rho_f (\partial v_f/\partial t) + \alpha_g \rho_g v_g (\partial v_g/\partial x) + \alpha_f \rho_f v_f (\partial v_f/\partial x)$$

$$= - \partial P/\partial x + \rho B_x - \alpha_g \rho_g v_g \, FWG - \alpha_f \rho_f v_f \, FWF - \Gamma_g (v_g - v_f) \, . \tag{13}$$

The difference of the phasic momentum equations is obtained by first dividing the vapor and liquid phasic momentum equations by $\alpha_g \rho_g$ and $\alpha_f \rho_f$ respectively and subsequently subtracting. Here again the interface conditions are used and the common area is divided out. The resulting equation is:

$$\partial v_g/\partial t - \partial v_f/\partial t + v_g (\partial v_g/\partial x) - v_f (\partial v_f/\partial x)$$

$$= - (1/\rho_g - 1/\rho_f)(\partial P/\partial x) - v_g FWG + v_f \, FWF$$

$$+ \Gamma_g [\rho v_I - (\alpha_f \rho_f v_g + \alpha_g \rho_g v_f)] / (\alpha_g \rho_g \alpha_f \rho_f)$$

$$- \rho FI (v_g - v_f) - C[\rho^2/(\rho_g \rho_f)][\partial (v_g - v_f)/\partial t$$

$$+ v_f (\partial v_g/\partial x) - v_g (\partial v_f/\partial x)] \, . \tag{14}$$

The total energy equation is transformed into the equivalent thermal energy equation by using the momentum equations to obtain a mechanical energy equation, which is subsequently subtracted from the total energy equation. The result of this algebraic manipulation is

$$\partial(\rho U)/\partial t + (1/A)\partial(\alpha_g \rho_g v_g U_g A + \alpha_f \rho_f v_f U_f A)/\partial x$$

$$= - (P/A)\partial(\alpha_g v_g A + \alpha_f v_f A)/\partial x + Q$$

$$+ (\alpha_g \rho_g) FWG (v_g)^2 + (\alpha_f \rho_f) FWF (v_f)^2 + (\alpha_g \alpha_f \rho_g \rho_f) FI (v_g - v_f)^2$$

$$+ \Gamma_g (1/2 - \lambda)(v_g - v_f)^2 + C \alpha_g \alpha_f \rho \, (v_g - v_f)[\partial(v_g - v_f)/\partial t$$

$$+ v_f (\partial v_g/\partial x) - v_g (\partial v_f/\partial x)] . \qquad (15)$$

where the interfacial velocity v_I has been defined as

$$v_I = \lambda v_g + (1-\lambda) v_f . \qquad (16)$$

This definition for v_I has the property that if $\lambda = 1/2$ the interphase momentum transfer process associated with mass transfer is reversible. Other constant values lead to either an entropy sink or source depending upon the sign of Γ_g. However, if λ is chosen to be 0 for Γ_g positive and +1 for Γ_g negative; i.e., a donor formulation, then the mass exchange process is always dissipative. The latter model for v_I has been chosen as the most realistic for the momentum exchange process and is used for the numerical scheme development.

The thermal energy source term associated with the virtual mass acceleration term is not necessarily positive or zero. However, consideration of the second law of thermodynamics dictates that such must be the case. This contradiction is not resolved at this time and since the energy dissipation associated with virtual mass acceleration force is small, the energy source terms associated

with this force are omitted. The resulting form of the mixture thermal energy equation which is used in the development of the RELAP5 numerical hydrodynamic model is thus

$$\partial(\rho U)/\partial t + (1/A)\partial(\alpha_g \rho_g v_g U_g A + \alpha_f \rho_f v_f U_f A)/\partial x$$

$$= (P/A)\partial(\alpha_g v_g A + \alpha_f v_f A)/\partial x + Q$$

$$+ (\alpha_g \rho_g)FWG(v_g)^2 + (\alpha_f \rho_f)FWF(v_f)^2 + (\alpha_g \alpha_f \rho_g \rho_f)FI(v_g - v_f)^2$$

$$+ (|\Gamma_g|/2)(v_g - v_f)^2. \qquad (17)$$

The reason for selecting the thermal energy equation rather than the total energy equation will become more apparent in development of the numerical scheme. However, at this point note that the thermal energy equation does not involve time derivatives of the kinetic energy and thus fewer new time variables will appear in the numerical approximation. The field equations which form the basis for the RELAP5 hydrodynamic model are summarized as Equations (10), (11), (13), (14) and (17). The field variables which appear in temporal derivatives are ρ, X, v_g, v_c and (ρU). These are the basic field variables which are used in the numerical scheme.

3. STATE RELATIONS

The dependent variables which appear in the five field equation temporal and spatial derivatives are: density, ρ; pressure, P; static quality, X; mixture internal energy, U; and the two phasic velocities, v_g and v_f. All of the phasic properties also appear in the derivatives and as coefficients of the derivatives. To obtain a determinant system the state relationship must be employed wherein density as well as all of the phasic properties are expressed as functions of the pressure, static

quality and mixture internal energy. The state of the system cannot be established from the information above since the phase temperatures are in general different. The indeterminancy is the result of using only the overall energy equation and is removed by specifying one of the phases to exist at the prevailing saturation conditions. Generally, the least massive phase will be assumed to be saturated; i.e., that phase which is either appearing or disappearing. This specification is considered to be an adequate approximation for LWR transient and LOCA analysis.

The state of each phase is established by specification of the pressure and phasic internal energy (only the pressure is needed to specify the state of the saturated phase). For the case of subcooled liquid or superheated vapor, those states are established using tabular equilibrium data as a function of the pressure and phasic internal energy. For the pseudo-states of superheated liquid and subcooled steam, the properties are extrapolated along isobars using properties and property derivatives evaluated at the corresponding saturation state. In addition to the state properties, derivatives of the mixture density with respect to the pressure, static quality and mixture internal energy are required in the numerical solution scheme. The way in which these derivatives are used will be explained in the course of numerical scheme development.

The necessary state relations will be developed for the two cases, vapor saturated and liquid saturated, by first assuming the vapor to be saturated and then indicating the juxtaposition required to obtain the corresponding relation for the case of the liquid phase saturated (the procedure for the pseudo-states will also be discussed separately).

The mixture energy is defined in terms of the phasic energies and quality by

$$U = XU_g^s(P) + (1-X)U_f(P,X,U), \qquad (18)$$

where the superscript s is used to designate the saturation state and the functional relationships are designated by parentheses (P,X,U are the independent variables and all other state properties are to be expressed in terms of these). The partial derivatives of the liquid phase energy are obtained by differentiation of Equation (18) with respect to P, X and U and solving for the respective derivatives to obtain.

$$(\partial U_f/\partial P)_{X,U} = -[X/(1-X)](dU_g^s/dP), \tag{19}$$

$$(\partial U_f/\partial X)_{P,U} = (U_f-U_g^s)/(1-X), \tag{20}$$

and

$$(\partial U_f/\partial U)_{P,X} = 1/(1-X). \tag{21}$$

Derivatives of density are required for the numerical scheme, however, the state relationships are in terms of specific volumes. Therefore, we will work in terms of specific volumes and later develop the required density derivatives in terms of the specific volume derivatives. The vapor specific volume is a function of pressure only

$$V_g^s = V_g^s(P), \tag{22}$$

and the corresponding derivatives are

$$(\partial V_g^s/\partial P)_{X,U} = dV_g^s/dP, \tag{23}$$

$$(\partial V_g^s/\partial X)_{P,U} \equiv 0, \tag{24}$$

and

$$(\partial V_g^s/\partial U)_{P,X} \equiv 0 . \tag{25}$$

The functional form of the liquid specific volume and the associated derivatives are:

$$V_f = V_f(P,U_f) = V_f(P,U_f(P,X,U)), \tag{26}$$

$$(\partial V_f/\partial P)_{X,U} = (\partial V_f/\partial P)_{U_f} + (\partial V_f/\partial U_f)_P \, (\partial U_f/\partial P)_{X,U}, \tag{27}$$

$$(\partial V_f/\partial X)_{P,U} = (\partial V_f/\partial U_f)_P \, (\partial U_f/\partial X)_{P,U}, \tag{28}$$

and

$$(\partial V_f/\partial U)_{P,X} = (\partial V_f/\partial U_f)_P \, (\partial U_f/\partial U)_{P,X}. \tag{29}$$

The properties needed in evaluating the derivatives are obtained using water property subroutines. First the properties at the saturation state are evaluated, which are a function of the pressure only. The saturation properties for the vapor include specific volume, V_g^s; internal energy, U_g^s; temperature, T_g^s; specific heat at constant pressure, C_p^s; enthalpy h_g^s; isothermal compressibility, κ_g^s; and the isobaric coefficient of thermal expansion, β_g^s. All other required properties can be derived.

The derivative of vapor phase specific volume with respect to pressure is obtained as follows

$$dV_g^s/dP = (\partial V_g/\partial P)_T^s + (\partial V_g/\partial T)_P^s \, (dT_g^s/dP), \tag{30}$$

where

$$dT_g^s/dP = T_g^s(V_g^s - V_f^s)/(h_g^s - h_f^s), \tag{31}$$

and

$$(\partial V_g/\partial P)_T^s = - V_g^s \kappa_g^s, \tag{32}$$

$$(\partial V_g/\partial T)_P^s = V_g^s \beta_g^s. \tag{33}$$

The final expression for the specific volume derivative is,

$$dV_g^s/dP = - V_g^s \kappa_g^s + V_g^s \beta_g^s (dT_g^s/dP) \tag{34}$$

The thermodynamic properties for use in evaluating the derivatives of the liquid phase specific volume are obtained as a function of the pressure and liquid phase internal energy, where the liquid phase internal energy is obtained by solving Equation (18) for U_f in terms of the mixture internal energy U; i.e.,

$$U_f(P,X,U) = [U-XU_g^s(P)]/(1-X). \tag{35}$$

Here it is assumed that U_f corresponds to a subcooled liquid state, later the generalization for the superheated state will be developed. The properties of the liquid phase are also obtained using a water properties subroutine. The properties required include specific volume, V_f; temperature T_f; specific heat at constant pressure, C_{pf}; enthalpy, h_f; isothermal compressibility, κ_f; and the isobaric coefficient of thermal expansion, β_f.

The required derivatives of liquid specific volume with respect to P and U_f are obtained by considering the functional relation

$$V_f = V_f(P,U_f), \tag{36}$$

and application of standard equilibrium single-phase thermodynamic relations[3]. Thus

$$(\partial V_f/\partial P)_{U_f} = -V_f\kappa_f C_{vf}/(C_{pf}-PV_f\beta_f) \tag{37}$$

and

$$(\partial V_f/\partial U_f)_P = V_f\beta_f/(C_{pf}-PV_f\beta_f), \tag{38}$$

where

$$C_{vf} = C_{pf} - T_fV_f\beta_f^2/\kappa_f . \tag{39}$$

The derivatives of density required by the numerical scheme can now be expressed entirely in terms of known quantities. The mixture specific volume in terms of the phasic properties is

$$V = XV_g^s + (1-X)V_f \tag{40}$$

and the mixture density is simply

$$\rho = \frac{1}{V} . \tag{41}$$

The derivatives of density are found by application of the chain rule to Equations (40) and (41) to obtain

$$(\partial\rho/\partial P)_{X,U} = -\rho^2[X(dV_g^S/dP) + (1-X)(\partial V_f/\partial P)_{X,U}], \tag{42}$$

$$(\partial\rho/\partial X)_{P,U} = -\rho^2[V_g^S - V_f + (1-X)(\partial V_f/\partial X)_{P,U}], \tag{43}$$

and

$$(\partial\rho/\partial U)_{P,X} = -\rho^2[(1-X)(\partial V_f/\partial U)_{P,X}] . \tag{44}$$

The corresponding thermodynamic relations for the case where the liquid phase is assumed to be at saturation can be obtained by juxtaposition of the f with g subscript and X with (1-X). The necessary relations for this case are summarized below.

$$(\partial U_g/\partial P)_{X,U} = -[(1-X)/X](dU_f^S/dP) \tag{45}$$

$$(\partial U_g/\partial X)_{P,U} = (U_g - U_f^S/dP) \tag{46}$$

$$(\partial U_g/\partial U)_{P,X} = 1/X \tag{47}$$

$$dV_f^S/dP = (\partial V_f/\partial P)_T^S + (\partial V_f/\partial T)_P^S(dT_f^S/dP) \tag{48}$$

$$(\partial V_g/\partial P)_{X,U} = (\partial V_g/\partial P)_{V_g} + (\partial V_g/\partial U_g)_P(\partial U_g/\partial P)_{X,U} \tag{49}$$

$$(\partial V_g/\partial X)_{P,U} = (\partial V_g/\partial U_g)_P(\partial U_g/\partial X)_{P,U} \tag{50}$$

$$(\partial V_g/\partial U)_{P,X} = (\partial V_g/\partial U_g)_P\ (\partial U_g/\partial U)_{P,X} \tag{51}$$

$$dT_f^S/dP = T_f^S(V_g^S - V_f^S)/(h_g^S - h_f^S) \tag{52}$$

$$dV_f^s/dP = - V_f^s\kappa_f^s + V_f^s\beta_f^s(dT_f^s/dP) \tag{53}$$

$$(\partial V_g/\partial P)_{U_g} = - V_g\kappa_s C_{vg}/(C_{pg}-PV_g\beta_g) \tag{54}$$

$$(\partial V_g/\partial U_g)_P = V_g\beta_g/(C_{pg}-PV_g\beta_g) \tag{55}$$

$$C_{vg} = C_{pg}-T_gV_g\beta_g^2/\kappa_g \tag{56}$$

$$(\partial\rho/\partial P)_{X,U} = -\rho^2[X(\partial V_g/\partial P)_{X,U} + (1-X)(dV_f/dP)] \tag{57}$$

$$(\partial\rho/\partial X)_{P,U} = -\rho^2[V_g-V_f^s + X(\partial V_g/\partial X)_{P,U}] \tag{58}$$

$$(\partial\rho/\partial U)_{P,X} = -\rho^2X(\partial V_g/\partial U)_{P,X} \tag{59}$$

The properties for cases where the vapor is subcooled or the liquid is superheated, are obtained both by using properties at saturation and extrapolation at constant pressure. The following properties are evaluated and held fixed at saturation; C_p,κ, and β. The temperature and specific volume are extrapolated at constant pressure from the values at saturation. This extrapolation is illustrated for the case of the liquid held at saturation and the vapor subcooled. The internal energy of the vapor phase is obtained by solving the mixture energy relation, Equation (18), in terms of the liquid phase energy and the mixture energy; i.e.,

$$U_g = [U-(1-X)U_f^s]/X \ . \tag{60}$$

The vapor will be subcooled if

$$U_g < U_g^s \ . \tag{61}$$

The temperature and specific volume are obtained by a two-term Taylor series extrapolation from saturation conditions holding pressure constant; i.e.,

$$T_g = T_g^s + (\partial T_g/\partial U_g)_P^s \ (U_g-U_g^s), \tag{62}$$

and

$$V_g = V_g^s + (\partial V_g/\partial U_g)_p^s \, (U_g - U_g^s). \tag{63}$$

The temperature and specific volume derivatives in Equations (62) and (63) are evaluated at saturation conditions from standard thermodynamic relations[13]

$$(\partial T_g/\partial U_g)_p^s = 1/(C_{pg}^s - PV_g^s\beta_g^s) \tag{64}$$

and

$$(\partial V_g/\partial U_g)_p^s = V_g^s\beta_g^s/(C_{pg}^s - PV_g^s\beta_g^s). \tag{65}$$

The derivative of density with respect to pressure, quality and mixture energy can now be evaluated in the same manner as previously described. The case of liquid superheated with the vapor phase at saturation occurs for the condition.

$$U_f > U_f^s \, . \tag{66}$$

The appropriate extrapolation equations for temperature and specific volume are obtained by juxtapositioning X and (1-X) and the subscripts f and g. In this case, the properties C_{pf}, β_f and κ_f are held fixed at saturation value.

4. VAPOR GENERATION MODEL

The preliminary vapor generation model used in the PILOT code is a simple relaxation model based on the work of Jones et al.[14]. Jones has shown that the vapor generation terms can be written as

$$\Gamma_g = A_I h_I (T_g - T_f)/(h_{fg} A). \tag{67}$$

It is also shown in Reference (14) that the temperature difference (where one phase is at saturation) is proportional to the difference between the local static quality and the equilibrium quality; i.e.,

$$(T_g - T_f^s) \sim (X - X_e). \tag{68}$$

It is further assumed for the PILOT code model that the product of the interphase energy transfer coefficient, h_I, and the energy of vaporization, h_{fg}, are constant and is proportional to the local quality with an additive constant. Thus, the volumetric vapor generation rate, Equation (67), can be written

$$\Gamma_g = -K\ (X+X_o)(X-X_e)\,, \tag{69}$$

where X_o is a constant which characterizes the early germination process (after nucleation has taken place) and K is an overall rate constant dependent upon flow regime.

The vapor generation model has been used to simulate blowdown and steady flow phase change experiments with good results. Values for the constant K and X_o, which give agreement with Reocreux's[15] data for steady critical flow experiments are:

$$K = 1.145\text{x}10^{7}\,, \tag{70}$$

and

$$X_o = 1.0\text{x}10^{-5}\,. \tag{71}$$

An empirical correlation is given in Reference (15) which could be used to give the dependence of K on local flow variables. For this case K becomes the function

$$K = -\left[P^{0.515}\alpha_g^{0.954}v_m^{1.89}\right]/660\ . \tag{72}$$

Nucleation depends upon the fluid properties as well as system variables such as, pressure, dissolved substances, surface roughness and turbulence level. The effect of delayed nucleation is to cause the liquid phase to superheat relative to the saturation temperature at the prevailing pressure (in the case of pure vapor, the vapor becomes subcooled relative to the saturation temperature). In situations occurring in nuclear reactor LOCA the maximum superheat is only a few ^{o}K and the associated nucleation delay does not have a major effect on system blowdown. In view of this, a simple nucleation model is included in the PILOT

code which is based on exceeding a given constant superheat. Nucleation is also assumed to have occurred if the vapor phase (or liquid for condensation) is present as a result of convective transport.

While a constant superheat criterion is used in the PILOT code, a correlation such as that found in Reference (16) could be as easily used. The referenced correlation gives the degrees of superheat as a logarithmic function of the mass velocity and is being considered as a nucleation model for use in the RELAP5 systems code. This correlation is

$$\ln(\Delta T_{s,f}) = 13.64 - \ln(G). \tag{73}$$

The vapor generation term can be a dominant term in the continuity relationship and for this reason the relaxation parameters are evaluated implicitly in the numerical scheme. Equilibrium quality is not one of the field variables and therefore must be expressed in terms of the field variables by means of a two-term Taylor series expansion about the old time level. This expansion requires the partial derivatives of the equilibrium quality with respect to the field variables P and U.

The required derivatives for a two-phase equilibrium state are obtained by starting with the definition of the mixture energy at equilibrium

$$U = X_e U_g^s(P) + (1-X_e)U_f^s(P) \tag{74}$$

and taking derivatives with respect to P and U to obtain

$$(\partial X_e/\partial P)_U = [X_e(dU_g^s/dP) + (1-X_e)(dU_f^s/dP)]/(U_f^s-U_g^s) \tag{75}$$

and

$$(\partial X_e/\partial U)_P = -1/(U_f^s-U_g^s) . \tag{76}$$

The derivatives of the phasic saturation energies are:

$$dU_g^s/dP = [C_{pg}^s - V_g^s \beta_g^s P + V_g^s(dP/dT)(P\kappa_g^s - T\beta_g^s)]/(dP/dT) \tag{77}$$

and

$$dU_f^s/dP = [C_{pf}^s - V_f^s \beta_f^s P + V_f^s (dP/dT)(P\kappa_f^s - T\beta_f^s)]/(dP/dT), \quad (78)$$

where the derivative of the saturation pressure is given by the Clasius-Clayperon relation; i.e.,

$$dP/dT = (h_g^s - h_f^s)/[T(V_g^s - V_f^s)] \ . \quad (79)$$

The derivatives of quality with respect to pressure and energy are zero for all single-phase equilibrium states. The numerical implementation of the mass transfer model will be developed in the next section along with the basic numerical scheme.

5. INTERPHASE DRAG

The interphase drag term appearing in the momentum equations, Equations (4), (5) and (14), is the force arising from viscous shear effects between phases. The drag term is written as FI $(v_g - v_f)$ where the FI is the drag coefficient which depends upon the relative velocity as well as other flow variables such as flow regime.

The PILOT code model includes three options for FI. These are a spherical particle drag formulation based on a constant particle/bubble population density, a free slip option (FI = 0) and a homogeneous or FI infinite option (FI = 10^{30} in the code). These options are user-selected and are based on simple flow regime considerations wherein the flow regime is a function of void fraction and mass velocity. The flow regimes and the associated model for FI are

$$\text{(i)} \quad G \geq G_o = 2700 \text{ KG/M}^2, \ 0 \leq \alpha \leq 1.0 \quad (80)$$

churn-turbulent (FI = 10^{30})

(ii) $G < G_o$, $\alpha \leq 0.5$ (81)

dispersed bubbly flow (FI = spherical bubble)

(iii) $G < G_o$, $\alpha > 0.5$ (82)

dispersed droplet flow (FI = spherical particle)

For case (i) the flow is assumed homogeneous and the interphase friction, FI, is set to 10^{30}, which causes the velocities of each phase to be equal. The interphase drag correlations used in cases (ii) and (iii) are based upon the drag of a single bubble (droplet) times the number N_p of bubbles (droplets) per unit volume [17]. In both regions

$$\alpha_g \alpha_f \rho_g \rho_f \, FI = (3/8)\, \rho[C_d |v_f - v_g| + 12(\nu/r_o)]A \tag{83}$$

and

$$\nu = \alpha_g \nu_g + \alpha_f \nu_f \, . \tag{84}$$

For region (ii) the frontal area A is given as

$$A = \alpha_g / r_o, \quad r_o = \left(\frac{3\alpha_g}{4\pi N_p}\right)^{1/3} \tag{85}$$

and for region (iii) as

$$A = \alpha_f / r_o, \quad r_o = \left(\frac{3\alpha_f}{4\pi N_p}\right)^{1/3} \, . \tag{86}$$

At present N_p is a specified constant, typically $1 \times 10^7 / M^3$.

In addition to the above three flow regimes, a separated flow regime can be approximated by setting FI equal to zero. This option has been used for some developmental testing of the code on problems in which the interphase drag is expected to be small.

The flow regimes and interphase drag correlations described above have been adequate for the PILOT code developmental objectives. Further refinements and generalizations will be added in the RELAP5 system code structure as they are needed. They will include a flow regime map similar to one proposed by Lekach [18] with four flow regions and five transition regimes. The additional interphase drag correlations needed in these regimes will be modeled in a manner similar to that proposed by Liles [19].

III. NUMERICAL HYDRODYNAMIC MODEL

1. GENERAL

The numerical solution scheme is based on replacing the system of differential equations with a system of finite difference equations which are partially implicity in time. The terms which are evaluated implicitly will be identified as the scheme is developed. In all cases, the implicit terms are formulated so as to be linear in the dependent variables at new time. This results in a linear time advancement matrix which is solved by either direct inversion or by an iterative scheme, whichever is faster. An additional feature of the scheme is that the implicitness has been selected such that the five field equations can be reduced to a single difference equation per fluid control volume or mesh cell in terms of the hydrodynamic pressure. Thus, only an NxN system of difference equations must be solved simultaneously at each time step (N is the total number of control volumes used to simulate the fluid system).

The system of five differential equations which form the basis for the numerical scheme consist of: (1) the overall continuity equation, Equation (10); (2) the difference of the phasic continuity equations in terms of quality, Equation (11); (3) and (4) the sum and difference of the phasic momentum equations, Equations (13) and (14); and (5) the mixture internal energy equation, Equation (17). The following discussion will describe the development of the difference or computing equations from these differential equations.

It is well known[10][15] that the system of differential equations constitute an ill-posed initial-value problem. This fact is of little concern physically since the addition of any second order differential effect, regardless of how small, such as viscosity or surface tension, results in a well-posed problem[20]. However, the ill-posedness is of some concern numerically since it is necessary that the numerical problem be well-posed. The approximations inherent in any

numerical scheme modify the solution somewhat (truncation error) and these effects can be either stabilizing or destabilizing.

A well-posed numerical problem is obtained in the method developed herein as the result of several factors. These include the selective use of implicitness (evaluation of spatial gradient terms at the new time), donor formulations for the mass and energy flux terms and use of a "donor like" formulation for the momentum flux terms. The term "donor like" is used because the momentum flux formulation consists of a centered formulation for the spatial gradient of velocity plus a numerical viscosity term which is similar to the form obtained when the momentum flux terms are donored with the conservative form of the momentum equations. The well-posedness of the final numerical scheme (as well as its accuracy) has been demonstrated by extensive numerical testing during development.

2. DIFFERENCE EQUATIONS

The difference equations are based on the concept of a control volume or "mesh cell" in which mass and energy are conserved by equating accumulation to rate of influx through the cell boundaries. This model results in defining mass and energy volume average properties and requiring knowledge of velocities at the volume boundaries. The velocities at the boundaries are most conveniently defined through use of momentum control volumes or "cells" which are centered on the mass and energy cell boundaries. This approach results in a numerical scheme having a staggered spatial mesh. The scalar properties (pressure, energy and quality) of the flow are defined at cell centers and the vector quantities (velocities) are defined on the cell boundaries. The resulting one-dimensional spatial noding is illustrated in Figure 1. The term cell is used throughout the discussion to mean an increment in the spatial variable, x, corresponding to the mass and energy control volume.

The difference equations for each cell were obtained by integrating the mass and energy equations, Equations (10), (11) and (17), with respect to the spatial variable, x, from the junction at x_j to x_{j+1}. The momentum equations, Equations (13) and (14), were integrated with respect to the spatial variable from cell center to adjoining cell center (X_K to X_L), see Figure 1.

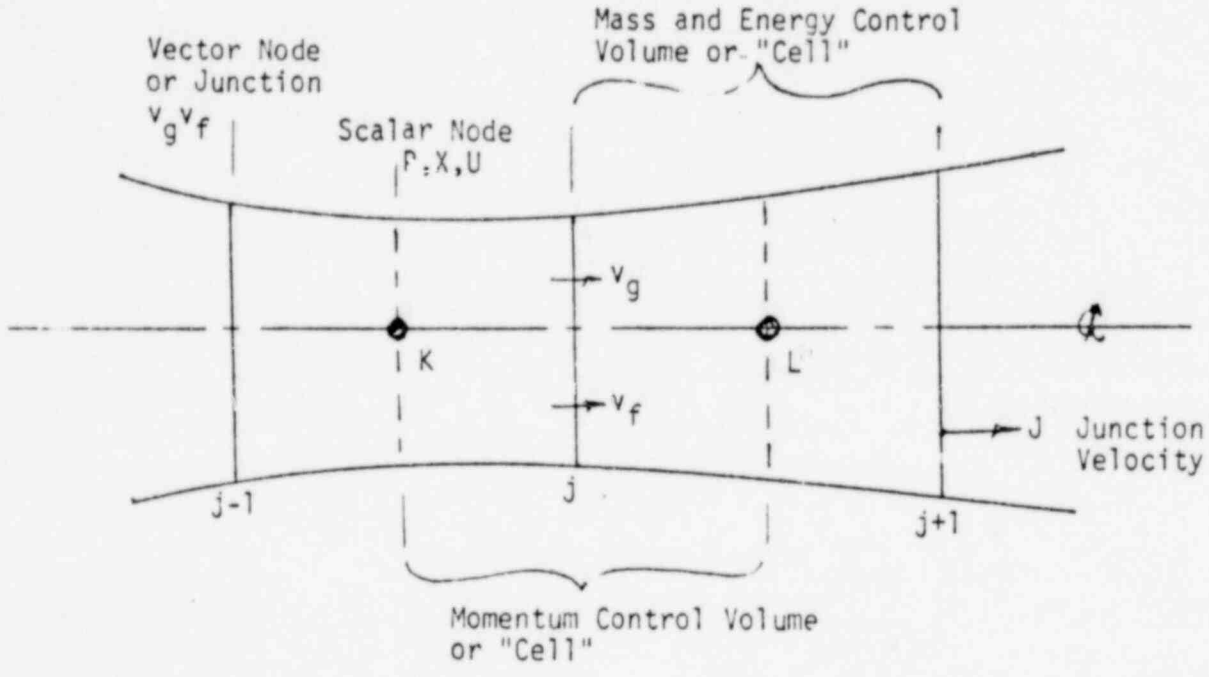

Figure 1. Difference Equation Nodalization Schematic

Each junction is assumed to move with velocity J_j in order to obtain a general numerical scheme applicable to time-dependent control volumes. This generalization is for the purpose of tracking points of discontinuous change such as might occur at material interfaces, hydrodynamic shocks, phase change fronts, etc. Aside from presenting the general numerical scheme, the methodology for interface tracking will not be developed herein.

When the mass and energy equations, Equations (10), (11) and (17), are integrated with respect to the spatial variable from junction j to j+1, differential equations in terms of cell average properties and cell boundary fluxes are obtained. The resulting equations are

$$\partial(\rho V)/\partial t + [\alpha_g\rho_g(v_g-J)A]_{x_j}^{x_{j+1}} + [\alpha_f\rho_f(v_f-J)A]_{x_j}^{x_{j+1}} = 0, \tag{88}$$

$$\rho[\partial(XV)/\partial t] + (1-X)[\alpha_g\rho_g(v_g-J)A]_{x_j}^{x_{j+1}} - X[\alpha_f\rho_f(v_f-J)A]_{x_j}^{x_{j+1}} = V\Gamma_g, \tag{89}$$

and

$$\begin{aligned}\partial(\rho UV)/\partial t &+ [\alpha_g\rho_g U_g(v_g-J)A]_{x_j}^{x_{j+1}} + [\alpha_f\rho_f U_f(v_f-J)A]_{x_j}^{x_{j+1}} \\ &= -P[\alpha_g v_g A + \alpha_f v_f A]_{x_j}^{x_{j+1}} + QV + \alpha_g\rho_g v_g^2(FWG)V \\ &+ \alpha_f\rho_f v_f^2(FWF)V + \alpha_g\rho_g\alpha_f\rho_f FI(v_g-v_f)^2V \\ &+ \Gamma_g(\tfrac{1}{2}-\lambda)(v_g-v_f)^2V,\end{aligned} \tag{90}$$

where the brackets with subscripts and superscripts indicate the integration limits for the enclosed quantity. The quantities not enclosed in brackets are volume averages and the energy source term due to virtual mass effects is omitted.

The sum and differenced momentum equations, Equations (13) and (14), are integrated from cell center to cell center to obtain

$$\begin{aligned}1/A\,[(\alpha_g\rho_g)\,\partial(v_gV)/\partial t &+ (\alpha_f\rho_f)\,\partial(v_fV)/\partial t] + \alpha_g\rho_g v_g[v_g-J]_{x_K}^{x_L} + \alpha_f\rho_f v_f[v_f-J]_{x_K}^{x_L} \\ &= -[P]_{x_K}^{x_L} + \rho F_x(x_L-x_K) - (\alpha_g\rho_g v_g FWG + x_f\rho_f v_f FWF)(x_L-x_K) \\ &- \Gamma_g(v_g-v_f)(x_L-x_K)\end{aligned} \tag{91}$$

and

$$(1/A)[1+C\rho^2/(\rho_g\rho_f)][\partial(v_gV)/\partial t-\partial(v_fV)/\partial t] + [v_g + Cv_f\rho^2/(\rho_g\rho_f)][v_g-J]_{x_K}^{x_L}$$

$$- [v_f+Cv_g\rho^2/(\rho_g\rho_f)][v_f-J]_{x_K}^{x_L} = - (1/\rho_g-1/\rho_f)[P]_{x_K}^{x_L} - [v_gFWG-v_fFWF](x_L-x_K)$$

$$+ \left\{\Gamma_g[\rho v_I-(\rho_f\rho_f v_g+\alpha_g\rho_g v_f)]/(\alpha_g\rho_g\alpha_f\rho_f)\right\}(x_L-x_K)-\rho FI(v_g-v_f)(x_L-x_K). \quad (92)$$

Here the common area term, A, has been factored from most terms. The quantities shown in square brackets with limits are evaluated at the indicated limits while the coefficients are averaged over the cell or integration interval. The indicated derivatives are now derivatives of cell average quantities. Since the integration interval is centered on the junction these averages are approximated by the junction values. In all cases, the correlation coefficients for averaged products are taken as unity so that averaged products are replaced directly with products of averages.

Several general guidelines were followed in developing numerical approximations for Equations (88), (89), (90), (91) and (92). These guidelines are summarized below.

(i) Mass and energy inventories are very important quantities in water reactor safety analysis and as such the numerical scheme should be consistent and conservative in these quantities (a greater degree of approximation for momentum effects was considered acceptable). Both mass and energy are convected from the same cell and each are evaluated at the same time level (i.e., mass density is evaluated at old time level so energy density is also evaluated at old time).

(ii) In order to achieve fast execution speed implicit evaluation is used only for: those terms necessary for numerical stability, elimination of the wave propagation time step limit, and those phenomena known to have small time constants. Thus, implicit evaluation is used for the velocity in mass and energy

transport terms, the pressure gradient in the momentum equations and the interphase mass and momentum exchange terms.

(iii) To further enhance computing speed, the time level evaluations were selected so that the resulting implicit terms are linear in the new time variables. Where it was necessary to retain nonlinearities, Taylor series expansions about old time values were used to obtain a formulation linear in the new time variables (higher order terms were neglected). Linearity results in high computing speed by eliminating the need to iteratively solve systems of nonlinear equations.

(iv) To allow easy degeneration to homogeneous, single-phase and drift-flux formulations, the momentum equations are used as a sum and a difference equation. The particular difference equation used is obtained by first dividing each of the phasic momentum equations by $\alpha_g\rho_g$ and $\alpha_f\rho_f$ for the vapor and liquid phase equations, respectively, and then subtracting.

Using the above guidelines, the finite difference equations for the mass and energy balances, corresponding to Equations (88), (89) and (90), are

$$\rho_L^{n+1}V_L^{n+1}-\rho_L^nV_L^n + \{[\dot{\alpha}_g^n\dot{\rho}_g^n(v_g-J)_{j+1}^{n+1} + \dot{\alpha}_f^n\dot{\rho}_f^n(v_f-J)_{j+1}^{n+1}]A_{j+1}$$

$$- [\dot{\alpha}_g^n\dot{\rho}_g^n(v_g-J)_j^{n+1} + \dot{\alpha}_f^n\dot{\rho}_f^n(v_f-J)_j^{n+1}]A_j\}\Delta t = 0 \qquad (93)$$

and

$$\rho_L^n(X_L^{n+1}V_L^{n+1}-X_L^nV_L^n) + (1-X_L^n)[\dot{\alpha}_g^n\dot{\rho}_g^n(v_g-J)_{j+1}^{n+1}A_{j+1}-\dot{\alpha}_g^n\dot{\rho}_g^n(v_g-J)_j^{n+1}A_j]\Delta t$$

$$- X_L^n[\dot{\alpha}_f^n\dot{\rho}_f^n(v_f-J)_{j+1}^{n+1}A_{j+1} - \dot{\alpha}_f^n\dot{\rho}_f^n(v_f-J)_j^{n+1}A_j]\Delta t = V^n(\Gamma_g)_j^{n+1}. \qquad (94)$$

$$(\rho_L U_L)^{n+1} V_L^{n+1} - (\rho_L U_L)^n V_L^n + [\dot{\alpha}_g^n \dot{\rho}_g^n \dot{U}_g^n (v_g - J)_{j+1}^{n+1} + \dot{\alpha}_f^n \dot{\rho}_f^n \dot{U}_f^n (v_f - J)_{j+1}^{n+1}] A_{j+1} \Delta t$$

$$- [\dot{\alpha}_g^n \dot{\rho}_g^n \dot{U}_g^n (v_g - J)_j^{n+1} + \dot{\alpha}_f^n \dot{\rho}_f^n \dot{U}_f^n (v_f - J)_j^{n+1}] A_j \Delta t$$

$$= - P_L^n [(\alpha_g^n v_g^n + \alpha_f^n v_f^n)_{j+1} A_{j+1} - (\alpha_g^n v_g^n + \alpha_f^n v_f^n)_j A_j] \Delta t$$

$$+ Q_L^n V_L^n \Delta t + DISS_L^n V_L^n \Delta t \, . \qquad (95)$$

The term $DISS_L^n$ which appears in Equation (95) is the sum of the energy dissipation terms which appear in Equation(90). These terms are evaluated at old time using volume averaged variables.

The quantities having a dot overscore are donored quantities based on the junction relative velocities, $v_g - J$ and $v_f - J$. The donored quantities are volume average scalar quantities and are defined analytically as

$$\dot{\phi} = \tfrac{1}{2}(\phi_K + \phi_L) + \tfrac{1}{2} [|v-J|/(v-J)](\phi_K - \phi_L), \; (v-J) \neq 0 \, , \qquad (96)$$

where ϕ is any of the donored properties and v is the appropriate velocity; i.e., vapor or liquid. For the degenerate case of $v-J \equiv 0$ a simple centered formulation is used

$$\dot{\phi} = \tfrac{1}{2}(\phi_K + \phi_L), \; (v-J) \equiv 0 \, . \qquad (97)$$

where donored values are not used at junctions, linear interpolations between neighboring cell values are used.

A similar approach is used to obtain the finite difference form for the phasic momentum equations. In this case, the volume average properties for the momentum control volume are taken as junction properties; i.e., linear interpolations between mass and energy control volume centers. The momentum flux terms are approximated using a "donor like" formulation which results in a centered velocity gradient term and a viscous like term. The resulting difference equations are:

$$(\alpha_g\rho_g)_j^n(v_g^{n+1}\Delta x^{n+1}-v_g^n\Delta x^n)_j + (\alpha_f\rho_f)_j^n(v_f^{n+1}\Delta x^{n+1}-v_f^n\Delta x^n)_j$$

$$+ (\alpha_g\rho_g v_g)_j^n[(v_g-J)_L^n - (v_g-J)_K^n]\Delta t + (\alpha_f\rho_f v_f)_j^n[(v_f-J)_L^n - (v_f-J)_K^n]\Delta t$$

$$-[(\alpha_g\rho_g)_j^n \, VISG_j^n - (\alpha_f\rho_f)_j^n \, VISF_j^n]\Delta t$$

$$= -(P_L-P_K)^{n+1}\Delta t + \{\rho_j^n - B_x - (\alpha_g\rho_g)_j^n(v_g)_j^{n+1}FWG_j^n$$

$$- (\alpha_f\rho_f)_j^n(v_f)_j^{n+1} \, FWF_j^n - (\Gamma_g)_j^n(v_g-v_f)_j^n\} \, \Delta x_j^n\Delta t, \qquad (98)$$

and

$$[1+C\rho^2/(\rho_g\rho_f)]_j^n[(v_g^{n+1}\Delta x^{n+1}-v_g^n\Delta x^n) - (v_f^{n+1}\Delta x^{n+1}-v_f^n\Delta x^n)]_j$$

$$+ [v_g+Cv_f\rho^2/(\rho_g\rho_f)]_j^n[(v_g-J)_L^n - (v_g-J)_K^n]\Delta t - VISG_j^n\Delta t$$

$$- [v_f+Cv_g\rho^2/(\rho_g\rho_f)]_j^n[(v_f-J)_L^n - (v_f-J)_K^n]\Delta t + VISF_j^n\Delta t$$

$$= -[(\rho_f-\rho_g)/(\rho_g\rho_f)]_j^n(P_L-P_K)^{n+1}\Delta t - \{FWG_j^n(v_g)_j^{n+1} - FWF_j^n(v_f)_j^{n+1}$$

$$- [\Gamma_g(\rho v_I-\alpha_f\rho_f v_g-\alpha_g\rho_g v_f)/(\alpha_g\rho_g\alpha_f\rho_f)]_j^n$$

$$(\rho FI)_j^n(v_g-v_f)_j^{n+1}\}\Delta x_j^n\Delta t \, , \qquad (99)$$

where the viscous terms are defined as

$$VISG_j = \tfrac{1}{2}\{|(v_g)_{j+1}+(v_g)_j|[(v_g)_{j+1}-(v_g)_j] - |(v_g)_j+(v_g)_{j-1}|[(v_g)_j-(v_g)_{j-1}]\} \qquad (100)$$

and

$$VISF_j = \tfrac{1}{2}\{|(v_f)_{j+1}+(v_f)_j|[(v_f)_{j+1}-(v_f)_j] - |(v_f)_j+(v_f)_{j-1}|[(v_f)_j-(v_f)_{j-1}]\} \qquad (101)$$

A multiplier which is zero or unity is included on the inertia terms in the subtracted equation, Equation (99), to allow reduction to a drift-flux formula. A second multiplier on the interphase drag term is used to permit reduction to homogeneous flow. In Equations (98) and (99), the scalar or thermodynamic variables needed at the junctions are linear interpolations between the neighboring cell values. The generalization of the momentum equations to model abrupt area changes, orifices, etc. has been documented in a previous report, Reference (14), and will not be described herein.

3. NUMERICAL SOLUTION SCHEME

The basic five difference equations for mass, monentum and energy, contain terms which involve six variables at the new (n+1) time level. The six variables are the pressure, P; mixture density, ρ; static quality, X; mixture energy, U, which appears as the product ρU; and the phase velocities, v_g and v_f. The additional relationship necessary to render the difference equations determinant is provided by the state relationship by which the density can be expressed as a function of the pressure, static quality and the mixture energy (an additional constraint is implicit in the state relation wherein one phase is assumed to be at saturation conditions). The state relationship is highly nonlinear and the basic data are in tabular form. Thus, in order to preserve the linearity of the numerical scheme, the density relationship in terms of the other state variables is expressed by a two-term Taylor series expansion about the old time level; i.e.,

$$\rho^{n+1} = \rho^n + (\partial\rho/\partial P)^n_{X,U}(P^{n+1}-P^n) + (\partial\rho/\partial X)^n_{P,U}(X^{n+1}-X^n)$$

$$+ (\partial\rho/\partial U)_{P,X}(U^{n+1}-U^n) \; . \qquad (102)$$

The energy variable which appears in the difference equations is the product, ρU, which contains two dependent variables. Application of the chain rule to accomplish a change in independent variable in the Taylor expansion produces the result

$$\rho^{n+1} = \rho^n + (\partial\rho/\partial P)^n_{X,\rho U}\,(P^{n+1}-P^n) + (\partial\rho/\partial X)^n_{P,\rho U}(X^{n+1}-X^n)$$

and

$$+ [\partial\rho/\partial(\rho U)]_{P,X}[(\rho U)^{n+1} - (\rho U)^n], \tag{103}$$

where the derivatives with respect to P, X and (ρU) are expressed in terms of the thermodynamic derivatives developed in Section II.3 and are as follows:

$$(\partial\rho/\partial P)^n_{X,(\rho U)} = \rho^n[(\partial\rho/\partial P)^n_{X,U}]/[\rho^n + U^n(\partial\rho/\partial U)^n_{P,X}], \tag{104}$$

$$(\partial\rho/\partial X)^n_{P,(\rho U)} = \rho^n[(\partial\rho/\partial X)^n_{P,U}]/[\rho^n + U^n(\partial\rho/\partial U)^n_{P,X}], \tag{105}$$

and

$$[\partial\rho/\partial(\rho U)]^n_{P,X} = [(\partial\rho/\partial U)^n_{P,X}]/[\rho^n + U^n(\partial\rho/\partial U)^n_{P,X}]. \tag{106}$$

Equation (103) can now be used to eliminate the density at the n+1 time level from the difference equations to obtain a system of five difference equations in terms of the five dependent variables, P, X, (ρU), v_g and v_f.

At this point the numerical time advancement (from the n^{th} time level to the n+1 level) could be accomplished by simultaneous solution of the 5Nx5N system of linear equations which results from application of the five difference equations at each of the N nodes (the application of appropriate boundary conditions is necessary, but will be discussed later). However, the judicious choice of implicit terms in the momentum equations permits the time advancement problem to be reduced to the solution of an NxN system of linear equations. This is accomplished by elimination at a node of all the dependent variables except the pressure. This elimination is possible because the difference equations are linear in the new time variables and because the momentum equations only involve the velocities

and the pressures. The elimination process consists of solving for the phasic velocities in terms of adjoining cell pressures. The velocity equations are then used to eliminate the velocities from the mass and energy equations. Three equations per cell result which involve energy and quality of only the cell under consideration. Thus, the system of three equations can be reduced to a single linear equation relating the cell pressure to the pressure of adjoining cells. This procedure is in effect carried out for each cell of the system so that the result is an NxN system of equations for the new time pressures. The procedure is reversed so that the remaining field variables are obtained by back substitution. The NxN system of linear equations is diagonally dominant, in all cases examined to date, and thus the solution may be obtained either by direct inversion or by iterative inversion, whichever proves more efficient. The PILOT code uses direct inversion by means of a sparse matrix routine.

After solution for the field variables as just described, only the product (ρU) is known rather than values of ρ and/or U. The energy is required in order to apply the state relationship and thus obtain density as well as all other thermodynamic variables. The density-energy separation is obtained without iteration by using an auxiliary difference equation for the mixture density, ρ. For this purpose the mixture continuity equation is used along with the momentum equation for the velocities as described earlier. Thus, the density may be solved at each cell in terms of the already established pressure field (This solution is accomplished very efficiently in the PILOT code since all the convective terms have already been calculated in the course of the pressure field solution). The mixture energy is then calculated from the relation

$$U^{n+1} = (\rho U)^{n+1} / \rho_m{}^{n+1}, \tag{107}$$

where $\rho_m{}^{n+1}$ in the mixture mass density calculated from the mixture continuity relation.

The state relation is used to calculate the mixture thermodynamic density, ρ, using the state variables, P, X and U, as described in Section II.2 of this report.

4. TIME STEP CONTROL

In general, the density obtained from the state relationship is not equal to the density calculated from the mixture continuity equation. The difference between these two densities is a measure of the truncation error associated with the use of the Taylor expansion, Equation (103). This truncation error is sensitive to change in the density derivatives, Equations (104), (105) and (106). In a two-phase system the density derivatives may be highly discontinuous at points of transition between single-phase and two-phase regions. Consequently, any numerical scheme will have significant truncation error at such points unless these points are explicitly tracked and appropriate jump conditions applied, or unless the time step is made sufficiently small for the time step which spans the single-phase to two-phase transition. This error is controlled in the PILOT code by the latter approach using an automatic time step control.

The truncation error measure provided by the density difference is used as the basis for the automatic time step control scheme and this approach has been very successful in controlling mass truncation error and at the same time making fast execution possible through use of efficient time step sizes. The error measure is defined by

$$\epsilon = \left\{ \left| (\rho_i - \rho_{mi})/\rho_{mi} \right| \right\}_{max} \quad i = 1,2,3...N \ . \tag{108}$$

If the error measure exceeds a preset value (5.0×10^{-5} KG/M^3 has been used in the PILOT code) then the time step is rejected and the time step is repeated with half the preceding time step. Likewise, if the error measure, Equation (108), is less than a preset minimum (1.0×10^{-5} has been used in the PILOT code)

then the next time step advancement is made at double the previous time step. At intermediate values for the error measure the integration is continued with the same time step.

The halving or doubling time step adjustment process is overriden for print interval control and the Courant stability limit. The print interval override assures that a time step will coincide with the times where output is desired. The Courant condition limits the maximum time step such that material is never transported through more than one spatial cell per time step. This condition is expressed analytically by

$$\Delta t < [\Delta x_i/(|v_{gi}|,|v_{fi}|)_{max}]_{min}, \quad i = 1,2,\ldots N . \tag{109}$$

Generally, the truncation error control is more restrictive than the Courant condition for transient problems.

5. BOUNDARY CONDITIONS

Boundary conditions are usually established by a combination of physical considerations combined with a characteristic analysis to establish permissible number/combinations of boundary conditions. However, because the system of differential equations are not totally hyperbolic it is not possible to use characteristic arguments directly. In view of this situation, it is necessary to draw on experience with single-phase hydrodynamic models, such as the Navier-Stokes equations, to conclude what combinations of boundary conditions are acceptable.

The first and most obvious boundary condition to be considered is a closed end or null condition. In this case it is clear that the appropriate boundary conditions are that both the phasic velocities are zero. The momentum equations at such a junction are not required and the solution of the difference equations is determinate.

The second case to be considered is that of a constant pressure source or sink. In the case of a source, all the volume properties are required so that the quality, X, and energy, U, must be specified (this situation exists if either or both phasic velocities are such as to cause inflow to the system). Specified pressure is sufficient for a pure sink. A less obvious situation arises in the momentum calculation at either a source or a sink. The momentum convective terms require velocities at junctions upstream and downstream from the boundary junction and thus information is required beyond the source or sink volume. In this case, the boundary conditions are supplemented by the numerical condition that the derivatives of velocity are zero beyond the last junction; i.e., the velocities are constant, which permits evaluation of the momentum convection terms.

The last and most subtle boundary condition is associated with specified nonzero velocities. In this case, the boundary volume properties must be specified for the inflow case. If both velocities are specified in addition to the pressure, quality and energy, then the problem is overspecified since there are only five field equations (the analogous case for a single phase flow would be specification of the pressure, energy and velocity, which could only be the case if the flow velocity were greater than the sound speed; i.e., supersonic). The specification of five conditions could only be correct if the flow were choked or supersonic. However, since the system of equations is not totally hyperbolic the criterion for choking is obscure. In general, the flow will be less than sonic so that one is forced to conclude that fewer than five specifications is appropriate. It can be shown that only one velocity need be specified and the remaining velocity can be calculated from momentum considerations. However, even in this case additional numerical boundary conditions must be employed in order to calculate the momentum flux terms as discussed previously. This requirement for additional boundary conditions is common to most finite

difference schemes and does not seem to cause any significant problem. In conclusion, one can specify both velocities as well as the state properties and generate reasonable results, but some caution should be exercised when posing and/or interpreting the results from such problems.

IV. PROCESS/COMPONENT MODELS

1. GENERAL

The PILOT code includes process/component models for abrupt area change, branching and choking. The models for area change and branching have been documented in a separate report, Reference (4), and will only be briefly described herein.

2. ABRUPT AREA CHANGE AND BRANCHING

The abrupt area change model is based on the Bourda-Carnot[21] formulation for a sudden enlargment and standard pipe flow relations, including vena-contracta effect for a sudden contraction and/or an orifice. Quasi-steady continuity and momentum balances are employed at points of abrupt area change. The numerical implementation of these balances is such that the hydrodynamic losses are independent of the upstream and the downstream nodalization. In effect, the quasi-steady balances are employed as jump conditions which couple fluid components having abrupt change in cross-sectional area. This coupling process is achieved without change to the basic linear semi-implicit numerical time advancement scheme. Thus, the fast execution time objective is not impacted by incorporation of these models.

The area change and parallel branching numerical models have been installed and tested in the RELAP5 PILOT code and have produced correct results for single-phase flows and two-phase flows with slip. The parallel branching model has been tested on a symmetrical system blowdown problem and correct results were obtained.

3. CHOKING

Choking is used to describe the process or flow condition under which the flow is independent of downstream conditions. Choking in single-phase flow occurs when the fluid velocity equals the local speed of sound. At such a condition, acoustic signals can no longer propagate upstream, the flow velocity is independent of downstream conditions and the flow is said to be choked. Usually the point at which a flow chokes will be a point of minimum area although not necessarily. The flow process in the vicinity of choked flow generally is characterized by large spatial gradients in pressure and fluid density, thus closely spaced spatial nodes are required for accurate numerical modeling of such a process.

In the case of two-phase flows, the criterion for choking is more obscure than in the single-phase flow case because the sound speed associated with acoustic signal propagation is not easily defined. On the other hand, to model such processes in detail requires fine spatial noding which limits the overall time step and requires excessive computational time. While it is possible to model choked flow in detail with the numerical scheme described herein, the approach was judged inefficient for modeling reactor blowdown problems. Particularly, where the blowdown occurs over an extended period of time and relatively coarse nodalization is used for the bulk of the system representation. The fine nodalization required at the break or point of choked flow is inconsistent with the representation of the remainder of the system and is computational inefficient.

Choked flow is modeled in the PILOT code by application of an appropriate criterion to detect choked flow and subsequent application of analytically based boundary conditions. The criterion for choking and the boundary conditions were derived from a characteristic analysis. A brief description of this analysis will be presented.

The RELAP5 system of partial differential equations can be written in vector/matrix notation as follows:

$$A(\partial\bar{U}/\partial t) + B(\partial\bar{U}/\partial x) = \bar{C} \qquad (110)$$

where $\bar{U}$ and $\bar{C}$ are vectors and A and B are fifth order square matrices. The characteristic problem is posed by raising the question: Do surfaces (lines) exist such that Equation (110) is an indeterminate or interior operator? This situation is investigated by choosing a surface orientation defined by a normal vector $\bar{n}$ and then transforming the system of equations, Equation (110), to a new set of coordinates, one direction of which coincides with the characteristic surface normal and the other being tangent to the surface. Transformation of Equation (110) yields:

$$A[(\partial\bar{U}/\partial n_1)(\partial n_1/\partial t) + (\partial\bar{U}/\partial n_2)(\partial n_2/\partial t)]$$

$$+ B[(\partial\bar{U}/\partial n_1)(\partial n_1/\partial x) + (\partial\bar{U}/\partial n_2)(\partial n_2/\partial x)] = \bar{C} \qquad (111)$$

If n_1 is chosen as the coordinate normal to a characteristic surface and n_2 tangent to the surface, then the characteristic property is expressed by the determinantal equation

$$|A(\partial n_1/\partial t) + B(\partial n_1/\partial x)| = 0 \qquad (112)$$

or

$$|A\lambda - B| = 0 \qquad (113)$$

where

$$\lambda = -(\partial n_1/\partial t)/(\partial n_1/\partial x) \qquad (114)$$

Here $-\lambda$ is the slope of the normal to a characteristic surface in the x, t plane.

The characteristic equation, Equation (113), has all real roots for a hyperbolic system. However, the system of equations used to model the RELAP5 hydrodynamics is such that the characteristic equation has a pair of complex conjugate roots as well as real roots. These complex roots are common to all

two-fluid two-phase models[20] and are the result of imperfections in the representation of high frequency phenomena. Thus, the complex nature of the roots is not of any physical significance and a well-posed numerical problem can be obtained by sufficient numerical dissipation (i.e., implicitness and donor flux formulations).

The propagation velocities associated with the complex roots can be shown to be between the phasic velocities, thus they do not govern choking behavior. A choking criterion is developed by looking at the real roots which are found after factoring out the complex conjugate pair. Of the remaining real roots, the smallest one (slope corresponding to the outermost characteristic surface) is the limiting path along which acoustic signals can propagate. The condition that the smallest root (λ) vanish, which corresponds to the condition that acoustic signals no longer propagate upstream, is the choking condition (the corresponding characteristic surface is vertical in the x,t plane);

$$[-\lambda_{real}]_{max} = 0 . \qquad (115)$$

The analytic factorization of the characteristic equation resulting from analysis of the RELAP5 system of equations is a near impossible task (A fifth order polynomial must be factored). This problem is made tractable by either assuming complete thermal equilibrium or assuming the interphase mass transfer rate to be zero. Each of these assumptions reduce the characteristic problem to factorization of a fourth order polynomial. Fortunately, the roots consist of a complex conjugate pair and a pair of real roots in each case. An approximate analytic factorization can be used to obtain the complex roots. The remaining two real roots are subsequently obtained using the quadratic formula.

Only the case of complete nonequilibrium without added mass effe ts will be presented since the general model is under development and will be the subject of a future report. The characteristic equation for this case is

$$\alpha_f\rho_g\,(\lambda+v_g)^2[(\lambda+v_f)^2/c_f^2-1] + \alpha_g\rho_f\,(\lambda+v_f)^2[(\lambda+v_g)^2/c_g^2-1] = 0 \qquad (116)$$

Disregarding fourth-order terms relative to second-order terms yields a second-order polynomial in λ which can be easily fa tored to obtain approximate values for the complex roots.

$$\lambda_{1,2} = (\alpha_f\rho_g v_g + \alpha_g\rho_f v_f)/(\alpha_f\rho_g + \alpha_g\rho_f)$$

$$\pm\,(i)\,(\alpha_f\alpha_g\rho_f\rho_g)^{\frac{1}{2}}\,(v_f-v_g)/(\alpha_f\rho_g + \alpha_g\rho_f) \qquad (117)$$

The original polynomial can now be divided by the product of the two complex conjugate factors to obtain a reduced second-order polynomial in λ. Analytic factorization of the second-order equation yield the remaining two roots, which are

$$\lambda_{3,4} = (\alpha_f\rho_g v_f + \alpha_g\rho_f v_g)/(\alpha_f\rho_g + \alpha_g\rho_f) \pm c$$

where c is the stratified sound speed. The choking criterion, Equation (115), yields

$$(\alpha_f\rho_g v_f + \alpha_g\rho_f v_g)/(\alpha_f\rho_g + \alpha_g\rho_f) = c. \qquad (118)$$

The sound speed appearing in Equation (118) is a function of the interphase coupling due to virtual mass effects and can be shown to be the homogeneous sound speed for large virtual mass coefficients (such as would be typical of dispersed droplet or bubbly flows).

Equation (118) provides a relation between the velocities and the scalar variables of the flow (the sound speed is a function of the pressure, quality and energy). When the two-phasic momentum equation are combined with Equation (118) the three simultaneous linear equations can be solved for the variables v_g, v_f and P at the point being investigated for choking.

If the values for v_g and v_f calculated by the normal solution scheme yield a value for the left-hand side of Equation (118) which exceeds c then the flow is choked and the values for v_g, v_f and P from the choked solution are imposed. This procedure numerically decouples the upstream solution from the downstream conditions, which is in agreement with the situation known to exist physically.

The choking model has been applied to modeling of Edwards'[22][23] pipe blowdown experiments for both 3 and 8 inch pipes. The results are in excellent agreement with data as illustrated in Section V of this report.

V. SAMPLE CALCULATIONS

1. GENERAL

The RELAP5 PILOT code has been tested on several hypothetical problems for the purpose of checking the code, model characteristics and constitutive data. The code has also been applied to the simulation of two two-phase experiments those of Edwards[22][23] and Reocreux[15]. The code results in both cases are in excellent agreement with the experimental data. Only the results for application to the Edward's experiment will be reported on herein; however, these results demonstrate all the features of the code, both the abrupt area change and choking models were used in producing these results. The application to Reocreaux data is still in progress and will be reported upon completion of that work.

2. EDWARD'S PIPE BLOWDOWN EXPERIMENT

Edwards[22][23] has performed transient blowdown experiments using 73 mm (3 in.) and 206 mm (8 in.) pipes which were both 4.09M in length. The pipes were filled with water, heated and pressurized. A glass disc at one end was ruptured to initiate the blowdown. The initial conditions which were used in the code to simulate the experiments are tabulated in Table I. All the results which are prescribed herein were obtained using 20 nodes or volumes to numerically model the pipe. However, the calculations were performed using 10 and 40 volume representations. The 10 and 20 volume representations differed only slightly (less than 10%) and the 20 and 40 nodalizations were essentially identical (less than 1%).

TABLE I

INITIAL CONDITIONS USED FOR SIMULATION OF EDWARDS' EXPERIMENT

	73 mm	206 mm
Pressure (N/M^2)	7.0×10^6	5.723×10^6
Temperature (^oK)	502^oK	527^oK
Pipe Length (M)	4.09	4.09
Pipe Area (M^2)	4.185×10^{-3}	3.333×10^{-2}
Exit Area (M^2)	3.641×10^{-3}	3.333×10^{-2}

The boundary conditions used were specified zero velocity at the closed end and the choking model described in Section IV of this report was used for choked flow at the open end. The abrupt area change model was used for the 73 mm pipe which had a 13% reduction at the exit due to fragments of the rupture disk remaining after initiation of the depressurization. The data taken were pressures at up to seven gauge stations stationed along the pipe from the open end (GS-1) to the closed end (^{GS}-7 for the 73 mm pipe and ^{GS}-8 for the 206 mm pipe) and void fraction measured at gauge station 5.

3. 73 MM PIPE BLOWDOWN RESULTS

The pipe blowdown calculated results are presented in two parts. The first part consists of the short-term results (0 to 20 ms) and the second, the long-term results (0 to 500 ms). At 500 ms, the pipe interior is approximately at ambient pressure. In all cases, the data are shown as solid curves with the PILOT calculations shown as dashed curves.

The short-term PILOT code calculated pressure histories are compared to Edwards' data, obtained from Reference (24), on Figures 2 and 3 for gauge stations 1 through 7, respectively. The results are in good agreement with the data. The calculated results do not show the large pressure undershoot measured at gauge station 7, although small undershoots at other gauge stations are in agreement with the data. Another interesting observation is that the calculated depressurization wave leads the data by about 0.5 ms at all gauge stations. The constant difference at all stations indicates that the depressurization wave propagation velocity is correct, but that the effective time of break initiation may be slightly different than reported.

Isometric plots of the short-term calculated results are presented in Figure 4. The pressure, liquid fraction, liquid velocity and vapor velocity are shown. In each of these plots, the condition all along the pipe are displayed as a function of time. The open end is on the left for the pressures and the void fractions while the open end is on the right for the velocity plots. Interesting features of these plots are the initial depressurization wave in the pressure plot and the high velocity gradients which exist near the open end in the velocity plots.

The long-term results (0 to 500 ms) are shown plotted on Figures 5 and 6 as pressure histories at gauge stations 1 through 7. The agreement with the data (solid curves) is excellent except at station 6. The lack of agreement at GS-6 is probably due to the use of a uniform energy corresponding to 502 K, while it is reported in Reference (24) that the initial temperature may have varied by as much as 8 K with the highest

temperature in the vicinity of gauge station 6. Note that the calculated pressure at GS-1 and GS-2 are in much better agreement with the data than reported in References (25) and (26). The improved result herein is due to the use of a choked flow velocity boundary condition rather than the pressure boundary conditions used in References (25) and (26). The analytical results presented in Reference (27) support this conclusion.

All results presented herein have been calculated both with and without pipe wall friction and thus support the findings in Reference (27) that pipe friction has no effect on the blowdown results.

The measured and calculated void fractions atgauge station 5 are shown on Figure 6. The long-term void fraction agrees very well with the data, but at early times (up to 0.250 sec) the calculated profile is very similar to the results obtained in other analytical investigations [References (25), (26) and (27)]. Here again nonuniform initial test energy may be responsible for the early time void fraction variation at gauge station 5. Void fraction profiles at other stations along the pipe did exhibit a variation similar to the data at gauge station 5.

Isometric plots of the long-term calculated results are shown on Figure 7. Here again, the open end is on the left for the pressure and liquid fraction plots while the open end is on the right for the velocity plots. The void propagation wave is very evident in the liquid fraction plot. Note that a small void wave is initiated at the closed end and this merges with the main wave from the open end. The velocity plots show that up to 50 m/s relative velocity is predicted to exist late in the blowdown.

4. 206 MM PIPE BLOWDOWN RESULTS

Edwards et al,[23] have repeated the pipe blowdown experiment using an 206 mm pipe in order to obtain better void fraction resolution. These experiments were also modeled using the RELAP5 PILOT code and results are compared to the data on Figures 8 through 11. The short-term (0 - 20 ms) pressure histories are presented on Figures 8 and 9. The calculated results show only fair agreement with the data. In general, the calculated pressures are lower than the measured pressures. However, the measured pressures show a continual decrease and approach the calculated values at 20 ms. The disagreement is suspected to be due to vertical temperature stratification in the pipe which is a result of the heating by free convection from the pipe walls (the temperature measurements confirm the existance of vertical gradients). The long-term calculated results are compared to the measured data on Figures 10 and 11. The calculated pressures agree well with the data except at the open end, GS-1 and at the closed end GS-8. The disagreement at the open end is probably due to the existence of large pressure gradients in both the axial and radial direction which exist due to the abrupt discharge. This effect does not appear to be significant since the correct rate of mass discharge was calculated (long-term pressure agreement at the pipe internal stations is evidence that the overall mass discharge rate is correct).

The measured and calculated void fractions are compared in Figure 11. The early and late time results are in good agreement. The discrepancy between 0.1 s and 0.2 s could be due to variation in the mean energy profile along the pipe as speculated in the case of the 73 mm results (the calculations were made using a uniform initial energy).

VI. REFERENCES

1. J. A. Trapp and V. H. Ransom, "RELAP5 Hydrodynamic Model: Progress Summary - Field Equations", SRD-126-76, EG&G Report (June 1976).

2. V. H. Ransom and J. A. Trapp, "RELAP5 Hydrodynamic Model: Progress Summary - PILOT Code", PG-R-76-013, EG&G Report (December 1976).

3. V. H. Ransom, "Completion of Buff Book Node 63126: 2VT$_K$T$_{sat}$ Pipe Flow Checkout" EG&G Interoffice Letter (April 29, 1977).

4. J. A. Trapp and V. H. Ransom, "RELAP5 Hydrodynamic Model Progress Summary - Abrupt Area Changes and Parallel Branching", PG-R-77-92, EG&G Report (November 1977).

5. V. H. Ransom, R. J. Wagner, J. A. Trapp, K. E. Carlson and D. M. Kiser, "RELAP5 Code Development and Results", Presented at the Fifth Water Reactor Safety Research Information Meeting, November 7-11, 1977.

6. M. Ishii, Thermo-Fluid Dynamic Theory of Two-Phase Flow, Direction des Etudes et Recherches d' Electricite de France (1975).

7. F. H. Harlow and A. A. Amsden, "Flow of Interpenetrating Material Phases", Journal of Computational Physics 18 (1975) pp 440-464.

8. J. R. Travis, F. H. Harlow, and A. A. Amsden, "Numerical Calculation of Two-Phase Flows", LA-5942-MS, Los Alamos Scientific Laboratory Report (June 1975).

9. R. T. Lahey, Jr., RPI Two-Phase Flow Modeling Program" Presented at Fifth Water Reactor Safety Research Information Meeting, November 7-11, 1977.

10. P. S. Andersen, P. Astrup, L. Eget, and O. Rathman, "Numerical Experience with the Two-Fluid Model RISQUE", Paper Presented at the ANS Water Reactor Safety Meeting July 31, August 4, 1977.

11. N. Zuber, "On the Dispersed Two-Phase Flow in the Laminar Flow Regime", Chem. Eng. Sci., 19 (1964) pp 897-917.

12. L. Van Wijngaarden, "Hydrodynamic Interaction Between Gas and Bubbles in Liquid", J. Fluid Mechanics, 77, Part 1 (1976) pp 27-44.

13. P. W. Bridgeman, The Thermodynamics of Electrical Phenomenon in Metal and a Condensed Collection of Thermodynamic Formulas, New York, Dover Publications, Inc. (1961).

14. O. C. Jones, Jr. and Pradip Saha, "Volumetric Vapor Generation in Non-Equilibrium, Two-Phase Flows", Notes Prepared for Advanced Code Review Group Meeting Water Reactor Safety Research Division U. S. Nuclear Regulatory Commission, Washington, D.C. 20555, June 2, 1977.

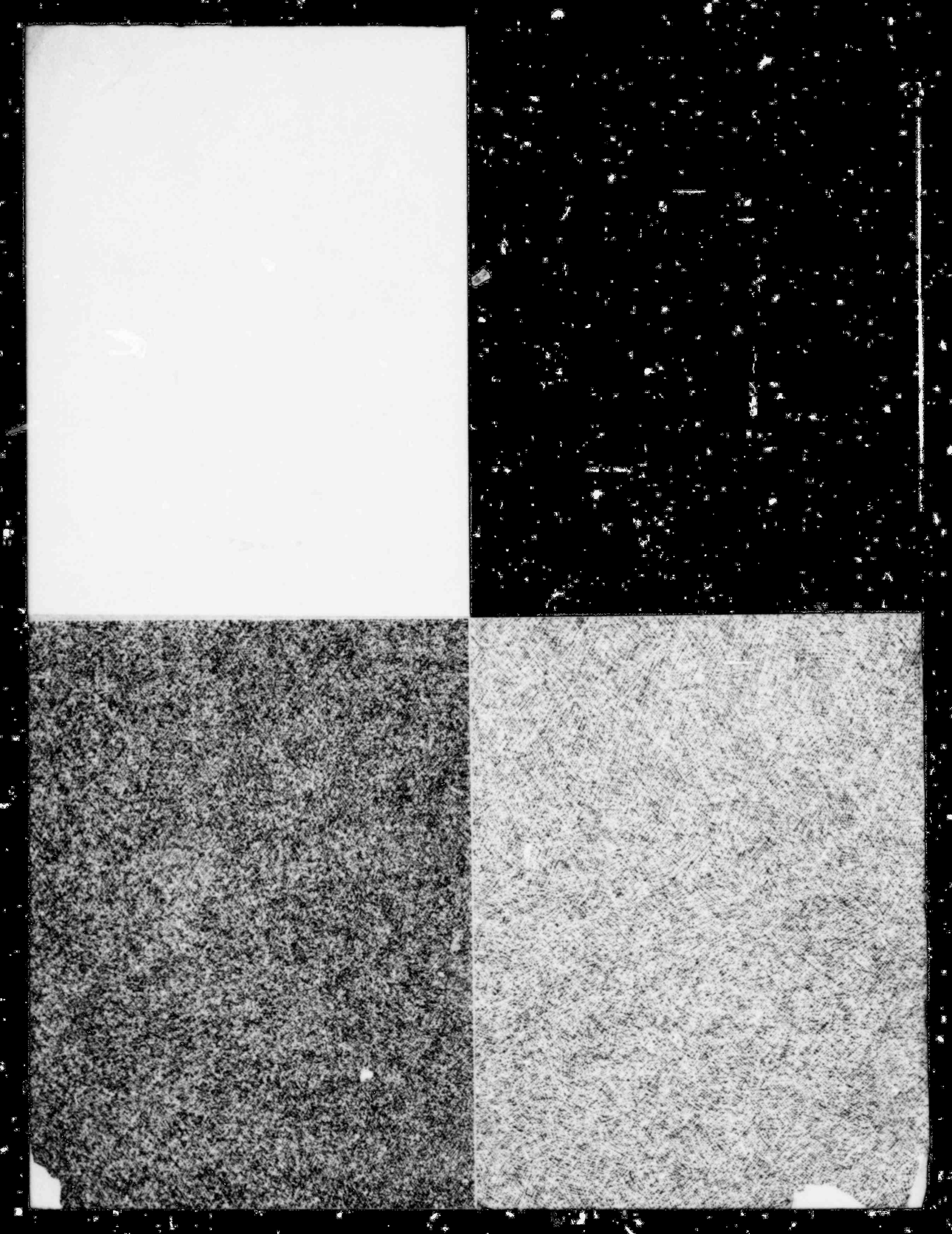

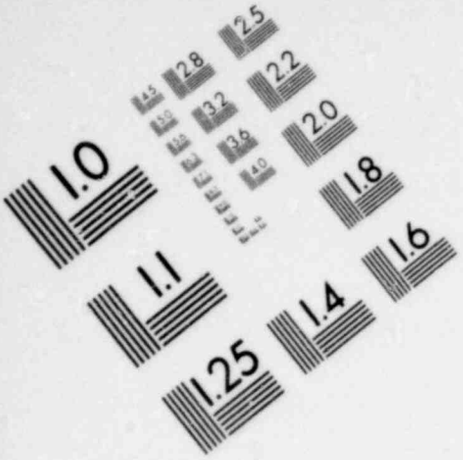

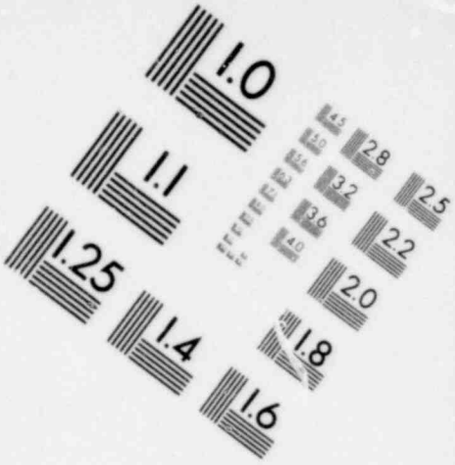

IMAGE EVALUATION
TEST TARGET (MT-3)

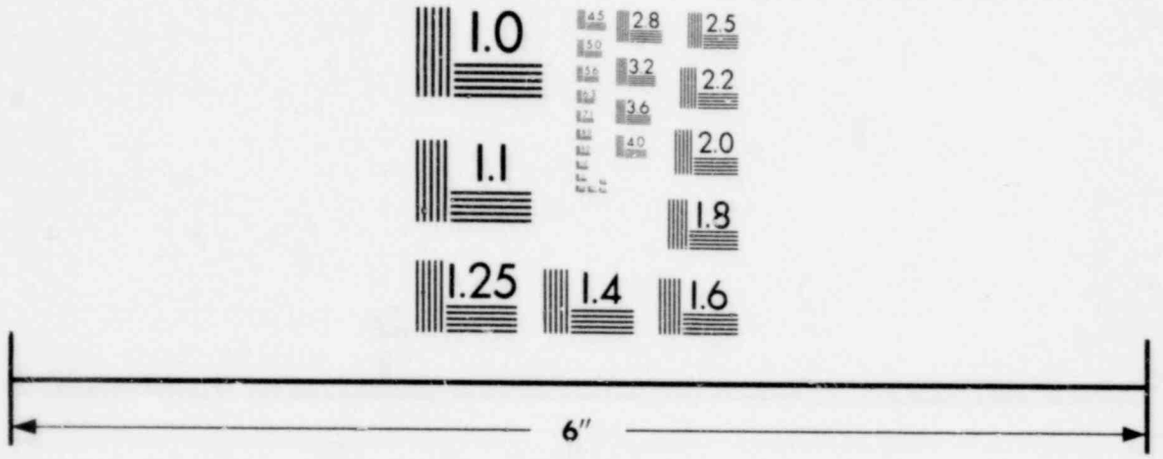

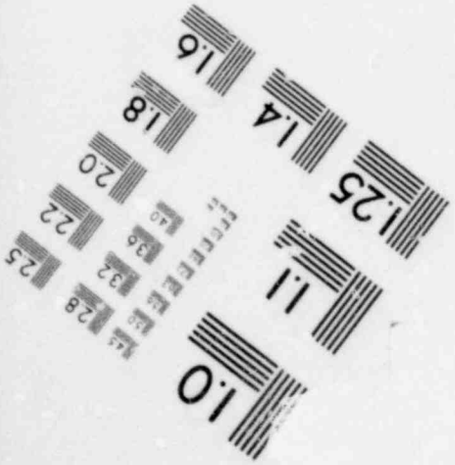

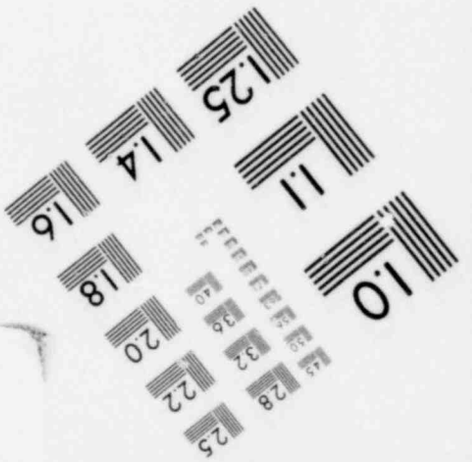

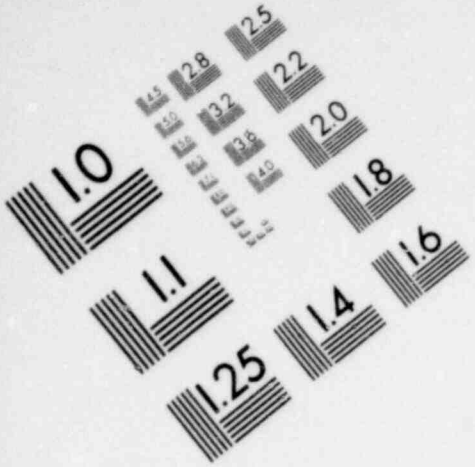

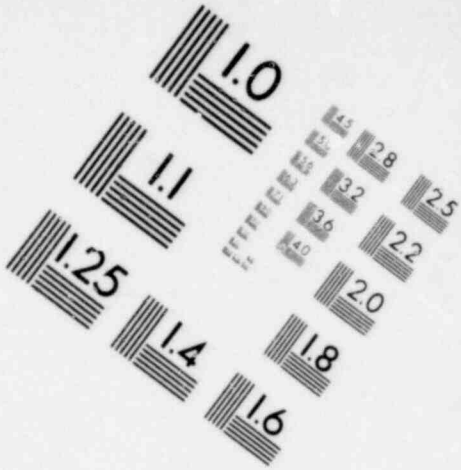

IMAGE EVALUATION TEST TARGET (MT-3)

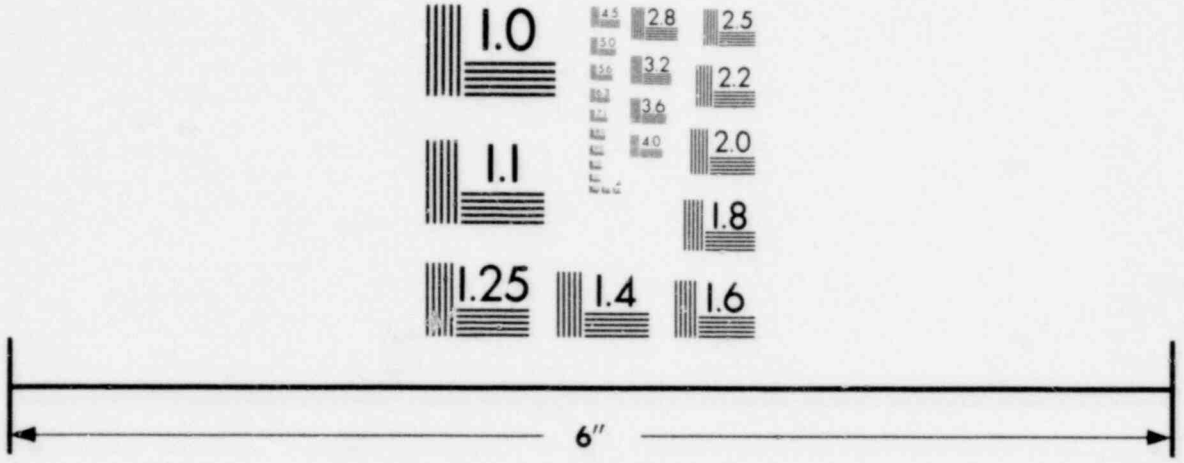

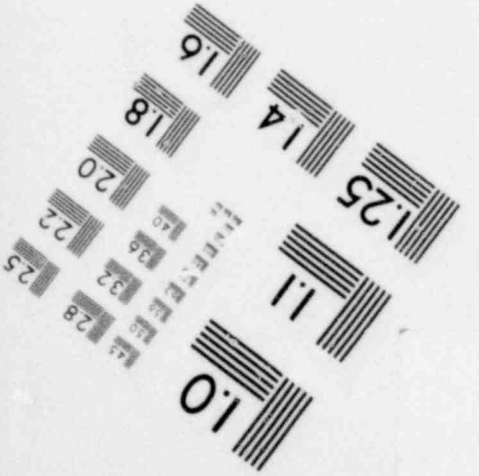

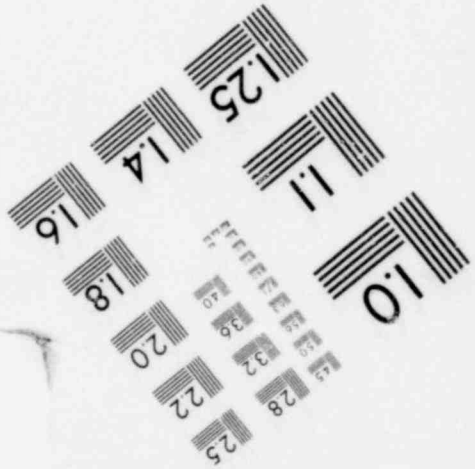

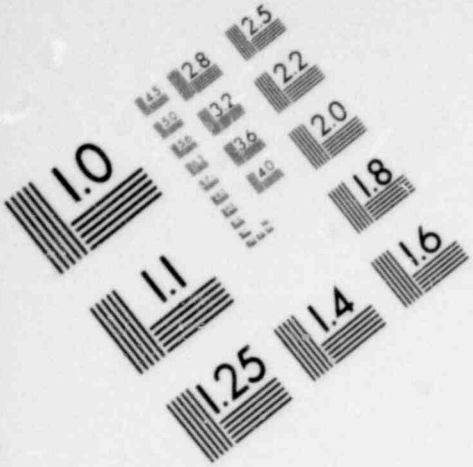

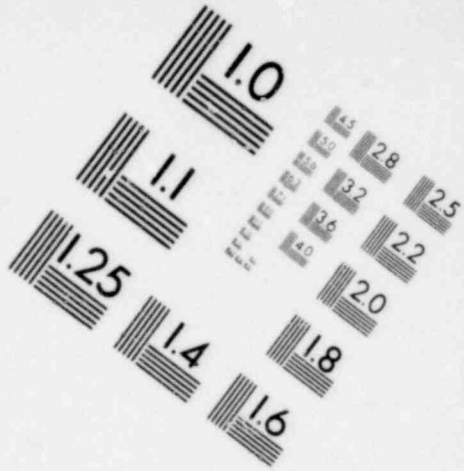

IMAGE EVALUATION TEST TARGET (MT-3)

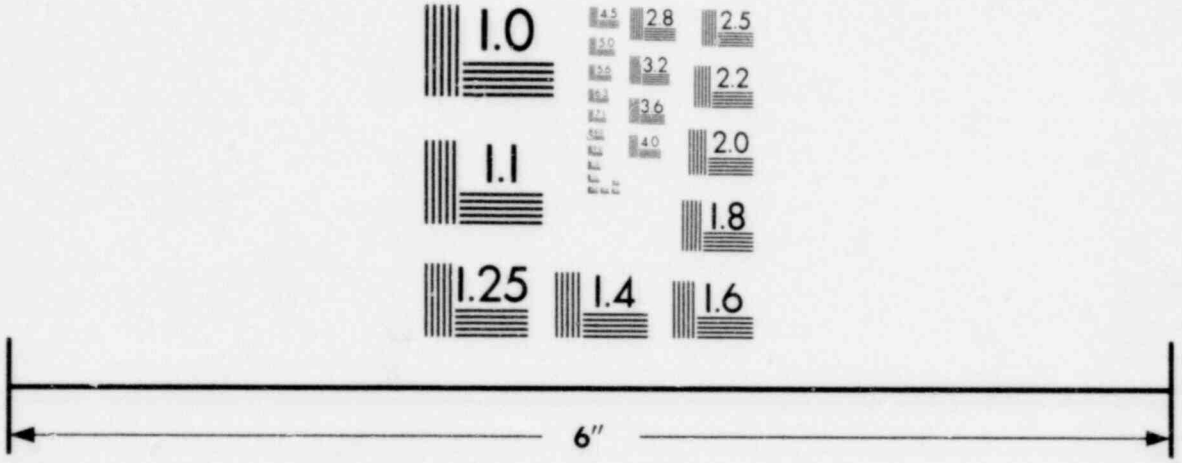

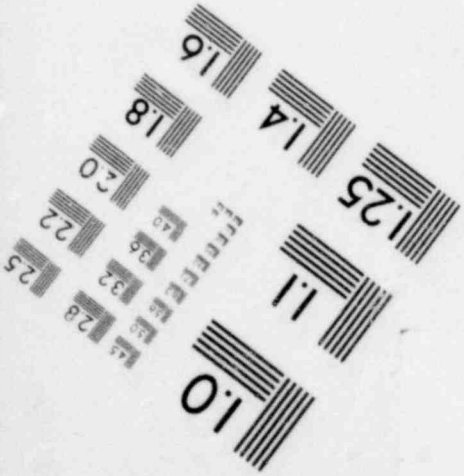

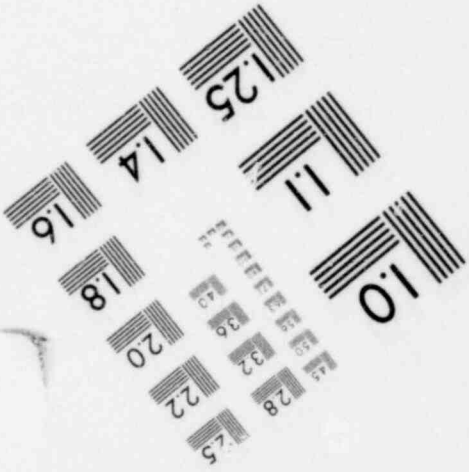

15. G. Houdayer, G. Lecoq, B. Pinet, M. Reocreux, and J. C. Rousseau, "Modeling of Two-Phase Flow with Thermal and Mechanical Non-Equilibrium", Paper Presented at the Fifth Water Reactor Safety Research Information Meeting, Washington, D.C., November 7-11, 1977.

16. J. M. Seynhaeve, M. M. Giot, and D. D. Fritte, "Non-Equilibrium Effects on Critical Flow Rates at Low Qualities", Paper Presented at the Specialists Meeting on Transient Two-Phase Flow - Totonto, Canada, August 1976.

17. C. W. Hirt and T. A. Oliphat, "SOLA-PLOOP: A Non-Equilibrium, Drift-Flux Code for Two-Phase Flow in Networks", Presented at Specialists Meeting on Transient Two Phase Flow - Toronto, Ontario, Canada, August 3-4, 1976.

18. S. Lekach, "Development of a Computer Code for Thermal Hydraulics of Reactors (THOR)", Brookhaven National Laboratory Quarterly Progress Report, BNL 19978 (1975).

19. D. R. Liles, "Nuclear Reactor Safety", Los Alamos Quarterly Progress Report, LA-NUREG-6934-PR.

20. J. D. Ramshaw and J. A. Trapp, "Characteristics, Stability and Short Wave Length Phenomena in Two-Phase Flow Equation Systems", Aerojet Nuclear Company Report, ANCR-1272 (1976).

21. J. K. Vennard, Elementary Fluid Mechanics, John Wiley and Sons, 4th Edition (1965).

22. A. R. Edwards and T. P. O'Brien, "Studies of Phenomena Connected with the Depressurization of Water Reactors", Journal of the British Nuclear Energy Society, Vol. 9 (April 1970) pp 125-135.

23. B. O. Borgartz, et al., Depressurization Studies, Phase 3: Results of Tests 142 and 143., DWRE/44/86/141, AWRE Fowlness Division Report (August 1977).

24. R. W. Garner, "Comparative Analyses of Standard Problems - Standard Problem 1 (Straight Pipe Depressurization Experiments)", ANC Interim Report I-212-74-5.1 (October 1973).

25. C. W. Hirt and N. C. Romero, "Application of a Drift-Flux Model to Flashing in Straight Pipes", Los Alamos Scientific Laboratory Report LA-6005-MS (July 1975).

26. W. C. Rivard and M. D. Torrey, "Numerical Calculation of Flashing from Long Pipes Using a Two-Fluid Model", Los Alamos Scientific Laboratory Report, LAMS-NUREG-6330 (May 1976).

27. P. G. Kroeger, "Application of a Nonequilibrium Drift Flux Model to Two-Phase Blowdown Experiments", Brookhaven National Laboratory Presented at Specialists Meeting on Transient Two-Phase Flow OECD Nuclear Energy Agency, Toronto, Canada, August 1976.

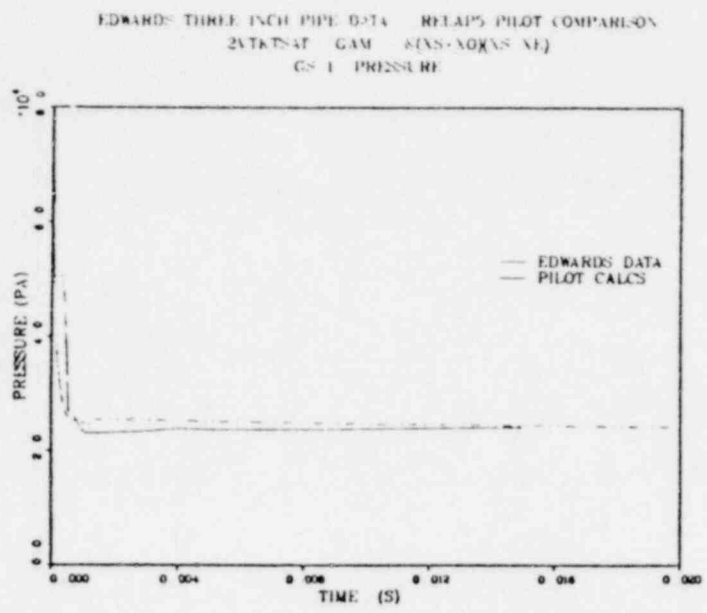

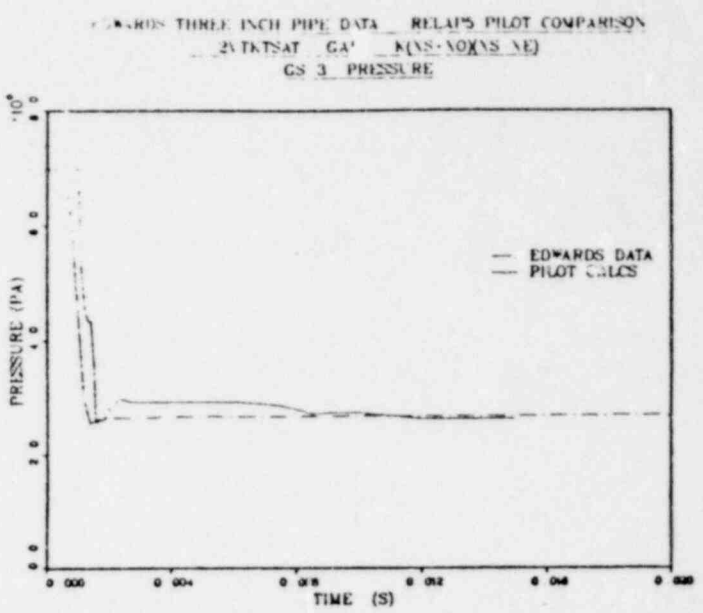

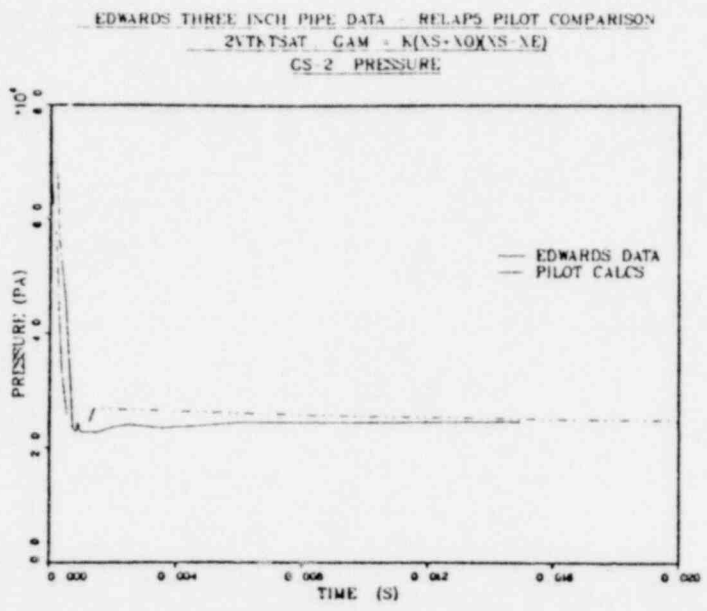

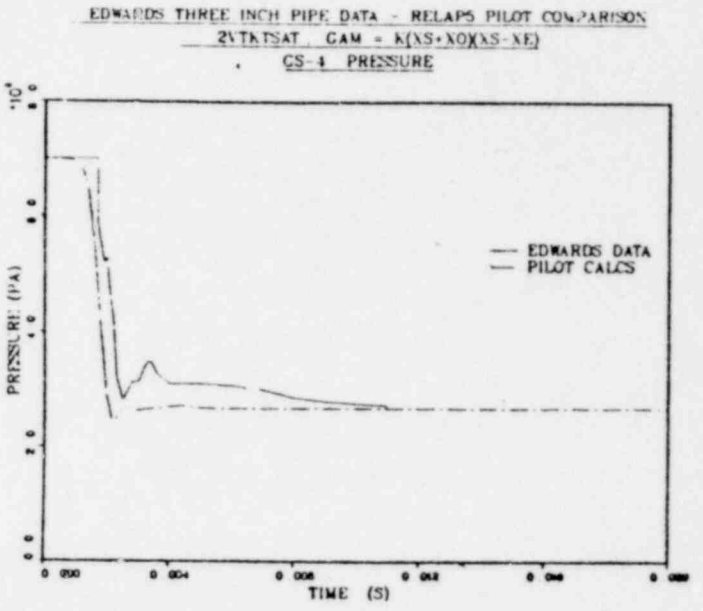

Figure 2. Comparison of RELAP5 PILOT Results to Edwards 73 mm Short-Term Pressure Data for Gauge Stations 1, 2, 3 and 4

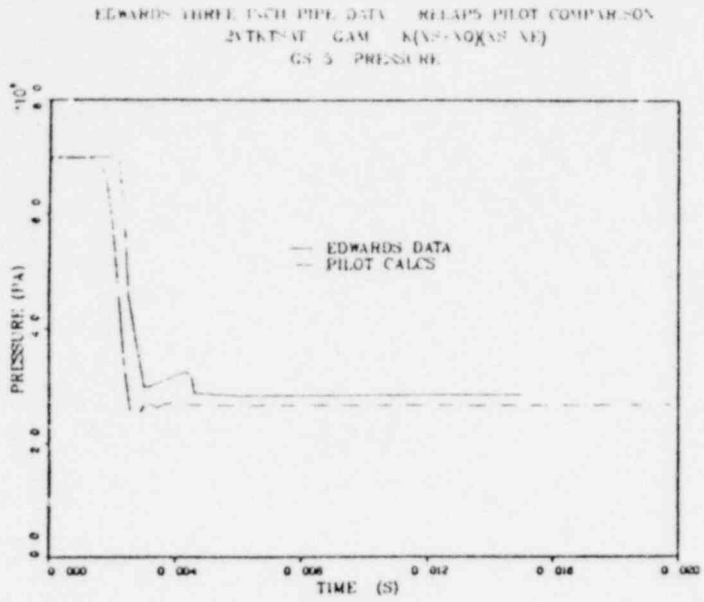

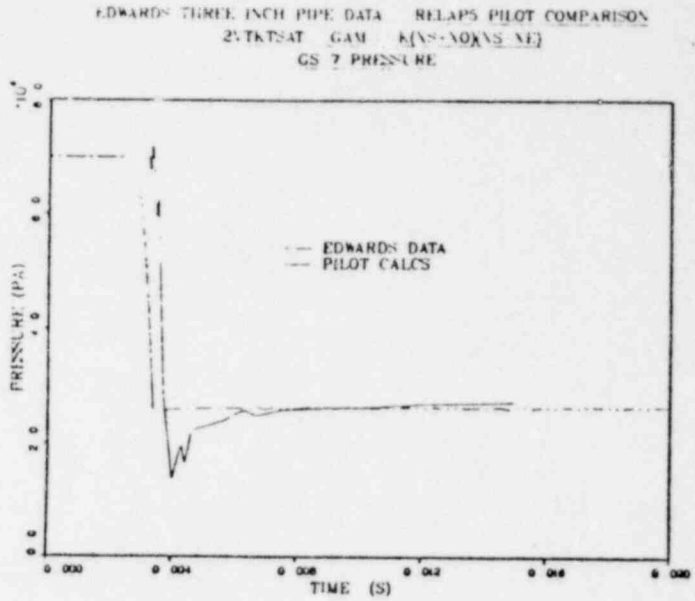

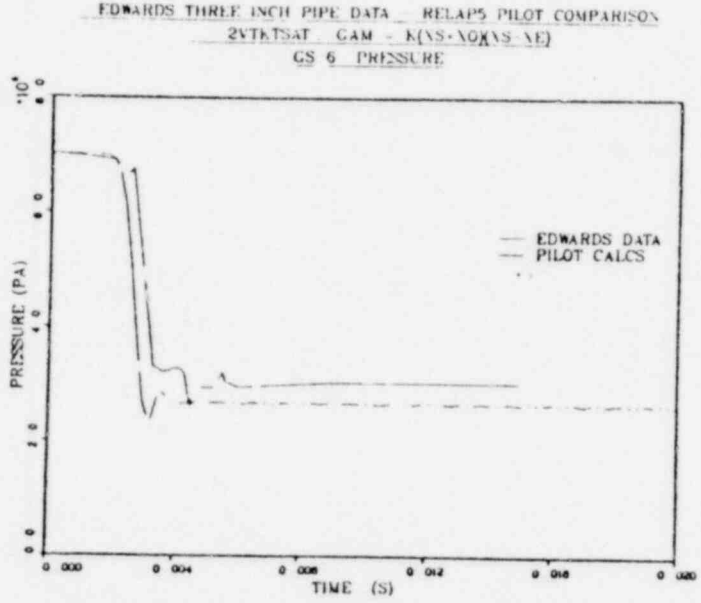

Figure 3. Comparison of RELAP5 PILOT Results to Edwards 73 mm Short Term Pressure Data at Gauge Stations 5, 6, and 7

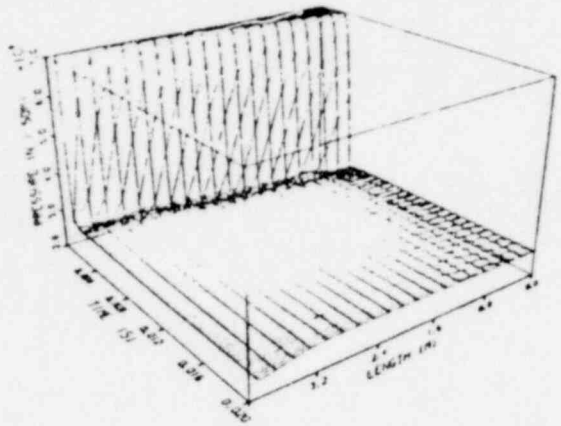

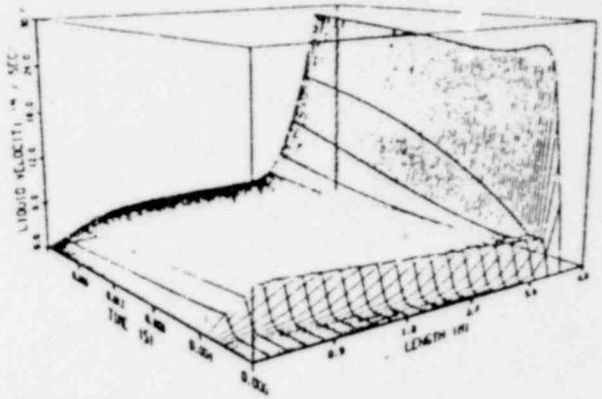

EDWARDS THREE INCH PIPE DATA - RELAP5 PILOT COMPARISON
2VT+TSAT, GAM = 1.15+0.15E5
VOLUME DATA

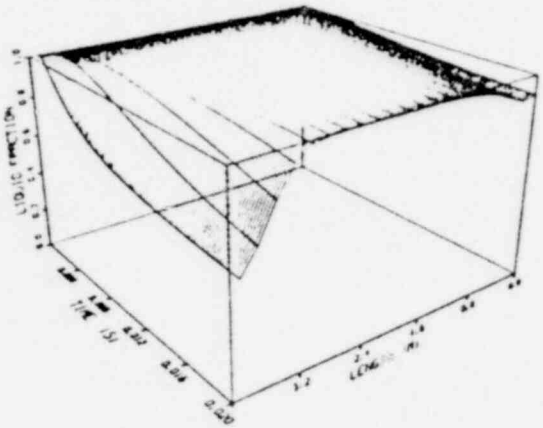

EDWARDS THREE INCH PIPE DATA - RELAP5 PILOT COMPARISON
2VT+TSAT, GAM = 1.15+0.15E5
JUNCTION DATA

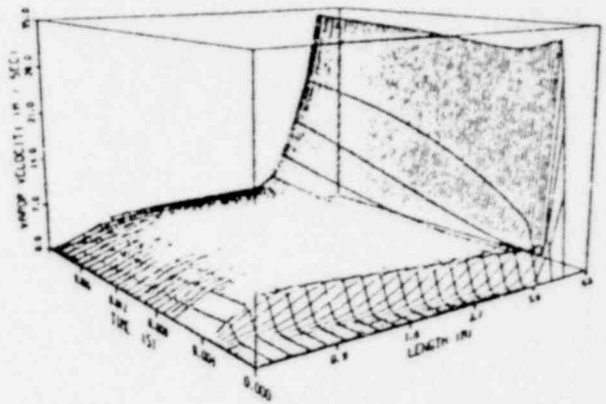

Figure 4. Isometric Plots of RELAP5 PILOT Short-Term Calculations for 73 mm Pipe

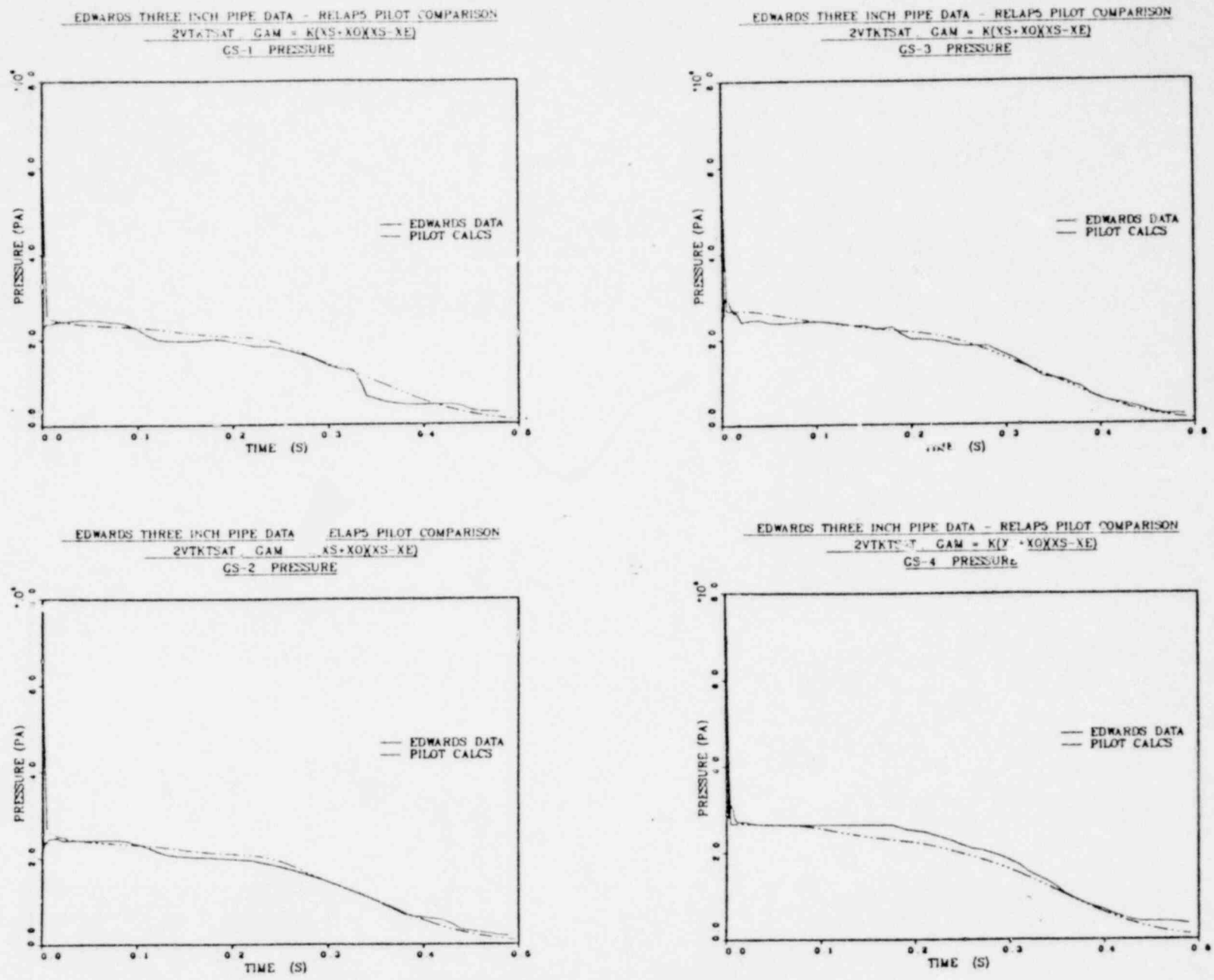

Figure 5. Comparison of RELAP5 PILOT Results to Edwards 73 mm Long Term Pressure Data for Gauge Stations 1, 2, 3, and 4

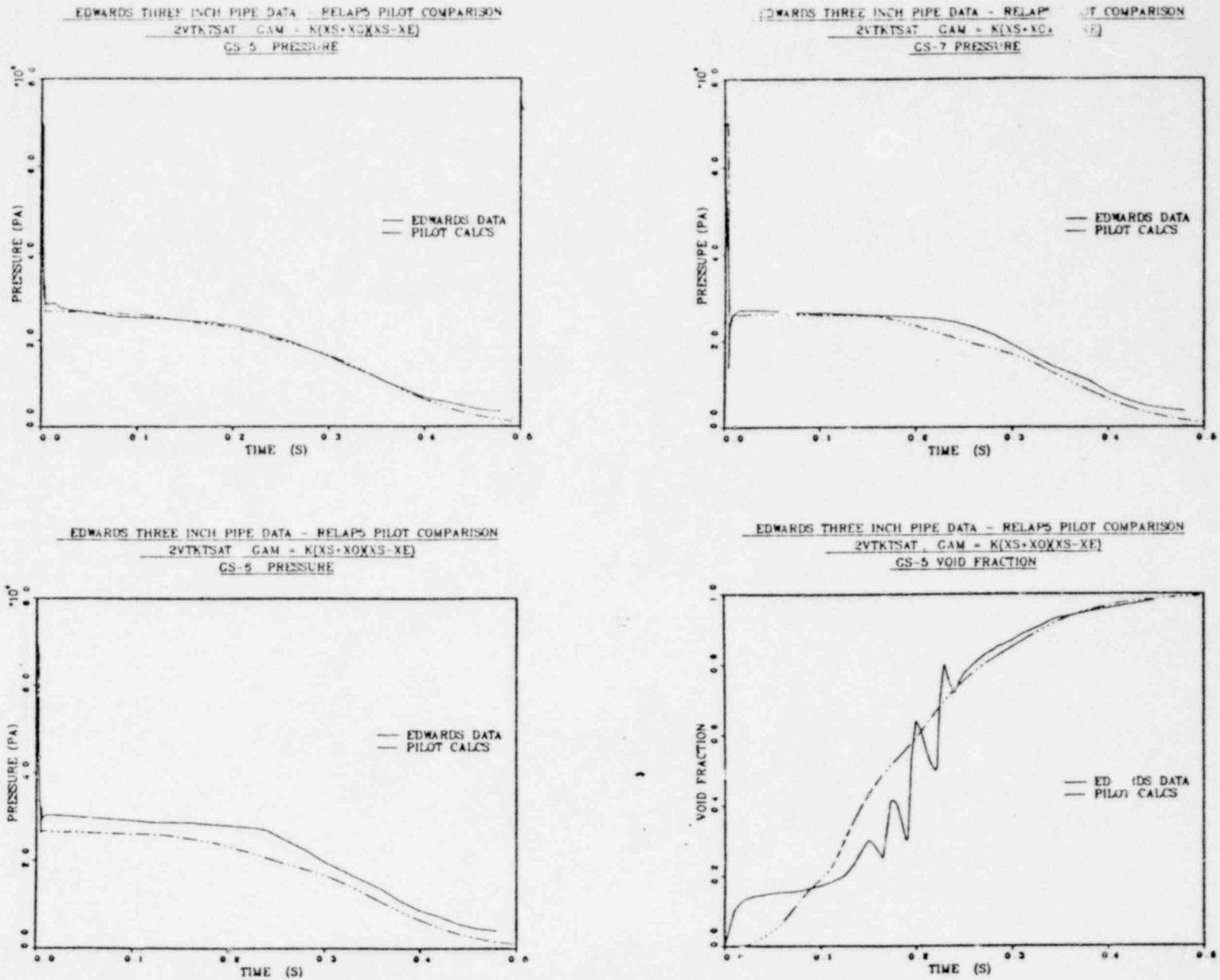

Figure 6. Comparison of RELAP5 PILOT Results to Edwards 73 mm Long Term Pressure and Void Fraction Data for Gauge Stations 5, 6, and 7

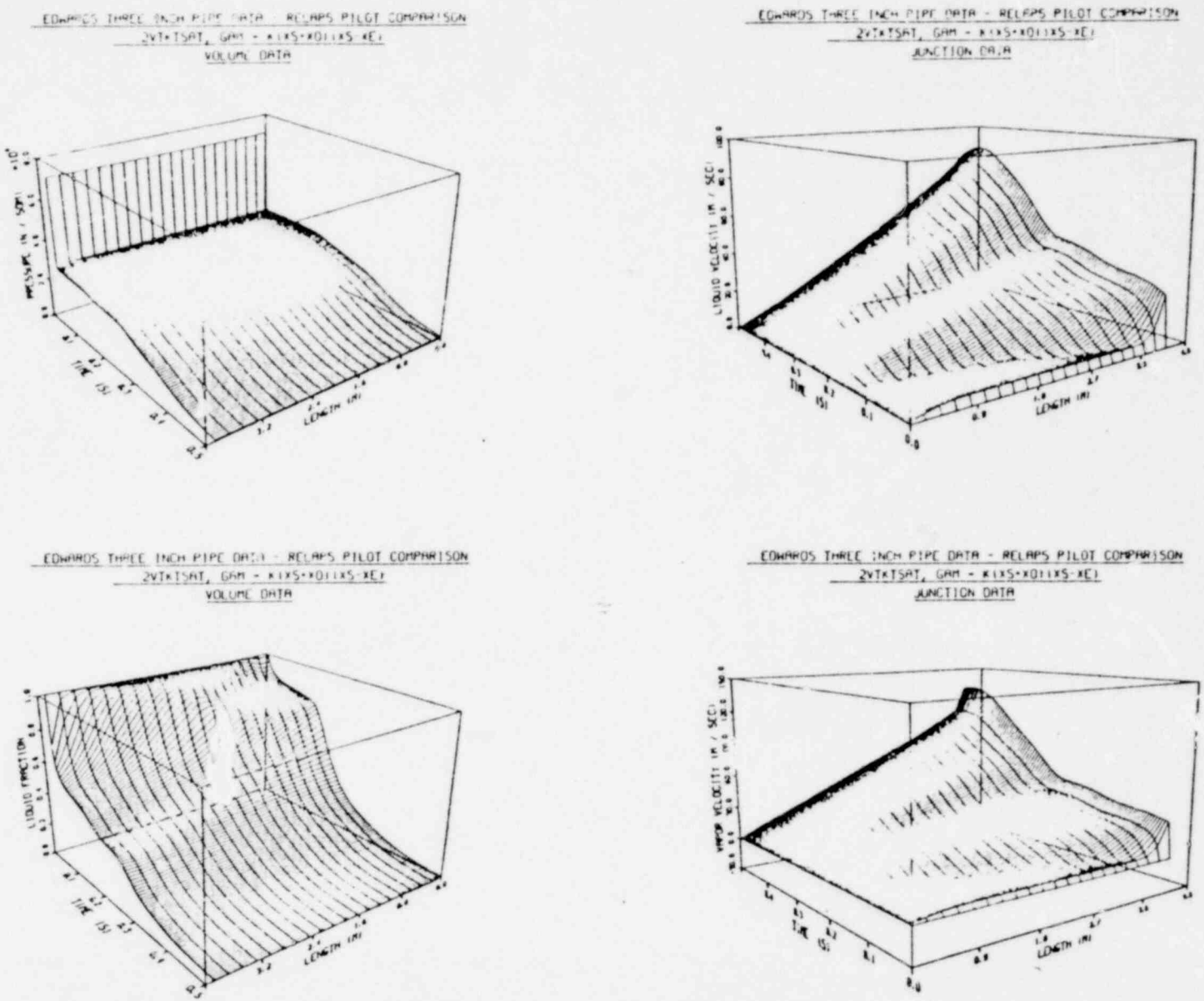

Figure 7. Isometric Plots of RELAP5 PILOT Long-Term Calculations for 73 mm Pipe

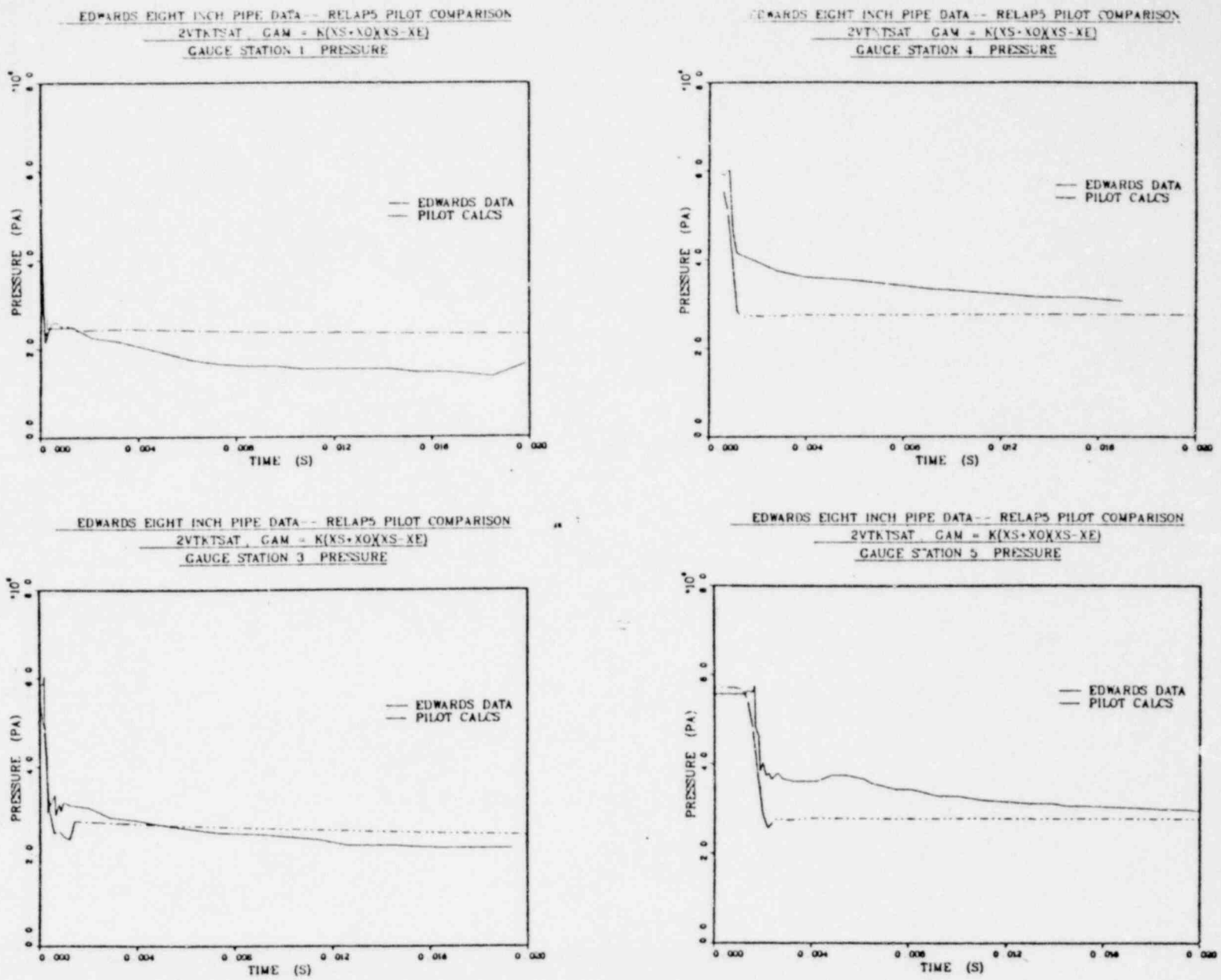

Figure 8. Comparison of RELAP5 PILOT Results to Edwards 206 mm Short-Term Pressure Data for Gauge Stations 1, 3, 4 and 5

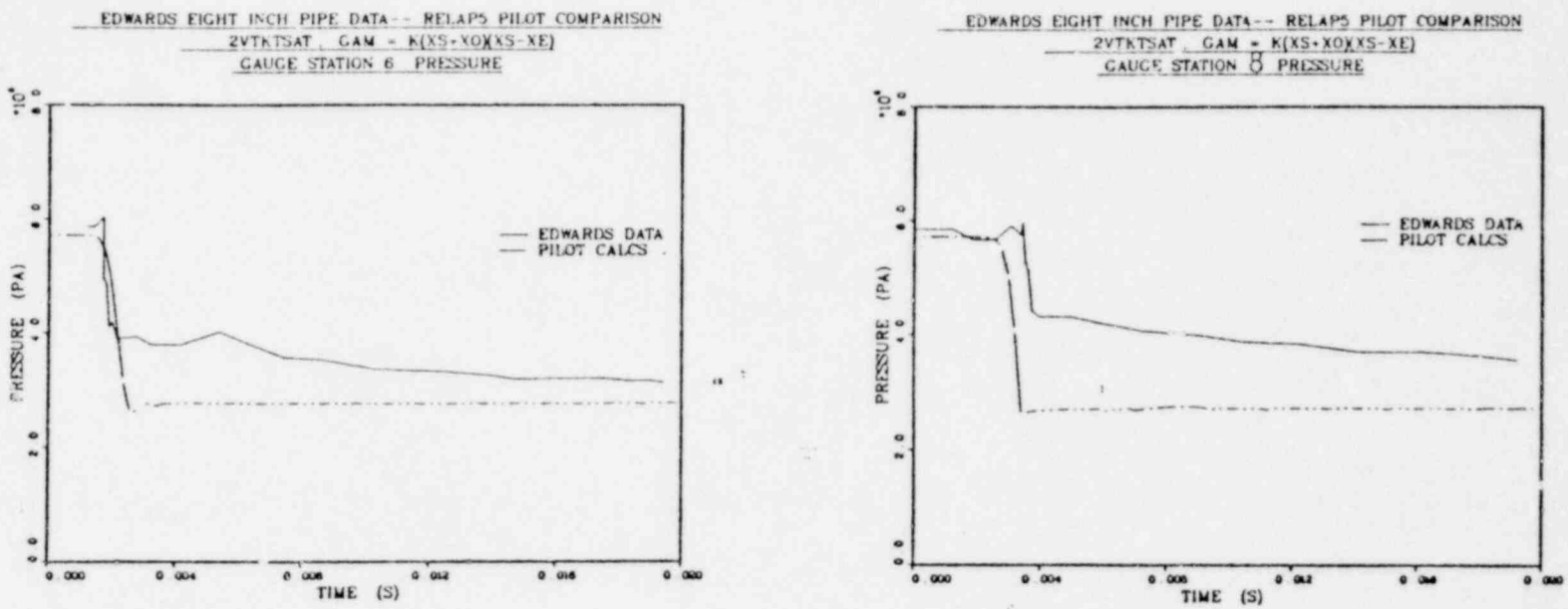

Figure 9. Comparison of RELAP5 PILOT Results to Edwards 206 mm Short-Term Pressure Data for Gauge Stations 6 and 8

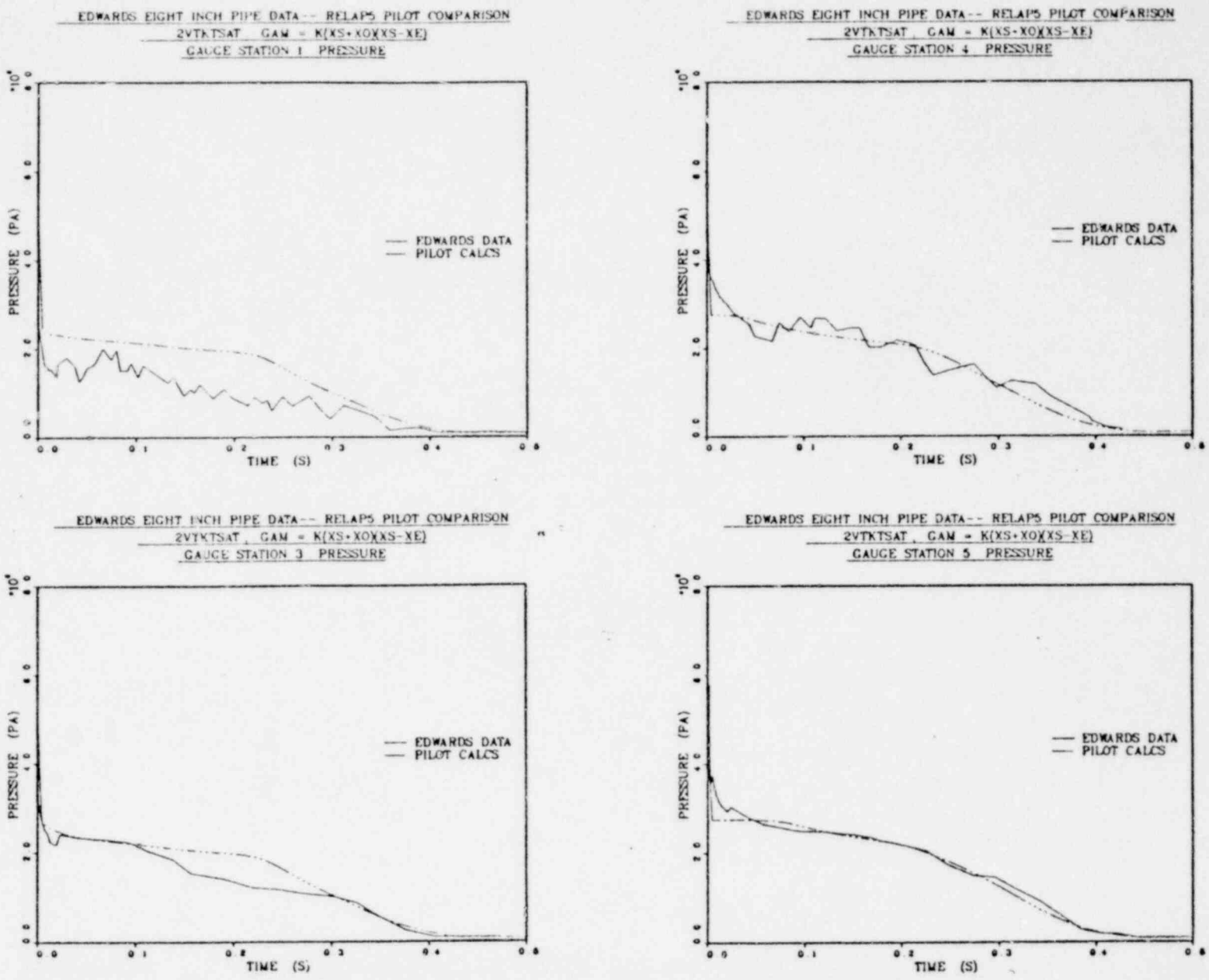

Figure 10. Comparison of RELAP5 PILOT Results to Edwards 206 mm Long-Term Pressure

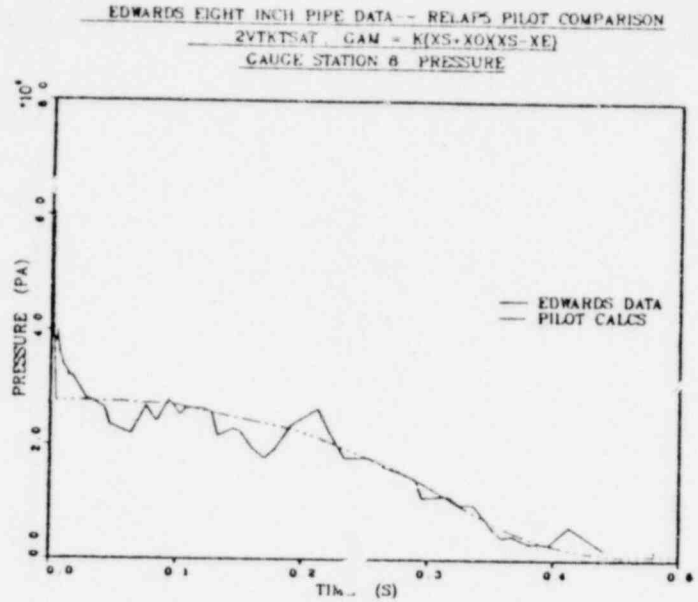

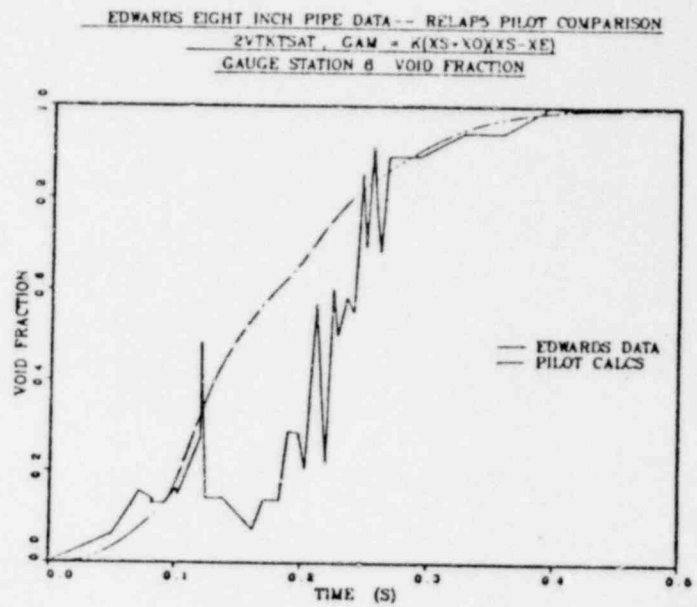

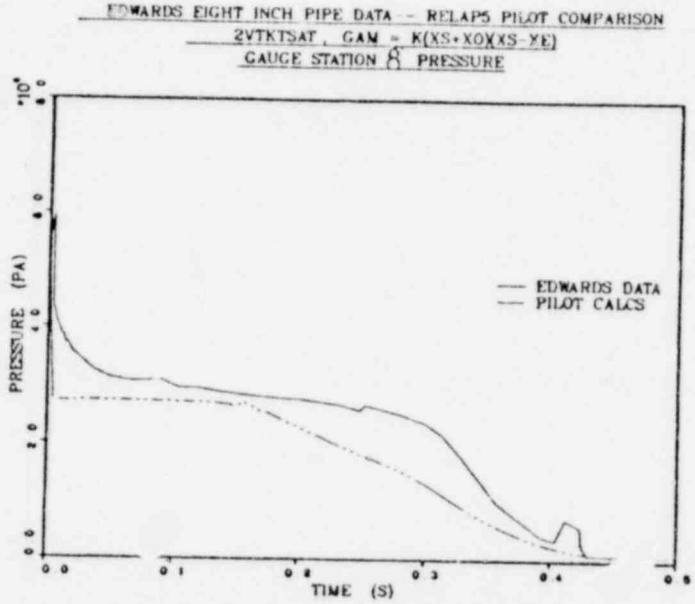

Figure 11. Comparison of RELAP5 PILOT Results to Edwards 206 mm Long-Term Pressure and Void Fraction Data at Gauge Stations 6 and 8

APPENDIX D

RELAP5 ABRUPT AREA CHANGES AND FLOW BRANCHING

REPORT NUMBER PG-R-77-42

DATE November 1977

CODE DEVELOPMENT-VERIFICATION-APPLICATION

REACTOR BEHAVIOR PROGRAM

SYSTEMS ANALYSIS-DATA ANALYSIS

RELAP5 HYDRODYNAMIC MODEL PROGRESS SUMMARY - ABRUPT AREA CHANGES AND PARALLEL BRANCHING

J. A. Trapp

V. H. Ransom

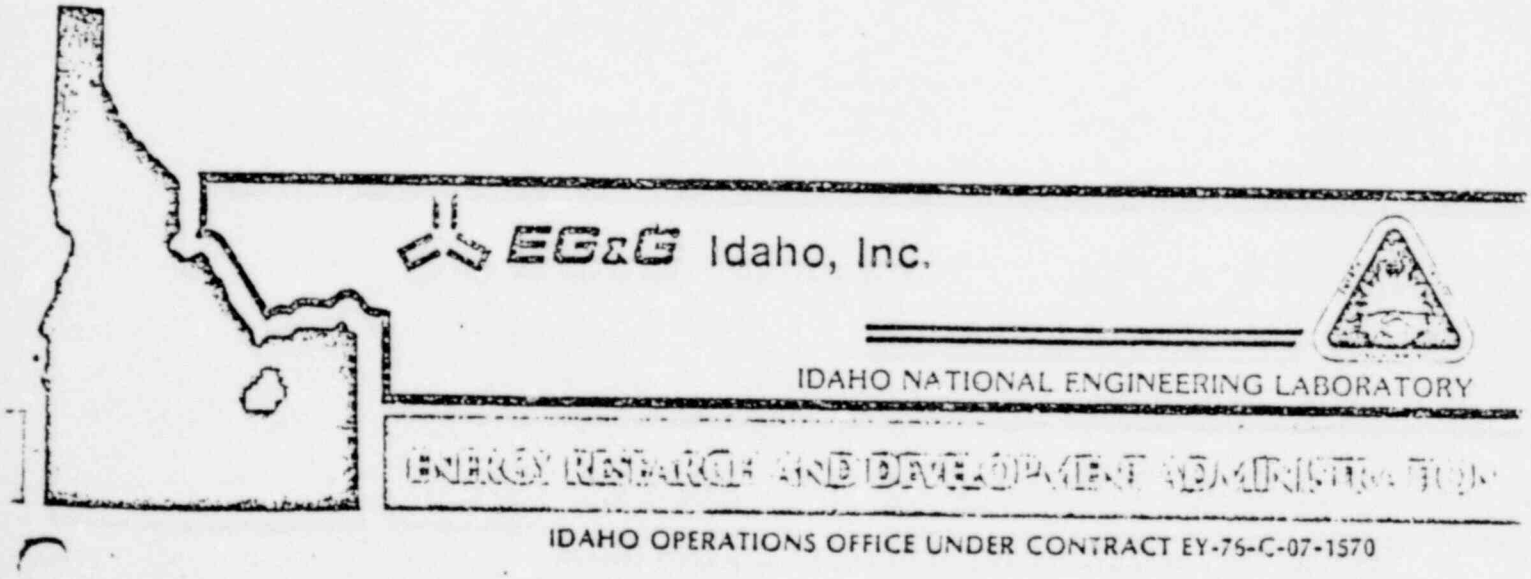

IDAHO OPERATIONS OFFICE UNDER CONTRACT EY-76-C-07-1570

ABSTRACT

As a part of the RELAP5 advanced two-phase hydrodynamic model development project, models have been developed for abrupt flow area change and flow branching. The area change models are based on accepted principles for single phase flow and are similar to two-phase models available in the literature, but with a significant improvement for establishing the void fraction change at the area change. With this improvement, a numerically simple and realistic model has been tested and found to produce qualitatively correct results.

A parallel branching model has been developed and subjected to limited testing. For the cases investigated, the model has produced correct results.

TABLE OF CONTENTS

LIST OF FIGURES

NOMENCLATURE

A	=	Area
α	=	Void fraction
ΔP_f	=	Dynamic pressure loss
ΔX	=	Length of hydrodynamic control volume
Δt	=	Time increment in finite difference equations
ϵ	=	Area ratio, A_2/A_1
ϵ_T	=	Area ratio, A_T/A_1
ϵ_c	=	Area ratio, A_c/A_T
Γ	=	Phase mass generation rate
FWL	=	Liquid phase wall friction coefficient
FWG	=	Vapor phase wall friction coefficient
FI	=	Interphase drag coefficient
g_Z	=	Acceleration due to gravity
h_L	=	Dynamic head loss
J	=	Multiple junction
L	=	Equivalent length for interphase drag
P	=	Pressure
ρ	=	Density
t	=	Time
v	=	Velocity
X	=	Length coordinate
Z	=	Elevation change coordinate

Subscripts

1 = Upstream station, or multiple junction index

2 = Downstream station, or multiple junction index

ℓ = Liquid phase

g = Vapor phase

c = Vena Contracta

T = Point of minimum area

j = Junction station

K = Center of upstream control volume

L = Center of downstream control volume

Superscripts

n = Time level in difference scheme

$\sim$ = Unit momentum for mass exchange

I. INTRODUCTION

The RELAP5 project is an effort to develop a transient one-dimensional two-phase hydrodynamic model for use in water reactor system analysis. A primary objective is to produce a fast running code having contemporary hydrodynamics which can be used for system safety analysis of nuclear power reactors. At the present time a two-velocity limited nonequilibrium fluid model ($2VT_K\ T_{SAT}$) has been developed and tested in a PILOT code. The model has been used to simulate pipe blowdown experiments and good agreement with data was obtained.

The general reactor system contains piping networks which consist of sudden area changes, orifices and flow branches. In order to apply the RELAP5 hydrodynamic model to such systems, analytical models for these components have been developed. This report documents the analytical formulation of these models. Included are a development of the two-phase one-dimensional transient flow equations for sudden enlargements, sudden contractions, an orifice, and parallel branching with area change. The basic hydrodynamic model is formulated for the case of slowly varying (continuous) flow area variations, therefore special models are not required for this case (the $2VT_K\ T_{SAT}$ hydrodynamic model is being documented separately).

The abrupt area change model developed herein is based on the Bourda-Carnot[1] formulation for a sudden enlargement and standard pipe flow relations, including vena-contracta effect, for a sudden contraction and/or an orifice. Quasi-steady continuity and momentum balances are employed at points of abrupt area change. The numerical implementation of these balances is such

that the hydrodynamic losses are independent of the upstream and the downstream nodalization. In effect, the quasi-steady balances are employed as jump conditions which couple fluid components having abrupt change in cross sectional area. This coupling process is achieved without change to the basic linear semi-implicit numerical time advancement scheme. Thus the fast execution time objective is not impeded by incorporation of these models.

The area changes and parallel branching numerical models have been installed and tested in the RELAP5 PILOT code and have produced correct results for single phase flows and two-phase flows with slip. The parallel branching model has been tested on a symmetrical system blowdown problem and correct results were obtained.

Future efforts will include testing the area change and parallel branching models on system type network problems for which experimental data are available (i.e. Semiscale Isothermal Blowdown Experiments).

1317 027

II. ABRUPT AREA CHANGE MODELING ASSUMPTIONS

The general assumptions which are used for transient calculation of two-phase flow in flow passages having points of abrupt area change are as follows: 1) the transient flow process can be approximated as a quasi-steady flow process that is instantaneously satisfied by the upstream and downstream conditions, 2) transient inertia, mass and energy storage at abrupt area change are neglected, however all upstream and downstream flow volumes are treated as a fully transient flow, 3) interphase mass and energy transfer are neglected in the area change flow process.

The bases for the above assumptions are several fold. A primary consideration is that the loss correlations which are available are based on data taken during steady flow processes, however transient investigations which are underway[2] have verified the adequacy of the quasi-steady assumption. The volume of fluid and associated mass, energy and inertia at points of abrupt area change is generally small compared to the volume of the upstream and downstream fluid components. The transient mass, energy and inertia effects are approximated by lumping them into the up and downstream flow volumes. Finally, the quasi-steady approach is consistent with the modeling of other important phenomena in transient codes, i.e. heat transfer, pumps, valves, and break flow.

III. REVIEW OF SINGLE PHASE ABRUPT AREA CHANGE MODELS

1. General

The modeling techniques which are used for dynamic pressure losses associated with abrupt area change in a single phase flow will be reviewed briefly before discussing the extension of these methods to two-phase flows. In a steady incompressible flow losses at area change are modeled by the inclusion of an appropriate dynamic head loss term, h_L, in the one dimensional modified Bernoulli equation.

$$(v^2/2 + P/\rho)_1 = (v^2/2 + P/\rho)_2 + h_L \qquad (1)$$

The particular form of the dynamic head loss is obtained by employing the Bourda-Carnot[1] assumption for calculating the loss associated with the expansion part of the flow process at points of abrupt area change.

2. Expansion

Consider a steady and incompressible flow undergoing a sudden increase in cross-sectional area (expansion) as shown in Figure 1. Here the flow is

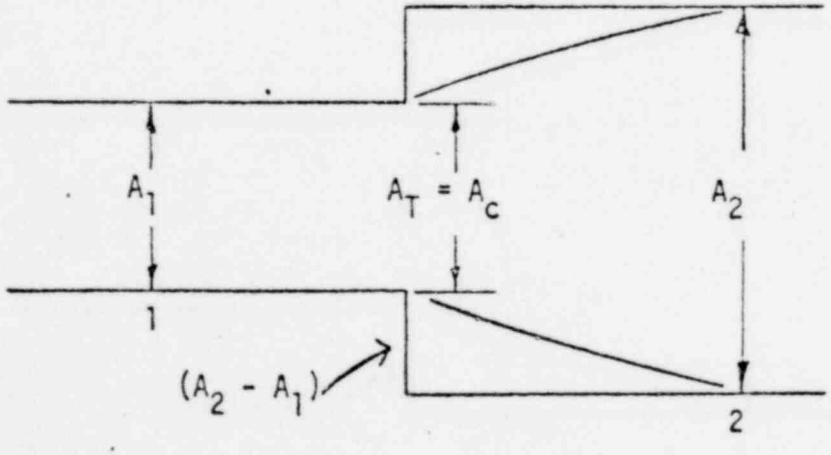

Figure 1. Abrupt Expansion

assumed to be from left to right with the upstream conditions denoted by the subscript 1 and the downstream condition by 2. Here the upstream and downstream conditions are assumed to be far enough removed from the point of area change that flow is one-dimensional, i.e. none of the two dimensional effects of the abrupt area change exist. These locations can range from several diameters upstream to as many as 30 diameters downstream. However, for purposes of modeling the overall dynamic pressure loss the entire process is assumed to occur as a discontinuous jump in flow condition at the point of abrupt area change. In this context, the stations 1 and 2 refer to locations immediately upstream and downstream of the abrupt area change.

The dynamic head loss for the abrupt expansion shown in Figure 1 can be obtained using the Bourda-Carnot[1] assumption, i.e. the pressure acting on the "washer shaped" area, $A_2 - A_1$, is the upstream pressure, P_1. When this assumption is employed in an overall momentum balance the head loss is

$$h_L = 1/2 \left(1 - \frac{A_1}{A_2}\right)^2 v_1^2 \qquad (2)$$

where $\varepsilon = A_2/A_1$ is the expansion area ratio. The loss is dynamic pressure associated with the area change is related to the head loss by

$$\Delta P_f = \rho h_L = 1/2 \cdot \rho \left(1 - \frac{1}{\varepsilon}\right)^2 v_1^2 \qquad (3)$$

3. Contraction

The flow process at a point of abrupt reduction in flow area (contraction) is idealized in much the same manner as for the expansion, except that an

additional process must be considered. The flow co. .es to contract beyond the point of abrupt area reduction and forms a vena contracta, see Figure 2. The point of vena contracta is designated by c. The far upstream and downstream conditions are designated by 1 and 2, respectively.

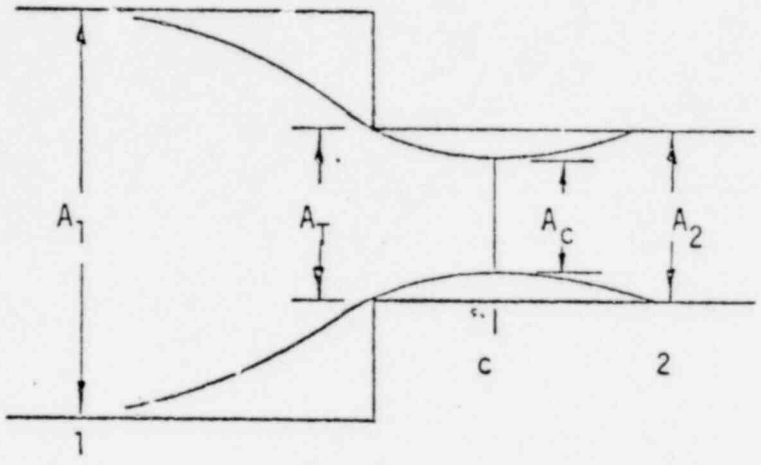

Figure 2. Abrupt Contraction

Consider a sudden contraction in a steady incompressible flow. The loss in dynamic pressure from the upstream station to the vena contracta is usually neglected (measurements indicated that the contracting flow experiences a loss no larger than $\Delta P_f \approx .05\ 1/2\rho\ v_c^2$,[1] where v_c is the velocity at the vena contracta). The dynamic pressure loss associated with the expansion from the area at vena contracta to the downstream area is modeled using the Bourda-Carnot assumption and is given by Equation (2) with the condition at vena contracta as the upstream condition, that is

$$\Delta P_f = 1/2\ \rho\ (1 - A_c/A_2)^2\ v_c^2 \quad , \tag{4}$$

where from continuity considerations

$$v_c = \frac{A_2 v_2}{A_c} \tag{5}$$

The contraction ratio A_c/A_2, is an empirical function of A_2/A_1 ranging between 0.617 and ~~0.000~~ 1.000 for values of A_2/A_1 ranging between 0 and 1.0 respectively (see Appendix A). Combining Equations (4) and (5) leads to

$$\Delta P_f = 1/2\ \rho\ (1 - \frac{A_2}{A_c})^2\ v_2^2 \quad , \tag{6}$$

as the dynamic pressure loss for a contraction[1].

4. Abrupt Area Change with an Orifice

The most general case of abrupt area change is a contraction with an orifice at the point of contraction. Such a configuration is illustrated in Figure 3. In this case an additional flow area, the orifice throat area,

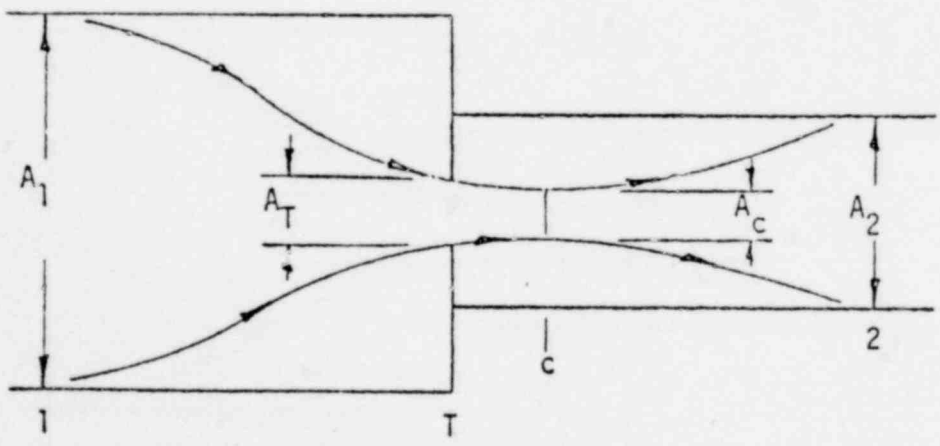

Figure 3. Orifice at Abrupt Area Change

1317 025

must be specified. Conditions at the orifice throat station will be designated by a subscript T. At this point it is convenient to define three area ratios which will be used throughout this development. The first is the contraction area ratio at vena contracta relative to the minimum physical area, $\varepsilon_c = A_c/A_T$, the second is the ratio of the minimum physical area to the upstream flow area, $\varepsilon_T = A_T/A_1$, and the third is the ratio of the downstream to upstream flow area, $\varepsilon = A_2/A_1$.

The dynamic pressure loss for an abrupt area contraction combined with an orifice is analyzed in a manner parallel to that for the simple contraction. The area A_T is the throat or minimum physical area. The loss associated with the contracting fluid stream from station 1 to c, the point of vena contracta, is neglected whereas the dynamic pressure loss associated with the expansion from the vena contracta to the downstream section is given by

$$\Delta P_f = 1/2\ \rho\ (1 - A_c/A_2)^2\ v_c^2 \quad , \qquad (7)$$

where $\varepsilon_c = A_c/A_T$ is the same empirical function of $\varepsilon_T = A_T/A_1$ as given in Appendix A. Using the continuity equations, $v_c = \frac{A_T v_T}{A_c} = v_T/\varepsilon_c$, and $v_T = \frac{A_2 v_2}{A_T} = \frac{\varepsilon}{\varepsilon_T}\ v_2$, Equation (7) can be written as

$$\Delta P_f = 1/2\ \rho\ (1 - \frac{\varepsilon}{\varepsilon_c \varepsilon_T})^2\ v_2^2 \qquad (8)$$

Equation (8) is a generalization applicable to all the cases previously treated. For a pure expansion $\varepsilon_T = 1$ and $\varepsilon_c = 1$, and $\varepsilon > 1$; for a con-

traction $\epsilon_T = \epsilon < 1$ and $\epsilon_c < 1$; hence each of these is a special case of Equation (3). The two-phase dynamic pressure loss model is based upon an adaptation of the general single-phase head loss given by Equation (8).

IV. TWO-PHASE ABRUPT AREA CHANGE MODEL

1. General

The two-phase flow through abrupt area change is modeled in a manner very similar to that for single phase flow by defining phasic flow areas. The two phases are coupled through the interphase drag, pressure gradient and the requirement that the phases coexist in the flow passage.

The one-dimensional phasic stream-tube momentum equations[3] are:

$$\alpha_\ell \rho_\ell \frac{\partial v_\ell}{\partial t} + \alpha_\ell \rho_\ell \frac{\partial(\frac{1}{2} v_\ell^2)}{\partial x} + \alpha_\ell \frac{\partial P}{\partial x} = \alpha_\ell \rho_\ell g_z + FWL\, v_\ell - FI\,(v_\ell - v_g) + \Gamma_\ell\,(\tilde{v}_\ell - v_\ell) \tag{9}$$

and

$$\alpha_g \rho_g \frac{\partial v_g}{\partial t} + \alpha_g \rho_g \frac{\partial(\frac{1}{2} v_g^2)}{\partial x} + \alpha_g \frac{\partial P}{\partial x} = \alpha_g \rho_g g_z + FWG\, v_g - FI\,(v_g - v_\ell) + \Gamma_g\,(\tilde{v}_g - v_g) \tag{10}$$

The flow at points of abrupt area change is assumed to be quasi-steady and incompressible. In addition the terms in the momentum equation due to body force, wall friction and mass transfer are assumed to be small in the region affected by area change (the effect of these terms is not neglected since the full transient equations are solved on both sides of the point of abrupt area change). The interphase drag terms are retained since the gradient in relative velocity can be large at points of abrupt area change.

Equations (9) and (10) can be integrated approximately for a steady incompressible smoothly varying flow to obtain modified Bernoulli type equations;

$$(1/2\ \rho_\ell v_\ell^2 + P)_1 = (1/2\ \rho_\ell v_\ell^2 + P)_2 + \left(\frac{FI}{\alpha_\ell}\right)_1 (v_{\ell 1} - v_{g1})\ L_1 + \left(\frac{FI}{\alpha_\ell}\right)_2 (v_{\ell 2} - v_{g2})\ L_2 \qquad (11)$$

and

$$(1/2\ \rho_g v_g^2 + P)_1 = (1/2\ \rho_g v_g^2 + P)_2 + \left(\frac{FI}{\alpha_g}\right)_1 (v_{g1} - v_{\ell 1})\ L_1 + \left(\frac{FI}{\alpha_g}\right)_2 (v_{g2} - v_{\ell 2})\ L_2 \qquad (12)$$

The interphase drag is divided into two parts, associated with the upstream and downstream parts of the flow affected by the area change.

2. General Model

Now consider the application of Equations (11) and (12) to the flow of a two-phase fluid through a passage having a generalized abrupt area change, in particular consider the flow passage illustrated in Figure 4.* Here the area A_T is the throat or minimum area associated with an orifice located at the point of abrupt area change. Since each phase is governed by a modified Bernoulli type equation it seems reasonable to assume that the losses associated with changes in the phasic flow area can be modeled by separate dynamic pressure loss terms for each of the liquid and gas phases. Hence we assume that the

*In Figure 4 the flow is shown as a separated flow for clarity. The models developed are equally applicable to separated and dispersed flow regimes.

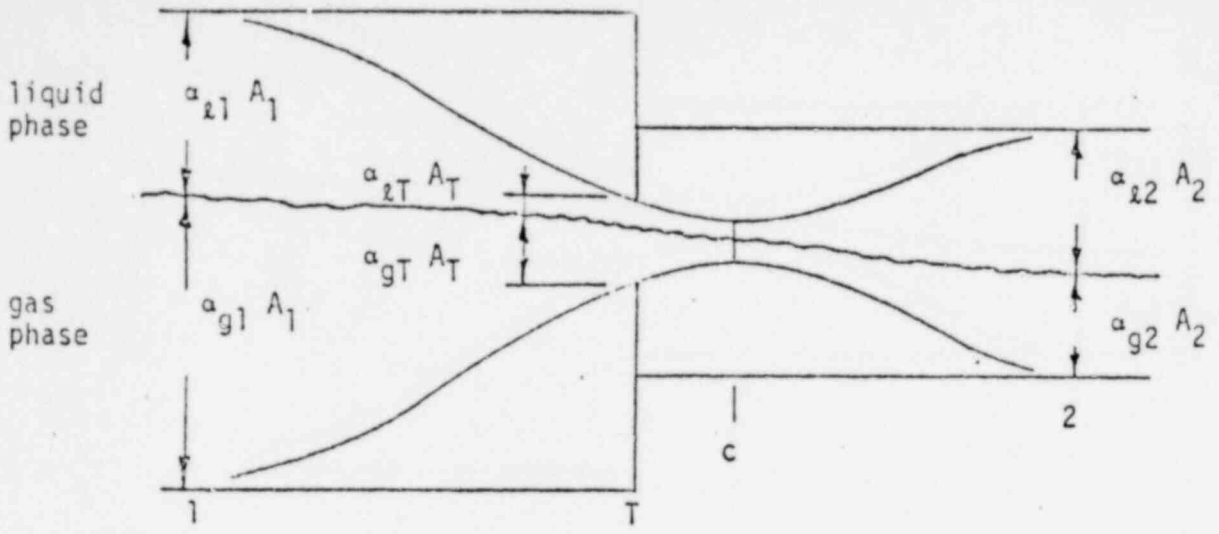

Figure 4. Schematic Flow of Two-Phase Mixture at Abrupt Area Change

liquid sustains a loss as if it alone (except for interphase drag) were experiencing an area change from $\alpha_{\ell 1} A_1$ to $\alpha_{\ell T} A_T$ to $\alpha_{\ell 2} A_2$ and the gas phase experiences a loss as if it alone were flowing through an area change from $\alpha_{g1} A_1$ to $\alpha_{gT} A_T$ to $\alpha_{g2} A_2$. (In particular, note that the area changes for each phase are the phasic area changes, see Figure 4.) When the losses for these respective area changes, based upon the Bourda-Carnot model and given by Equation (8), are added to Equations (11) and (12) we obtain

$$(1/2\ \rho_\ell v_\ell^2 + P)_1 = (1/2\ \rho_\ell v_\ell^2 + P)_2 + 1/2\ \rho_\ell \left(1 - \frac{\alpha_{\ell 2}\ \epsilon}{\alpha_{\ell T}\ \epsilon_{\ell c}\ \epsilon_T}\right)^2 (v_{\ell 2})^2$$

$$+ \left(\frac{FI}{\alpha_\ell}\right)_1 (v_{\ell 1} - v_{g1})\ L_1 + \left(\frac{FI}{\alpha_\ell}\right)_2 (v_{\ell 2} - v_{g2})\ L_2 \qquad (13)$$

and

$$(1/2\ \rho_g\ v_g^2 + p)_1 = (1/2\ \rho_g v_g^2 + P)_2 + 1/2\ \rho_g\left(1 - \frac{\alpha_{g2}\,\varepsilon}{\alpha_{gT}\,\varepsilon_{gc}\,\varepsilon_T}\right)^2 (v_{g2})^2$$

$$+ \left(\frac{FI}{\alpha_g}\right)_1 (v_{g1}-v_{\ell 1})\ L_1 + \left(\frac{FI}{\alpha_g}\right)_2 (v_{g2} - v_{\ell 2})\ L_2 \qquad (14)$$

as phasic momentum equations to be used across an abrupt area change. In Equations (13) and (14) $\varepsilon_{\ell c}$ and ε_{gc} are the same tabular function of area ratio as in the single-phase case except that the area ratios used are the phasic area ratios,

$$\varepsilon_{\ell T} = (\alpha_{\ell T}/\alpha_{\ell 1})\ \varepsilon_T \qquad (15)$$

and

$$\varepsilon_{gT} = (\alpha_{gT}/\alpha_{g1})\ \varepsilon_T \qquad (16)$$

respectively. The area ratios $\varepsilon = A_2/A_1$ and $\varepsilon_T = A_T/A_1$ are the same as for single phase flow. The interphase drag effects in Equations (13) and (14) are important. These terms govern the amount of slip induced by an abrupt area change and if they are omitted the model would always predict a slip at the area change appropriate to completely separated flow situation and hence give erroneous results for dispersed flow.

3. Model Application

A few remarks concerning the way in which Equations (13) and (14) are applied to expansions and contractions both with and without an orifice are necessary. In a single-phase steady flow situation if one is given the up-

stream conditions v_1 and P_1 then by use of the continuity equation ($v_1A_1 = v_2A_2$) and Equation (1) we can solve for v_2 and P_2. Equations (13) and (14) along with the two phasic continuity equations can be used in a similar manner except now the downstream void fraction is an additional unknown which must be determined.

3.1 Expansion

For the purpose of explanation, consider the case of an expansion ($\alpha_{\ell T} = \alpha_{\ell 1}$, $\varepsilon > 0$, $\varepsilon_T = 1$, $\varepsilon_{\ell c} = \varepsilon_{gc} = 1$, $FI_1 = 0$) for which Equations (13) and (14) reduce to

$$(1/2\ \rho_\ell v_\ell^2 + P)_1 = (1/2\ \rho_\ell v_\ell^2 + P)_2 + 1/2\ \rho_\ell \left(1 - \frac{\alpha_{\ell 2}\varepsilon}{\alpha_{\ell 1}}\right)^2 (v_{\ell 2})^2 + \left(\frac{FI}{\alpha_\ell}\right)_2 (v_{\ell 2} - v_{g2})\ L_2 \qquad (17)$$

and

$$(1/2\ \rho_g v_g^2 + P)_1 = (1/2\ \rho_g v_g^2 + P)_2 + 1/2\ \rho_g \left(1 - \frac{\alpha_{g2}\varepsilon}{\alpha_{g1}}\right)^2 (v_{g2})^2 + \left(\frac{FI}{\alpha_g}\right)_2 (v_{g2} - v_{\ell 2})\ L_2 \ . \qquad (18)$$

These two equations along with the continuity equations (incompressible)

$$\alpha_{\ell 1}\ v_{\ell 1}\ A_1 = \alpha_{\ell 2}\ v_{\ell 2}\ A_2 \ , \qquad (19)$$

and

$$\alpha_{g1}\ v_{g1}\ A_1 = \alpha_{g2}\ v_{g2}\ A_2 \qquad (20)$$

are a system of four equations having four unknowns $\alpha_{\ell 2}$ ($\alpha_{g2} = 1-\alpha_{\ell 2}$), $v_{\ell 2}$, v_{g2}, and P_2 in terms of the upstream conditions $\alpha_{\ell 1}$ ($\alpha_{g1} = 1-\alpha_{\ell 1}$), $v_{\ell 1}$, v_{g1} and P_1. It is important to note that the downstream value for the liquid fraction ($\alpha_{\ell 2}$) is an additional unknown compared to the single-phase case and is determined (along with the downstream velocities and pressure) by similtaneous solution of the four equations, Equations (17), (18), (19) and (20) without additional assumptions. It is reassuring that by taking a proper linear combination of Equations (17) and (18) the usual overall momentum balance obtained using the Borda-Carnot[1] assumption can be obtained.[4,5,6,7] The resulting expression is (see Appendix B for development)

$$\alpha_{\ell 1}\rho_{\ell 1}v_{\ell 1}^2 A_1 + \alpha_{g1}\rho_{g1}v_{g1}^2 A_1 + A_2 P_1 = \alpha_{\ell 2}\rho_{\ell 2}v_{\ell 2}^2 A_2$$

$$+ \alpha_{g2}\rho_{g2}v_{g2}^2 A_2 + A_2 P_2 \quad . \qquad (21)$$

If, as is the case in the cited literature,[4,5,6,7] only the overall momentum balance is used at an expansion there will be an insufficient number of equations to determine all the downstream flow parameters $\alpha_{\ell 2}$, $v_{\ell 2}$, v_{g2}, and P_2. The indeterminacy has been overcome in the cited work by means of several different assumptions concerning the downstream void fraction.* In the model developed herein, Equations (13) and (14), the division of the overall loss into liquid and gas parts respectively results in sufficient conditions to determine all the downstream flow variables including $\alpha_{\ell 2}$. In addition, the

---

*J. G. Collier[4] mentions three different assumptions that have been used: i) α = $\alpha_{\ell 1}$, (ii) $\alpha_{\ell 2}$ is given by a homogeneous model, and iii) $\alpha_{\ell 2}$ is given by the Hughmark void fraction correlation.

present model includes the force terms due to interphase drag in Equations (13) and (14), which are necessary in order to predict the proper amount of slip and void redistribution that occurs at points of abrupt area change. An example illustrating this particular effect will be given later.

3.2 Contraction

Next consider the application of Equation (13) and (14) to a contraction. An additional consideration needs to be made in this case in order to determine both the downstream conditions and the throat conditions from the upstream values of $\alpha_{\ell 1}$ (α_{g1}), $v_{\ell 1}$, v_{g1}, and P_1. To obtain the throat values we apply the momentum equations valid for the contracting section of flow (here the L_1 portion of the interphase force is associated with the contraction):

$$(1/2\ \rho_\ell v_\ell^2 + P)_1 = (1/2\ \rho_\ell v_\ell^2 + P)_T + FI_1(v_{\ell 1}-v_{g1})\ L_1 \qquad (22)$$

$$(1/2\ \rho_g v_g^2 + P)_1 = (1/2\ \rho_g v_g^2 + P)_T + FI_1(v_{g1}-v_{\ell 1})\ L_1 \qquad (23)$$

$$\alpha_{\ell 1}\ v_{\ell 1}\ A_1 = \alpha_{\ell T}\ v_{\ell T}\ A_T \ , \qquad (24)$$

$$\alpha_{g1}\ v_{g1}\ A_1 = \alpha_{gT}\ v_{gT}\ A_T \ . \qquad (25)$$

These four equations are solved simultaneously for the values of $\alpha_{\ell T}(\alpha_{gT})$ $v_{\ell T}$, v_{gT}, P_T at the throat section (minimum physical area). No additional or special assumptions are made concerning the throat conditions since they follow as a direct consequence of the unique head loss models for each phase.

After the throat values have been obtained, the conditions at the point of vena contracta are established assuming the void fraction is the same as at the throat. Thus $\epsilon_{\ell c}$ and ϵ_{gc} are established using the tabular function from Appendix A and the throat area ratios $\epsilon_{\ell T}$ and ϵ_{gT} defined by Equations (15) and (16). Equations (13) and (14) can be applied directly from station 1 to 2 or the expansion loss equations can be used from the throat section to station 2. Both approaches produce identical downstream solutions. As in the case of an expansion, because the proper upstream and downstream interphase drag is included, this modeling approach establishes the phase slip and resulting void redistribution. An orifice at an abrupt area change is treated exactly as the contraction explained above, i.e. with two separate calculations to establish first the throat and then the downstream flow variables.

4. Countercurrent Flow

In the preceeding development it has been implicitly assumed that the flow is cocurrent. The changes necessary to model countercurrent flow are described below. These changes have not been tested numerically yet. Equations (13) and (14) are applied exactly as is the case of cocurrent flow except that the upstream sections (section 1) for the respective phases are located on different sides of the abrupt area change. The difference appears in the manner in which the throat and downstream voids are determined. To determine the throat properties equations similar to Equations (22), (23), (24), (25) are used with the upstream values appropriate for each phase. These four equations are then solved for $\alpha_{\ell T}$ (α_{gT}), $v_{\ell T}$, v_{gT}, P_T. After these throat values are known, a straight forward application of the appropriate steady-

state momentum and mass equation for each phase gives the downstream properties for each phase (remembering that the downstream sections are on opposite sides of the abrupt area change in countercurrent flow).

V. TRANSIENT TWO-PHASE NUMERICAL MODEL FOR ABRUPT AREA CHANGE

The basic finite difference scheme used for the RELAP5 $2VT_K\ T_{SAT}$ transient model is partially described in References [3] and [8]. A complete description is being prepared. The scheme is based on staggered spatial control volumes. The relationship between the cell centered control volume for mass and energy and the junction centered control volume for momentum is illustrated in Figure 5. The scalar quantities are located at cell centers (K and L) and velocities are located at cell boundaries (j-1, j and j+1), see Figure 5.

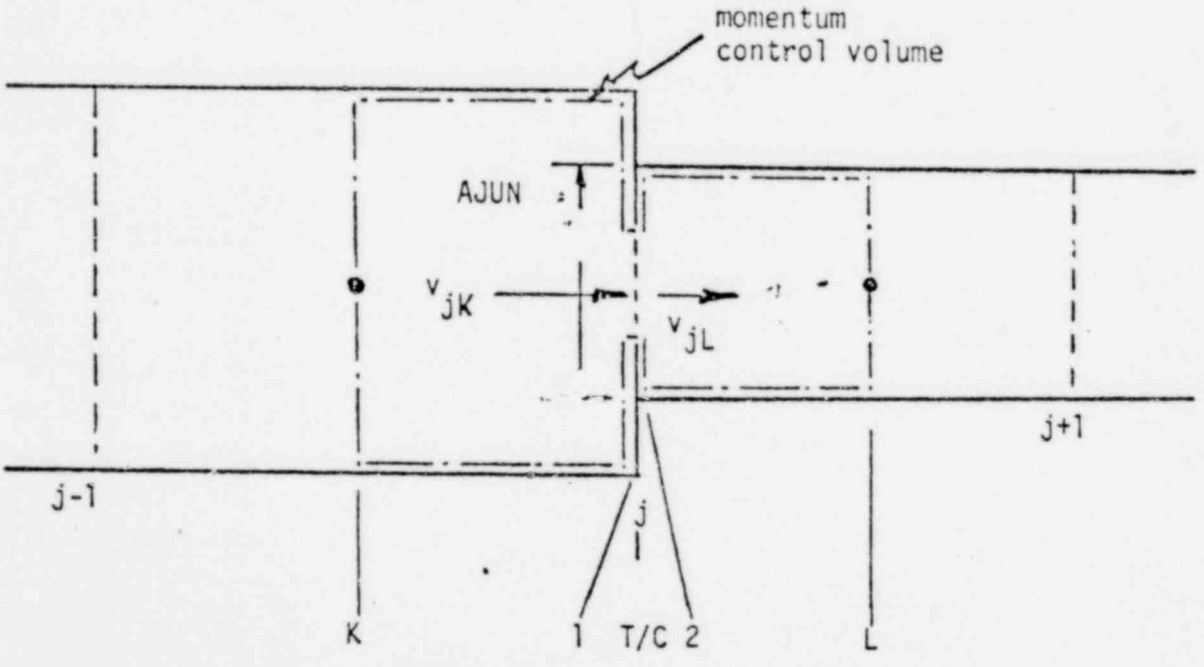

Figure 5. Cell Configuration Used in Numerical Scheme at Area Change

For the purpose of developing the numerical scheme it is convenient to define two additional stations, K and L, see Figure 5. The other

stations: 1, upstream; 2, downstream; T, throat or minimum area; and c, vena contracta have been previously defined in the development of the abrupt area change model. The additional stations, K and L, designate the upstream and downstream momentum control volume halves respectively, while the stations immediately upstream of the junction and station 2 is immediately downstream, see Figure 5. Recall that the flow process associated with abrupt area change is modeled as a quasi-steady process occurring at a point (upstream and downstream lengths occur as parameters at a junction for the purpose of defining the effect of interphase drag, however these lengths do not correspond to physical lengths in the transient numerical model). Thus the numerical model for momentum calculation at a point of abrupt area change consists of three parts. The normal momentum effects for a constant area passage corresponding to the K half cell, a quasi-steady model of the flow process at the abrupt area change, and the normal momentum effects for the L half cell. The momentum control volume associated with this process is illustrated in Figure 5.

In general, at a junction j, two velocities are defined, one for each phase. When an abrupt area change occurs at a junction j three velocities need to be defined for each phase: (i) $(v_\ell)_{j1}$ representing the liquid velocity immediately upstream of the abrupt area changes, (ii) $(v_\ell)_{j2}$ representing the liquid velocity downstream of the area change and (iii) $(v_\ell)_j$, a reference junction velocity which is calculated in the transient solution and will be defined later. Three corresponding velocities are defined for the gas phase. The jump conditions, represented by Equations (13) and (14), are applied at junction j across an element of zero length.

1. Phasic Momentum Equation

The basic approach to obtain the momentum equations at an abrupt area change junction is to sum up three separate contributions: (i) the momentum equations for the K half cell upstream from the area change, (ii) the momentum jump conditions defined by Equations (13) and (14), and (iii) the momentum equations for the L half cell. The wall drag, gravity and inertia terms are included in the K and L half cell momentum expressions. In these expressions the friction drag and inertia terms are functions of $(v_\ell)_{jK}$ and $(v_\ell)_{jL}$ for the liquid phase, and $(v_g)_{jK}$ and $(v_g)_{jL}$ for the vapor phase in the K and L half cells respectively. When these three contributions are added we obtain for the liquid momentum equation at junction j:

$$1/2(\alpha_\ell\rho_\ell)_j^n \left[\Delta X_K \left(\frac{(v_\ell)_{j1}^{n+1} - (v_\ell)_{j1}^n}{\Delta t}\right) + \Delta X_L \left(\frac{(v_\ell)_{j2}^{n+1} - (v_\ell)_{j2}^n}{\Delta t}\right)\right]$$

$$+ 1/2\,(\alpha_\ell\rho_\ell)_j^n \left[(v_\ell^n)^2_L - (v_\ell^n)^2_K\right] + \text{Viscous Damping}$$

$$= -(\alpha_\ell)_j^n \left(P_L^{n+1} - P_K^{n+1}\right) + (\alpha_\ell)_j^n \left(\Delta P_f\right)_\ell^{n+1}$$

$$- 1/2\left[FWL_K (v_\ell)_{jk}^n + FWL_L\,(v_\ell)_{jL}^n\right] + (\alpha_\ell\rho_\ell)_j^n\, g\,\Delta Z_j$$

$$- 1/2\left[FI_K^n\,(v_\ell - v_g)_{j1}^{n+1} + FI_L^n\,(v_\ell - v_g)_{j2}^{n+1}\right] + (\Gamma_\ell)_j^n\,(\tilde{v}_\ell - v_\ell)_j^n$$

(26)

A similar equation is obtained for the gas phase. In Equation (26) $(\Delta P_f)_\ell^{n+1}$ is given as

$$(\Delta P_f)_\ell^{n+1} = 1/2\ (\rho_\ell)_j^n \left(1 - \frac{\alpha_{\ell 2}^n\ \epsilon}{\alpha_{\ell T}^n\ \epsilon_{\ell c}^n\ \epsilon_T}\right)^2 |(v_\ell)_{j2}^n|(v_\ell)_{j2}^{n+1} \qquad (27)$$

The values for $\alpha_{\ell T}^n$ and $\alpha_{\ell 2}^n$ are obtained by the solution scheme described following Equation (25) with upstream values* $(\alpha_\ell)_{j1}^n = (\alpha_\ell)_K^n$, $(v_\ell)_{j1}^n$, $(v_g)_{j1}^n$, P_{j1}^n.

Equation (26) involves two velocities $(v_\ell)_{j1}$ and $(v_\ell)_{j2}$ which are related by steady state continuity considerations. However, we need to write Equation (26) in terms of a single velocity. This requirement is satisfied by defining a reference velocity, $(v_\ell)_j$, at junction j based upon the junction void fraction (donored), junction area A_j and continuity i.e.,

$$(\alpha_\ell)_j\ (v_\ell)_j\ A_j = \alpha_{\ell 1}\ (v_\ell)_{j1}\ A_K \qquad (28)$$

or

$$(\alpha_\ell)_j\ (v_\ell)_j\ A_j = (\alpha_\ell)_2\ (v_\ell)_{j2}\ A_L \ . \qquad (29)$$

When Equations (28) and (29) are used to express $(v_\ell)_{j1}$ and $(v_\ell)_{j2}$ in terms of $(v_\ell)_j$ and substituted into Equation (26) only a single velocity, $(v_\ell)_j^{n+1}$ remains as follows:

*Note that $(\alpha_\ell)_K^n$ has been used as the upstream void fraction in the jump conditions. This is consistent with the donor cell approximation and gives stable results.

$$1/2(\alpha_\ell \rho_\ell)_j^n \alpha_{\ell j} A_j \left[\frac{\Delta X_K}{\alpha_{\ell 1} A_K} + \frac{\Delta X_L}{\alpha_{\ell 2} A_L}\right] \left[(v_\ell)_j^{n+1} - (v_\ell)_j^n\right]/\Delta t$$

$$+ 1/2(\alpha_\ell \rho_\ell)_j^n \left[(v_\ell^2)_L^n - (v_\ell^2)_K^n\right] + \text{viscous damping}$$

$$= -(\alpha_\ell)_j^n \left(P_L^{n+1} - P_K^{n+1}\right) + (\alpha_\ell)_j^n (\Delta P_f)_\ell^{n+1}$$

$$- 1/2 (\alpha_\ell)_j^n A_j \left[\frac{FWL_K^n}{(\alpha_\ell)_1^n A_K} + \frac{FWL_L^n}{(\alpha_\ell)_2^n A_L}\right] (v_\ell)_j^{n+1} + (\alpha_\ell \rho_\ell)_j^n g \Delta Z_j$$

$$1/2 A_j \left\{\frac{FI_K^n}{A_K}\left[\frac{(\alpha_\ell)_j^n (v_\ell)_j^{n+1}}{(\alpha_\ell)_1^n} - \frac{(\alpha_g)_j^n (v_g)_j^{n+1}}{(\alpha_g)_1^n}\right] + \frac{FI_L^n}{A_L}\left[\frac{(\alpha_\ell)_j^n (v_\ell)_j^{n+1}}{(\alpha_\ell)_1^n}\right.\right.$$

$$\left.\left. - \frac{(\alpha_g)_j^n (v_g)_j^{n+1}}{(\alpha_g)_1^n}\right]\right\} + 1/2 A_j \left\{\frac{(\Gamma_\ell)_K^n}{A_K}\left[\frac{\alpha_{\ell j}^n (\tilde{v}_\ell)_j^{n+1}}{(\alpha_\ell)_1^n} - \frac{(\alpha_\ell)_j^n (v_\ell)_j^{n+1}}{(\alpha_\ell)_1^n}\right]\right.$$

$$\left. + \frac{(\Gamma_\ell)_L^n}{A_L}\left[\frac{(\alpha_\ell)_j^n (\tilde{v}_\ell)_j^{n+1}}{(\alpha_\ell)_2^n} - \frac{(\alpha_\ell)_j^n (v_\ell)_j^{n+1}}{(\alpha_\ell)}\right]\right\} - \qquad (30)$$

Equation (30) is the phasic momentum equation for the liquid phase. The vapor phasic momentum equation is obtained by interchanging the ℓ and g subscripts. The two phasic momentum equations are used in the numerical scheme as a sum and difference equation. The difference equation is formed by first dividing each phasic momentum equation by the respective αρ products and then taking the difference of the liquid and vapor equations.

The numerical formulation of the momentum equations described above was tested on single-phase expansions, contractions and orifices and gave correct results. Several two-phase problems were also run. The results of three of these are presented below. In each case a transient calculation was made until steady-state was achieved and the steady-state results are shown on the figures. All the results appear reasonable.

2. Sample Calculations

The numerical results for two different expansion cases, which demonstrate the capability of the model, are shown in Figures 6 and 7. The first case is an idealized problem with the interphase drag equal to zero which simulates a separated flow with an area ratio of 1:2. In this case an approximate analytic solution can be obtained because the pressure rise has little effect upon the liquid flow rate ($\rho_\ell >> \rho_g$). The approximate solution shows the liquid moving through the expansion with little or no change in velocity. The area change is then accommodated by a large reduction in the vapor velocity. The code

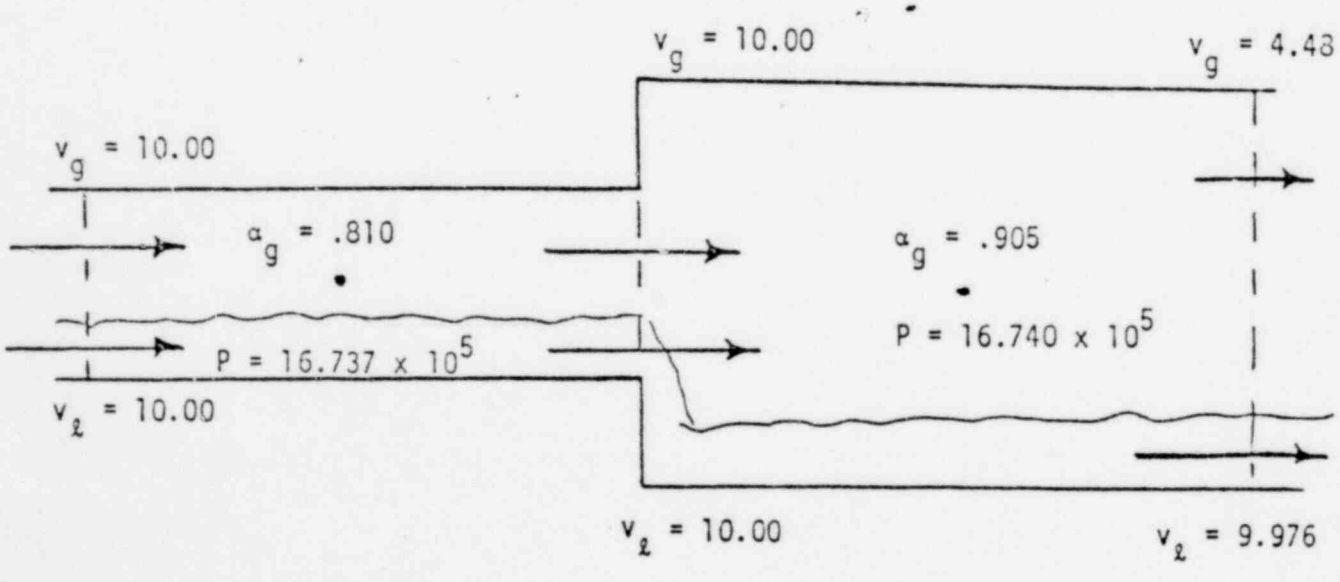

Figure 6. Separated Flow Expansion

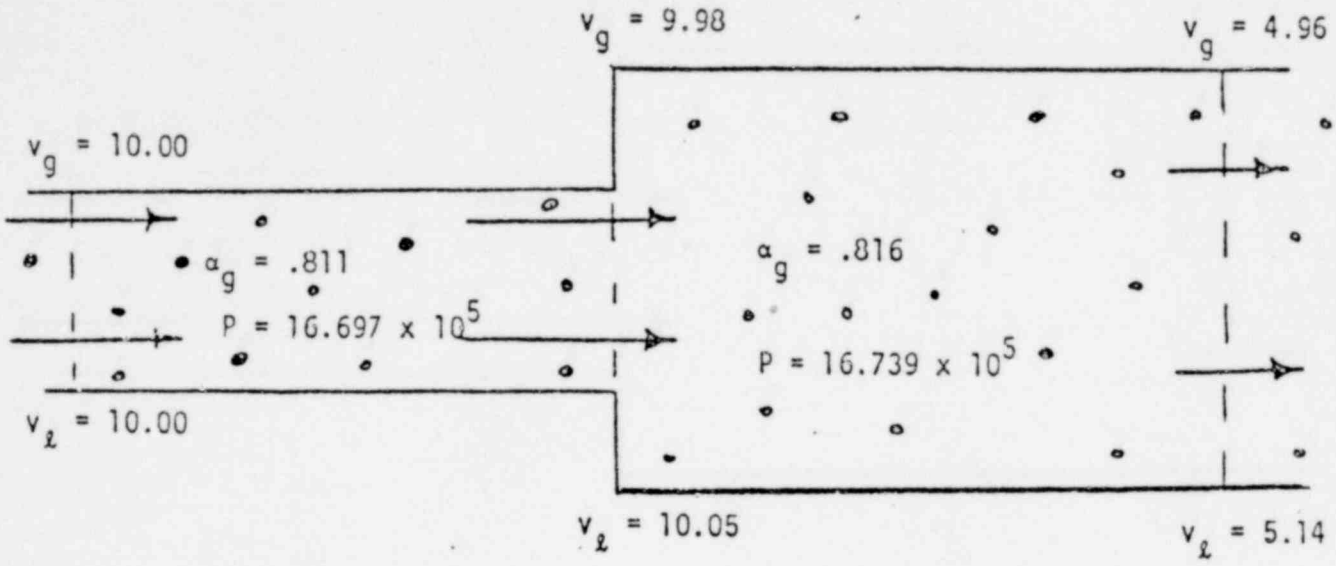

Figure 7. Dispersed Flow Expansion

results for this case are within 0.5% of the idealized analytic solution. The second example is for the same expansion geometry and boundary conditions but with an interphase drag, FI, appropriate to a dispersed flow regime. In this case we see that the interphase drag is sufficient to force the liquid to slow down approximately to the same velocity as that of the gas. Since both phases remain at approximately the same velocity the void fraction change is approximately zero across the expansion. This is in contrast to the free slip case where the void fraction changes abruptly as a result of the small change in liquid velocity, i.e. for free slip $\alpha_{\ell 2} \approx \alpha_{\ell 1} A_1/A_2$. These expansion examples demonstrate the range of capability of the numerical model. With the appropriate interphase drag the correct phase velocity and

void distributions downstream from an area change can be calculated.

Figure 8 shows the calculated results for a typical contraction and an interphase drag appropriate to the dispersed flow region. Here again qualitatively correct results were obtained and only a small change in void fraction occurs due to the large interphase drag associated with dispersed flow.

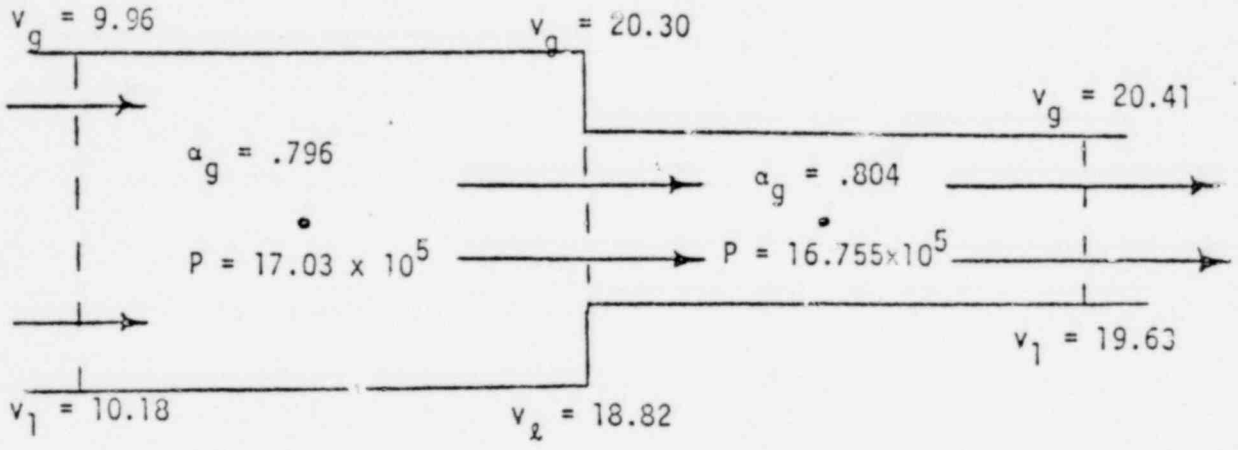

Figure 8. Dispersed Flow Contraction

Using the described model and associated numerical scheme, all the loss calculations are independent of the adjoining cell sizes (cells K and L). Hence there are no time step or nodalization restrictions due to the inclusion of abrupt area change. The calculated magnitude of the losses at abrupt area change also is independent of the volume of the adjoining cells.

VI. PARALLEL "TEE" MODEL

In order to model flow in interconnected piping networks it is necessary to model the two-phase fluid process at tees. A general description of the two-phase flow process is complicated by the possibility of phase separation effects which can occur at a tee where flow division occurs.[4] However, there are many situations where a parallel or plenum branching tee model is adequate for both flow merging and division. Typical situations when such a parallel model is adequate are parallel flow paths through the reactor core, jet pump flow mixing sections and any branch from a vessel of large cross-section (in this case the fluid momentum is small and it is entirely permissible to neglect the momentum convective terms). Further generalizations of the parallel tee are planned in which it will be possible to partially model phase separation effects from mechanistic momentum considerations and where this approach is found to be inadequate, empirical separation/loss models will be used to augment the mechanistic model.

The parallel tee model which has been formulated and tested consists of a single control volume that has multiple junctions (three or more) at its

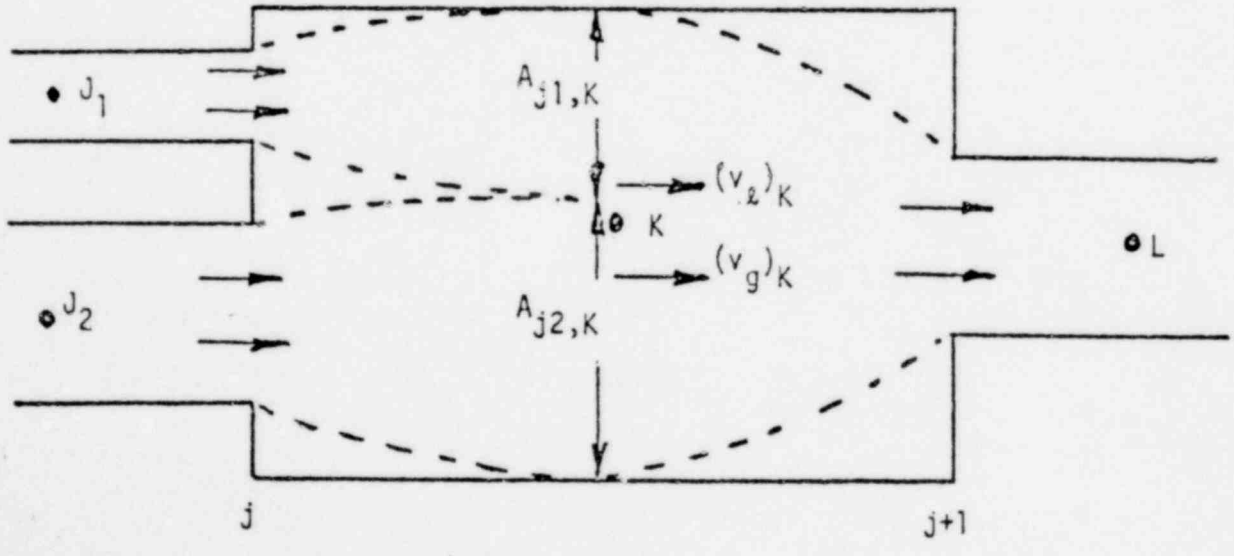

Figure 9. Typical Parallel Branching Junctions

1317 045

edges but the junction velocities are all parallel (see Figure 9). An additional distinction is made wherein junctions are identified as right or left junctions on a volume. Junction J_1 and J_2, shown in Figure 9, are left junctions while junction j + 1 is a right junction relative to volume K.

The modeling for this case is relatively simple. We assume ideal mixing in cell K. The volume velocities, $(v_\ell)_K$ and $(v_g)_K$ associated with the left junctions of cell K are obtained from a quasi-steady mass balance

$$(\alpha_\ell)_K^n (\rho_\ell)_K^n [(v_\ell)_K^n]_{LEFT} A_K = \sum_{j=J_1}^{J_N} (\alpha_\ell)_j^n (\rho_\ell)_j^n (v_\ell)_j^n A_j \quad , \tag{30}$$

$$(\alpha_g)_K^n (\rho_g)_K^n [(v_g)_{j2}^n]_{LEFT} A_K = \sum_{j=J_1}^{J_N} (\alpha_g)_j^n (\rho_g)_j^n (v_g)_j^n A_j \quad . \tag{31}$$

These volume velocities are then used to evaluate the momentum flux terms $(1/2\rho v^2)$ in the momentum equations for all left junctions connected to cell K.

To calculate the losses associated with these junctions an assumption must be made for the fraction of the area A_K that is "seen" by a typical junction connected to cell K. A junction flow with high mass flow rate would be expected to "see" a larger proportion of the volume area A_K than a junction flow with a low mass flow rate. We assume that each junction on cell K expands or contracts from the area of the junction, A_j, to an aportioned area in volume K (see Figure 9). The flow area of volume K is

assumed to be aportioned according to a mass flow fraction defined as follows:

$$(A_K)_j = \frac{\left\{\left|(\alpha_\ell)_j^n(\rho_\ell)_j^n\,(v_\ell)_j^n A_j\right|+\left|(\alpha_g)_j^n(\rho_g)_j^n\,(v_g)_j^n\,A_j\right|\right\} A_K}{\sum_{j=J_1}^{J_N}\left\{\left|(\alpha_\ell)_j^n\,(\rho_\ell)_j^n\,(v_\ell)_j^n A_j\right|+\left|(\alpha_g)_j^n(\rho_g)_j^n(v_g)_j^n\,A_j\right|\right\}} \qquad (32)$$

With the above areas defined the standard abrupt area change model described in the previous sections is applied at all junction connected to cell K. Other assumptions are possible for (A_K) but the one defined by Equation (32) has proved satisfactory in limited tests.

The only other additions to the basic code structure necessary to incorporate the parallel tee capability were a generalized indexing of the junctions and the flow logic necessary to keep track of which junctions are connected to a multiple junction volume. All this information is processed in the input routine for user controlled input.

Limited check out runs have been made using this branching option. Figure 10 shows the results of a symmetric two channel core through flow problem. The problem was run solely to see if the flow which developed was symmetric throughout the transient and at steady state. No deviation from symmetry was present in the six significant figures printed out. The final steady state pressures are seen in Figure 10.

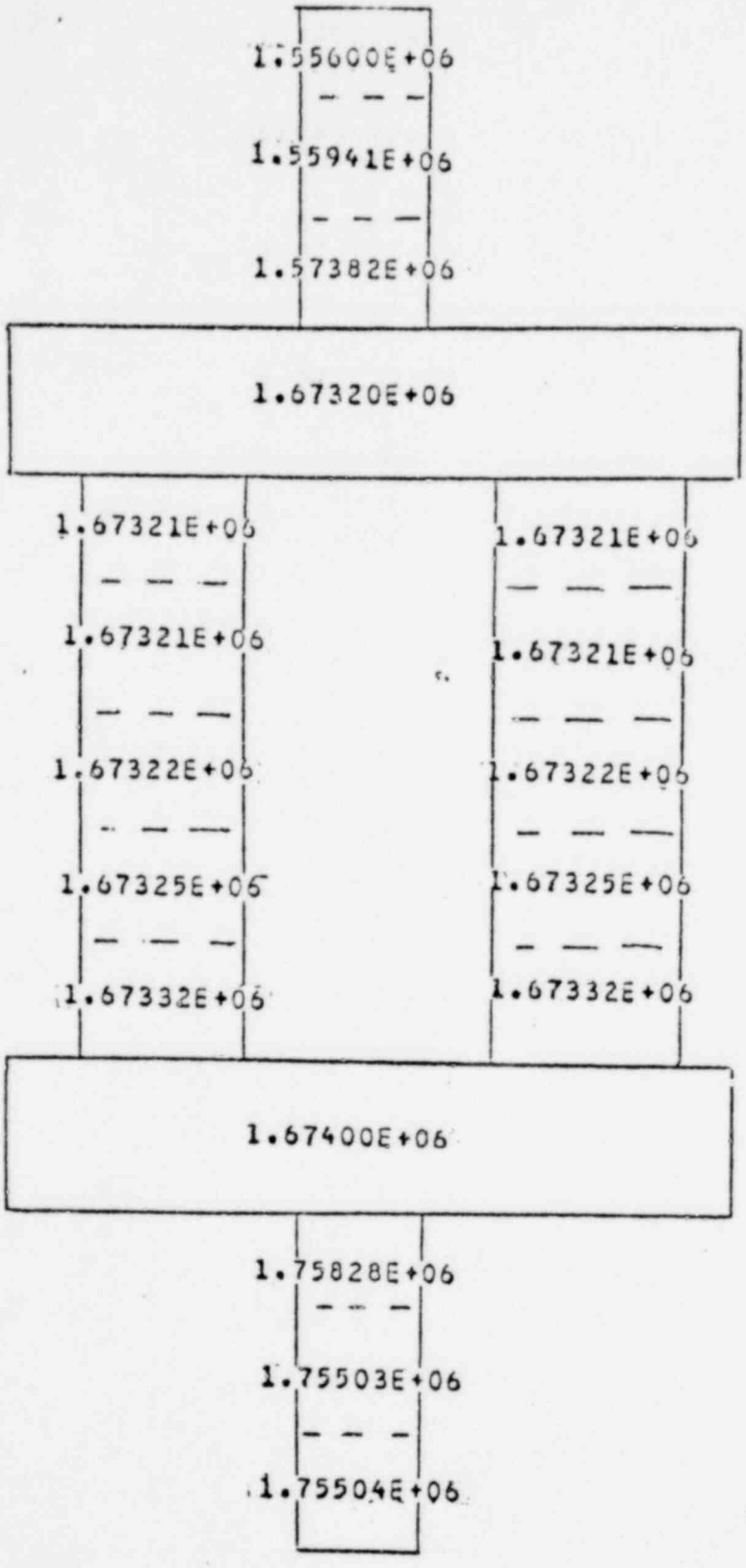

1317 048

Figure 10. Symmetric Pressure in Typical Parallel Channels

REFERENCES

1. Vennard, J. K., Elementary Fluid Mechanics, John Wiley and Sons, 4th Edition, 1965.

2. Weisman, J., Ake, T. and Knott, R., "Two-Phase Pressure Drop Across Abrupt Area Changes in Oscillatory Flow", Nuclear Science & Engineering, 61, 297-309, 1976.

3. Trapp, J. A. and Ransom, V. H., "RELAP5 Hydrodynamic Model: Progress Summary - Field Equation", SRD-126-76, Idaho National Engineering Laboratory, June 1976.

4. Collier, J. G., Advanced Study Institute on Two-Phase Flows and Heat Transfer, ASI Proceedings, Istanbul-Turkey, August 1976.

5. El-Wakil, M. M., Nuclear Heat Transport, International Textbook Company, 1971.

6. Harshe, B., Hussain, A. and Weisman, J., "Two-Phase Pressure Drop Across Restrictions and Other Abrupt Area Changes", NUREG-0062, University of Cincinnati, April 1976.

7. Lottes, P. A., "Expansion Losses in Two-Phase Flows", Nuclear Science and Energy, 9, 26 - 31, 1961.

8. Ransom, V. H. and Trapp, J. A., "RELAP5 Hydrodynamic Model: Progress Summary - PILOT Code," PG-R-76-013, Idaho National Engineering Laboratory, December 1976.

APPENDIX A

The table below tabulates the contraction coefficient, ε_c, normally used in single phase flow as a function of the area ratio[1].

$$\varepsilon_T = \frac{\text{Area at Throat}}{\text{Upstream Area}}$$

ε_T, ε_{gT}, $\varepsilon_{\ell T}$	ε_c, ε_{gc}, $\varepsilon_{\ell c}$
0.0	0.617
0.1	0.624
0.2	0.632
0.3	0.643
0.4	0.659
0.5	0.681
0.6	0.712
0.7	0.755
0.8	0.813
0.9	0.892
1.0	1.00

APPENDIX B

The purpose of this appendix is to show how Equation (21) can be derived from Equations (17) and (18). To this end consider Equation (17)

$$1/2\ \rho_\ell v_{\ell 1}^2 + P_1 = 1/2\ \rho_\ell\ v_{\ell 2}^2 + P_2 + 1/2\ \rho_\ell\ (1 - \frac{\alpha_{\ell 2}}{\alpha_{\ell 1}}\frac{\varepsilon}{})^2\ v_{\ell 2}^2$$

$$+\ (\frac{FI}{\alpha_\ell^2})_2\ (v_{\ell 2} - v_{g2})\ L_2\ . \qquad (B1)$$

Using the steady state mass conservation, Equation (19), in (B1) gives

$$1/2\ \rho_\ell\ v_{\ell 1}^2 + P_1 = 1/2\ \rho_\ell v_{\ell 2}^2 + P_2 + 1/2\ \rho_\ell v_{\ell 1}^2\ (1 - \frac{\alpha_{\ell 1}}{\alpha_{\ell 2}}\frac{}{\varepsilon})^2$$

$$+\ (\frac{FI}{\alpha_\ell})_2\ \ (v_{\ell 2} - v_{g2})\ L_2 \qquad (B2)$$

or

$$1/2\ \rho_\ell v_{\ell 1}^2 + P_1 = 1/2\ \rho_\ell v_{\ell 2}^2 + P_2 + 1/2\ \rho_\ell\ (v_{\ell 1} - v_{\ell 2})^2$$

$$+\ (\frac{FI}{\alpha_\ell})_2\ (v_{\ell 2} - v_{g2})\ L_2 \qquad (B3)$$

Multiplying (B3) by $\alpha_{\ell 2} A_2$ we obtain after some rearrangement

$$\alpha_{\ell 2}\ A_2\ P_1 = \alpha_{\ell 2}\rho_\ell v_{\ell 2}^2\ A_2 + \alpha_{\ell 2}\ A_2 P_2 - (\alpha_{\ell 2}\ v_{\ell 2} A_2)\ \rho_\ell v_{\ell 1}$$

$$+\ A_2\ FI_2\ (v_{\ell 2} - v_{g2})\ L_2 \qquad (B4)$$

If we again use Equation (19) to rewrite the last term in Equation (B4) we obtain

$$\alpha_{\ell 1}\, \rho_{\ell}\, v_{\ell 1}^2\, A_1 + \alpha_{\ell 2} A_2 P_1 = \alpha_{\ell 2} \rho_{\ell} v_{\ell 2}^2\, A_2 + \alpha_{\ell 2}\, A_2 P_2$$

$$+ A_2\, FI_2\, (v_{\ell 2} - v_{g2})\, L_2 \qquad \text{(B5)}$$

A similar development starting from Equations (18) and (20) leads to

$$\alpha_{g1}\, \rho_g\, v_{g1}^2\, A_1 + \alpha_{g2}\, A_2\, P_1 = \alpha_{g2}\, \rho_g\, v_{g2}^2\, A_2 + \alpha_{g2}\, A_2\, P_2$$

$$+ A_2\, FI_2\, (v_{g2} - v_{\ell 2})\, L_2 \qquad \text{(B6)}$$

Adding Equations (B5) and (B6) will then give the desired Equation (21) of the text, i.e.

$$\alpha_{\ell 1}\, \rho_{\ell 1}\, v_{\ell 1}^2\, A_1 + \alpha_{g1}\, \rho_{g1}\, v_{g1}^2\, A_1 + A_2\, P_1 = \alpha_{\ell 2}\, \rho_{\ell 2}\, v_{\ell 2}^2\, A_2$$

$$+ \alpha_{g2}\, \rho_{g2}\, v_{g2}^2\, A_2 + A_2\, P_2 \quad . \qquad \text{(B7)}$$

APPENDIX E

RELAP5 ANALYTIC CHOKING CRITERION

Report No. CDAP-TR-013

Date April 1978

CODE DEVELOPMENT AND ANALYSIS PROGRAM

RELAP5 PROGRESS SUMMARY
ANALYTIC CHOKING CRITERION FOR TWO-PHASE FLOW

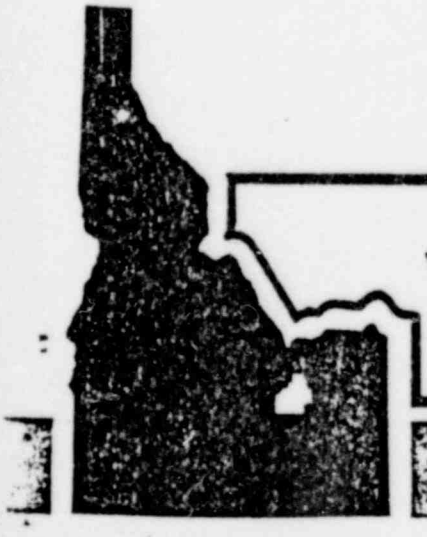

EG&G Idaho, Inc.

IDAHO NATIONAL ENGINEERING LABORATORY

DEPARTMENT OF ENERGY

IDAHO OPERATIONS OFFICE UNDER CONTRACT EY-76-C-07-1570

PRELIMINARY ANALYSIS REPORT

Report No. CDAP-TR-013

Date April 1978

Contract Program or Project Title: Loss-of-Coolant Accident Analysis, A6052

Subject of this Document: RELAP5 Progress Summary, Analytic Choking Criterion for Two-Phase Flow

Type of Document: Technical Report

Author(s): V. H. Ransom, J. A. Trapp

Date of Document: April 1978

Responsible NRC Individual and NRC Office or Division: S. Fabic, Reactor Safety Research

Idaho National Engineering Laboratory
Idaho Falls, Idaho 83401
Operated by
EG&G Idaho, Inc.
for the
U.S. Department of Energy

Prepared for
U.S. Nuclear Regulatory Commission
Washington, D.C. 20555

PRELIMINARY ANALYSIS REPORT

Report No. CDAP-TR-013

Date April 1978

RELAP5 PROGRESS SUMMARY
ANALYTIC CHOKING CRITERION FOR TWO-PHASE FLOW

V. H. Ransom
J. A. Trapp

REVIEWED BY:

Paul North
Acting Branch Manager

APPROVED BY:

Paul North, Manager
Code Development and
Analysis Program

ABSTRACT

The conditions for chcked two-phase flow are investigated analytically by application of the theory of characteristics to a one-dimensional transient model. Two situations are considered, that of thermal equilibrium between phases and the case where the phases are isolated thermally. The basic hydrodynamic model which is analyzed is a two-fluid model including relative phasic acceleration terms.

The analytical results provide an algebraic choking criterion analogous to that for a single-phase flow except that terms due to relative phase motion are included. The criterion has been applied to pipe blowdowns with choked discharge and the thermal equilibrium model is found to agree very well with data.

INTRODUCTION AND SUMMARY

The choked flow of a two-phase mixture is an important phenomenon in many two-phase flow situations. In particular, the depressurization rate (and the resulting water inventory) in a nuclear reactor during blowdown under loss-of-coolant accident conditions is controlled by the choked mass discharge rate. In the past relatively simple semi-empirical models have been used to predict the choked mass discharge rate for use with system transient analytical models, such as RELAP4. The development of more general and physically based models for the two-phase flow process, being undertaken in the RELAP5 project, has necessitated development of consistent choked flow models.

The two-fluid nonequilibrium hydrodynamic model which is used in the RELAP5 code[1] embodies additional degrees of freedom compared to the homogeneous equilibrium model used in RELAP4. An associated choked flow model is developed herein which is analogous to the transient choked flow criterion for single-phase flows. Choking is known to occur in single-phase flow when the fluid velocity attains the local speed of sound[2]. In two-phase flows the speed of sound governing choked flow is much lower than the phasic sound speeds, but the exact value has been difficult to establish analytically except in very special cases, such as homogeneous equilibrium flow.

In this report, a new choking criterion is developed for nonhomogeneous equilibrium and frozen (thermally isolated) flows. It is based on the two-fluid analytical model for two-phase flow and an analytic expression is developed which relates the phasic velocities to a mixture sound speed. The mixture sound speed is a function of the interphase momentum coupling due to relative acceleration (virtual mass) and it is shown that the well-known two-phase sound speed depression[3] is a direct result of this coupling. The choking criterion has been used to model choked two-phase flow from pipe blowdowns and the results

obtained using the equilibrium model are in excellent agreement with data. While the choking criterion is based on the thermal equilibrium assumption, the nonequilibrium RELAP5 hydrodynamic model is used to model the transient flow throughout the system.

The analytic expressions which are developed can be used to establish the choked mass flow rate for a variety of fluid flow conditions. These relations are particularly useful in conjunction with numerical calculations of transient two-phase flows. The use of a choking criterion eliminates the need to model the flow process numerically in the immediate vicinity of the choked flow point. Normally, large spatial gradients in the flow properties occur near points of choked flow and fine spatial noding is required for accurate resolution. The use of the choking criterion and appropriate boundary conditions eliminates the need for this detail which can be expensive in terms of computer storage and computational time.

NOMENCLATURE

A,B	General Matrix Functions
a	Sound Speed
C	General Vector Function
c	Coefficient of Virtual Mass
D	Coefficient of Relative Mach Number in Choking Criterion
L	Length
M	Mach Number
P	Pressure
S	Phasic Entropy
t	Time Coordinate
U	Vector of Dependent Variables
v	Mixture or Phasic Velocity with Subscript
x	Spatial Coordinate
α	Void Fraction
λ	Characteristic Operator
ρ	Mixture Density or Phasic Density with Subscript

SUBSCRIPTS

f	Liquid Phase
g	Vapor Phase
HE	Homogeneous Equilibrium
HF	Homogeneous Fr ..en
v	Mass Mean Mach Number
r	Relative Mach Number

SUPERSCRIPTS

I	Imaginary Part of Complex Number
R	Real Part of Complex Number
s	Saturation Property
*	Total Derivative of a Saturation Property With Respect to Pressure
'	Partial Derivative With Respect to Pressure

CONTENTS

FIGURES

RELAP5 PROGRESS SUMMARY

ANALYTIC CHOKING CRITERION FOR TWO-PHASE FLOW

I. CHOKING THEORY

Choking is defined as the condition wherein the mass flow rate becomes independent of the downstream conditions; i.e., that point at which further reduction in the downstream pressure does not result in change to the mass flow rate. The fundamental reason that choking occurs is that acoustic signals can no longer propagate upstream. This occurs when the fluid velocity just equals the propagation velocity.

For a differential operator, the path lines for signal propagation are established from a characteristic analysis. Consider a system of n first-order quasi-linear, partial differential equations of the form

$$A(\bar{U})[\partial\bar{U}/\partial t] + B(\bar{U})[\partial\bar{U}/\partial x] + \bar{C}(\bar{U}) = 0 \qquad (1)$$

The characteristic directions (or characteristic velocities) of the system are defined[4][5] as the roots, $\lambda_i (i \leq n)$, of the characteristic polynomial

$$(A\lambda - B) = 0. \qquad (2)$$

The real part of any root, λ_i^R, gives the velocity of signal propagation along the corresponding characteristic path in the space-time plane. The imaginary part of any complex root, λ_i^I, gives the rate of growth or decay of the signal propagating along the respective path. For a hyperbolic system in which all the roots of Equation (2) are real and nonzero, it can be shown that the number of boundary conditions required at any boundary point equals the number of characteristic lines entering the solution region as t increases. If we consider the system, Equation (1), for a particular region $0 \leq x \leq L$ and examine the boundary conditions at x = L, it follows that as long as any λ_i is less than

zero we must supply some boundary information in order to obtain the solution. If, on the other hand, all the λ_i are greater than or equal to zero, then no boundary conditions are needed at x = L and, hence, the interior solution is unaffected by conditions beyond this boundary.

A choked condition exists when no information can propagate into the solution region from the exterior. Such a condition exists at the boundary point x = L when

$$\lambda_j = 0 \text{ for } j \leq n \tag{3}$$

$$\lambda_i \geq 0 \text{ for all } i \neq j. \tag{4}$$

These are the mathematical conditions which are satisfied by the equations of motion for a flowing fluid when reduction in downstream pressure ceases to result in increased flowrate. It is well-known[2] that the choked condition for single-phase flow occurs when the fluid velocity just equals the local sound speed.

In the following sections the appropriate conditions for choked flow of a two-phase fluid are developed for two cases: (1) thermal equilibrium between phases, and (2) adiabatic phases without phase change (frozen). These two cases bound actual two-phase flows in which thermal nonequilibrium as well as nonhomogeneous flow exist (it will be shown in what follows that current interphase mass transfer models are not adequate to enable analysis of the nonequilibrium flow case).

II. CHOKING IN NONHOMOGENEOUS EQUILIBRIUM TWO-PHASE FLOW

The two-fluid model for the conditions of thermal equilibrium (equilibrium interphase mass transfer) is described by the overall mass continuity equation, two phasic momentum equations and the mixture energy equation. This system of equations is as follows

$$\partial(\alpha_g\rho_g+\alpha_f\rho_f)/\partial t + \partial(\alpha_g\rho_g v_g + \alpha_f\rho_f v_f)/\partial x = 0 \tag{5}$$

$$\alpha_g\rho_g[\partial v_g/\partial t+v_g(\partial v_g/\partial x)] + \alpha_g(\partial P/\partial x)$$

$$+ c\alpha_g\alpha_f\rho[\partial v_g/\partial t+v_f(\partial v_g/\partial x) - \partial v_f/\partial t - v_g(\partial v_f/\partial x)] = 0 \tag{6}$$

$$\alpha_f\rho_f[\partial v_f/\partial t+v_f(\partial v_f/\partial x)] + \alpha_f(\partial P/\partial x)$$

$$+ c\alpha_f\alpha_g\rho[\partial v_f/\partial t+v_g(\partial v_f/\partial x) - \partial v_g/\partial t - v_f(\partial v_g/\partial x)] = 0 \tag{7}$$

$$\partial(\alpha_g\rho_g S_g+\alpha_f\rho_f S_f)/\partial t + \partial(\alpha_g\rho_g S_g v_g + \alpha_f\rho_f S_f v_f)/\partial x = 0 \tag{8}$$

The momentum equations include the interphase force terms due to relative acceleration[6]. These force terms have a significant effect on wave propagation velocity and consequently also on the choked flow velocity. The particular form chosen is frame invarient and symmetric and the coefficient of virtual mass, $c\alpha_g\alpha_f\rho$, is chosen so that a smooth transition between pure vapor and pure liquid is assured. For a dispersed flow the constant c has a theoretical value of 0.5, while for a separated flow the value may approach zero. The energy equation is written in terms of mixture entropy which is constant for adiabatic equilibrium flow (the energy dissipation associated with interphase mass transfer and relative phase acceleration is neglected).

The nondifferential source terms, $\bar{C}(\bar{U})$, in Equation (1) do not enter into the characteristic analysis and thus do not affect the propagation velocities. For this reason the source terms associated with wall friction, interphase drag and heat transfer are omitted for brevity in Equations (5) through (8).

In the thermal equilibrium case ρ_g, ρ_f, S_g and S_f are known functions of the pressure only (the vapor and liquid values along the saturation curve). The derivatives of these variables are designated by an asterisk as follows

$$\rho_g^* = d\rho_g^S/dP, \qquad \rho_f^* = d\rho_f^S/dP \tag{9}$$

$$S_g^* = dS_g^S/dP, \qquad S_f^* = dS_f^S/dP \tag{10}$$

The system of governing equations, Equation (5) through (8), can be written in terms of the four dependent variables, α_g, P, v_g and v_f, by application of the chain rule and the property derivatives, Equations (9) and (10). Thus, the system of equations can be written in the form of Equation (1) where the A and B are fourth-order square coefficient matrices. The characteristic determinantal equation, Equation (2), corresponding to this system is

$$\begin{aligned}
&\rho c(\lambda-v_f)(\lambda-v_g) + \alpha_f\rho_g(\lambda-v_g)^2 + \alpha_g\rho_f(\lambda-v_f)^2 \\
&+ \left\{[\rho_g(\lambda-v_g) - \rho_f(\lambda-v_f)]\,[\alpha_g\rho_g S_g^* (\lambda-v_g) + \alpha_f\rho_f S_f^* (\lambda-v_f)]/(S_g-S_f)\right. \\
&\left. - (\alpha_f\rho_g\rho_f^* + \alpha_g\rho_f\rho_g^*)(\lambda-v_f)(\lambda-v_g)\right\} \times \left\{(\lambda-v_f)(\lambda-v_g)\right. \\
&\left. + (c\rho\alpha_f/\rho_g)(\lambda-v_f)^2 + (c\rho\alpha_g/\rho_f)(\lambda-v_g)^2\right\} = 0
\end{aligned} \tag{11}$$

The characteristic polynomial is fourth-order in λ and factorization can only be carried out approximately to obtain the roots for λ and thus establish the

choking criterion. The factorization is presented in Appendix A and produces the following results. The first two roots are:

$$\lambda_{1,2} = \frac{\left\{\alpha_f\rho_g + \rho c/2 \pm [(\rho c/2)^2 - \alpha_g\alpha_f\rho_g\rho_f]^{1/2}\right\} v_g + \left\{\alpha_g\rho_g + \rho c/2 \mp [(\rho c/2)^2 - \alpha_g\alpha_f\rho_g\rho_f]^{1/2}\right\} v_f}{(\alpha_f\rho_g + \rho c/2) + (\alpha_g\rho_f + \rho c/2)} \qquad (12)$$

These two roots are obtained by neglecting the fourth-order factors relative to the second-order factors in $(\lambda - v_g)$ and $(\lambda - v_f)$ (there are no first- or third-order factors). Inspection of Equation (12) shows that the $\lambda_{1,2}$ have values between v_g and v_f, thus the fourth-order factors $(\lambda - v_g)$ and $(\lambda - v_f)$ are small (i.e., neglecting these terms is justified). The values for $\lambda_{1,2}$ may be real or complex depending on the sign of the quantity $[(\rho c/2)^2 - \alpha_g\alpha_f\rho_g\rho_f]$.

The remaining two roots are obtained by dividing out the quadratic factor containing $\lambda_{1,2}$, neglecting the remainder and subsequent factorization of the remaining quadratic terms (this procedure can be shown to be analogous to neglecting the second and higher order terms in the relative velocity, $(v_g - v_f)$. The remaining roots are:

$$\lambda_{3,4} = v + D\,(v_g - v_f) \pm a \qquad (13)$$

where

$$v = (\alpha_g\rho_g v_g + \alpha_f\rho_f v_f)/\rho\ , \qquad (14)$$

$$a = a_{HE}\left\{[(c\rho^2 + \rho(\alpha_g\rho_f + \alpha_f\rho_g)]/(c\rho^2 + \rho_g\rho_f)\right\}^{1/2} \qquad (15)$$

and

$$D = \tfrac{1}{2}\left\{\frac{(\alpha_g\rho_f - \alpha_f\rho_g)}{(\rho c + \alpha_f\rho_g + \alpha_g\rho_f)} + \frac{\rho_g\rho_f(\alpha_f\rho_f - \alpha_g\rho_g)}{\rho(\rho_g\rho_f + c\rho^2)} - a_{HE}^2\,\frac{\rho(\alpha_g\rho_g S_g^* + \alpha_f\rho_f S_f^*)}{\rho_g\rho_f(S_g - S_f)}\right\} \qquad (16)$$

The quantity a_{HE} is the homogeneous equilibrium speed of sound and is defined in Appendix A. The roots $\lambda_{3,4}$ have only real values.

The general nature and significance of these roots is revealed by applying the characteristic considerations discussed in Section I. The speeds with which small disturbances propagate are related to the values of the characteristic roots. In general, the velocity of propagation corresponds to the real part of a root and the growth or attenuation is associated with the complex part of the root. The choked flow condition concerns the velocity with which a disdurbance propagates from a boundary, thus, the criterion for choking is established from examination of the real part of a characteristic root. Choking will occur when the signal, which propagates with the largest velocity relative to the fluid, is just stationary; i.e.,

$$\lambda_j^R = 0 \text{ for } j \leq 4 \tag{17}$$

and

$$\lambda_i^R \geq 0 \text{ for all } i \neq j. \tag{18}$$

The existance of complex roots for $\lambda_{1,2}$ makes the initial-boundary-value problem ill-posed. This problem has been discussed by many investigators[7][8] and we only note here that the addition of any small second-order viscous effect renders the problem well-posed[7][9]. The whole phenomena of systems with mixed orders of derivatives, and in particular a first-order system with the addition of a small second-order term, has been discussed and analyzed by Whitham[5]. He has shown that the second-order viscous terms do give infinite characteristic velocities, but very little information is propagated along these characteristic lines and the bulk of the information is propagated along the characteristic lines defined by the first-order system. We conclude that the ill-posed nature of Equations (5)-(8) can be removed by the addition of small second-order viscous terms and that these terms will have little effect upon the propagation of information. Therefore, the choking criterion for the two-phase flow system analyzed here is established from Equation (17).

The explicit character of the choking criterion for the two-phase flow model defined by Equations (5) through (8) will now be examined. Since the two roots $\lambda_{1,2}$ are between the phase velocities v_f and v_g, the choking criterion is established from the roots $\lambda_{3,4}$ and Equation (17). The choking criterion is

$$v + D(v_g - v_f) = \pm a \tag{19}$$

The choking criterion can be rewritten in terms of the mass mean and relative Mach numbers

$$M_v = v/a, \quad M_r = (v_g - v_f)/a \tag{20}$$

as

$$M_v + DM_r = \pm 1 . \tag{21}$$

This relation is very similar to the choking criterion for single-phase flow wherein only the mass average Mach number appears and choking also corresponds to a Mach number of unity.

The choking criterion, Equation (21), is a function of the two parameters D and a. In Figure 1, a is plotted as a function of the void fraction α_g for a typical steam-water system at 7.5 MPA with c equal zero (the stratified equilibrium sound speed), c equal 0.5 (the typical value for a dispersed flow model) and in the limiting case when c becomes infinite (homogeneous equilibrium sound speed). From Figure 1 it is evident that the virtual mass coefficient has a significant effect upon the choked flow dynamics in two-phase flows[8].

To establish the actual choked flow rate for two-phase flow with slip, the relative velocity term in Equation (21) must also be considered. The relative Mach number coefficient, D, is shown plotted on Figure 2 for values of c equal to 0, 0.5 and ∞. It is evident from these results that the choked flow velocity can differ appreciably from the mass mean velocity when slip occurs. It is significant, that the variation of the choked flow criterion from the homogeneous result is entirely due to velocity nonequilibrium, since these results have been obtained under the assumption of thermal equilibrium.

III. CHOKING IN NONHOMOGENEOUS FROZEN TWO-PHASE FLOW

In Section I the extreme of thermal equilibrium was analyzed to show the effect of nonhomogeneity on choked flow. These results will now be contrasted with the case of frozen nonhomogeneous two-phase flow (this case is more specifically characterized as two-component immiscible flow without mass or energy transfer between components). The governing equations are similar to those for equilibrium flow except that continuity and energy equations must now be written for each phase. The system of equations is

$$\partial(\alpha_g\rho_g)/\partial t + \partial(\alpha_g\rho_g v_g)/\partial x = 0 \tag{22}$$

$$\partial(\alpha_f\rho_f)/\partial t + \partial(\alpha_f\rho_f v_f)/\partial x = 0 \tag{23}$$

$$\alpha_g\rho_g[\partial v_g/\partial t + v_g(\partial v_g/\partial x)] + \alpha_g(\partial P/\partial x)$$
$$+ c\alpha_g\alpha_f\rho[\partial v_g/\partial t + v_f(\partial v_g/\partial x) - \partial v_f/\partial t - v_g(\partial v_f/\partial x)] = 0 \tag{24}$$

$$\alpha_f\rho_f[\partial v_f/\partial t + v_f(\partial v_f/\partial x)] + \alpha_f(\partial P/\partial x)$$
$$+ c\alpha_f\alpha_g\rho[\partial v_f/\partial t + v_g(\partial v_f/\partial x) - v_g/\partial t - v_f(\partial v_g/\partial x)] = 0 \tag{25}$$

$$\partial(\alpha_g\rho_g S_g)/\partial t + \partial(\alpha_g\rho_g S_g v_g)/\partial x = 0 \tag{26}$$

$$\partial(\alpha_f\rho_f S_f)/\partial t + \partial(\alpha_f\rho_f S_f v_f)/\partial x = 0 \tag{27}$$

The phasic equations of state for the frozen system are

$$\rho_g = \rho_g(P,S_g) \text{ and } \rho_f = \rho_f(P,S_f). \tag{28}$$

The system of Equations, Equations (22) through (27), can be written in terms of the six dependent variables α_g, P, v_g, v_f, S_g and S_f through use of the equation of state and the chain rule as was explained in Section II. When the corresponding characteristic determinant is expanded, the following polynomial equation for λ is obtained.

$$(\lambda-v_g)(\lambda-v_f)\{\rho c(\lambda-v_g)(\lambda-v_f) + \alpha_f\rho_g(\lambda-v_g)^2 + \alpha_g\rho_f(\lambda-v_f)^2$$

$$- [(\alpha_f\rho_g\rho_f' + \alpha_g\rho_f\rho_g')(\lambda-v_g)(\lambda-v_f)]$$

$$x[(\lambda-v_g)(\lambda-v_f) + (c\alpha_f/\rho_g)(\lambda-v_f)^2 + (c\alpha_g\rho/\rho_f)(\lambda-v_g)^2]\} = 0 \quad (29)$$

where

$$\rho_g' = (\partial\rho_g/\partial P)_{S_g}, \quad \rho_f' = (\partial\rho_f/\partial P)_{S_f}. \quad (30)$$

Except for the added factor of $(\lambda-v_g)(\lambda-v_f)$, Equation (29) is identical to the case for thermal equilibrium with the following values for the entropy and density derivatives:

$$S_g^* = 0, \; S_f^* = 0, \; \rho_g^* = \rho_g', \text{ and } \rho_f^* = \rho_f' \quad (31)$$

Thus, the factorization completed for Equation (11) in Section II is equally valid for Equation (29).

The roots of Equation (29) are:

$$\lambda_{1,2} = \frac{\left\{\alpha_f\rho_g + \rho c/2 \pm [(\rho c/2)^2 - \alpha_g\alpha_f\rho_g\rho_f]^{1/2}\right\}v_g + \left\{\alpha_g\rho_f \mp [(\rho c/2)^2 - \alpha_g\alpha_f\rho_g\rho_f]^{1/2}\right\}v_f}{(\alpha_f\rho_g + \rho c/2) + (\alpha_g\rho_f + \rho c/2)} \quad (32)$$

and

$$\lambda_{3,4} = v + D(v_g - v_f) \pm a \tag{33}$$

where

$$a = a_{HF}\left\{[(c\rho^2 + \rho(\alpha_g\rho_f + \alpha_f\rho_g)]/(c\rho^2 + \rho_g\rho_f)\right\}^{\frac{1}{2}} \tag{34}$$

and

$$D = \tfrac{1}{2}\left\{\frac{(\alpha_g\rho_f - \alpha_f\rho_g)}{(\rho c + \alpha_f\rho_g + \alpha_g\rho_f)} + \frac{\rho_g\rho_f(\alpha_f\rho_f - \alpha_g\rho_g)}{\rho(\rho_g\rho_f + c\rho^2)}\right\}. \tag{35}$$

The homogeneous frozen sound speed, a_{HF}, which appears in Equation (34), is a special case of the homogeneous equilibrium sound speed in which $S_g^* = 0$ and $S_f^* = 0$ (see Appendix A).

The choking criterion is identical to the equilibrium case; i.e.,

$$M_v + DM_r = \pm 1$$

except that the sound speed and the factor D, given by Equations (34) and (35) respectively, are simply special cases of the previous result. The variation of a and D with the void fraction and c (all other conditions are the same as for the results presented in Section II) are shown plotted on Figures 4 and 5. The trends with c are similar for both the sound speed and D, but the trend with void fraction is quite different, particularly at low void fraction (compare Figures 1 and 3 for the sound speed and Figures 2 and 4 for D). The significance of this difference and the implications as far as nonequilibrium models are concerned is discussed further in Section IV.

IV. APPLICATION OF THE CHOKING CRITERION

The choking criterion is established from Equation (21) with the consideration that either right or left traveling acoustic waves, corresponding to the $\pm$, may satisfy the criterion. The result is

$$|M_v + DM_r| = 1 \tag{36}$$

When a flow is known to be choked or it is desired to calculate the flow rate for a choked flow, Equation (36) is used as a boundary condition for the flow solution. Since the relative velocity, in addition to the mass average velocity, enter into the choking criterion, Equation (36) must be solved simultaneously with the equations of motion. The amount of slip, $(v_g - v_f)$, which exists in a flow approaching a point of choked flow, will affect significantly the choked flow rate. This fact makes the calculation of a choked flow more complex for two-phase flow than for a single-phase flow.

In the RELAP5 code, the choking criterion, Equation (36), is checked each time step at each flow junction and if the quantity

$$M_{exp} = |[M_v + DM_r]_{exp}| \tag{37}$$

exceeds unity the flow is assumed to be choked (the subscript exp is used to indicate that the criterion is checked using explicit calculations for the velocities). When choking occurs, Equation (36) is solved implicitly with the upstream vapor and liquid momentum equations for v_g, v_f and P at the point of flow choking (upstream is with reference to the mass average velocity, v). This solution is used as a boundary condition so that the upstream solution is decoupled from the downstream conditions. If M_{exp} on any time step is less than unity, then the process is reversed and the flow is calculated as in the normal unchoked case.

The application of this criterion is illustrated on Figures 5 and 6 for the two cases of equilibrium and frozen flow which have been analyzed in Sections II and III of this report. The results shown on Figure 5 are for an equilibrium flow having velocities of v_g = 150 M/S and v_f = 110 M/S and for values of c equal to 0, 0.5 and ∞. The Mach number defined by

$$M = |M_v + DM_r| \tag{38}$$

is plotted as a function of the void fraction. The points where choked flow exists for these conditions are where the curves intersect the Mach number unity line. Similar results for the frozen flow case are illustrated on Figure 6. These results are for values of the velocities v_g = 400 M/S and v_f = 360 M/S. Here again, choked flow is attained at those points where M = 1.0 is satisfied.

The conditions and/or parameters which enter into the choked flow criterion include all of the flow parameters as well as the added mass coefficient and the thermal equilibrium or frozen assumption. Of these variables only the degree of thermal nonequilibrium which exists is free or must be established by comparisons to data. The flow variables and the value of the virtual mass coefficient are established from independent analytical modeling considerations. The flow variables are established from solution of the equations of motion for the flow preceding the point of flow choking and the virtual mass coefficient has been established from analytical considerations[11]. For dispersed bubbly and droplet flows the value of the virtual mass coefficient has been established to be approximately 0.5 and for separated flows the value approaches zero. Thus, the coefficient is known within a narrow range.

The degree of thermal nonequilibrium which exists in a two-phase flow has a large effect on the choked flow rate. This can be seen by comparison of the equilibrium calculations shown on Figure 5 are for $v_g = 150$ and $v_f = 110$ with the frozen flow results shown on Figure 6 are for $v_g = 400$ and $v_f = 360$. The choked flow velocities differ by more than a factor of two in these cases. This range becomes even larger at low void fractions.

The effect of partial thermal nonequilibrium cannot be included in the choked flow analysis at present due to limitations of current relaxation-type vapor generation models. In particular, a differential model for the vapor generation terms, such as is the case for equilibrium, is necessary in order for the nonequilibrium effects to be reflected in the choking analysis (algebraic relaxation models appear in the analysis as nondifferential source terms). A relaxation model correctly predicts transient nonequilibrium effects in the finite difference hydrodynamic model, but does not enter into the characteristic analysis. For this reason, the degree of nonequilibrium which should be included in the choking analysis must be investigated empirically. Both the equilibrium and the frozen models have been used to model the results of pipe blowdown experiments, wherein the discharge flow is choked and pipe internal pressures are known functions of time, and to limited cases of steady choked nozzle flow. It has been found that the choking model in which thermal equilibrium is assumed to exist agrees well with data while the frozen model predicts blowdown to occur in about half the actual time.

The comparison of the calculated results, using the equilibrium model, with pipe blowdown data is presented on Figures 7 through 11. The data are those of Edwards'[10] for blowdown of a pipe 0.073 M in diameter by 4.09 M long. The pipe is initially pressurized to 7 MPA and heated to approximately

510^{o}, then a glass disk is ruptured at one end allowing the pipe to blowdown. The pressures are plotted versus time on Figures 7 through 10 for Gauge Stations 1, 3, 5 and 7. Gauge Station 1 is near the open end while 3 and 5 are at intermediate points and 7 is at the closed end. The pressure histories are very dependent upon the mass discharge rate; however, the results are in excellent agreement with data. These same calculations using the frozen model show blowdown being completed in about half the actual time shown by data. Further evidence that the blowdown characteristics are properly predicted by the thermal equilibrium model is provided by comparisons of the calculated and measured void fractions at Gauge Station 5 which is shown on Figure 11.

V. CONCLUSIONS

A computationally efficient choking model for the choked mass discharge of a two-phase mixture has been developed for the RELAP5 system code. Calculations using the model agree with data in the limited number of cases examined. Future work will include comparison of the model to more of the choked two-phase flow data available in the literature. In particular, the applicability of the model to flows near saturated liquid conditions will be investigated in order to determine if nonequilibrium effects need to be considered in more detail.

VI. REFERENCES

1. V. H. Ransom, J. A. Trapp, RELAP5 Progress Summary, PILOT Code Hydrodynamic Model and Numerical Scheme, Idaho National Engineering Laboratory Report No. CD-AP-TR-005 (January 1978).

2. A. H. Shapiro, The Dynamics and Thermodynamics of Compressible Fluid Flow, Vol. II, New York: Ronald, 1954.

3. G. B. Wallis, One-Dimensional Two-Phase Flow, New York: McGraw-Hill Book Company, Inc., 1969.

4. P. R. Garabedian, Partial Differential Equations, New York: John Wiley and Sons, 1964.

5. G. B. Whitham, Linear and Nonlinear Waves, New York: John Wiley and Sons, 1974.

6. R. T. Lahey, Jr., "RPI Two-Phase Flow Modeling Program," NRC Fifth Water Reactor Safety Research Meeting, Gaithersburg, Maryland, November 7, 1977.

7. D. Gidaspow (Chairman), "Modeling of Two-Phase Flow," Proceedings of Round Table Discussion RT-1-2 at the Fifth International Heat Transfer Conference, Tokyo, Japan, September 3-7, 1974, also in Heat Trans., 3, 1974.

8. P. S. Anderson, P. Astrup, L. Eget, O. Rathmann, "Numerical Experience With the Two-Fluid Model, RISQUE," Proceedings of ANS Water Reactor Safety Meeting, July 31 - August 4, 1977.

9. R. Jackson, "The Present Status of Fluid Mechanical Theories of Fluidization," Chemical Engineering Progress Symposium Series, Number 105, Vol. 66, 1970.

10. A. R. Edwards and T. P. O'Brien, "Studies of Phenomena Connected With the Depressurization of Water Reactors," Journal of the British Nuclear Energy Society, Vol. 9 (April 1970), pp 128-135.

11. N. Zuber, "On the Dispersed Two-Phase Flow in the Laminar Flow Region," Chemical Engr. Sci., Vol. 19 (1964) pp 897-917.

APPENDIX A

FACTORIZATION OF CHARACTERISTIC POLYNOMIAL

The fourth-order polynomial obtained as the solution to the characteristic analysis must be factored in order to obtain a choking criterion. This can only be carried out approximately for the general case of unequal phase velocities. However, some useful insight can be obtained by first considering the case of equal phase velocities; i.e., $v_g = v_f = v_o$. For this case, Equations (11) and (29) of the main text can be factored exactly with the results;

$$\lambda_{1,2} = v_o \tag{A-1}$$

$$\lambda_{3,4} = v_o \pm a. \tag{A-2}$$

where the sound speed, a, is defined as before by Equation (15) of the text. Hence, for small values of $(v_g - v_f)$, we expect two of the roots to be near the mixture velocity, v, and thus the factors $\lambda - v_g$ and $\lambda - v_f$ will be of the same order as $(v_g - v_f)$. This being the case, it is possible to obtain a close approximation to two of the roots by neglecting the fourth-order factors in $\lambda - v_g$ and $\lambda - v_f$ relative to the second-order factors. The remaining two roots are expected to be of the order $(v \pm a)$ and the factors $\lambda - v_g$ and $\lambda - v_f$ to be of the order $\pm a$,; i.e., not small. The root $\lambda_{1,2}$ may be interpreted physically as the paths along which kinematic effects propagate at the fluid velocity while the roots, $\lambda_{3,4}$, are the paths along which acoustic phenomena propagate at speeds $v \pm a$.

The slower kinematic roots are obtained by neglecting the fourth-order factors in $\lambda - v_g$ and $\lambda - v_f$ and subsequently exactly factoring the remaining second-order polynomial; i.e.,

$$\rho c(\lambda - v_g)(\lambda - v_f) + \alpha_f \rho_g (\lambda - v_g)^2 + \alpha_g \rho_f (\lambda - v_f)^2 = 0 \qquad \text{(A-3)}$$

The corresponding roots are:

$$\lambda_{1,2} = \frac{\left\{\alpha_f \rho_g + \rho c/2 \pm [(\rho c/2)^2 - \alpha_g \alpha_f \rho_g \rho_f]\right\} v_g + \left\{\alpha_g \rho_f + \rho c/2 \mp [(\rho c/2)^2 - \alpha_g \alpha_f \rho_g \rho_f]\right\} v_f}{(\alpha_f \rho_g + \rho c/2) + (\alpha_g \rho_f + \rho c/2)} \qquad \text{(A-4)}$$

The remaining two roots are obtained by neglecting other than the first-order factors in $v_g - v_f$. Each of the phasic velocities can be written as the sum of a mean velocity and a relative velocity term as follows:

$$v_g = v + [(\alpha_f \rho_f)/\rho](v_g - v_f) \qquad \text{(A-5)}$$

$$v_f = v - [(\alpha_g \rho_g)/\rho](v_g - v_f). \qquad \text{(A-6)}$$

When Equations (A-5) and (A-6) are substituted into the fourth-order polynomial, Equation (11), the factors expanded, and only the terms first order in $(v_g - v_f)$ retained, the following roots can be obtained

$$\lambda_1 = v$$

$$\lambda_2 = v + \frac{2(v_g - v_f)}{\rho} \left[\frac{(\frac{\rho c}{2} + \alpha_f \rho_g)\alpha_f \rho_f - (\frac{\rho c}{2}) + \alpha_g \rho_f)\alpha_g \rho_g}{\rho c + \alpha_f \rho_g + \alpha_g \rho_f} \right] \qquad \text{(A-7)}$$

which are slightly different approximations to the kinematic roots, Equation A-4, obtained by exact factorization of the second-order polynomial, Equation (A-3).

The remaining roots of the fourth-order polynomial are:

$$\lambda_{3,4} = v + D(v_g - v_f) \pm a \tag{A-8}$$

where

$$v = (\alpha_g \rho_g v_g + \alpha_f \rho_f v_f)/\rho \tag{A-9}$$

$$D = \tfrac{1}{2}\left\{\frac{\alpha_g \rho_f - \alpha_f \rho_g}{\rho c + \alpha_f \rho_g + \alpha_g \rho_f} + \frac{\rho_g \rho_f (\alpha_f \rho_f - \alpha_g \rho_g)}{\rho(\rho_g \rho_f + c\rho^2)} - \frac{\rho a_{HE}^2 (\alpha_g \rho_g^2 S_g^* + \alpha_f \rho_f^2 S_f^*)}{\rho_g \rho_f (S_g - S_f)}\right\} \tag{A-10}$$

$$a = a_{HE}\left\{[c\rho^2 + \rho(\alpha_g \rho_f + \alpha_f \rho_g)]/(c\rho^2 + \rho_g \rho_f)\right\}^{\frac{1}{2}} \tag{A-11}$$

The homogeneous equilibrium sound speed is defined as

$$a_{HE}^2 = (\rho_g \rho_f/\rho)[\alpha_f \rho_g \rho_f^* + \alpha_g \rho_f \rho_g^* - (\rho_g - \rho_f)(\alpha_g \rho_g S_g^* + \alpha_f \rho_f S_f^*)/(S_g - S_f)]^{-1} \tag{A-12}$$

where the asterisk denotes differentiation with respect to pressure (see Equations (9) and (10) of the text).

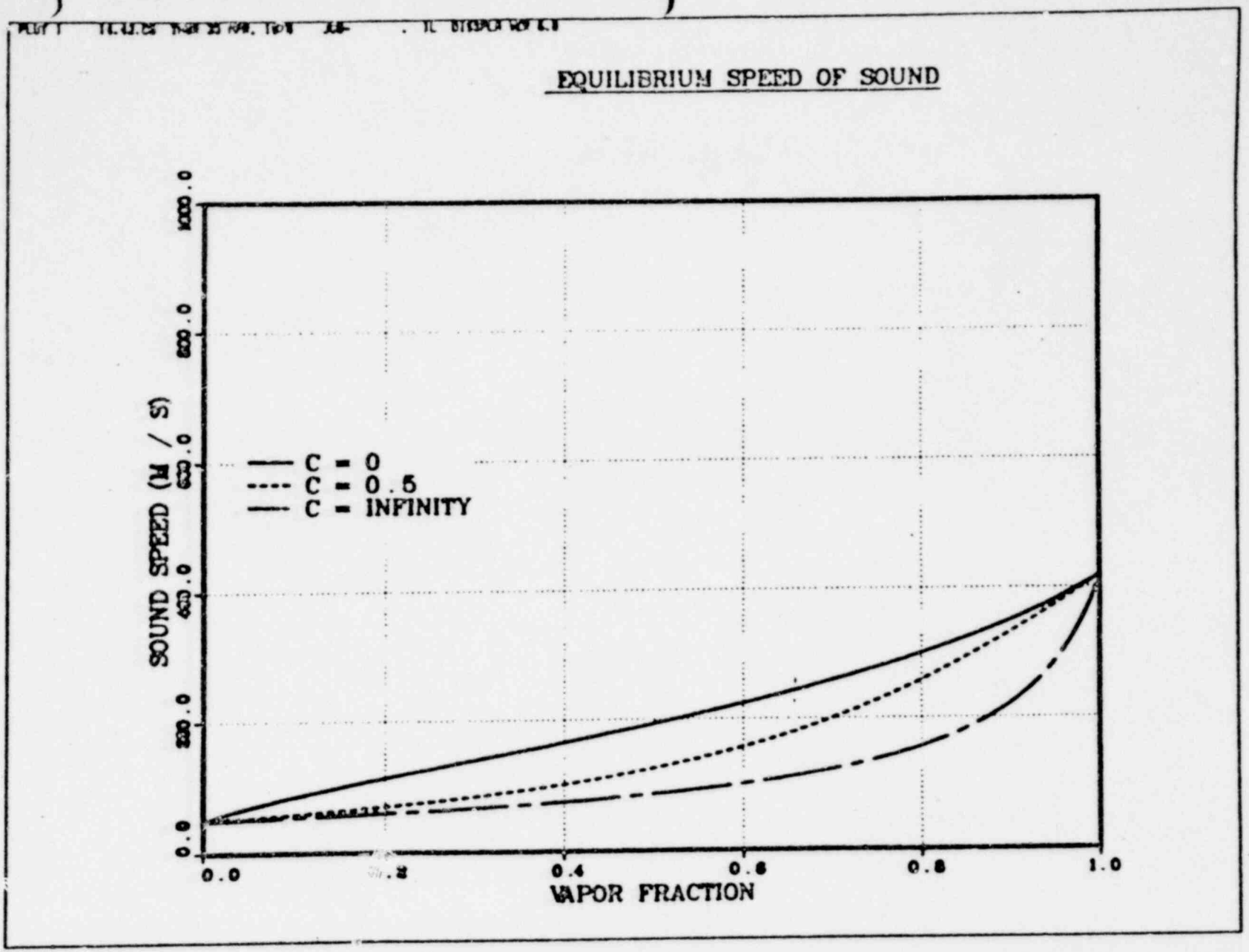

Figure 1. Equilibrium speed of sound as a function of void fraction and virtual mass coefficient

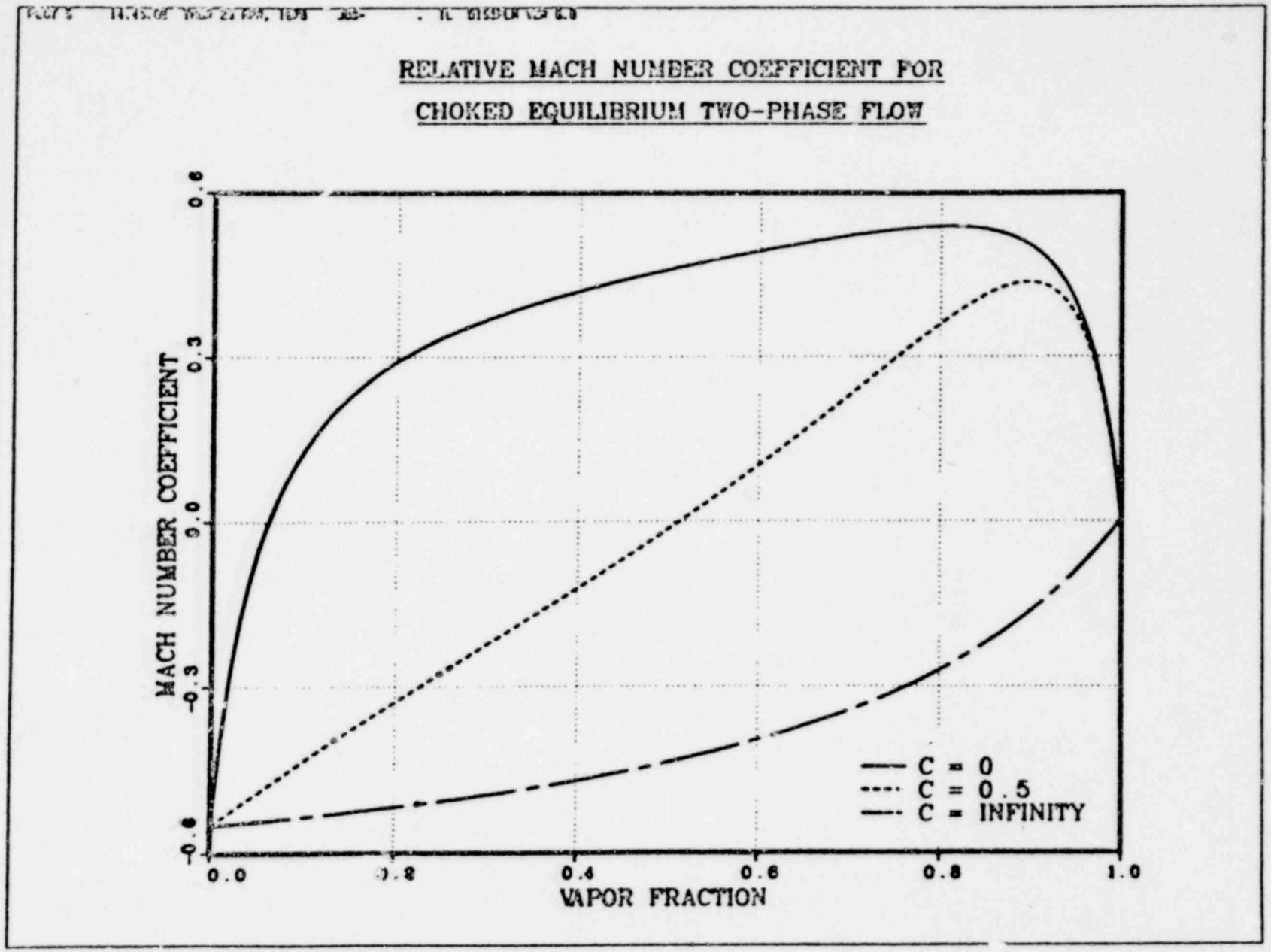

Figure 2. Coefficient of relative Mach number for thermal equilibrium flow as a function of void fraction and virtual mass coefficient

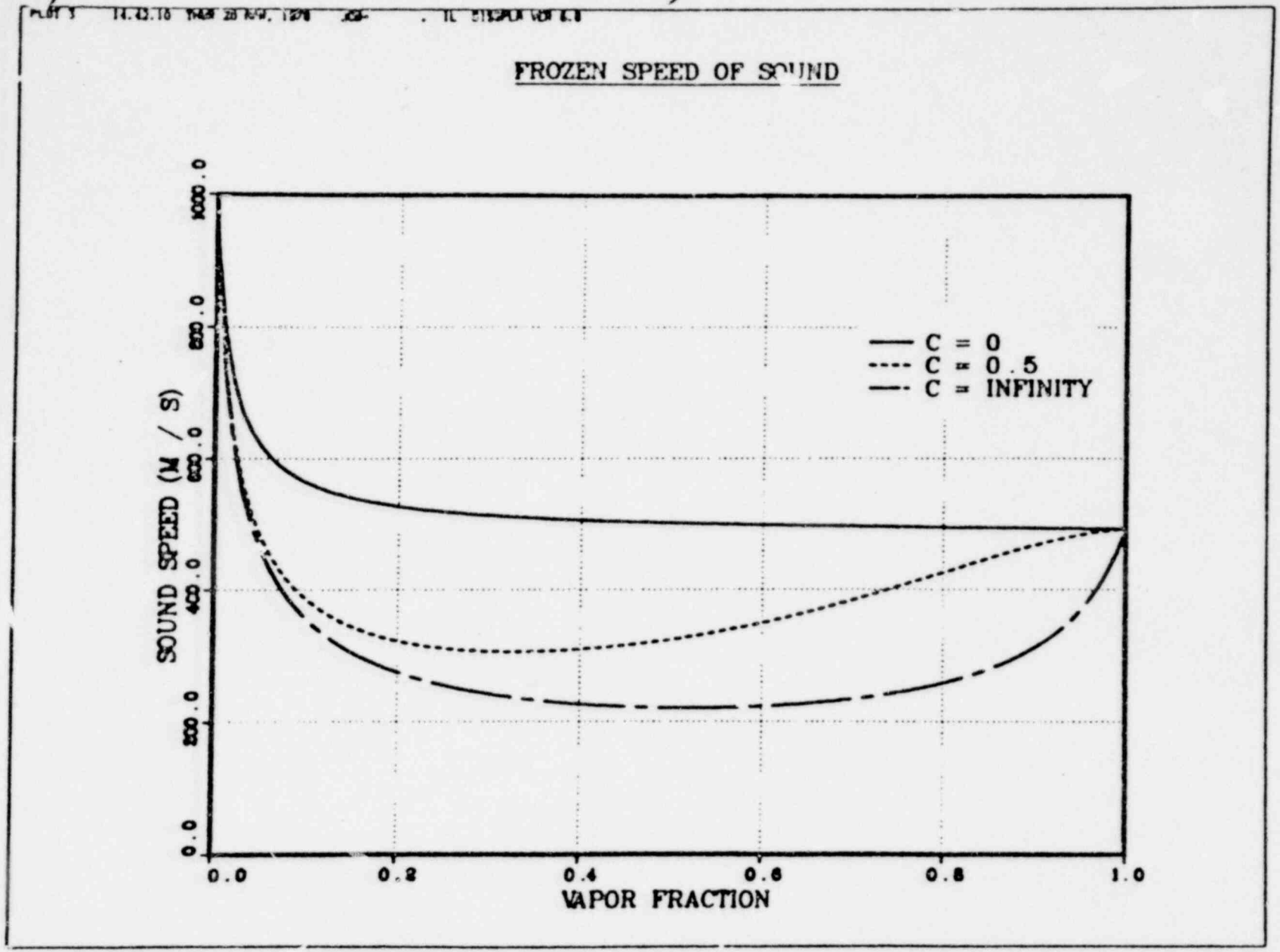

Figure 3. Frozen speed of sound as a function of void fraction and virtual mass coefficient

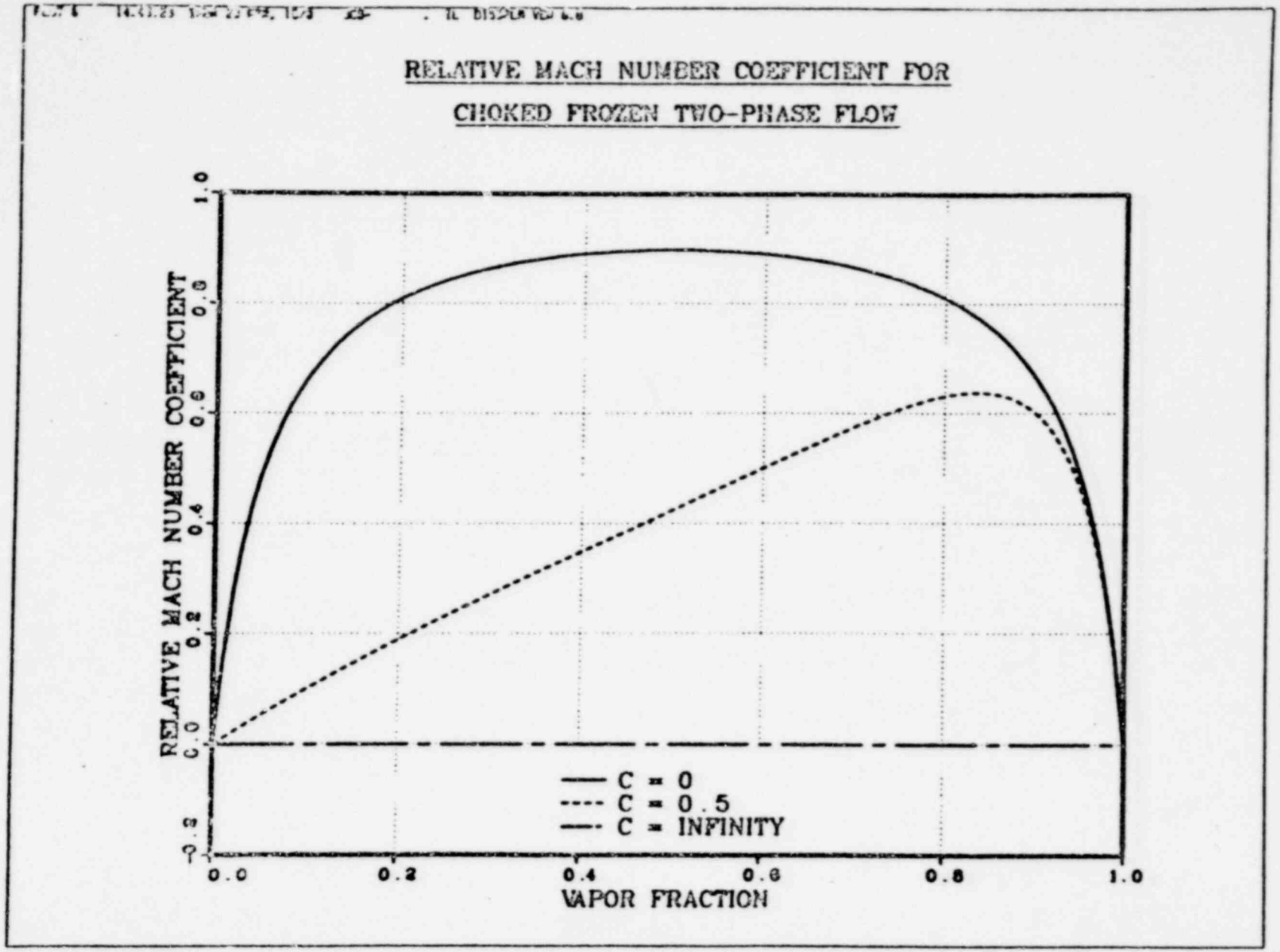

Figure 4. Coefficient of relative Mach number for frozen flow as a function of void fraction and virtual mass coefficient

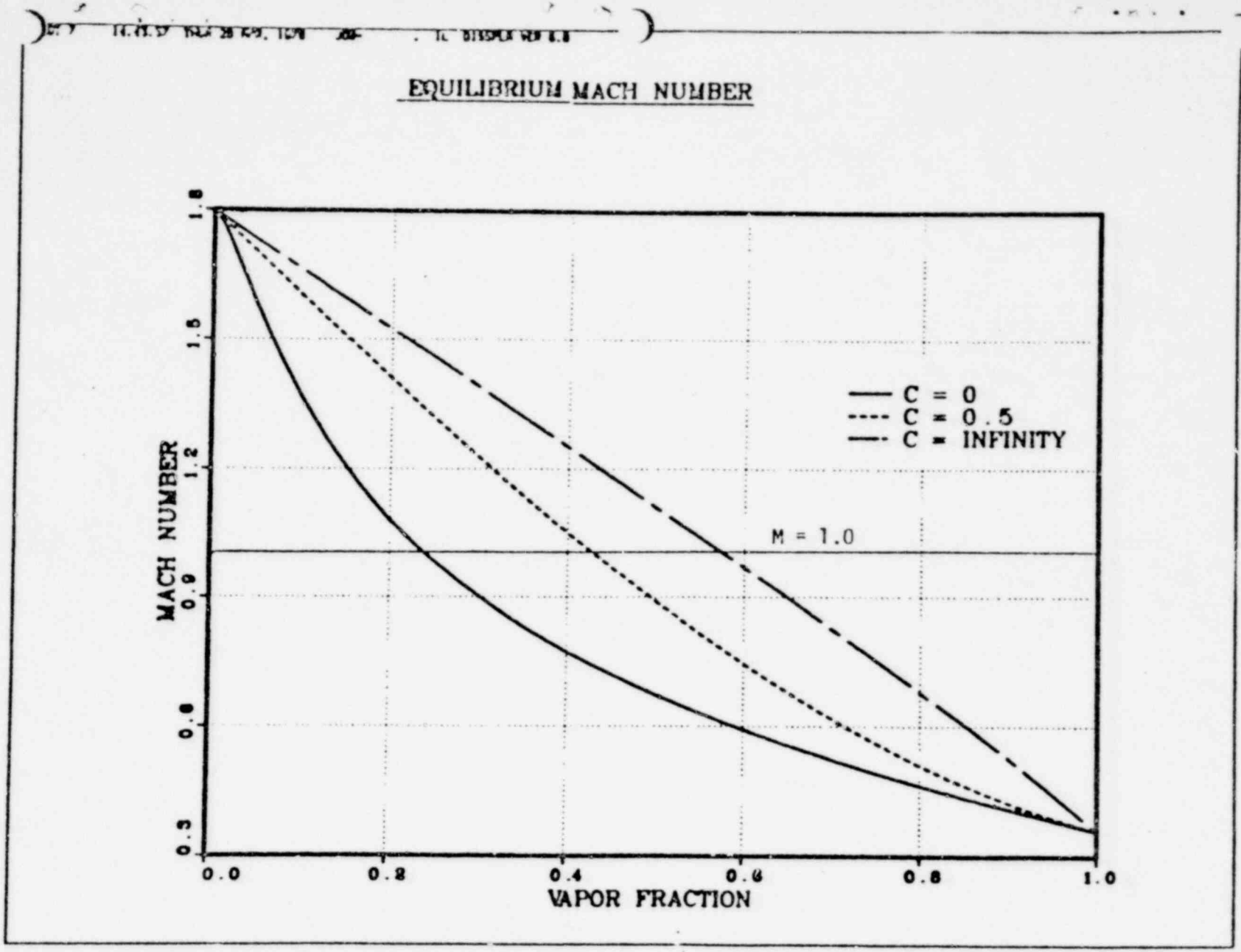

Figure 5. Two-phase equilibrium Mach number as a function of void fraction and virtual mass coefficient for v_g = 150 M/S and v_f = 110 M/S

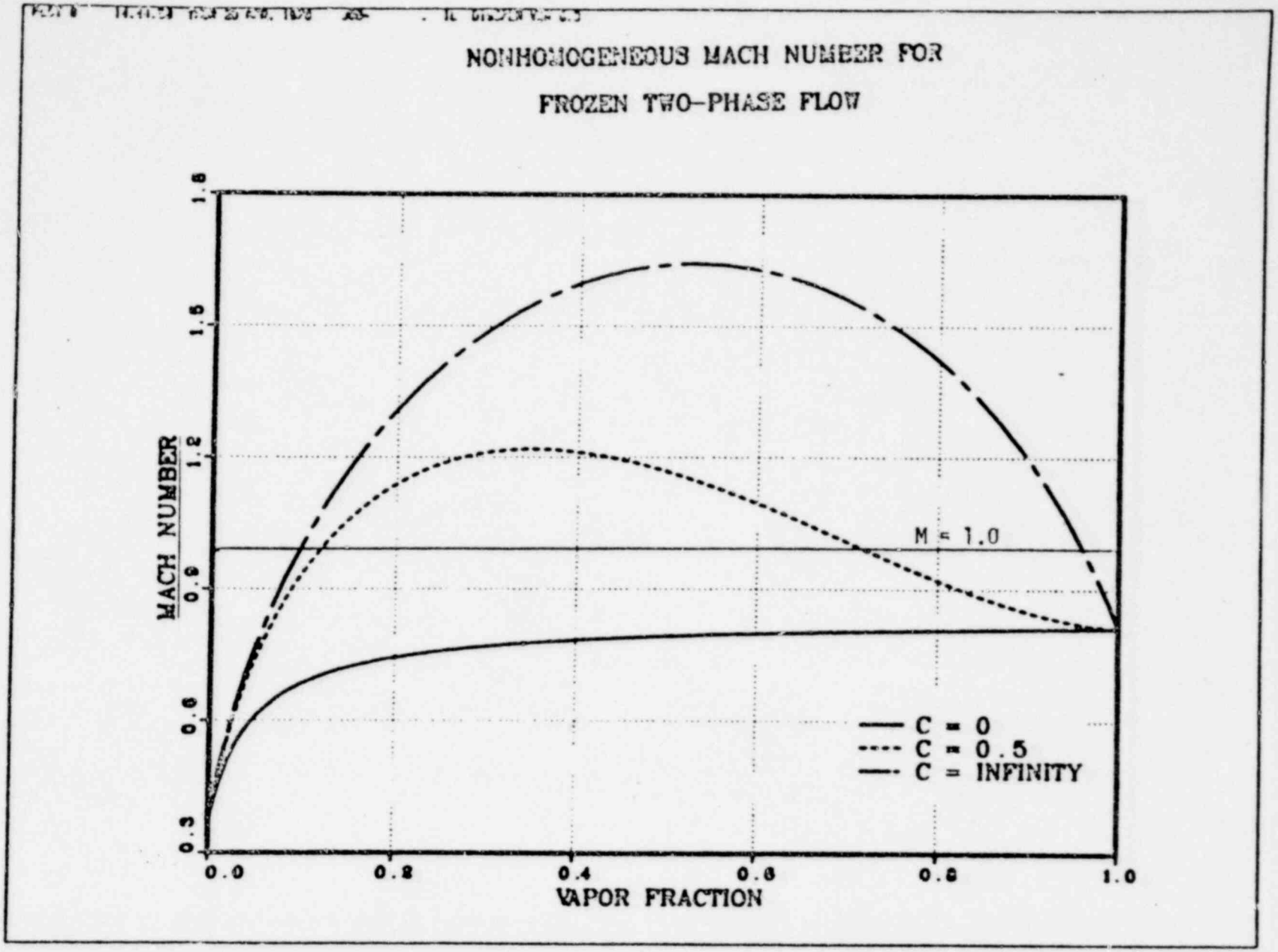

Figure 6. Two-phase frozen Mach number as a function of void fraction and virtual mass coefficient for v_g = 400 M/S and v_f = 360 M/S

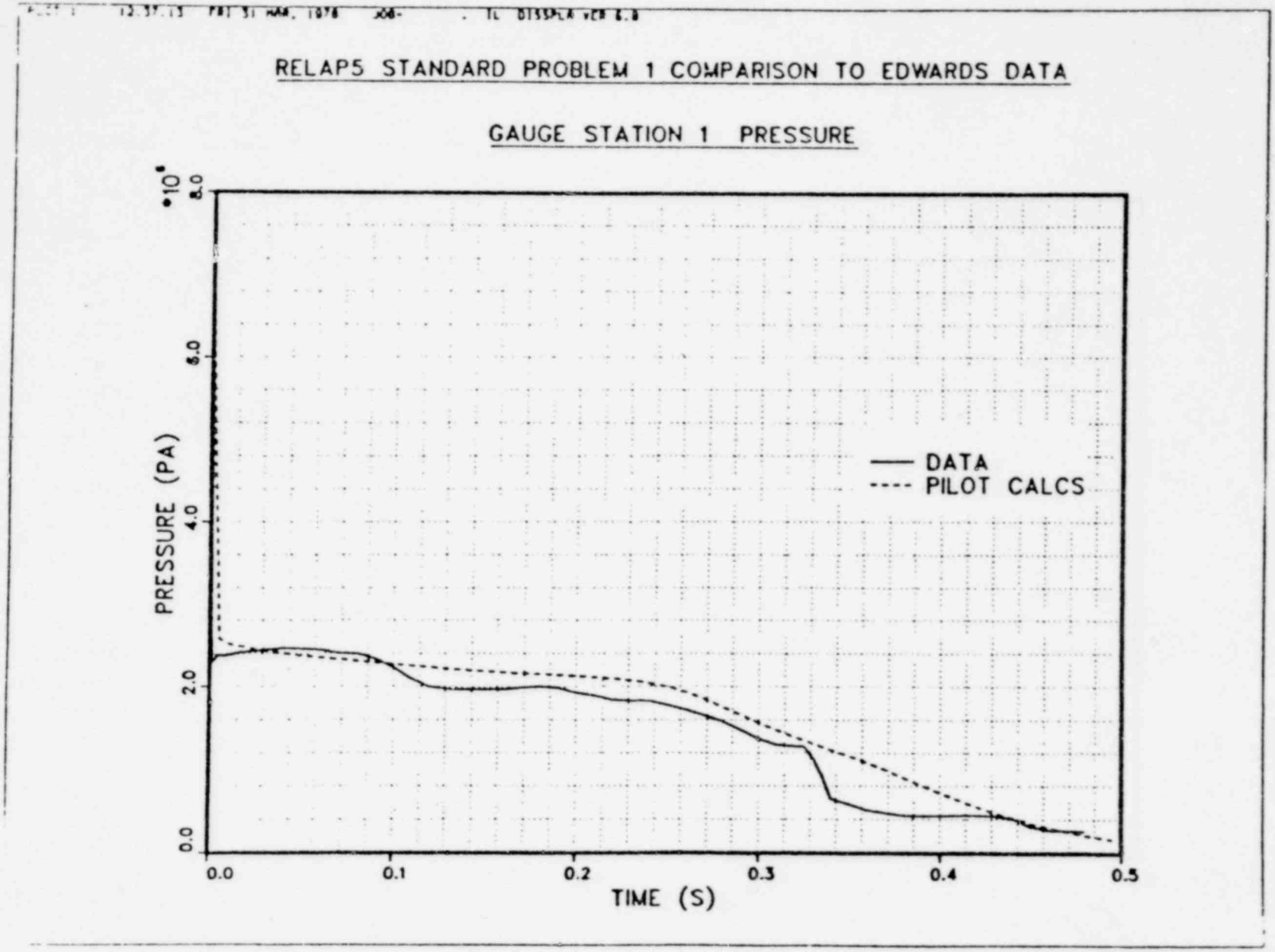

Figure 7. Edwards' pipe blowdown, pressure at gauge station 1

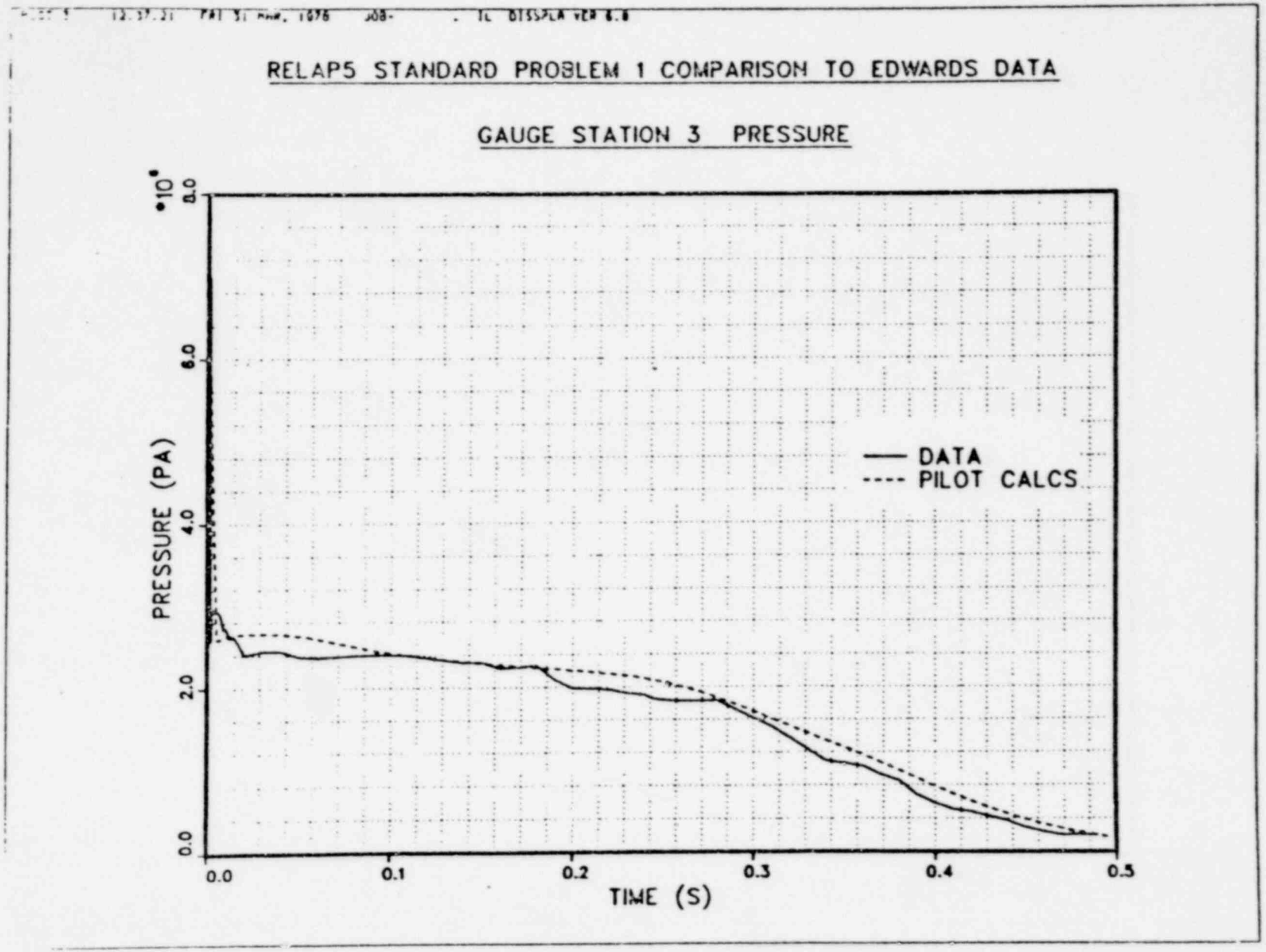

Figure 8. Edwards' pipe blowdown, pressure at gauge station 3

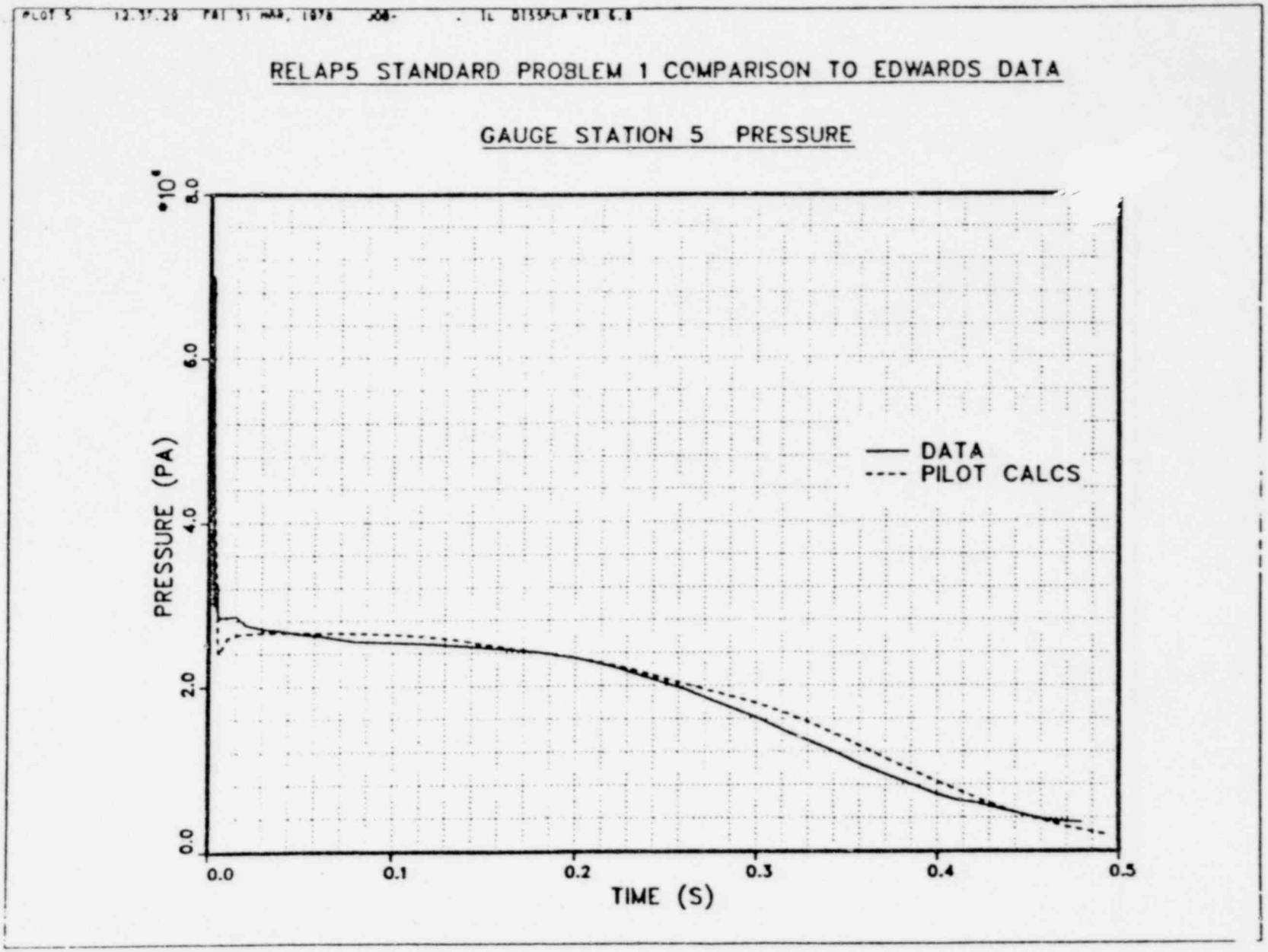

Figure 9. Edwards' pipe blowdown, pressure at gauge station 5

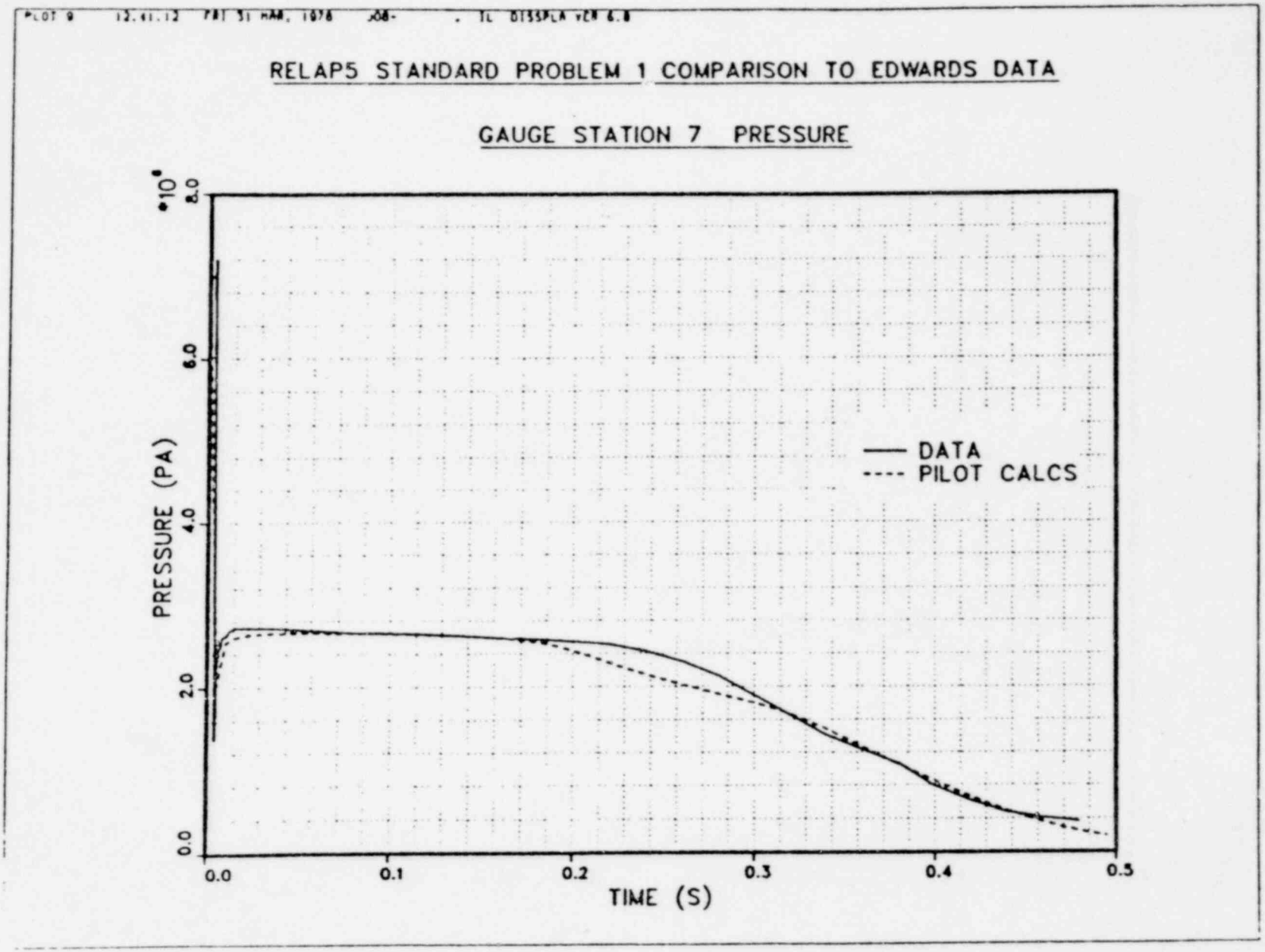

Figure 10. Edwards' pipe blowdown, pressure at gauge station 7

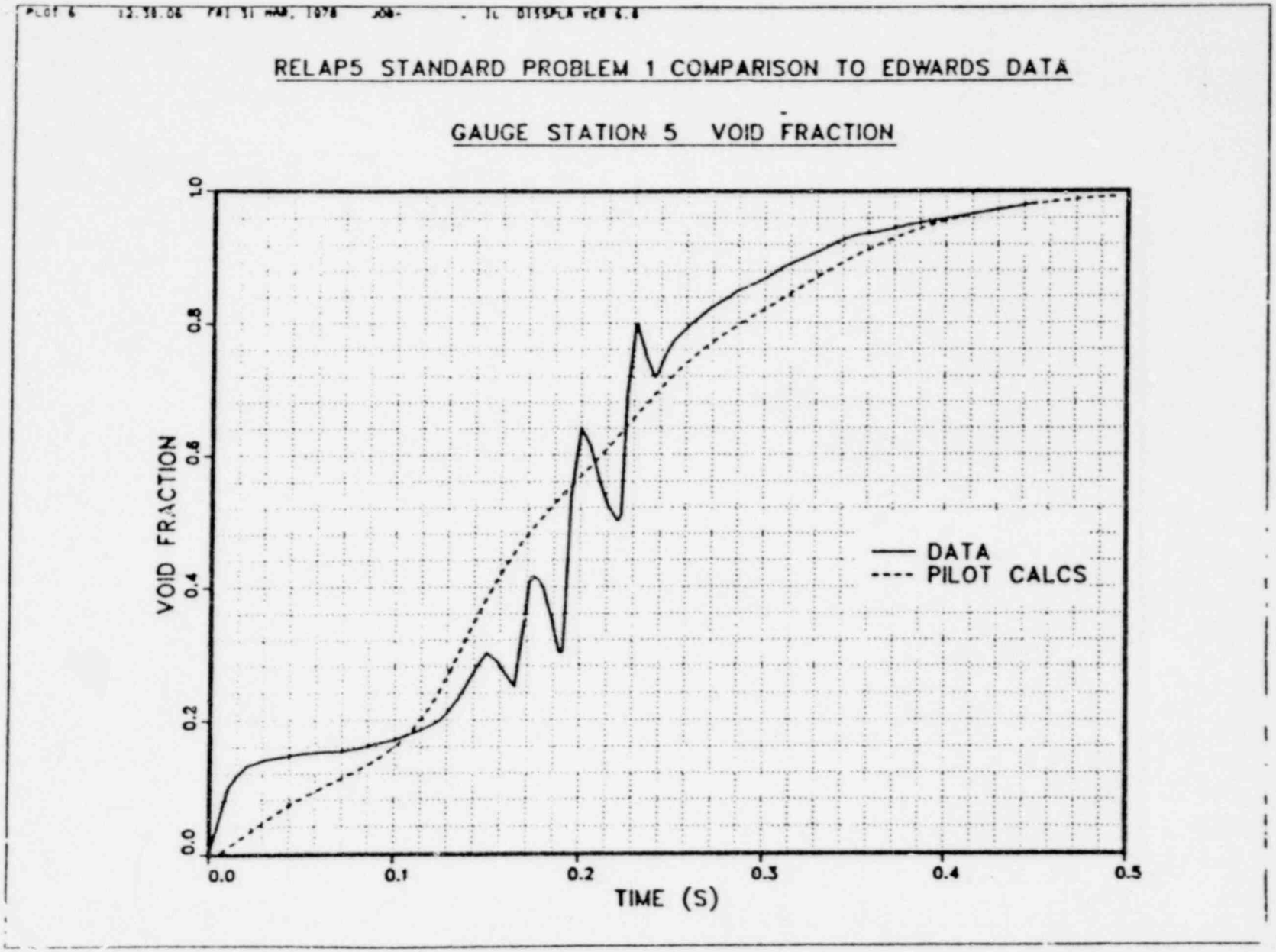

Figure 11. Edwards' pipe blowdown, void fraction at gauge station 5